The ethology of stress in nematodes

Thesis by

Pei-Yin Shih

In Partial Fulfillment of the Requirements for

the Degree of

Doctor of Philosophy in Biology

CALIFORNIA INSTITUTE OF TECHNOLOGY

Pasadena, California

2019

(Defended September 10, 2018)

Pei-Yin Shih
ORCID: 0000-0003-3082-9242

ACKNOWLEDGEMENTS

Doing science at Caltech has been an intellectually stimulating and exciting experience. I am very lucky to have had the opportunity to get to know and work with so many amazing and inspiring scientists here. I am also very grateful for having support from my friends and family along the way.

First and foremost, I would like to thank my advisor Paul Sternberg. His vision and guidance have challenged me to think in a more creative and critical way. His encouragement and passion toward science have also helped me to build confidence toward the science I do and love. I also would like to thank my committee members: Professors Ellen Rothenberg, Michael Elowitz, and David Prober. I appreciate them for taking time out of their busy schedules and giving me great advice and support. I owe thanks to Professor Dianne Newman for believing in me and giving me the opportunity work with her as a TA: leading recitation section was daunting in the beginning, but the experience has helped me grow a lot in my public speaking and teaching skills.

I would like to thank many good friends and colleagues in the Sternberg lab. Mihoko Kato is my go-to person for advice on experiments and life in general. She is also my role model for being a great mentor and assertive scientist. I would like to thank Amir Sapir and Ryoji Shinya for showing me how great discovery comes from earnest curiosity, the love and caring for the living world, and optimistic attitudes. I am also grateful for Oren Schaedel's help on developing my interest in the dauer field and Porfirio Quintero-Cadena's help on statistical analysis for dauer assays. I would also like to thank the following individuals from the Sternberg lab: Christopher Cronin for answering all sorts

of engineering questions and inspiring me to build; Hillel Schwartz for helping me start my nematode journey and always providing helpful edits and critiques; Han Wang for insightful ideas and suggestions; Paul Minor and Julie Cho for showing me what an outstanding graduate student is like; Margaret Ho for being my lovely running buddy; and Kerckhoff 209 residents Meennakshi Doma, Ping Hsueh, Wen Chen, Cynthia Chia, and Liz Holman for making coming to work enjoyable. There are many others from the lab that I would like to thank, including Heenam Park, Ravi Nath, Jonathan Liu, Katie Brugman, Daniel Leighton, Daniel Oh, Sarah Cohen, Sandy Wong, Mandy Tan, Chun-Hao Chen, Mengyi Cao, David Angeles, Mary Alvarez, Sarah Torres, Barbara Perry, Shala Gharib, and John DeModena.

I have also built a lot of precious friendships outside of the lab. I would like to thank Tsui-Fen Chou for being like my sister and second PI, taking good care of me in life and in science. I am also grateful for having my classmate from high school in Taiwan here in LA with me. Thank you Ting-Hwan Lee for always being there for me. I would like to thank Alicia Rogers and Scott Saunders for the coffee breaks, board game time, and the trail running adventure. It was tough the first few years of studying abroad, so I would like to thank the following wonderful people for helping me through: Min-Yu Yang for his support, snacks, and morning calls; KJ (Tiffiany) Chang for helping me set up my life in the US; Va Si, Xun Wang, and Can Li for doing problem sets together and celebrating with delicious food afterwards; Yi-Chun Chen and Ting-Ni Lu for keeping me company and always making me happy; Susan Liao for exploring Pasadena with me; fitness buddies Yun Mou, Mike Yang, and Mike Anaya for keeping me in shape.

Running a marathon is a metaphor for life. With every self-doubt and setback, there

are also assurance, and breakthroughs. Training for the LA marathon and running with the Pasadena Pacers 11-Minute group has been a blessing. They showed me how dedication and consistency can redefine difficulty in life. I can stay strong mentally and physically at the last stretch of my graduate school because of their encouragement and positive energies. I also would like to thank Kate for her Wednesday spinning class, which has always been a great stress-reliever and highlight of my week.

I have grown to appreciate great coffee, music, and podcasts during graduate school. I would like to thank various coffee shops and stores for keeping me awake with great taste and providing good spaces for inspiration: Highlight Coffee, Copa Vida, Philz, Float, and Vromans/Jones coffee. I would also like to thank Mayday, Pinegrove, Spotify, and various podcasts (the Daily, Marathon Training Academy, Pop Culture Happy Hour, Moth Radio Hour) for entertaining and educating me during all the worm-picking and pheromone-boiling hours.

I am lucky to have the warmth of a family with the following people's love and caring: Grandma Hong, Uncle Frank, Aunt Jenny, Benjamin Hong, Grandpa Jinsung Koo, Uncle Yonghwan Lee, Aunt Michelle Lee, and William Lee. I am very grateful for all their support.

I owe a lot of thanks to James Lee, my best roommate, collaborator, and partner during my graduate career. I am always inspired by his intelligence and curiosity. At the same time, he ensures I know my own strength and ability, and helps me build up my confidence. For that I am very glad to have had him with me during the journey.

Finally, I would like to thank my family for their love and support. Even though they can only see me a few weeks a year, they have always been very supportive of me

pursuing my dream. I am especially thankful for my mom for showing me how strong and resilient I can be.

ABSTRACT

Animals can respond to stress in two ways: one is through innate, reflexive behaviors and physiological responses. For example, bees sting invaders when they feel threatened, and heat shock proteins in our body ensure the proper folding of proteins under stressful conditions. The other strategy is through the more active and dynamic phenotypic plasticity responses, for example the transformation of spadefoot tadpoles into cannibals in crowded environments.

When *Caenorhabditis elegans* roundworms face harsh environmental conditions they can develop into the dauer larvae stage instead of reproductive adult. Dauers are long-lived, stress-resistant, and specialized for dispersal. Dauer biology has much to reveal about stress resistance, neural state, and tissue coordination.

Using RNA-seq we compared dauers vs non-dauers and found 8,042 genes that are differentially expressed. By bioinformatically clustering these genes, we discovered the significant up-regulation of neuropeptide genes during dauer development. In particular, the FMRFamide neuropeptides are coordinatelly up-regulated as a family. Peptidergic signaling downstream of *sbt-1* promotes dauer entry decision and nication coordination, and it is necessary for CO_2 chemoattraction. We further identified that *flp-10* and *flp-17* together have the same effect as *sbt-1* on nictation and CO_2 attraction. Finally, we showed that the upregulation of *flp* might be a shared strategy in the host-seeking parasitic infective juvenile (IJ) stage.

From the RNA-seq data we also identified four good marker genes for labeling the dauer entry decision and driving gene expression, specifically during dauer commitment. By overexpressing *daf-9* in the hypodermis during dauer-commitment, we can

manipulate the decision and promote reproductive development. Combining the markers with partial dauer mutants allowed me to confirm their subtle phenotypes in tissue-coordination breakdown. Furthermore, this approach allowed me to uncover the novel neuronal partial dauer phenotype for *daf-18* mutants.

In work done outside of the lab, I investigated the innate stress response of extremophiles to Mono Lake. I isolated nine new nematode species that were diversely related in phylogeny, morphology, and feeding lifestyles. We were able to culture one of the species, *Auanema tufa*, in the laboratory, and demonstrated a high level of arsenic stress-resistance in the species. These data suggest that Mono Lake—particularly its more buffered tide zone—has been invaded independently and multiple times by nematodes. We also speculate that pre-adaptation to arsenic in the tide zones on Mono Lake could lead to the genomic evolution necessary to adapt to the high pH and salinity of inner Mono Lake.

Altogether, I have investigated innate and plastic stress responses in and outside of the lab through my work on dauer development and arsenic resistance in Mono Lake. This has allowed me to survey the strategies nematodes use to maximize the use of their simple body plans. In particular, dauers up-regulate 64 neuropeptide genes that encode for 215 peptides to massively rewire their neural state. This likely allows them to overcome the physical limitations of their un-compartmentalized nervous system, and I speculate that such a strategy would be useful in other organisms lacking compartmentalized brains, as well as in local regions of a brain that are low complexity.

PUBLISHED CONTENT AND CONTRIBUTIONS

Lee JS*, **Shih PY***, Schaedel ON, Quintero-Cadena P, Rogers AK and Sternberg PW (2017) FMRFamide-like peptides expand the behavioral repertoire of a densely connected nervous system. *Proceedings of the National Academy of Sciences USA* 114(50): E10726-E10735. doi: 10.1073/pnas.1710374114
*Equal contribution

P.-Y.S. participated in designing research, performing experiments, contributing new reagents, analyzing data, and writing the manuscript.

TABLE OF CONTENTS

Acknowledgements……...iii
Abstract ……...vii
Published Content and Contributions…….....ix
Table of Contents…….....x
List of Illustrations and/or Tables……....xii
Chapter 1: Introduction 1
1.1 Thesis overview.....2
1.2 Figures 17
1.3 References 21
Chapter 2: FMRFamide-like peptides expand the behavioral repertoire of a densely connected nervous system 33
2.1 Abstract 34
2.2 Introduction 35
2.3 Results 38
2.4 Discussion 53
2.5 Materials and Methods.....57
2.6 Figures 69
2.7 References 88
Chapter 3: Genetic markers enable the verification and manipulation of the *Caenorhabditis elegans* dauer entry decision 102
3.1 Abstract 103
3.2 Introduction 105
3.3 Results 107
3.4 Discussion 113
3.5 Materials and Methods.....116
3.6 Figures 121
3.7 References 135
Chapter 4: Extremophile nematodes in and around Mono Lake demonstrate adaptation to an arsenic-rich environment 139
4.1 Abstract 140
4.2 Introduction 141
4.3 Results 144
4.4 Discussion 151
4.5 Materials and Methods.....153
4.6 Figures 156
4.7 References 184
Chapter 5: Conclusion 190
5.1 Concluding remarks 191
5.2 References 193
Appendix A: *Caenorhabditis elegans* can use mechanosensation to predict

environmental collapse....194
A.1 Abstract....195
A.2 Introduction....196
A.3 Results....198
A.4 Discussion....204
A.5 Materials and Methods....207
A.6 Figures....210
A.7 References....221

LIST OF ILLUSTRATIONS AND/OR TABLES

Figure *Page*

1.1 Two developmental trajectories in *C. elegans* 17

1.2 The major signaling pathways involved in reproduction and dauer developmental decision 18

1.3 The differential CO_2 preference in *C. elegans* dauer and non-dauer .. 19

1.4 The hypothesized evolution of parasitism 20

2.1 39% of the *C. elegans* genome is differentially expressed during dauer and reproductive development. 69

2.2 *daf-9(dh6)* RNA-seq dataset summaries 71

2.3 Differential expression was detected at high accuracy and single-cell resolution 72

2.4 Clustering revealed six common expression profiles during dauer and reproductive development. 74

2.5 Enriched GO terms and KEGG pathways in clusters 1 to 6. 75

2.6 Differential expression of the neuronal effector genome of *C. elegans* during dauer and reproductive development 77

2.7 Nictation initiation and the proportion of time spent nictating are not significantly affected in *sbt-1* null mutants. 78

2.8 Neuropeptide signaling promotes dauer entry and dispersal behaviors 79

2.9 FMRFamide-like peptides are coordinately up-regulated during dauer development 81

2.10 FMRFamide-like peptides are coordinately up-regulated during dauer development 83

2.11 FMRFamide-like peptides are coordinately up-regulated in host-seeking infective juveniles of parasitic nematodes 85

2.12 Model of circuit changes during dauer development via

non-synaptic FLP signaling.....87
3.1 Expression profiles of collagen gene.....121
3.2 *col-183*, *ets-10*, *nrh-246* and *led-1*(*F53F1.4*) Genetic markers demonstrates dauer- or reproductive-specific expression pattern....122
3.3 Expression profiles of transcription factors.....124
3.4 *ets-10* expression pattern in non-dauer stages (L4-adult).....126
3.5 *nhr-246* expression pattern in non-dauer stage (embryo-L1).....128
3.6 Expression profiles of genes that are down-regulated in dauer.....129
3.7 The appearance of fluorescence correlates with the dauer-commitment decision and stays on in dauer 130
3.8 Overexpressing daf-9 in the hypodermis during commitment increases the reproduction decision 131
3.9 Partial dauers mis-express dauer markers.....133
4.1 Nematodes were isolated from in and around Mono Lake 156
4.2 Pictures of three sampling sites around Mono Lake 158
4.3 Nematodes isolated from the three sites are diverse in morphology159
4.4 The nematodes isolated are phylogenetically and in morphologically diverse.....161
4.5 Nematodes isolated from the three sites are diverse in morphology165
4.6 Percent of sequence identity of each isolates compared to its closest related species.....166
4.7 Phylogenetic tree of species a (based on LSU sequence).....167
4.8 Phylogenetic tree of species a (based on SSU sequence).....168
4.9 Phylogenetic tree of species b (based on LSU sequence) 169
4.10 Phylogenetic tree of species b (based on SSU sequence).....170
4.11 Phylogenetic tree of species c (based on LSU sequence).....171
4.12 Phylogenetic tree of species c (based on SSU sequence).....172
4.13 Phylogenetic tree of species d (based on LSU sequence) 173
4.14 Phylogenetic tree of species d (based on SSU sequence).....174
4.15 Phylogenetic tree of species e (based on LSU sequence).....175

4.16 Phylogenetic tree of species e (based on SSU sequence).....176
4.17 Phylogenetic tree of species f (based on LSU sequence).....177
4.18 Phylogenetic tree of species g (based on SSU sequence).....178
4.19 Phylogenetic tree of species h (based on SSU sequence).....179
4.20 Species g and h SSU sequence alignment 180
4.21 Characteristics of *Auanema tufa* 181
4.22 *Auanema tufa* is resistant to arsenic.....182

Table *Page*

4.1 Detailed information of the soil samples collected 163

Appendix Figure *Page*

A.1 The dauer entry life cycle decision is modulated by mechanosensation 210
A.2 *mec-4* and *mec-10* CRISPR alleles are putative nulls.....212
A.3 *mec-4* promotes dauer entry.....213
A.4 Touch and pheromone are parallel inputs into the dauer entry decision.....215
A.5 *mec-4* and *trp-4* act additively with *pezo-1* to promote dauer entry .218
A.6 Direct mechanical stimulation promotes dauer entry.....219
A.7 Model of the complex dauer entry decision 220

Appendix Table

A.1 Expression pattern and allele effects of mechanosensation genes.....217

2.1 Metadata of our *daf-9(dh6)* RNA-seq experiment
2.2 Normalized expression values for each detected gene in the RNA-seq dataset
2.3 Differentially expressed genes from the twelve pairwise comparisons
2.4 Genes in clusters 1 to 6
2.5 Differentially expressed neuronal effector genes

Appendix Video

2.1 Wild type nictation

2.2 *sbt-1(-)* nictation

2.3 Wild type CO_2 response

2.4 Wild type control gas response

2.5 *sbt-1(-)* CO_2 response

2.6 *sbt-1(-)* control gas response

C h a p t e r 1

INTRODCUTION

1.1 Thesis overview

Phenotypic plasticity

Living organisms constantly interact with the surroundings they live in, including environmental stresses that might be harmful for them. Phenotypic plasticity is a way for organisms to adjust for survival under stress. For example, the water flea changes its morphology in the presence of predator to become a less favorable prey (1), and high population density can transform the behavior of the spadefoot tadpole to become cannibalistic (2). The immune system is an example in humans for constant adaptation against the invasion of foreign organisms (3). To me, it is especially interesting to think about how the genome and nervous system of an organism encode the information so that it can properly respond to the environment and maximize its fitness.

C. elegans can avoid stress by entering into dauer stage

Caenorhabditis elegans roundworms provide perhaps the best example for studying molecular basis of phenotypic plasticity. *C. elegans* can switch developmental trajectories depending on environmental conditions (**Figure 1.1**). In favorable environments, they proceed from L1, L2, L3, and L4 larvae stages to reproductive adults. When the L1 animals sense harsh stimulus, including high temperature, low food, and high population density—as measured by conspecific pheromone—they can enter an alternative pre-dauer stage, the L2d, and commit to become a dauer if the unfavorable conditions persist. Dauer larvae have specialized physiology (*e.g.* thickened cuticle) that makes them highly resistant to environmental insults, including desiccation, heat, and oxidative stress (4). Their ability to

convert stored fat to carbohydrate through glyoxylate cycle enables them to have an extended life span despite not feeding (4, 5). If environmental conditions improve, dauers can then resume reproductive development (6, 7).

This developmental choice is important for *C. elegans*, especially because making the wrong dauer entry decision can lead to a significant fitness cost (8). The animals can be disadvantaged by not having as many progeny if they misjudge environmental conditions and enter dauer at the wrong time; or they can be at risk of dying if they continue reproductive development while the environment is harsh. On the other hand, there is, of course, an energy cost to entering dauer. Dauer development requires the remodeling of tissues (*e.g.* hypodermis, intestine, gonad, and neurons) throughout the whole animal, as well as the coordination of the tissues in executing the decision. In addition, there is an opportunity cost to not reproducing when other organism are doing so.

Food, pheromone, and temperature are the three known environmental cues that *C. elegans* use to gauge the quality of the environment and make the dauer or reproduction decision (9, 6). Food signal promotes reproductive development, but the specific component of food that the animals are sensing is still unknown. Pheromone is an indicator of crowding (9). Dauer pheromone promotes dauer formation, and its several dauer-inducing components have been identified, including ascarosides: ascr#1, ascr#2, ascr#3, ascr#5, ascr#8, and indolecarboxy ascaroside icas#9 (10–12). The difference in the side chains attached to the sugar ascarylose base make different ascrosides distinct both structurally and functionally (13). While ascr#2 and ascr#3 are the most potent ones, ascr#8 can enhance their effect on dauer induction even more (14). The complex composition of dauer pheromone and the synergistic effect of ascarosides suggest there might be multiple

receptors mediating pheromone sensation. Increased temperature can also input into dauer decision by enhancing pheromone-induced dauer formation (6), suggesting the modulatory role of temperature. The importance of temperature is also highlighted by the finding that the population density of *C. elegans* in the wild and the dauer dispersal behavior are season dependent (15, 16).

C. elegans perceive environmental inputs through their amphid chemosensory organ, which includes 12 pairs of chemosensory neurons (ADF, ADL, AFD, ASE, ASG, ASH, ASI, ASJ, ASK, AWA, AWB, and AWC) (17). Through cell ablation experiments using a laser microbeam, the importance of four of the pairs in dauer decision were revealed. ADF, ASG, and ASI, were identified to inhibit dauer formation in favorable conditions (18); ASJ, on the contrary, functions to promote dauer formation in dauer-inducing conditions (19). Although how food signals are sensed by *C. elegans* is still not well understood, it was shown that ASI and AWC integrate food availability to regulate dauer decision (20). ASI, along with ASK, were also found to function in ascaroside-mediated dauer induction. G-protein-coupled receptors (GPCRs) SRG-36, SRG-37, and DAF-37 in ASI mediate the perception of ascr#5 and ascr#2 (21, 22), and SRBC-64 and SRBC-66 in ASK detect ascr#1, ascr#2, and ascr#3 (23). Further biochemical analysis on the structure of ascaroside receptors might help reveal how the specific recognition of ascarosides is achieved and expand our understanding on GPCRs in general.

Chemosensory neurons rely the environmental information to the animal through TGF-β and insulin signaling, whose activation promote reproductive and inhibit dauer development. DAF-7/TGF-β ligand is expressed solely in the ASI neurons, and its expression level is downregulated in dauer-inducing conditions (19). In the case of insulin

signaling, *C. elegans* have 40 insulin-like peptides (ILPs) (24, 25) and only one known insulin receptor ortholog, DAF-2 (26), suggesting potential complex patterns of redundancy (27). In fact, there are agonistic and antagonistic DAF-2 ligands regulating dauer decision (28, 29). Agonistic ligands that inhibit dauer formation include INS-6 and DAF-28 from ASI and ASJ, and INS-4 from motor neuron. Dauer-promoting DAF-2 ligands including INS-1 and INS-18 are from sensory neurons, but the specific neurons were not identified. Under favorable condition, high level of agonistic to antagonistic ligands promotes reproductive development. In harsh environment, on the other hand, reduced agonistic and increased antagonistic ligands facilitates animals to become dauers.

The convergent point of TGF-β and insulin signaling is the steroid hormone pathway involving DAF-9 and DAF-12 (30, 31) (Figure 1.2). DAF-9 is a P450 enzyme that synthesize bile acid-like steroids dafachronic acids (DAs), the ligands for the nuclear hormone receptor transcription factor DAF-12 (32, 33). Under favorable condition, the activation of TGF-β and insulin signaling stimulate the production of DAs, and the DA-bounded DAF-12 promote reproductive growth. When the environment is unfavorable, reduced TGF-β and insulin signaling result in unliganded DAF-12, which together with corepressor DIN-1 specify dauer development (34, 35).

The XXX cells are considered to be the integration site of TGF-β, insulin and the steroid hormone pathway for several reasons. First of all, XXX is the main source of *daf-9* expression and thus DA synthesis. *daf-9* expression was observed in only three tissues, XXX, the hypodermis, and the spermatheca (30, 31). While *daf-9* is expressed in XXX expression is at all stages, the hypodermal expression is highly variable depending on the environmental inputs and the spermatheca expression only exists in adult. It was shown

that under favorable condition, DA originating from XXX amplifies the hypodermal *daf-9* expression in a *daf-12* dependent manner, and the positive feedback loop ensure the reproductive development (Figure 1.2) (30, 31, 36). Second, many components involved in dauer regulatory pathways are also expressed in the XXX cells (*e.g. sdf-9*, which regulates both steroid hormone and insulin-like pathways) (37–39), further highlighting the important role of XXX in the decision. Finally, the XXX cells are required for L2d animals to bypass dauer and carry out reproductive development when the environmental condition improves (36). Notably, for L1 animals, the XXX cells are sufficient but not necessary to grow into adult under favorable condition (30, 31, 37), suggesting there might be a compensation mechanism for the loss of the XXX cells at early developmental stage.

Although a wealth of knowledge regarding the molecules and signaling pathways involved in the developmental decision have been accumulated, many aspects of the decision are still not well understood.

At the sensory sensation level, first of all, it was suspected that there might be other environmental inputs controlling dauer decision in addition to food, temperature, and pheromone (40), but no report has proven the idea yet. In the Appendix chapter, we demonstrated for the first time that touch is an overlooked input, and that touch promotes dauer development. One plausible explanation is that touch serves as a population density indicator on top of pheromone. Touch as an input into the dauer decision also opens up the possibility that other environmental signals, such as light, O_2 and CO_2, can also contribute to the developmental choice.

Moreover, it is not clear how the sensory neurons interact with each other. Since ascaroside and food signals have opposing effects on dauer entry decision, do ascaroside-

sensing and food-sensing neurons modulate each other's activity? As food-to-pheromone ratio, rather than their absolute amount, is important for dauer recovery (9), is it possible for dauer entry that the food and pheromone also affect each other's threshold, and that the signals are summed up at an interneuron? Reproductive-promoting insulins were not expressed in the food-sensing neuron AWC, and the pheromone and temperature sensing neurons ASK and AFD were not identified to express *daf-7* or dauer-promoting insulins (19, 20, 28, 29). It is possible that the endogenous genes are actually expressed in those neurons, but because of the promoter region included in the transcriptional reporter, the observed anatomic expression pattern does not completely reflect that of the endogenous gene. In the case that the expression patterns are correct, it then raise the question of how AWC transduce the food information to the TGF-β and insulin signaling neurons, including ASI and ASJ. Similarly, how do ASI and ASJ receive the pheromone and temperature information from ASK and AFD? They might be connected together directly through physical connection, or indirectly through interneurons. We could obtain a more comprehensive understanding of the neuron circuit controlling the information relay by studying the neuronal connections, and genetically or optogenetically manipulating the neuronal activities.

There are also multiple parts unknown at the signaling transduction and integration level. First, while the initial genetic screens looked solely for Daf-c (dauer formation abnormal constitutive) or Daf-d (dauer formation abnormal defective) mutants and identified main components and signaling pathways (41, 42), the studies overlooked the modulators mediating the decision. For example, *daf-28* is the only insulin mutant identified through genetic screen (23, 41), but other insulins were later discovered to play

roles (of smaller effect size) in the decision as well (28, 29). In addition, it is still unclear where the sites of action are for several signaling components. As mentioned above, TGF-β and insulin were observed only in ASI, ASJ, and motor neurons, but not in AWC, ASK or AFD (19, 20, 28, 29). Another example is the insulin receptor DAF-2. Whether DAF-2 acts predominately in nervous system or intestine to regulate the dauer decision is still inconclusive, as different results were reported suggesting one or the other (29, 44, 45). Solving the site of action mystery would improve our understanding of the spatial control of the dauer entry decision.

Although the choice between dauer or reproductive development is considered as a binary decision (36), it in fact requires the coordination across different tissues to execution of the decision. Dauer development involves the remodeling of multiple tissues, including the changes in the cuticle, muscle, nervous system, pharynx, gut, gonad, and excretory system, to meet the specialized physiological and behavioral needs of dauers (46). Partial dauer phenotype describes the mutant dauers that have incomplete or missing dauer features in some of the tissues. For instance, *daf-9(e1406)*/cytochrome P450 dauers have a non-dauer intestine, cuticle, pharynx, and neurons (42). Although studying partial dauer mutants would elucidate how the tissue-tissue signaling ensures the correct remodeling of the whole animal, our knowledge regarding it is still limited due to the limited quantitative tools. The only two available tools are SDS sensitivity and fluorescent beads for identifying dauer hypodermis and pharynx selection (47, 48), but not for other tissues.

In Chapter 2, I describe our findings that the FMRFamide family of neuropeptides helps to improve dauer entry decision-making, possibly at the level of sensory perception and signal integration. Using RNA-seq data collected from dauer- or reproductive-

developing animals, I helped discover 8,042 genes that are differentially expressed between the two developmental tracks. Neuropeptides, in particular the FMRFamide-like peptides (*flp*s), were enriched for up-regulation starting from dauer-commitment. With mutant analysis, I found that several *flp*s have opposing effects on the dauer entry decision, but overall peptidergic signaling (from insulins, *nlp*s, and *flp*s) promotes dauer development.

Understanding how the *flp* gene family is coordinately up-regulation might expand our knowledge of how dauers are programmed transcriptionally. We analyzed promoter regions of the 31 *flp* genes, but we were not able to pinpoint specific *cis*-regulatory elements that are shared within the *flp* gene family. To find upstream regulators might require unbiased genetic screen or biased RNAi screen on transcription factors on animals expressing transcriptional reporter of *flp* genes.

Neuropeptides can act as neurotransmitters that control the activity, polarity, sensitivity and even gene expression of their recipient neurons (49–51). We propose two possible mechanisms for neuropeptides to mediate the dauer decision at the input sensation or signaling integration level. First, neuropeptides might modulate the sensitivity of sensory neurons and thus the animals' perception to the environmental inputs (52, 53). We used a pheromone reporter, whose intensity correlate with the amount of pheromone sensed by the animal (23, 54), to test this hypothesis. Our preliminary data showed that pheromone sensitivity indeed is lower in *sbt-1* mutant, which have reduced levels of active neuropeptides (55) (data not shown), suggesting the modulation of pheromone sensation by neuropeptides. Further imaging analysis of the activity of different sensory neurons is necessary to make a definite conclusion. Second, neuropeptides might influence how TGF-β and insulin signaling are integrated. Previous study suggested that unfavorable

environment might inhibit reproductive development by raising the DA threshold and preventing DA amplification in the hypodermis (36). It is thus conceivable that neuropeptides might modulate XXX cells and set how sensitive it is to TGF-β and insulin signaling, or set the DA threshold in the hypodermis. To test the hypothesis might require direct measurements of XXX activity and DA levels in XXX and hypodermis.

In Chapter 3, I used the RNA-seq dataset that I analyzed in chapter 2 to identify candidate genes to use as molecular markers to selectively label dauers and non-dauers. As discussed above, the tools for identification of dauer tissue remodeling are limited to SDS sensitivity for dauer hypodermis and fluorescent beads for identifying dauer pharynx (47, 48). Through developing molecular markers, we hope to conveniently assay the dauer entry decision, and to parse the subtle phenotypes of partial dauers for better understanding of the coordinately execution of the decision. Indeed, I was able to engineer four markers that label specifically the dauer or reproduction decision, and I verified that the lighting up of the dauer fluorescent markers marks dauer commitment. I also used the markers to manipulate the decision by driving gene overexpression during dauer-commitment. Finally, by combining the markers with partial dauer mutants, I confirmed their physiological defects and uncovered previously unknown defects as well. Previous study suggested that *C. elegans* might take into account the uncertainty of the environment to make the dauer decision, but the idea has not been verified by experiments yet (56). Since the expression of the markers can be a readout of the dauer decision, it is foreseeable to utilize them to study how environmental signals are integrated over time, and how discontinuous inputs might change the dynamics of the dauer decision.

We have only explored the neuropeptide part of the huge RNA-seq dataset, and there is

still a lot of interesting information worth looking into. For instance, we noticed that many GPCRs are highly expressed at the time point preceding dauer, when the expression levels of most neuropeptides are the highest, suggesting a possible anticipatory preparation of receptors for their corresponding ligands. Moreover, studying the transcription factors that are turned on before dauer commitment (*e.g.* at L2d.26 time point) might reveal important control for the commitment decision.

Dauers have specialized behaviors

In addition to the developmental switch, entering dauer switches their behavior as well. Only dauers have the ability to nictate, a hitchhiking behavior where the animals stand on their tail and wave their body , and also only dauers are attracted to CO_2 while non-dauers are repelled by it (57–59). These two dauer-specific behaviors are thought to help dauers find carrier animals and disperse, because dauer, the most common life stage of *C. elegans* found in the wild, are often found to be associated with invertebrates and even inside the intestine of predatory slugs (60, 61).

The molecular basis regulating the nictation behavior in *C. elegans* was not characterized until the recent advance in the design of artificial micro-dirt chip for precise quantification of the behavior (62). The measurements include nication ratio (the percentage of the observation time during which the dauers spend on nictating), initiation index (the frequency the dauers start a new nictation event), and average duration (the average duration of each nictation event). Using this assay, it was shown that insulin, TGF-β, and piRNA pathways are involved in nictation behavior (63, 64). Interestingly, unlike in the dauer entry, insulin and TGF-β signaling control nictation in opposite ways

(63). Moreover, the property of the IL2 neuron are essential for nictation, including its cholinergic transmission and proper dendritic remodeling through proprotein convertase *kpc-1* during dauer (62, 65). As the mechanism controlling nictation started to unfold, there are still many missing pieces. For example, it is not known how the duration of the nictation events is controlled since all the mutants identified in previous studies are defective in only nictation ratio and initiation index. It would also be interesting to pinpoint the new connections downstream of IL2 neuron during dauer to understand how the new behavior is generated.

An animal's response to sensory stimulus can be mediated by developmental stage and life history. For example, *Drosophila melanogaster* larvae and adults showed different preference for certain fruit odors (66). For *C. elegans*, CO_2 is repulsive for non-dauers, but an attractive cue for dauers (Figure 1.3). Since CO_2 can be an environmental signal that indicates the presence of food, carriers, or predators (67, 59, 68), it suggests that dauers might use CO_2 to facilitate dispersal or recovery from dauer despite the potential risks. The CO_2 preference change was also observed in adult animals depending on their nutritional status and prior experience. The CO_2 avoidance is suppressed in food-deprived adults via insulin and TGF-β signaling (57, 58). Adults that were cultivated in higher CO_2 are attracted to as opposed to repelled by CO_2, and the preference and degree of change is mediated by the activity of four interneurons and a combination of neuropeptides (69).

Despite our understanding of the context-dependent modulation of CO_2 preference, how developmental stage switches the response to the same CO_2 stimulus in *C. elegans* is still not clear. Interestingly, a single pair of sensory neurons, the BAG neurons, is necessary for CO_2-sensing in both dauer and non-dauer (56, 57), suggesting that the CO_2 responses in

dauer and non-dauer might mediated by the distinct signals from the BAG neurons. Two simple hypotheses are that the BAG neurons secrete different molecules, or the BAG neurons have different downstream neuronal circuit connections in dauer compared to non-dauer animals. More investigations of the mechanism would provide a deeper insight of how neuronal plasticity can be engaged under stress.

In Chapter 2, I describe our findings that the FMRFamide family of neuropeptides helps enable hitchhiking/carrier-seeking behaviors (70). Using the micro-dirt chip, I observed a less vigorous nictation movement and as a result a longer nictation duration in *sbt-1* mutant compared to wild type animals. Although it might require an additional tool, such as movement tracking and nictation angle analysis, to fully capture and describe the phenotype, and it was the first mutant reported to have nictation duration defect. I also found that peptidergic signaling downstream of *sbt-1* is necessary for dauer CO_2 chemoattraction, and to our knowledge, *sbt-1* mutant was the first reported *C. elegans* duaer that avoid CO_2 like adults. Moving forward, it would be intriguing to find out how neuropeptide signaling changes the neuronal properties in dauer using calcium imaging. The change in physical connections between neurons in dauer might also contribute to the acquisition of new behaviors in dauer. As the techniques for identifying synaptic partners in living animals are advancing (71, 72), and the dauer neuronal connectome is being constructed (Mei Zhen, personal communication), a great progress in the field is conceivable.

Dauers and IJs

Dauer and the infective juvenile (IJ) stage of many parasitic nematodes are both

non-feeding and similar in morphologically (73). Therefore, it has been hypothesized that the evolution of dauer is a pre-adaption toward developing parasitism (Figure 1.4) (74, 75). The close association of nematodes with non-specific insects or invertebrate, like the hitchhiking behavior in *C. elegan*s dauer, is considered phoresy (76). In some species when the association becomes more specific, the dauers would wait for the host species to die and feed on their carcass, and it is considered necromeny (76). The relationship eventually evolved into parasitism, where the association becomes harmful for the host. The molecular similarities in regulating dauer and IJ formation have also been identified, including sensory neuroanatomy, insulin signaling, steroid hormone pathway and *daf-12* (77).

In Chapter 2, through meta-analysis, I helped discover the similar up-regulation of *flp*s in IJ stages of several parasitic nematodes, including semiobligate and obligate parasites, revealing the potential shared strategy for carrier-seeking in dauer and host-seeking in IJs. As more tools for genetic intervention, such as RNAi and CRISPR, are being developed in parasitic nematodes (78, 79), it will be possible to test the function of the neuropeptides in host-seeking in parasites and potentially develop *sbt-1* as an anthelminthic target.

Since neuropeptides, which function in modulating behaviors, can evolve over time (80, 81), it is conceivable that neuropeptide expansion could be important for the evolution of behavior. For example, the acquisition of jumping behavior in *Steinernema carpocapsae* IJ might involve neuropeptides for changing the wiring between the motor neuron and CO_2 neurons to achieve a different dynamic (59). Neuropeptides can also mediate the sensing of the internal state through connecting the intestine, to sensory, inner and motor neurons (82). All those changes could affect how active and how quickly dauers and IJs burn through their fat stores, considering the tradeoff and balance between

hibernating and actively trying to find carriers and hosts.

The study of stress in other nematodes

Extremophiles organisms have revealed much about the biology of stress-resistance, re-defined the limits of life, and have been useful to biotechnology. For example, from studying antioxidant defense in the African lungfish *Protopterus dolloi* during their stress-resistant estivation period, we have learned how human brains deal with the increasing oxidative stress associated with aging (83). Moreover, the heat-stable DNA polymerase isolated from the thermophile *Thermus aquaticus* is widely used for efficient DNA amplification in polymerase chain reactions (PCR) (84).

Nematodes have been found in a variety of hostile environments, including deep underground diamond mines (85), extreme arid soil (86), and frozen Antarctic water (87). They were even found alive after being frozen for 30,000 to 40,000 years (88). Those findings represent a fertile ground for further exploring stress response in nematodes and plasticity and resilience to stress. Especially because the stress-resistant dauer stage of *C. elegans* is well characterized (35), studying the nematodes isolated from extreme environments offer an opportunity to apply the good lessons and methodology learned from dauers to learn novel biology.

I was interested in exploring natural environmental stresses—outside of the laboratory. In Chapter 4, I describe hunting for extremophile nematodes in and around Mono Lake, an environment that is high in pH, salt and arsenic. I helped isolate and characterize nine new nematode species from the extreme environment. The diverse morphologies of the species suggest that nematodes have adapted to Mono Lake via diverse lifestyles. I also found that

Auanema tufa, which is lab-culturable, could be a potential model for studying arsenic resistance in a multicellular organism.

One of the exciting future direction is to sequence the genome of *A. tufa* and find the genes that contribute to the arsenic resistance in *A. tufa*. Especially because *A. tufa* is possibly hermaphroditic and culturable in lab, it would be easier to single out individual animal, drive the genome into homozygosity, and assemble the genome. Once we have the genome assembled, it would be interesting to look for potential gene duplication in genes important for *C. elegans* arsenic resistance. For example, there might be duplications of *gcs-1* genes, which catalyze the redox reaction of arsenic and facilitate the expel of arsenic outside of the cell (89).

Summary

When I began my PhD, the molecular correlates of the dauer commitment decision were unknown. How the tissues coordinate during the dauer entry decision was also unknown. And importantly, how dauers switch their behaviors was only partially known, in the case of the neuronal rewiring (of the IL2 neuron) that underlies nictation (65).

During my PhD, my contribution to the field is a better understanding of how *C. elegans* establishes a "new brain" to cope with stress through neuropeptide signaling. Moreover, the molecular tools I built not only open up a new way of studying and manipulating dauer entry decision, but also provide a quantitative assay for studying tissue-tissue communication in executing the whole animal developmental decision. and how nematodes have evolved to survive in harsh environments.

1.2 Figures

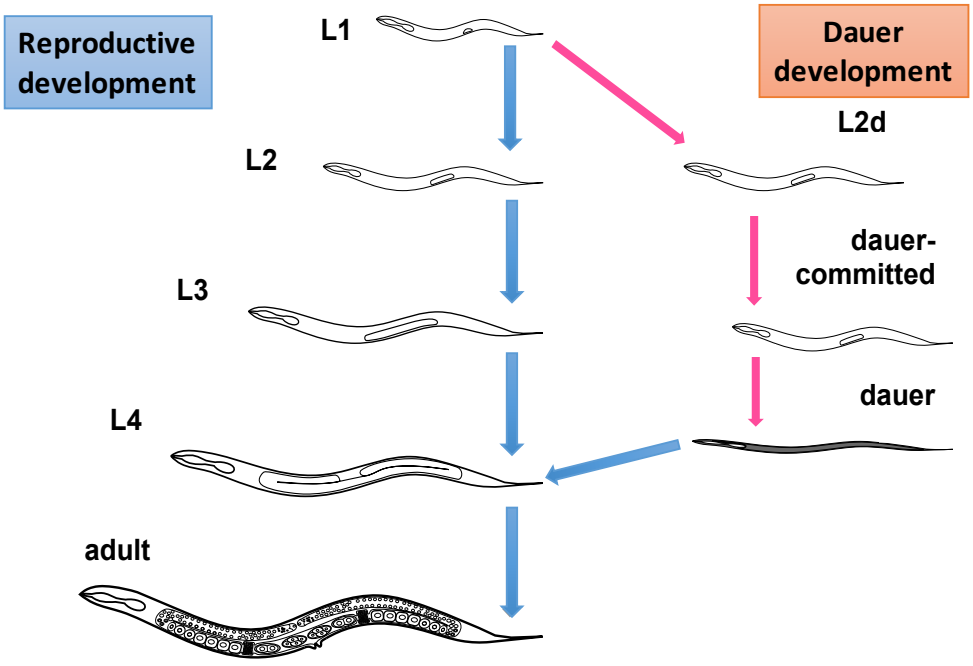

Figure 1.1. Two developmental trajectories in *C. elegans*. The blue and red arrows indicate the reproductive or dauer developmental trajectories under favorable or unfavorable conditions, respectively.

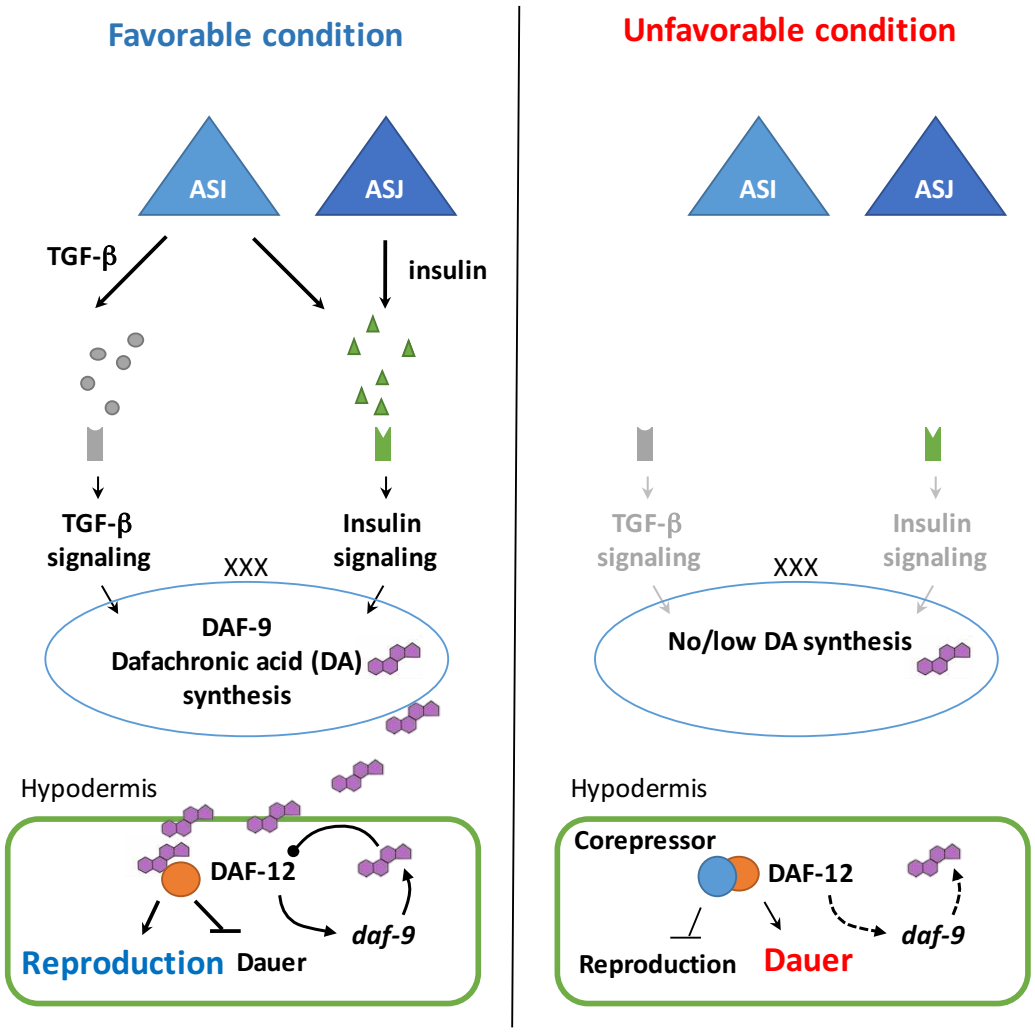

Figure 1.2. The major signaling pathways involved in reproduction and dauer developmental decision. Dafachronric acid (DA) is shown in its chemical structure in purple. Dash arrows represent reduction, and the oval arrow indicates the binding of DA to DAF-12. For simplicity, only two of the sensory neurons, ASI and ASJ, are shown.

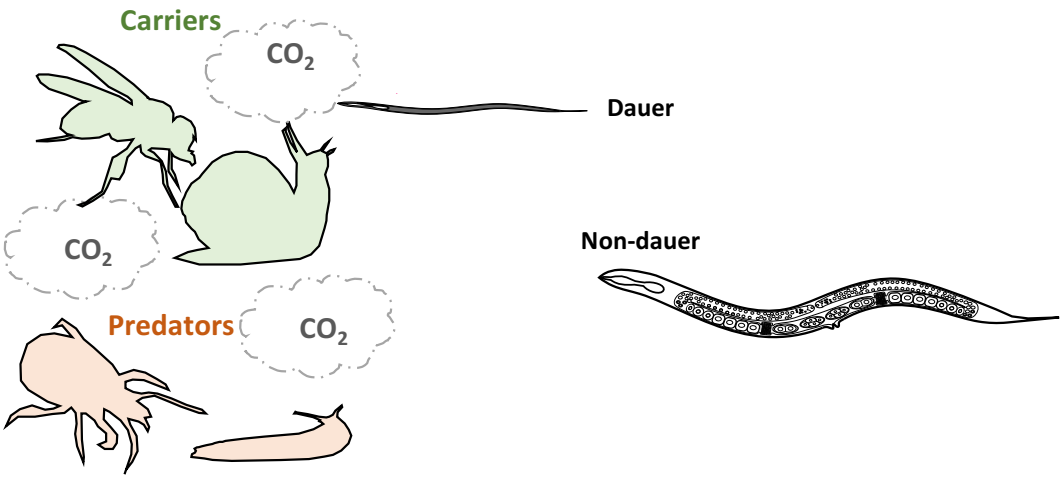

Figure 1.3. The differential CO_2 preference in *C. elegans* dauer and non-dauer. A fly and snail shown in green are potential carrier animals, and a mite and slug shown in orange are potential predators of *C. elegans*.

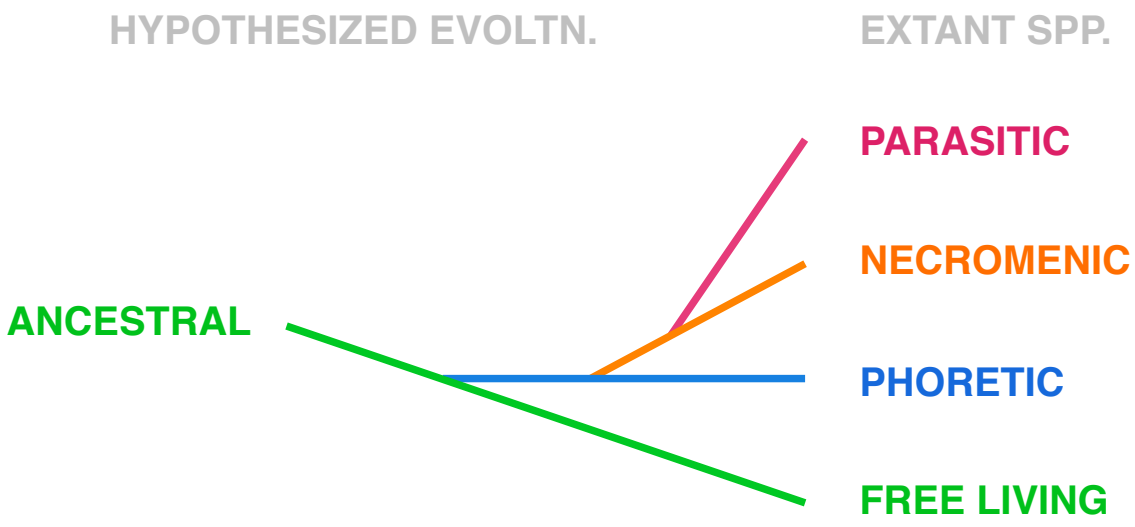

Figure 1.4 The hypothesized evolution of parasitism

1.3 References

1. Agrawal AA (2001) Phenotypic Plasticity in the Interactions and Evolution of Species. *Science* 294(5541):321–326.

2. Pfennig DW, Reeve HK, Sherman PW (1993) Kin recognition and cannibalism in spadefoot toad tadpoles. *Animal Behaviour* 46(1):87–94.

3. Fusco G, Minelli A (2010) Phenotypic plasticity in development and evolution: facts and concepts. Introduction. *Philos Trans R Soc Lond, B, Biol Sci* 365(1540):547–556.

4. Riddle DL, Albert PS (1997) Genetic and environmental regulation of dauer larva development. *C. Elegans II*, eds Riddle DL, Blumenthal T, Meyer BJ, Priess JR (Cold Spring Harbor (NY)). 2nd Ed.

5. Vanfleteren JR, Braeckman BP (1999) Mechanisms of life span determination in Caenorhabditis elegans. *Neurobiol Aging* 20(5):487–502.

6. Golden JW, Riddle DL (1984) The Caenorhabditis elegans dauer larva: developmental effects of pheromone, food, and temperature. *Dev Biol* 102(2):368–378.

7. Vowels JJ, Thomas JH (1992) Genetic analysis of chemosensory control of dauer formation in Caenorhabditis elegans. *Genetics* 130(1):105–23.

8. Sommer RJ, Ogawa A (2011) Hormone signaling and phenotypic plasticity in nematode development and evolution. *Current biology : CB* 21(18):R758-66.

9. Golden JW, Riddle DL (1982) A pheromone influences larval development in the nematode Caenorhabditis elegans. *Science* 218(4572):578–80.

10. Jeong P-Y, et al. (2005) Chemical structure and biological activity of the Caenorhabditis elegans dauer-inducing pheromone. *Nature* 433(7025):541–545.

11. Butcher RA, Fujita M, Schroeder FC, Clardy J (2007) Small-molecule pheromones that control dauer development in Caenorhabditis elegans. *Nat Chem Biol* 3(7):420–422.

12. Butcher RA, Ragains JR, Clardy J (2009) An indole-containing dauer pheromone component with unusual dauer inhibitory activity at higher concentrations. *Org Lett* 11(14):3100–3103.

13. Ludewig AH, Schroeder FC (2013) Ascaroside signaling in C. elegans. *WormBook*:1–22.

14. Pungaliya C, et al. (2009) A shortcut to identifying small molecule signals that regulate behavior and development in Caenorhabditis elegans. *Proc Natl Acad Sci USA* 106(19):7708–7713.

15. Frézal L, Félix M-A (2015) C. elegans outside the Petri dish. *Elife* 4. doi:10.7554/eLife.05849.

16. Kaplan F, et al. (2012) Interspecific nematode signals regulate dispersal behavior. *PLoS ONE* 7(6):e38735.

17. Inglis PN, Ou G, Leroux MR, Scholey JM (2007) The sensory cilia of Caenorhabditis elegans. *WormBook*:1–22.

18. Bargmann CI; H HR (1991) Control of Larval Development by Chemosensory Neurons in Caenorhabditis elegans. *Science* 251:1243–1246.

19. Schackwitz WS, Inoue T, Thomas JH (1996) Chemosensory neurons function in parallel to mediate a pheromone response in C. elegans. *Neuron* 17(4):719–728.

20. Neal SJ, et al. (2015) Feeding state-dependent regulation of developmental plasticity via CaMKI and neuroendocrine signaling. *Elife* 4. doi:10.7554/eLife.10110.

21. McGrath PT, et al. (2011) Parallel evolution of domesticated Caenorhabditis species targets pheromone receptor genes. *Nature* 477(7364):321–325.

22. Park D, et al. (2012) Interaction of structure-specific and promiscuous G-protein-coupled receptors mediates small-molecule signaling in Caenorhabditis elegans. *Proc Natl Acad Sci USA* 109(25):9917–9922.

23. Kim K, et al. (2009) Two chemoreceptors mediate developmental effects of dauer pheromone in C. elegans. *Science* 326(5955):994–998.

24. Pierce SB, et al. (2001) Regulation of DAF-2 receptor signaling by human insulin and ins-1, a member of the unusually large and diverse C. elegans insulin gene family. *Genes Dev* 15(6):672–686.

25. Li W, Kennedy SG, Ruvkun G (2003) daf-28 encodes a C. elegans insulin superfamily member that is regulated by environmental cues and acts in the DAF-2 signaling pathway. *Genes Dev* 17(7):844–858.

26. Kimura KD, Tissenbaum HA, Liu Y, Ruvkun G (1997) daf-2, an insulin receptor-like gene that regulates longevity and diapause in Caenorhabditis elegans. *Science* 277(5328):942–946.

27. Ritter AD, et al. (2013) Complex expression dynamics and robustness in C. elegans insulin networks. *Genome Res* 23(6):954–965.

28. Cornils A, Gloeck M, Chen Z, Zhang Y, Alcedo J (2011) Specific insulin-like peptides encode sensory information to regulate distinct developmental processes. *Development* 138(6):1183–1193.

29. Hung WL, Wang Y, Chitturi J, Zhen M (2014) A Caenorhabditis elegans developmental decision requires insulin signaling-mediated neuron-intestine communication. *Development* 141(8):1767–1779.

30. Gerisch B, Antebi A (2004) Hormonal signals produced by DAF-9/cytochrome P450 regulate C. elegans dauer diapause in response to environmental cues. *Development* 131(8):1765–1776.

31. Mak HY, Ruvkun G (2004) Intercellular signaling of reproductive development by the C. elegans DAF-9 cytochrome P450. *Development* 131(8):1777–1786.

32. Motola DL, et al. (2006) Identification of ligands for DAF-12 that govern dauer formation and reproduction in C. elegans. *Cell* 124(6):1209–23.

33. Mahanti P, et al. (2014) Comparative Metabolomics Reveals Endogenous Ligands of DAF-12, a Nuclear Hormone Receptor, Regulating C. elegans Development and Lifespan. *Cell Metabolism* 19(1):73–83.

34. Hu PJ (2007) Dauer. *WormBook*:1–19.

35. Fielenbach N, Antebi A (2008) C. elegans dauer formation and the molecular basis of plasticity. *Genes Dev* 22(16):2149–2165.

36. Schaedel ON, Gerisch B, Antebi A, Sternberg PW (2012) Hormonal signal amplification mediates environmental conditions during development and controls an irreversible commitment to adulthood. *Plos Biology* 10(4). doi:10.1371/journal.pbio.1001306.

37. Ohkura K, Suzuki N, Ishihara T, Katsura I (2003) SDF-9, a protein tyrosine phosphatase-like molecule, regulates the L3/dauer developmental decision through hormonal signaling in C. elegans. *Development* 130(14):3237–3248.

38. Li J, Brown G, Ailion M, Lee S, Thomas JH (2004) NCR-1 and NCR-2, the C. elegans homologs of the human Niemann-Pick type C1 disease protein, function upstream of DAF-9 in the dauer formation pathways. *Development* 131(22):5741–5752.

39. Hu PJ, Xu J, Ruvkun G (2006) Two membrane-associated tyrosine phosphatase homologs potentiate C. elegans AKT-1/PKB signaling. *PLoS Genet* 2(7):e99.

40. Karp X (2018) Working with dauer larvae. *WormBook*:1–19.

41. Riddle DL, Swanson MM, Albert PS (1981) Interacting genes in nematode dauer larva formation. *Nature* 290(5808):668–671.

42. Albert PS, Riddle DL (1988) Mutants of Caenorhabditis elegans that form dauer-like larvae. *Developmental biology* 126(2):270–93.

43. Malone EA, Thomas JH (1994) A screen for nonconditional dauer-constitutive mutations in Caenorhabditis elegans. *Genetics* 136(3):879–886.

44. Apfeld J, Kenyon C (1998) Cell nonautonomy of C. elegans daf-2 function in the regulation of diapause and life span. *Cell* 95(2):199–210.

45. Wolkow CA, Kimura KD, Lee MS, Ruvkun G (2000) Regulation of C. elegans life-span by insulinlike signaling in the nervous system. *Science* 290(5489):147–150.

46. Androwski RJ, Flatt KM, Schroeder NE (2017) Phenotypic plasticity and remodeling in the stress-induced Caenorhabditis elegans dauer. *Wiley interdisciplinary reviews Developmental biology* 6(5). doi:10.1002/wdev.278.

47. Cassada RC, Russell RL (1975) The dauerlarva, a post-embryonic developmental variant of the nematode Caenorhabditis elegans. *Developmental biology* 46(2):326–42.

48. Nika L, Gibson T, Konkus R, Karp X (2016) Fluorescent Beads Are a Versatile Tool for Staging Caenorhabditis elegans in Different Life Histories. *G3* 6(7):1923–33.

49. Nusbaum MP, Blitz DM, Swensen AM, Wood D, Marder E (2001) The roles of co-transmission in neural network modulation. *Trends Neurosci* 24(3):146–154.

50. Salio C, Lossi L, Ferrini F, Merighi A (2006) Neuropeptides as synaptic transmitters. *Cell Tissue Res* 326(2):583–598.

51. Rojo Romanos T, Petersen JG, Pocock R (2017) Control of Neuropeptide Expression by Parallel Activity-dependent Pathways in Caenorhabditis elegans. *Sci Rep* 7:38734.

52. Russo AF (2017) Overview of Neuropeptides: Awakening the Senses? *Headache* 57 Suppl 2:37–46.

53. Morris R, et al. (2017) A neuropeptide modulates sensory perception in the entomopathogenic nematode Steinernema carpocapsae. *PLoS Pathog* 13(3):e1006185.

54. Peckol EL, Troemel ER, Bargmann CI (2001) Sensory experience and sensory activity regulate chemosensory receptor gene expression in Caenorhabditis elegans. *Proceedings of the National Academy of Sciences of the United States of America* 98(20):11032–8.

55. Husson SJ, Schoofs L (2007) Altered neuropeptide profile of Caenorhabditis elegans lacking the chaperone protein 7B2 as analyzed by mass spectrometry. *Febs Letters* 581(22):4288–4292.

56. Avery L (2014) A model of the effect of uncertainty on the C elegans L2/L2d decision. *PLoS ONE* 9(7):e100580.

57. Bretscher AJ, Busch KE, Bono M de (2008) A carbon dioxide avoidance behavior is integrated with responses to ambient oxygen and food in Caenorhabditis elegans. *PNAS* 105(23):8044–8049.

58. Hallem EA, Sternberg PW (2008) Acute carbon dioxide avoidance in Caenorhabditis elegans. *Proceedings of the National Academy of Sciences of the United States of America* 105(23):8038–43.

59. Hallem EA, et al. (2011) A sensory code for host seeking in parasitic nematodes. *Current biology : CB* 21(5):377–83.

60. Felix MA, Braendle C (2010) The natural history of Caenorhabditis elegans. *Current biology : CB* 20(22):R965-9.

61. Schulenburg H, Félix M-A (2017) The Natural Biotic Environment of Caenorhabditis elegans. *Genetics* 206(1):55–86.

62. Lee H, et al. (2011) Nictation, a dispersal behavior of the nematode Caenorhabditis elegans, is regulated by IL2 neurons. *Nature neuroscience* 15(1):107–12.

63. Lee D, Lee H, Kim N, Lim DS, Lee J (2017) Regulation of a hitchhiking behavior by neuronal insulin and TGF-β signaling in the nematode Caenorhabditis elegans. *Biochem Biophys Res Commun* 484(2):323–330.

64. Lee D, et al. (2017) The genetic basis of natural variation in a phoretic behavior. *Nat Commun* 8(1):273.

65. Schroeder NE, et al. (2013) Dauer-specific dendrite arborization in C. elegans is regulated by KPC-1/Furin. *Current biology : CB* 23(16):1527–35.

66. Dweck HKM, et al. (2018) The Olfactory Logic behind Fruit Odor Preferences in Larval and Adult Drosophila. *Cell Reports* 23(8):2524–2531.

67. Scott K (2011) Out of thin air: sensory detection of oxygen and carbon dioxide. *Neuron* 69(2):194–202.

68. Ma DK, Ringstad N (2012) The neurobiology of sensing respiratory gases for the control of animal behavior. *Front Biol* 7(3):246–253.

69. Guillermin ML, Carrillo MA, Hallem EA (2017) A Single Set of Interneurons Drives Opposite Behaviors in C. elegans. *Curr Biol* 27(17):2630-2639.e6.

70. Lee JS, et al. (2017) FMRFamide-like peptides expand the behavioral repertoire of a densely connected nervous system. *Proceedings of the National Academy of Sciences of the United States of America* 114(50):E10726–E10735.

71. Feinberg EH, et al. (2008) GFP Reconstitution Across Synaptic Partners (GRASP) defines cell contacts and synapses in living nervous systems. *Neuron* 57(3):353–363.

72. Desbois M, Cook SJ, Emmons SW, Bülow HE (2015) Directional Trans-Synaptic Labeling of Specific Neuronal Connections in Live Animals. *Genetics* 200(3):697–705.

73. Viney ME (2009) How did parasitic worms evolve? *Bioessays* 31(5):496–499.

74. Barriere A, Felix MA (2005) Natural variation and population genetics of Caenorhabditis elegans. *WormBook : the online review of C elegans biology*:1–19.

75. Hong RL, Sommer RJ (2006) Pristionchus pacificus: a well-rounded nematode. *Bioessays* 28(6):651–659.

76. Kiontke K, Sudhaus W (2006) Ecology of Caenorhabditis species. *WormBook*:1–14.

77. Crook M (2014) The dauer hypothesis and the evolution of parasitism: 20 years on and still going strong. *International journal for parasitology* 44(1):1–8.

78. Ward JD (2015) Rendering the Intractable More Tractable: Tools from Caenorhabditis elegans Ripe for Import into Parasitic Nematodes. *Genetics* 201(4):1279–1294.

79. Gang SS, et al. (2017) Targeted mutagenesis in a human-parasitic nematode. *PLoS Pathog* 13(10):e1006675.

80. Li C, Kim K (2014) Family of FLP Peptides in Caenorhabditis elegans and Related Nematodes. *Front Endocrinol (Lausanne)* 5:150.

81. Li C, Kim K (2008) Neuropeptides. *WormBook*:1–36.

82. Lin X, et al. (2015) Neuropeptide Y genotype, central obesity, and abdominal fat distribution: the POUNDS LOST trial. *Am J Clin Nutr* 102(2):514–519.

83. Garbarino VR, Orr ME, Rodriguez KA, Buffenstein R (2015) Mechanisms of oxidative stress resistance in the brain: Lessons learned from hypoxia tolerant extremophilic vertebrates. *Archives of biochemistry and biophysics* 576:8–16.

84. Saiki RK, et al. (1988) Primer-directed enzymatic amplification of DNA with a thermostable DNA polymerase. *Science* 239(4839):487–91.

85. Borgonie G, et al. (2015) Deep subsurface mine stalactites trap endemic fissure fluid Archaea, Bacteria, and Nematoda possibly originating from ancient seas. *Frontiers in microbiology* 6:833.

86. Treonis AM, Wall DH (2005) Soil nematodes and desiccation survival in the extreme arid environment of the antarctic dry valleys. *Integrative and comparative biology* 45(5):741–50.

87. Wharton D, Ferns D (1995) Survival of intracellular freezing by the Antarctic nematode Panagrolaimus davidi. *The Journal of experimental biology* 198(Pt 6):1381–7.

88. Shatilovich AV, et al. (2018) Viable Nematodes from Late Pleistocene Permafrost of the Kolyma River Lowland. *Doklady biological sciences : proceedings of the Academy of Sciences of the USSR, Biological sciences sections* 480(1):100–102.

89. Liao VH-C, Yu C-W (2005) Caenorhabditis elegans gcs-1 confers resistance to arsenic-induced oxidative stress. *Biometals* 18(5):519–528.

C h a p t e r 2

FMRFAMIDE-LIKE PEPTIDES EXPAND THE BEHAVIORAL REPERTOIRE OF A DENSELY CONNECTED NERVOUS SYSTEM

Lee JS*, **Shih PY***, Schaedel ON, Quintero-Cadena P, Rogers AK and Sternberg PW (2017) FMRFamide-like peptides expand the behavioral repertoire of a densely connected nervous system. *Proceedings of the National Academy of Sciences USA* 114(50): E10726-E10735. doi: 10.1073/pnas.1710374114
*Equal contribution

2.1 Abstract

Animals, including humans, can adapt to environmental stress through phenotypic plasticity. The free-living nematode *Caenorhabditis elegans* can adapt to harsh environments by undergoing a whole-animal change, involving exiting reproductive development and entering the stress-resistant dauer larval stage. The dauer is a dispersal stage with dauer-specific behaviors for finding and stowing onto carrier animals, but how dauers acquire these behaviors, despite having a physically limited nervous system of 302 neurons, is poorly understood. We compared dauer and reproductive development using whole-animal RNA-seq at fine time points, and at sufficient depth to measure transcriptional changes within single cells. We detected 8,042 differentially expressed genes during dauer and reproductive development, and observed striking up-regulation of neuropeptide genes during dauer entry. We knocked down neuropeptide processing using *sbt-1* mutants, and demonstrate that neuropeptide signaling promotes the decision to enter dauer over reproductive development. We also demonstrate that during dauer, neuropeptides modulate the dauer-specific nictation behavior (carrier animal-hitchhiking), and is necessary for switching from repulsion to CO_2 (a carrier animal cue) in non-dauers to CO_2 attraction in dauers. We tested individual neuropeptides using CRISPR knockouts and existing strains, and demonstrate that the combined effects of *flp-10* and *flp-17* mimic the effects of *sbt-1* on nictation and CO_2 attraction. Through meta-analysis, we discovered similar up-regulation of neuropeptides in the dauer-like infective juveniles of diverse parasitic nematodes, suggesting the anti-parasitic target potential of SBT-1. Our findings reveal that under stress, increased neuropeptide signaling in *C. elegans* enhances their decision-making accuracy, and expands their behavioral repertoire.

2.2 Introduction

Stress during development can have long-lasting effects on animal physiology and behavior. For instance, trauma during early human childhood can lead to difficulties with coping against depression and anxiety in adults (1-4). Phenotypic plasticity allows animals to adapt to stresses from the environment (5). Examples of phenotypic plasticity include the production of new antibodies by the mammalian immune system (6), temperature-dependent sex determination in reptiles (7, 8), and crowding-induced cannibalism in the spadefoot toad (5, 9).

The free-living bacterivore *Caenorhabditis elegans* can adapt to stressful conditions by exiting reproductive development and entering the stress-resistant dauer larval stage (10-12). In reproductive development, *C. elegans* develops through four larval stages (L1, L2, L3, and L4) to become a reproductive adult. Declining food, temperature, and crowding conditions, however, promote L1 entry into pre-dauer L2d. If conditions improve, L2d commit to reproductive development through amplification of dafachronic acid growth hormone across the animal body (13). Unimproved conditions cause L2d to commit to dauer development, through a process that is not well understood. Following this event, L2d larvae molt into dauer larvae and halt their feeding.

Dauers are less metabolically active than non-dauers, and can survive long periods of starvation by utilizing stored lipids, in lieu of aerobic respiration (14, 15). Morphologically, they have a highly impermeable cuticle that allows them to resist environmental assaults (10). In addition, they have a rewired nervous system (16, 17), and specialized dispersal behaviors for finding and stowing onto carrier animals (18, 19).

Dauer lifespans are ten times longer than those of non-dauers (20), and dauers can resume reproductive development with an unaffected adult lifespan once they recover under favorable conditions (21). Thus, dauers have much to reveal about the biological control of longevity, stress-resistance, and neural state.

The genetic and anatomical tractability of *C. elegans* make it an advantageous model for studying phenotypic plasticity in a whole organism. Previous systems-level studies have analyzed the *C. elegans* transcriptome during molt into dauer, during dauer, and during recovery from dauer (22-24). However, the transcriptome of L2d during the dauer entry decision has not been characterized, likely because L2d lack strong distinguishing traits that can be used to isolate them (25). Furthermore, dauer and reproductive development have not been compared under parallel growth conditions, which has limited the discovery of genes that are differentially expressed between the two developments.

Therefore, we have used techniques from our previous analysis of *daf-9(dh6)* loss-of-function animals (13) to add crucial detail to dauer development. Using dafachronic acid, we controlled the developmental decisions of *daf-9(dh6)* L2d, under parallel conditions. We coupled this with our previous timing of *daf-9(dh6)* development to collect pure populations of uncommitted L2d, dauer-committed L2d, L3-committing L2d, dauers, and L4. We performed whole-animal RNA-seq on these populations, revealing 8,042 differentially expressed genes during dauer and reproductive development. Through enrichment analysis, we observed striking up-regulation of neuropeptide genes during dauer-commitment. Using the *sbt-1(ok901)* null mutant to knock down neuropeptide processing (26), we demonstrate that peptidergic signaling promotes the dauer entry

decision, promotes coordination during nictation (a hitchhiking behavior), and is necessary for switching from CO_2 repulsion in non-dauers to CO_2 attraction in dauers.

Testing individual neuropeptides using CRISPR knockouts and existing strains, we demonstrate uncoordinated nictation and CO_2 avoidance phenotypes in *flp-10(n4543) flp-17(n4894)* double mutants, similar to *sbt-1(ok901)*. Through a meta-analysis, we discovered similar up-regulation of neuropeptides in the dauer-like infective juveniles of diverse parasitic nematodes, suggesting the anti-parasitic target potential of SBT-1. Our results reveal that the *C. elegans* nervous system responds to environmental stress by increasing neuropeptide signaling to enhance decision-making, and to enable specialized dispersal behaviors. The expansion of the neuropeptide genes, especially the FMRFamide-like neuropeptide (*flp*) genes, in nematodes has been a puzzle (27, 28), and our results provide one reasonable explanation.

2.3 Results

RNA-seq was used to investigate dauer and reproductive development

Our previous analysis of the *daf-9(dh6)* null mutant in (13) allowed us to sequence cDNA from large quantities of dauer- and reproductive-developing animals. Briefly, *C. elegans* DAF-9 is a cytochrome P450 enzyme that synthesizes the growth hormone dafachronic acid (DA) (29, 30). Commitment to reproductive development only occurs when the level of DA in the animal body is high enough to trigger feedback amplification of DA across the entire organism, thus locking the developmental decision (13). *daf-9(dh6)* null mutants cannot produce their own DA, and therefore constitutively form dauers unless synthetic DA is added to induce reproductive development (13, 30, 31). We previously characterized the timing of development in *daf-9(dh6)* animals: dauer-commitment occurs at 33 hours post hatch (hph), followed by molt into dauer at 48 hph (13). However, if DA is added at 24 hph, *daf-9(dh6)* L2d commit to reproductive development by 27 hph, and molt into L4 at 34 hph.

Using these conditions, we grew synchronized populations of dauer-developing *daf-9(dh6)* by withholding synthetic DA, and we collected L2d animals (at 24 hph and 26 hph), dauer-committed L2d (at 34 hph), and fully developed dauers (at 60 hph) for RNA sequencing (**Figure 2.1A**). In parallel, we added synthetic DA to a sub-culture, forcing it into reproductive development, and from which we collected L3-committing larvae (at 26 hph) and L4 (at 34 hph) for sequencing. We sequenced each sample using two biological replicates, at an average depth of 100 million reads (the sum of the replicates) (**Appendix Table 2.1**). Since *C. elegans* animals contain 959 cells (32), and each cell likely expresses

100,000 mRNA transcripts (33, 34), we estimated that we had sequenced one read for every transcript in the whole animal at each time point. Therefore, we expected to detect signals from transcripts as long as they were not expressed in few cells at low abundance. For each sample, we detected between 20,519 to 22,672 expressed genes, of the total 20,362 coding and 24,719 non-coding genes of the *C. elegans* genome (35, 36) (**Figure 2.2A** and **Appendix Table 2.2**).

PCA analysis revealed the extent of variation between developmental stages

We analyzed the variation between our transcriptomes using principal component analysis (PCA) (**Figure 2.2B-C**). Replicate samples had similar PC scores to each other, indicating that our biological replicates were well correlated in their gene expression. Our analysis also revealed that the largest sources of variation between our transcriptomes were the differences between dauer-commitment/differentiation versus the remaining time points (principal component 1, 65% of overall variation), and the difference between 24 hph L2d and 26 hph L2d (principal component 2, 17% of overall variation). Along the first two principal components, 24 hph L2d and L4 demonstrated close similarity, as did 26 hph L2d and L3-committing larvae, as well as dauer and dauer-committed larvae.

8,042 genes are differentially expressed during dauer and reproductive development

Using the differential gene expression analysis program DESeq (37, 38), we performed pairwise comparisons between 24 hph L2d and 26 hph L2d to identify gene expression changes during L2d sensory integration; between L2d and dauer-committed larvae for changes during dauer-commitment; and between L2d and dauer larvae for changes during

differentiation and maintenance of dauer (**Figure 2.1B**). With our reproductive development samples, we performed pairwise comparisons between L2d and L3-committing larvae for changes during commitment to reproductive development, and between L2d and L4 for changes during reproductive growth. In addition, our design allowed us to perform pairwise comparisons between age-matched dauer- and reproductive-developing animals at 26 hph (L2d versus L3-committing larvae) and 34 hph (dauer-committed larvae versus L4) to identify gene expression changes specific to one developmental track (**Figure 2.1C**). We avoided sequencing an age-matched reproductive sample for 60 hph dauer since reproductive animals at 60 hph are gravid and inappropriate for studying a stage-specific transcriptome. In total, we performed twelve pairwise comparisons between our dauer and reproductive time points. In each comparison, we detected between 484 to 2,276 up-regulated genes, and 280 to 2,824 down-regulated genes (**Figure 2.1D** and **Appendix Table 3**). Overall, we observed 8,042 differentially expressed genes from the twelve comparisons. These genes corresponded to 7,866 coding genes and 77 ncRNA genes, indicating that 39% of the *C. elegans* protein-coding genome is differentially expressed during dauer and reproductive development.

Differential expression was detected at high accuracy and single-cell resolution

To analyze the resolution of our RNA-seq dataset, we used WormBase anatomical-level gene expression data to search our 8,042 differentially expressed genes for genes previously reported to have tissue-specific expression. We detected transcriptional changes in 47 epithelial system genes (of 74 total epithelium-specific genes in WormBase), 56 muscular system genes (of 89 total), 181 alimentary system genes (of 310 total), 108

reproductive system genes (of 233 total), 139 nervous system genes (of 599 total), 9 amphid sensillum genes (of 62 total), and 1 XXX cell gene (of 4 total) (**Figure 2.3A**). This analysis suggests that we could detect differential expression from within tissues and single cells. Indeed, we constructed fluorescent transcriptional reporters for *col-40* and *srt-41*, which were up-regulated in our data during dauer development, and we observed previously unreported, specific expression for the two genes in the hypodermis and the AWC neuron, respectively (**Figure 2.3B-O**).

We examined the accuracy of our dataset by comparing to SAGE data published by Jones, *et al*. (2001), and microarray data published by Wang & Kim (2003), which have identified genes that are enriched in wild type dauers versus mixed-populations or post-dauer adults, respectively (24, 39). When tested for differential expression in our data, 141 (45%) of the dauer-enriched genes from (39) were significantly up-regulated at dauer-commitment and dauer, relative to L2d and L4 (**Figure 2.3P**). Similarly, 312 (69%) of the dauer-enriched genes from (24) were significantly up-regulated at dauer-commitment and dauer. Thus, our calculations for differential expression (negative binomial testing at a Benjamini-Hochberg controlled false discovery rate < 0.01) may have been more stringent than the calculations in (24, 39). Other differences may be explained by gene expression changes that are only observable between dauer and post-dauer, and by differences in the *daf-9(dh6)* strain we used versus the wild type strain. Nonetheless, we conclude from this analysis that *daf-9(dh6)* and wild type transcriptomes demonstrate high comparability, and that our differential expression testing is conservative.

Clustering revealed six common expression profiles during dauer and reproductive development

Soft clustering is a sensitive method for identifying common expression profiles within a dataset (40, 41). We performed soft clustering on our 8,042 differentially expressed genes to group the genes by similarities in their expression profiles. This revealed six clusters (clusters 1-6), indicating that differential gene expression through dauer and reproductive development can be described by six common expression profiles (**Figure 2.4**): the expression levels of 1,102 genes gradually decreased into dauer (cluster 1), 1,921 genes gradually increased into dauer (cluster 2), 1,025 genes increased transiently at 26 hph (cluster 3), 1,497 genes increased transiently during dauer-commitment (cluster 4), 1,332 genes decreased after dauer-commitment (cluster 5), and 1,165 genes increased in L4 (cluster 6) (**Appendix Table 2.4**).

The genes from clusters 2 and 4 encompass 3,418 genes likely involved in commitment, differentiation, and maintenance of dauer. These highly dauer-specific genes represent a 7.6-fold expansion over the 449 'dauer-enriched' genes described previously (24). In addition, the genes from clusters 1, 3, 5, and 6 encompass 4,624 genes whose expressions are largely excluded during dauer-commitment and dauer.

We examined the six clusters for enriched biochemical pathways and gene ontology (GO) terms using KEGG biochemical pathway data (42-44), and the PANTHER Classification System (45). We observed that cluster 1 (genes with decreasing expression into dauer) was enriched for the "peroxisome" KEGG pathway, suggesting that peroxisomal activity is reduced in dauers (**Figure 2.4**). This is consistent with the reduction of ascarocide pheromone production in dauers (46), since a key step of ascarocide

biosynthesis occurs via peroxisomal β-oxidation (47). In fact, cluster 1 contains genes for the β-oxidation enzymes ACOX-1, MAOC-1, and DHS-28, which perform 3 of the 4 steps of ascarocide side chain biosynthesis (47).

Cluster 2 (genes with increasing expression into dauer) was enriched for the "FoxO signaling pathway" and "longevity regulating pathway – worm" KEGG pathways, as may be expected from the extended longevity of dauers (20), and the role of FOXO signaling in modulating longevity and stress resistance (11) (**Figure 2.4** and **Appendix Table 2.4**). We observed 13 members (18%) of the "longevity regulating pathway – worm" in cluster 2, including members in the branches of the pathway that respond to environmental cues, dietary restriction, oxidative stress, germline state, and the mitochondrial unfolded protein response to affect lifespan (42-44). The remaining input into the longevity regulating pathway, the hypoxia branch, did not have any members in cluster 2. This suggests the intriguing possibility that the extreme longevity of dauer arises from the simultaneously enhanced activity of five of the six branches of the longevity pathway.

We also observed enrichment of the "neuropeptide signaling pathway" GO term in cluster 2 (**Figure 2.4**), suggesting that neuropeptides modulate the dauer-commitment decision and/or neural functions downstream of the decision. Indeed, some neuropeptides have been shown to affect dauer biology: insulin signaling via DAF-28, INS-4, and INS-6 promotes reproductive growth over dauer development, and INS-1 and INS-18 antagonize this pathway (reviewed in (48)). In addition, FMRFamide signaling via FLP-18 acts in parallel with the TGF-β signaling pathway to inhibit dauer development (49). Furthermore, *ins-3*, *6*, *18*, *20*, *27-28*, *31*, *34*, and *daf-28* have been shown to affect the fraction of time that is spent nictating in dauer (50).

In cluster 3 (genes with increased expression at 26 hph), we observed enrichment for biomolecule synthesis and turnover pathways, including the "proteasome," "lysosome," "fatty acid degradation," and "fatty acid elongation" KEGG pathways (**Figure 2.4**, **Figure 2.5**, and **Appendix Table 2.4**). This observation may reflect the developmental uncertainty in L2d, and perhaps represents a bet-hedging strategy of cycling biomolecules in preparation for either commitment decision. Consistent with the prediction of developmental uncertainty, genes with the "molting cycle" GO term were enriched (2.9-fold enrichment, $p = 2.54 \times 10^{-14}$) among the genes up-regulated in 26 hph L2d versus 24 hph L2d (**Appendix Table 2.3**), despite molt into dauer, one of the two possible molts from L2d, occurring 22 hours later at 48 hph.

In cluster 4 (genes with increased expression at dauer-commitment), we observed enrichment of the "neuroactive ligand-receptor interaction" and "calcium signaling pathway" KEGG pathways (**Figure 2.4**, **Figure 2.5**, and **Appendix Table 2.4**). Together with cluster 2, this indicates that several genes with neuronal functions have increased expression during dauer-commitment and dauer.

Genes that are down-regulated during dauer-commitment are likely repressed to exclude non-dauer physiologies, and indeed, our enrichment data for cluster 5 (genes with decreased expression after dauer-commitment) are consistent with the reduction of TCA cycle activity in favor of long-term lipid metabolism in dauer (51), as we observed enrichment of the "fatty acid degradation" and "citrate cycle (TCA cycle)" KEGG pathways (**Figure 2.5** and **Appendix Table 2.4**).

Cluster 6 (genes with increased expression at L4) was enriched for terms related to translation and respiration, including the "mitochondrial electron transport, ubiquinol to

cytochrome c" GO term and the "ribosome" KEGG pathway (**Figure 2.4**), which likely reflects growth during reproductive development and gametogenesis in the L4 (52-54).

Differential expression of the neuronal genome during dauer development

Our KEGG and GO enrichment analyses indicated the strong involvement of neuronal effector genes during dauer-commitment and dauer. To investigate this further, we examined the expression of the neuronal genome of *C. elegans* during dauer and reproductive development. The neuronal genome of *C. elegans* encodes 3,114 genes from 30 gene classes, including the calcium channels, neurotransmitters, G protein-coupled receptors (GPCRs), and CO_2 receptors (55). We detected the differential expression of 606 neuronal genes during dauer and reproductive development, corresponding to 19% of the total neuronal genome, with members from all of the 30 gene classes (**Figure 2.6**).

Five gene classes were enriched in one of the soft clusters 1 to 6, indicating that for these classes, a high proportion of their members followed a certain expression profile during dauer and reproductive development (**Appendix Table 2.5**). The extracellular immunoglobulin and leucine rich repeat domain gene class was over-represented in cluster 1 (decreasing expression into dauer), with 2.8-fold enrichment and $p = 6.42 \times 10^{-3}$. The neuropeptide gene class was over-represented in cluster 2 (increasing expression into dauer), with 3.1-FE and $p = 6.32 \times 10^{-21}$. Finally, the GPCR (2.9-FE, $p = 2.41 \times 10^{-8}$), CO_2 and O_2 receptor (4.9-FE, $p = 7.86 \times 10^{-5}$), and potassium channel gene classes (3.0-FE, $p = 2.84 \times 10^{-3}$) were over-represented in cluster 4 (increased expression at dauer-commitment).

GPCR gene expression increases sharply during dauer-commitment, before neuropeptide gene expression reaches its peak during dauer (**Figure 2.6**). In addition, the 34 GPCRs in cluster 4 include 1 biochemically de-orphanized neuropeptide GPCR (*npr-11*) and 9 putative neuropeptide GPCRs (*ckr-1*, *frpr-7*, *-19*, *npr-17*, *-31*, C01F1.4, F13H6.5, Y37E11AL.1, and Y70D2A.1) (27, 55) (**Appendix Table 2.5**). This suggests that neuropeptide receptors are up-regulated during dauer-commitment in anticipation of increasing neuropeptide gene expression during dauer-commitment and dauer.

Notably, the neuropeptide gene class was the only class that was enriched for increasing expression into dauer. We observed extensive up-regulation of the neuropeptides during dauer development: in dauer-commitment (34 hph) versus L2d (24 hph), 60 of the 118 total neuropeptide genes were up-regulated while 9 were down-regulated (**Figure 2.9A**). Similarly, at dauer-commitment (34 hph) versus L4 (34 hph), 43 neuropeptide genes were up-regulated while 10 were down-regulated (**Figure 2.10A**), and in dauer (60 hph) versus L2d (24 hph), 64 neuropeptide genes were up-regulated while 9 were down-regulated (**Figure 2.10B**). The up-regulation of 64 neuropeptide genes during dauer versus L2d is remarkable, as it corresponds to the majority of all neuropeptide genes in the *C. elegans* genome. Furthermore, the 64 genes encode for 215 putative or biochemically isolated peptides (48). By comparison, the human genome contains a total of 97 neuropeptide genes that encode for 270 peptides (56).

Peptidergic signaling downstream of SBT-1 promotes dauer entry and nictation coordination, and is necessary for CO_2 chemoattraction in dauer

Neuropeptides become functional transmitters and neuromodulators only after they are cleaved from longer proneuropeptide chains (48) (**Figure 2.8A**). SBT-1/7B2 is a chaperone for the proprotein convertase EGL-3/PC2, which cleaves proneuropeptides (57), and as a result, *sbt-1*(*ok901*) null mutants have reduced levels of mature neuropeptides compared to wild type (26) (**Figure 2.8B**). Previously, *sbt-1*(*ok901*) mutants were reported to possess aldicarb resistance and extended lifespans (58, 59), but to our knowledge, no functions for *sbt-1* in dauer biology have been reported.

Because we observed up-regulation of neuropeptides starting from dauer commitment, we tested the ability of *sbt-1*(*ok901*) mutants to enter dauer, using crude pheromone to induce dauer entry. Under the same dauer-inducing conditions, wild type animals entered dauer 49% of the time, while *sbt-1*(*ok901*) mutants entered dauer 16.5% of the time (**Figure 2.8C**). We also observed that expressing *sbt-1* genomic DNA in *sbt-1(ok901)* mutants (under the control of the endogenous promoter) rescued the dauer entry phenotype in two independent lines: rescue line 1 entered dauer 46% of the time, and rescue line 2 entered dauer 37% of the time (**Figure 2.8C**). These results suggest that the net effect of peptidergic signaling downstream of SBT-1 promotes dauer entry over reproductive development.

We examined if neuropeptides play a role during dauer, when the majority of the *C. elegans* neuropeptide genes were expressed the highest in our dataset. *C. elegans* dauers have been found to associate with invertebrate carriers, likely for transportation to new niches (60). Nictation, where dauers stand on their tail and wave their body, and CO_2 chemoattraction are two dauer-specific behaviors that likely enable dauers to migrate toward and attach onto carriers (18, 61). We tested *sbt-1*(*ok901*) nictation on micro-dirt

chips, which provide substrates for dauers to nictate on, and observed that the average nictation duration doubled in *sbt-1(ok901)* mutants (μ = 28.90 seconds, max = 139.63 seconds) as compared to wild type (μ = 14.44 s, max = 32.32 s). Moreover, the phenotype was rescued by *sbt-1* genomic DNA expression under the endogenous promoter (line 1: μ = 14.35 s and max = 78.00 s, line 2: μ = 14.50 s and max = 52.27 s) (**Figure 2.8D**). We observed a difference in the degree of three-dimensional movement during nictation in wild type and *sbt-1(ok901)* mutant animals that may explain the increased duration of nictation in *sbt-1(ok901)* mutants: while wild type animals displayed a wide range of motion and fell back to the chip easily, *sbt-1(ok901)* animals displayed a limited range of motion and slow, uncoordinated waving that likely increased stability during nictation (**Appendix Video 2.1** and **2.2**). We did not observe significant differences in other components of the nictation behavior, such as initiation frequency and the proportion of time spent nictating (19) (**Figure 2.7A-B)**.

CO_2 has been shown to be attractive to dauers and replusive to non-dauers (18, 62). Using chemotaxis assays, we observed attraction to CO_2 in wild type dauers (chemotaxis index = 0.59) and repulsion to CO_2 in *sbt-1(ok901)* dauers (chemotaxis index = -0.53) (**Figure 2.8E**). We further performed CO_2 acute avoidance assays by delivering CO_2 directly to the nose of forward-moving dauers and scoring reversal. While wild type dauers did not avoid CO_2 (avoidance index = -0.11), we observed rapid reversal in *sbt-1(ok901)* mutants in response to CO_2 (avoidance index = 0.64). In addition, the CO_2 repulsion phenotype of *sbt-1(ok901)* was rescued by *sbt-1* genomic DNA (line 1: avoidance index = 0.04, line 2: avoidance index = 0.06) (**Figure 2.8F** and **Appendix Video 2.3-2.6**). Together, our results indicate that the neuropeptides downstream of SBT-1 modulate

proper nictation coordination, and are necessary for the correct CO_2 preference switch from aversion in non-dauers to attraction in dauers. To our knowledge, we have reported for the first time the genetic control of the CO_2 preference switch in dauer.

The 31-gene *flp* family is coordinately up-regulated during dauer development

The *C. elegans* genome encodes for three families of neuropeptides: the FMRFamide-like peptides (31 *flp* genes), the insulin related peptides (40 *ins* genes) and the neuropeptide-like proteins (47 *nlp* genes) (48). In dauer-commitment versus L2d, we observed the up-regulation of almost all of the *flp* genes, with significant increases in expression for *flp-1-2*, *4-9*, *11-22*, *24-28*, and *32-34* (28 of 31 total) (**Figure 2.9A** and **Appendix Table 2.3**). In contrast, a smaller proportion of *ins* and *nlp* genes were up-regulated during dauer-commitment versus L2d: *ins-1*, *17-18*, *24*, *28*, *30*, and *daf-28* (7 of 40 total); and *nlp-1-3*, *6*, *8-15*, *17-18*, *21*, *35*, *37-38*, *40-42*, *47*, *ntc-1*, *pdf-1*, and *snet-1* (25 of 47). Similar results were observed during dauer-commitment versus L4 (**Figure 2.10A**), and dauer versus L2d (**Figure 2.10B**). Therefore, the *flp* genes, more than the *ins* or *nlp* genes, are coordinately up-regulated during dauer development.

We quantified this coordination in *flp* gene expression by pairing every combination of the 31 *flp* genes and scoring the correlation between the expression of each pair of genes across our RNA-seq dataset. The average correlation score between the *flp* genes was 0.88, with possible scores ranging from -1 (perfectly anti-correlated) to 1 (perfectly correlated) (**Figure 2.9B**). By comparison, the average correlation scores for random sets of 31 genes (mimicking the size of the *flp* family) were distributed around a bootstrapped mean of 0.02. In addition, the *ins* and *nlp* genes had an average score of 0.21 and 0.28, respectively.

Furthermore, we obtained similar results when we expanded our correlation analysis to include expression data from 246 publically available RNA-seq datasets describing a broad range of *C. elegans* life stages and experimental conditions (23) (**Figure 2.10C-D**). Using dotplot analysis (63), we examined whether the 31 *flp* genes share regions of sequence similarity (**Figure 2.10E**). We observed that there are no regions of shared sequence among the *flp* genes that extends beyond 20 nucleotides, with only two regions sharing a 20-nucleotide match (between *flp-2* and *flp-22*, and between *flp-27* and *flp-28*). Therefore, it is unlikely that the high correlation between *flp* gene expressions was caused by any cross-mapping of RNA-seq reads among the 31 *flp* genes, since our sequenced reads were 50 to 100 base pairs in length. Together, these results strongly suggest that the *flp* genes are co-regulated and are coordinately up-regulated during dauer development.

FLPs modulate the dauer entry decision, nictation, and CO_2 chemoattraction

We investigated whether FLP neuropeptides modulate the dauer entry decision by assaying 4 CRISPR-generated knockout alleles and 19 available *flp* alleles, corresponding to mutations in 18 *flp* genes. We induced dauer entry using crude pheromone and compared the dauer entry percentage of each genotype to the wild type control. We recapitulated the previously reported increased dauer entry phenotype of *flp-18(db99)* as a positive control (49). We observed increased dauer entry in three additional *flp* mutants: *flp-2(ok3351)*, *flp-6(ok3056)*, and *flp-34(sy810)*. Furthermore, we detected decreased dauer entry in 8 mutants: *flp-1(yn4)*, *flp-8(pk360)*, *flp-10(ok2624)*, *flp-11(tm2706)*, *flp-17(n4894)*, *flp-21(pk1601)*, *flp-25(gk1016)*, and *flp-26(gk3015)* (**Figure 2.9C**). These results suggest that FLPs can act redundantly and with opposed effects on dauer entry.

flp-10 and *flp-17* are expressed in the CO_2 sensing BAG neuron (64, 65), and act synergistically with the neurotransmitter acetylcholine, which promotes the nictation behavior (19), to inhibit egg-laying (66). Because of these connections to nictation and CO_2-sensing, we examined nictation and CO_2 chemoattraction in *flp-10(n4543) flp-17(n4894)* double mutant animals. Using the micro-dirt chip, we observed an average nictation duration of 14.44 seconds for wild type, and an increased average duration of 25.02 seconds in *flp-10(n4543) flp-17(n4894)* mutants (**Figure 2.9D**). For CO_2 avoidance, we observed that *flp-10(n4543) flp-17(n4894)* mutants displayed increased reversal behavior in response to CO_2 (avoidance index = 0.56) as compared to wild type (avoidance index = -0.11) (**Figure 2.9E**). These data suggest that *flp-10* and *flp-17* contribute to SBT-1 functions in mediating nictation coordination and the switch to CO_2 attraction in dauers.

flp genes are coordinately up-regulated in parasitic nematode IJs

The infective juvenile (IJ) dispersal stage of parasitic nematodes is similar to dauer in several ways: both are non-feeding stages with a resistant cuticle (67), and both recognize and exploit carriers/hosts similarly (18, 68). One gene class that has been shown to affect dauers and IJs is the neuropeptide-encoding set of genes (27, 48). To investigate if the coordinated up-regulation of *flp* genes is a strategy shared by dauers and IJs, we performed a meta-analysis on *flp* gene expression in IJs of the semi-obligate animal parasite *Strongyloides stercoralis*, the obligate animal parasite *Ancylostoma ceylanicum*, the obligate plant parasite *Globodera pallida*, and the filarial parasite *Brugia malayi*. We selected these distantly related parasitic species because the orthologs/analogs of *C. elegans flp* genes have been identified in these nematodes (69). In addition, the transcriptomes of

these species had been collected using RNA-seq, from stages during, before, and after IJ (70-73).

There are 21 *flp* genes in *S. stercoralis*, 25 in *A. ceylanicum*, 14 in *G. pallida*, and 13 in *B. malayi*. We observed that each *flp* gene was expressed at its highest level during the IJ or post-infection IJ in *S. stercoralis*, *A. ceylanicum*, and *G. pallida*, and was expressed lowly in other stages, including the egg, the first larval, third larval, fourth larval, and adult stages (**Figure 2.11B-D**). Specifically, *S. stercoralis* expressed 16 *flp* genes highly in IJ, and 5 highly in the post-infection IJ (**Figure 2.11B**); *A. ceylanicum* expressed 18 *flp* genes highly in IJ, and 5 highly in the post-infection IJ (**Figure 2.11C**); and *G. pallida* expressed 14 *flp* genes highly in IJ (**Figure 2.11D**).

By contrast, only 4 of the 13 *flp* genes in *B. malayi* were expressed at high levels in the IJ. The expressions of the remaining *flp* genes were specialized to other stages, such as the microfilariae and the adult male (**Figure 2.11E**). Unlike the other three parasitic nematodes, *B. malayi* spends its life cycle entirely within its hosts. Notably, the IJs of *B. malayi* infect humans through the aid of a mosquito vector (74). This differs from the IJs of *S. stercoralis*, *A. ceylanicum*, and *G. pallida*, which must find and infect their hosts (**Figure 2.11**). We therefore observe that *C. elegans* dauers and the host-seeking IJs of *S. stercoralis*, *A. ceylanicum*, and *G. pallida* share a strategy of coordinately up-regulating the *flp* family.

2.4 Discussion

In the wild, *Caenorhabditis elegans* feeds on transient microbial communities that collapse approximately every three generations (75). To persist, *C. elegans* can enter the stress-resistant dauer larval stage, which can seek improved conditions by stowing onto carrier animals (60). We sequenced cDNA from dauer- and reproductively-developing animals by culturing *daf-9*(*dh6*) animals under identical conditions apart from exposure to DA. This allowed us to collect the first transcriptomes, to our knowledge, of L2d during dauer-commitment and commitment to reproductive development. Our design also allowed us to compare dauer and reproductive development to identify gene expression changes along, and between, the two tracks. We have demonstrated that 8,042 genes are differentially expressed during dauer and reproductive development, including the up-regulation of 51% of the neuropeptide genes during dauer-commitment.

Neuropeptides are short sequences of amino acids that are derived from longer proneuropeptide chains, and can act as transmitters and neuromodulators. As neuromodulators, they can control the activity, polarity, sensitivity, and signaling repertoire of neurons (76, 77). Neuropeptides can also diffuse to facilitate signaling between synaptically unconnected neurons (78, 79). Through these modulatory functions, neuropeptides can shape which circuits are active in the nervous system, the membership of these circuits, and their functions (79).

C. elegans encodes three families of neuropeptides: the insulin-like peptides (INS), the neuropeptide-like proteins (NLP), and the FMRFamide-related peptides (FLP) (48). We have shown that the *flp* genes are coordinately up-regulated during dauer-commitment. On

the other hand, few of the *ins* genes, and approximately half of the *nlp* genes are up-regulated during dauer-commitment. The low level of *ins* up-regulation is not surprising since insulins have conserved roles in growth and metabolism in Metazoa (80). In addition, signaling through the *C. elegans* insulin-like receptor DAF-2 promotes reproductive growth (48). Indeed, the only *ins* gene that was up-regulated between dauer-commitment and L4 was *ins-1*, which is known to increase dauer entry, likely by antagonizing DAF-2 signaling (28). Likewise, the *nlp* genes would not be expected to be up-regulated as a family either, since the NLPs are a miscellaneous group of non-INS, non-FLP neuropeptides (48) that likely function in several independent processes. On the other hand, FLPs have conserved roles in regulating feeding and reproduction in nematodes, arthropods, mollusks, and vertebrates (80-83). These roles correlate well with the inhibition of feeding and reproduction, and the activation of specialized food-seeking behaviors in dauer. Therefore, the coordinated up-regulation of the *flp* family may function to generate a wide response to stress that is centered on feeding and reproduction control.

We took advantage of the knockdown of neuropeptide processing in *sbt-1(ok901)* null mutants (26) to investigate the function of the neuropeptides during dauer development. We have shown that the net effect of peptidergic signaling downstream of *sbt-1* is to promote dauer entry, perhaps by encoding pro-dauer information from the sensed environment, or by modulating the food, temperature, and pheromone signaling pathways to affect the threshold (13) for dauer entry. We have also assayed 23 *flp* mutants and observed increased dauer entry in 4 mutants and decreased entry in 8 mutants. These results suggest that FLPs can act redundantly and with opposed effects on dauer entry, perhaps to fine-tune the entry decision in response to environmental signals.

Following dauer entry, dauer larvae demonstrate behaviors and preferences that are not observed in non-dauers. For instance, dauers are the only stage that can nictate (10, 19), and are attracted to CO_2 while non-dauers are repelled (18, 84). These changes indicate that dauers possess a different neural state from non-dauers, likely involving different or altered circuits in the nervous system. Yet, *C. elegans* possesses only 302 neurons that are densely interconnected (79, 85), with no synaptically compartmentalized circuits to switch between during dauer and non-dauer. To overcome this constraint, dauers can rewire their neurons to access new behaviors (16, 19). We observed that in addition to this strategy, peptidergic signaling downstream of *sbt-1* promotes coordination during nictation, and is necessary for the switch from CO_2 repulsion to CO_2 attraction in dauer. We have also shown that the combined effects of *flp-10* and *flp-17* strongly promote nictation coordination and the switch to CO_2 attraction. Therefore, we have demonstrated that neuropeptides change the neural state of *C. elegans* during dauer, possibly by altering the composition and function of the active circuits in the nervous system (**Figure 2.12**).

Considering these results, it is notable how many neuropeptides are up-regulated during dauer development. By dauer, 64 neuropeptide genes encoding 215 peptides are up-regulated, and by comparison, the entire human genome only contains 97 neuropeptide genes encoding 270 peptides (56). Indeed, the neuropeptide gene families are expanded in *C. elegans* (48), and the FLP neuropeptides are especially expanded in the phylum Nematoda (27). We observed that FLPs are involved in establishing the *C. elegans* dauer neural state, and RNAi knockdown experiments have also shown that FLPs regulate the IJ dispersal behaviors of *G. pallida* (*flp-12*), *Meloidogyne incognita* (*flp-18*), and *Steinernema carpocapsae* (*flp-21*) (86, 87), indicating that they are involved in establishing the IJ neural

state as well. Because we observed coordinated up-regulation of the FLPs during dauer, and in the IJs of the distantly related nematodes *S. stercoralis*, *A. ceylanicum*, and *G. pallida*, we speculate that the computational challenges of dauer and IJ were the driving force for *flp* expansion in Nematoda. This hypothesis is supported by the lack of such expansion in the nematodes *Trichinella spiralis* and *Trichuris muris* (69), which do not posses dauer or IJ stages (88, 89), and only encode 4 *flp* genes each. Therefore, *flp* expansion may have provided ancestral nematodes the means to overcome their constrained nervous systems (90) in order to effectively adapt to stress during dauer and IJ.

Our genetic data and meta-analysis also suggest that SBT-1 would be a potent target for anthelminthic control. Since *sbt-1* nulls are strongly defective in dauer entry and dispersal behaviors, we predict that targeting SBT-1 in parasitic nematodes will severely impair dispersal and host-seeking in their IJs. While RNAi against individual FLPs can affect IJ dispersal (86, 87), our meta-analysis indicates that multiple FLPs are up-regulated in several types of parasitic nematodes. We propose that inhibition of SBT-1 could be used to efficiently knock down multiple FLPs at once, and in a wide range of parasitic nematodes. SBT-1 would also be an excellent target, since nematode SBT-1 is distinct in sequence from vertebrate 7B2 (57), reducing the risks of cross-species effects.

Altogether, we have investigated phenotypic plasticity in a whole organism by studying *C. elegans* adaptation to stress during development. We uncovered the transcriptional dynamics of *C. elegans* during dauer development, and discovered a strategy of massively up-regulating neuropeptide expression. This strategy functions to enhance the dauer entry decision and expand the behavioral repertoire of dauers, and appears to be evolutionarily shared by dauers and host-seeking IJs, suggesting SBT-1 as a potent anthelminthic target.

2.5 Materials and Methods

Animal strains

C. elegans strains were grown using standard protocols with the *E. coli* strain OP50 (for plate cultures) or HB101 (for liquid cultures) as a food source (91). The wild type strain was N2 (Bristol). PS5511 *daf-9(dh6)*; *dhEx24* was a gift from the Antebi lab. Strains obtained from the *Caenorhabditis* Genetics Center (CGC) include: NY16 *flp-1(yn4)*, VC2324 *flp-6(ok3056)*, RB1990 *flp-7(ok2625)*, PT501 *flp-8(pk360)*, RB1989 *flp-10(ok2624)*, FX02706 *flp-11(tm2706)*, RB1863 *flp-12(ok2409)*, AX1410 *flp-18(db99)*, RB2188 *flp-20(ok2964)*, RB982 *flp-21(ok889)*, VC1982 *flp-25(gk1016)*, and VC3017 *flp-26(gk3015)*. AX1129 *flp-21(pk1601*) was a gift from the De Bono lab. MT15933 *flp-17(n4894)* and MT15973 *flp-10(n4543); flp-17(n4894)* were gifts from the Horvitz lab. PS7112 *sbt-1(ok901)* was outcrossed 6 times from CGC RB987; PS7370 *flp-2(ok3351)* was outcrossed 3 times from CGC VC2591; PS7378 W07E11.1 & *flp-2(gk1039)* was outcrossed 3 times from CGC VC2490; PS7379 *flp-3(ok3265)* was outcrossed 3 times from CGC VC2497; PS6813 *flp-13(tm2427)* was outcrossed 3 times from the Mitani strain FX02427; and PS7221 *flp-34(ok3071)* was outcrossed 3 times from CGC RB2269.

Transgenic strains

sbt-1 genomic DNA rescue strains were generated by injecting 15 ng/µL of *sbt-1* genomic DNA (amplified by PCR with forward primer CTGTGAAGCGCTCATCTGAA and reverse primer TTCAGGCAAATCCATCATCA), 50 ng/µL coelomocyte-specific *ofm-1p::rfp* co-injection marker, and 135 ng/µL 1 kb DNA ladder (New England Biolabs,

Beverly, MA) carrier DNA into the adult gonads of *sbt-1(ok901)* animals, followed by integration into the genome by X-ray (92, 93). Two independent integration lines were generated: PS7274 *sbt-1(ok901); Is444[sbt-1p::sbt-1; ofm-1p::rfp]* (line 1, outcrossed 2 times) and PS7275 *sbt-1(ok901); Is445[sbt-1p::sbt-1; ofm-1p::rfp]* (line 2, outcrossed 3 times).

Transcriptional reporter strains

Transcriptional reporter constructs were built using fusion PCR (1). The promoter regions of *srt-41* and *col-40* were fused to *mCherry*::*unc-54* 3'UTR (amplified from pGH8 from Addgene). The flanking sequences of the amplified *srt-41* promoter were GCACAGTTTTAAGTTTTTCTGTCTT and TGCTGCCAACCTGTTCTG. The flanking sequences of the amplified *col-40* promoter were ATGATGACCGCCTGATTTTC and AATTATTGTAGTAAAGGGGGAAGTC. Injection mixtures were prepared at a concentration of 20 ng/µL reporter construct, 50 ng/µL *unc-119(+)* rescue construct, and 130 ng/µL 1 kb DNA ladder carrier DNA. Transgenic animals were obtained by microinjecting the mixtures into the adult gonads of *unc-119(ed4)* animals (2, 3). The fluorescent transcriptional reporter strains that were generated are:

PS7128 *unc-119(ed4); syEx1534[srt-41p::mCherry; unc-119(+)]* and

PS6727 *unc-119(ed4); syEx1338[col-40p::mcherry; unc-119(+)]*

CRISPR-generated strains

CRISPR mutagenesis with co-conversion (94) was used to generate the deletion strains. Guide RNA (gRNA) target sequences of 19 bp (corresponding to sequence upstream of an

NGG PAM site) were cloned into pRB1017 single-guide RNA (sgRNA) vector (Addgene). Four distinct gRNA sequences were used to target each gene. Injection mixtures were prepared at a concentration of 25 ng/µL per sgRNA expression plasmid, 50 ng/µl Cas9 plasmid (Addgene #46168), 25 ng/µl *dpy-10* sgRNA plasmid (pJA58 from Addgene), and 500 mM *dpy-10(cn64)* donor oligonucleotide (synthesized by Integrated DNA Technologies, Coralville, IA). Injected P_0 hermaphrodites were transferred to individual Petri plates to produce F_1 progeny. F_1 progeny exhibiting a Rol or Dpy phenotype were picked to individual Petri plates four days after injection. F_1s that produced Rol or Dpy F_2s were genotyped for the presence of a deletion allele. Homozygous deletion mutants were isolated from the F_2 or F_3 population, and the deletion alleles were confirmed by Sanger sequencing (Laragen, Culver City, CA).

The 1343bp *flp-21(sy880)* deletion is flanked by the sequences TATGTACACTATTTAA GATTTGATTGTGTA and CATTCGGGGCCACAAACTCCTGCTTCGATC. *flp-32(sy853)*, *flp-34(sy810)* and *flp-34(sy811)* deletion alleles have short DNA fragment insertions. The 460bp *flp-32(sy853)* deletion is flanked by the sequences TATGAATATGTTCCGGAGCGCATGTCAAAC and AACTAAAGATACACCACTAC CACCTGAACC, with a TAACT insertion. The 1365bp *flp-34(sy810)* deletion is flanked by the sequences TCAAATTTTTTGAGGAAATCCTCCTGAAAC and AATATTTTCGA GTTTCGAAACATTTCAAAT, with a AATATATTTTCGAGTTTCGAAACATATTTT CGAGTTTCGAAACAC insertion. The 1607bp *flp-34(sy811)* deletion is flanked by the sequences TTTGTGTCTAGCAAAAGGAGATGCTCTTTA and CATAGGCGTAGGCC ATAGGCGTAGGCCATA, with a AATAAATTAATTAAATATCTGAAATAAAAACA

AAACCTCGAGAGAGAAAATTTAGAAAAAAAAACGAGACGGCTACGGACGGCT
GACGTGATGGAATTATTTACGGCCAAATCTGAAAATAAAATGGATTATATTTT
GTTTTAGGCCATAGACGTAGGTCATAGGCGTAGACCATAGGCGTAGGC
insertion.

***daf-9(dh6)* culturing and harvesting for RNA-seq**

Synchronous, single-stage populations of *daf-9(dh6)* animals were grown using our previously described method for liquid culturing *daf-9(dh6)* (13). *daf-9(dh6)* animals were collected at 6 points over a branching time series along 24 hours post hatch (hph) to 60 hph. This period, as we have previously analyzed, includes L2d sensory integration, dauer-commitment, dauer maintenance, reproductive-commitment, and reproductive development (13) (**Figure 2.1A**). The dauer-developing branch was obtained by withholding dafachronic acid (Δ7-DA), and animals were collected at 24 hph (L2d), 26 hph (L2d), 34 hph (dauer-commitment), and 60 hph (dauer). The reproductive-developing branch was obtained by adding 100 nM Δ7-DA at 24 hph, and animals were collected at 26 hph (L3-committing) and 34 hph (L4). Reproductive animals at 60 hph are gravid, making them inappropriate for single-stage transcriptome analysis, and were therefore not collected.

Cultures from the dauer and reproductive branches were grown in parallel, fed at the same time, and experienced the same batches of HB101 and Δ7-DA in order to minimize asynchronous development between the cultures. Each time point was collected using two independently cultured biological replicates. Each biological replicate was maintained separately for at least 5 generations. Harvested animals were spun in S. Basal three times to

help clear the bacteria. The worm pellets (approximately 10,000 worms per pellet) were then treated with 1 mL Trizol and 0.6 mg/mL linear polyacrylamide carrier, before being flash frozen in liquid nitrogen and stored at -80°C. RNA was purified as previously described (13).

RNA-sequencing and computational analysis

cDNA was prepared from the collected samples using the Illumina TruSeq RNA Sample Preparation kit or mRNA-Seq Sample Preparation kit. cDNA was sequenced using the Illumina HiSeq2000 to generate paired-end or single-end libraries. Paired-end libraries were not multiplexed, were sequenced at a read length of 100 bp, and were sequenced to an average depth of 76 million reads. Single-end libraries were multiplexed at 4 libraries per lane, sequenced at a read length of 50 bp, and sequenced to an average depth of 33 million reads. All raw sequences have been deposited into the NCBI Sequence Read Archive (SRA) database (accession number SRP116980). **Appendix Table 2.1** contains the detailed metadata for the sequenced libraries. Codes used for data analysis have been deposited into GitHub at https://github.com/WormLabCaltech/dauerRNAseq.

***Read mapping and differential expression testing*:** Reads that did not pass the Illumina chastity filter were removed using Perl. Read mapping, feature counting, library normalization, quality checks, and differential gene expression analysis was performed using R version 3.1.0, bowtie2 version 2.2.3, tophat2 version 2.0.12, SAMtools version 0.1.19, HTSeq version 0.6.1, and DESeq, as described in (38). The *C. elegans* reference genome and gene transfer format files were downloaded from Ensembl release 75 and genome assembly WBcel235. Gene dispersion estimates were obtained after pooling all

sequenced samples. Each pairwise comparison for differential gene expression was performed at a Benjamini-Hochberg controlled false discovery rate < 0.01.

***RNA-seq data summaries*:** Principal component analysis was performed using the DESeq package in R (37). Violin plotting was done in R using ggplot2 (95). KEGG biochemical pathway enrichment analysis was performed using clusterProfiler in R (96), at a cutoff of BH-corrected *q*-value < 0.01. Gene Ontology (GO) enrichment analysis was performed using the PANTHER Overrepresentation Test for GO Biological Process, at a Bonferroni-adjusted *p*-value cutoff of < 0.05. GO and KEGG terms were ranked based on descending fold-enrichment for GO, and ascending *q*-value for KEGG.

***Soft clustering*:** Soft clustering was performed using the mFuzz package in R (40, 41). Gene expression data were standardized before clustering, and cluster numbers were chosen based on cluster stability, minimum cluster centroid distance, and visual clarity of the clusters. Over-represented neuronal gene classes in clusters 1 to 6 were determined by hypergeometric test, using a cutoff of Bonferroni-corrected *p*-value < 0.05.

***Heatmaps*:** Heatmaps were drawn using the gplots and RColorBrewer packages in R (97, 98). Mean count values were used for each time point, calculated by averaging the biological replicates. Heatmap dendrograms were drawn using correlation distances and average-linkage hierarchical clustering. Expression values were centered and scaled for each gene.

***Gene expression correlation analysis*:** Spearman correlation scores were computed using Python 2.7.9 and the Scipy library (99) by ranking the transcripts per million (TPM) values in each RNA-seq experiment, then calculating the Pearson correlation on the ranked values for each pairwise combination of genes: ρ = covariance(gene1, gene2) /σ_{gene1} σ_{gene2}, where

σ represents standard deviation. *p*-values were computed by comparing average correlation scores to the bootstrap distribution of average scores for random sets of 31 genes (mimicking the size of the *flp* family), and calculated as the fraction of times that bootstrapping produced a score greater than or equal to the score being tested. Because the *ins* and *nlp* families have more than 31 genes, the *p*-value is an upper estimate. Bootstrapping was performed 10,000 times. The RNA-seq datasets that were used were our *daf-9(dh6)* RNA-seq data, re-quantified using kallisto (100) into TPM counts; and processed RNA-seq data from 246 publically available libraries (23), obtained using WormBase SPELL and converted to TPM counts (101). Genes detected in less than 80% of the experiments were discarded.

***Dotplot analysis*:** Dotplot analysis of the *flp* coding sequences was performed using Gepard (63). Coding sequences from the 31 total *flp* genes (taking only the a isoform for genes with multiple isoforms) were used in the analysis.

Dauer entry assay on pheromone plates

The preparation of crude pheromone and the dauer entry assay were performed with modifications to previously described methods (102). Crude pheromone was extracted from exhausted liquid culture medium, re-suspended with distilled water and stored at -20°C. Pheromone plates (NGM-agar with added crude pheromone and no peptone) were freshly prepared the day before each experiment and dried overnight at room temperature. Heat-killed *E. coli* OP50 was used as a limited food source for the dauer entry assays, and was prepared by re-suspending OP50 overnight cultures in S. Basal to 8 g/100 mL, and heating at 100°C for 5 minutes. On the day of the experiment, seven to ten

young adults were picked onto each plate, and allowed to lay approximately 50-60 eggs before being removed. 20 μl of heat-killed OP50 was added to the plates as a food source for the un-hatched larvae. After 48 hours of incubation at 25.5°C, dauers and non-dauers were counted on each plate based on their distinct morphologies.

Dauer entry can exhibit day-to-day variation caused by environmental conditions such as humidity or temperature (25). To control for this variation, wild type controls were run in every trial. The wild type results from the same batch of pheromone were pulled together for better statistical power, and each statistical analysis was done with samples treated with the same batch of pheromone.

Statistical analysis for dauer entry assay

The mean and 99% confidence interval of the dauer entry percentage were calculated non-parametrically for each genotype by pooling the data from all the plates and computing 10,000 bootstrap replicates (103). Pairwise comparisons were performed through a non-parametric permutation test with 10,000 replicates. The difference in dauer entry probability between two genotypes was estimated using a Bayesian approach (104) to compute the posterior probability of dauer entry for each genotype. Bootstrapping, permutation, and Bayesian statistics were performed using Python 3.5 and the SciPy library (105).

For each genotype, the data from all of the plates tested for that genotype were pooled and the number of dauers and non-dauers were converted into a Boolean array (1 for dauer, 0

for non-dauer). Non-parametric bootstrapping was used to sample the data array (with replacement) to calculate a corresponding dauer entry percentage. This procedure was repeated 10,000 times to construct a dauer entry percentage distribution, from which the mean and 99% confidence interval were calculated.

For each comparison between two genotypes, data arrays from the two genotypes were concatenated, shuffled, and split into two datasets of original size as before concatenation, and a difference of means was calculated between the two new datasets. This procedure was repeated 10,000 times to generate a distribution of differences of means that simulated the null hypothesis. The *p*-value was calculated as the fraction of the distribution where the simulated difference was greater than or equal to the observed difference.

A binomial likelihood was used with a uniform prior for values in the range [0, 1], so that the log posterior probability distribution was proportional to the log bionomial distribution in the allowed range. The data for each genotype were pooled, and the posterior distribution was sampled using Markov chain Montecarlo (MCMC). The difference between mutant and wild-type was computed by subtracting the respective MCMC samples.

Dauer behavior assays

Crude pheromone plates were used to induce synchronized dauers for behavior assays: for each pheromone plate, 20 μL of heat-killed OP50 (8 g/100 mL) were spotted and 12-15 young adult animals were picked onto the plate to lay eggs at 20°C for 12 hours before being removed. After 2-4 days of incubation at 25.5°C, dauers were identified by their morphology and isolated for the following assays.

***Nictation assay*:** Nictaiton assay was performed on micro-dirt chips with modifications to previously described methods (19). Dauers suspended in distilled water were transferred onto the micro-dirt chip (4% agarose in distilled water) and allowed to nictate. Each nictating dauer was observed for at least 3 minutes or until the end of nictation. The time recording began when a dauer initiated nictation (by lifting its neck region of the body), and the total duration of each nictation event was also recorded. If the dauer stopped nictating and exhibited quiescence in a standing posture during the recording, the data were excluded from further analysis. The average nictation duration was calculated by dividing the total duration of nictation by the number of nictation events. At least 20 dauers were assayed for each genotype. The mean of average duration and 99% confidence interval, and the pairwise *p*-value, were computed non-parametrically as described for the dauer entry assay.

***CO_2 chemotaxis assay*:** CO_2 chemotaxis assays were performed on dauers with modifications to previously described methods (18). Dauers were washed three times with distilled water and transferred to standard chemotaxis assay plates (106). Two gas mixtures were delivered to the plate at a rate of 0.5 mL/min through PVC tubing and holes drilled through the plate lid. The CO_2 gas mixture was 10% CO_2 and 21% O_2 balanced with N_2, and the control gas mixture was 21% O_2 balanced with N_2 (Airgas). The two holes were positioned on opposite sides of the plate along a diameter line, with each of them positioned 1 cm from the edge of the plate. The scoring regions were set as the areas of the plate beyond 1 cm from a central line drown orthogonally to the diameter on which the gas mixtures were presented. At the end of 1 hour, the numbers of animals in each scoring region was counted and the chemotaxis index was calculated as ($N_{at\,CO2}$ scoring region $- N_{at}$

$_{\text{control gas}}$ scoring region) / ($N_{\text{at CO2}}$ scoring region + $N_{\text{at control gas}}$ scoring region). Statistical analysis (two-tailed t test) was performed using GraphPad Prism.

***Acute CO_2 avoidance assay*:** CO_2 avoidance assays were performed as previously described (62), with slight modifications. Dauers were washed three times with distilled water and transferred to unseeded NGM plates. A 50 mL gas-tight syringe was filled with either a CO_2 gas mixture or a control gas mixture, and connected to a pipet tip using PVC tubing. Gas was pumped out through the pipet tip at a rate of 1.5 mL/min using a syringe pump, and the tip was presented to the head of forward-moving dauers. A response was scored if the animal reversed within 4 seconds. For each plate, at least 20 animals were assayed per gas mixture, with each plate counted as a trial. The avoidance index was calculated as ($N_{\text{reversed to CO2}}$ / $N_{\text{presented with CO2}}$) − ($N_{\text{reversed to control gas}}$ / $N_{\text{presented with control gas}}$). Statistical analysis (one-way ANOVA with Bonferroni post-correction test) was performed using GraphPad Prism.

flp gene expression in infective juveniles

Orthologs/analogs of *C. elegans flp* genes exist in other nematodes (69, 80, 107). Identified *flp* orthologs/analogs in (69, 107) were matched to transcript IDs in *S. stercoralis*, *A. ceylanicum*, *G. pallida*, and *B. malayi* using BLAST via WormBase ParaSite. Published RNA-seq data was downloaded for *S. stercoralis* (73) and *G. pallida* (71) using the ENA; *B. malayi* (70) using WormBase SPELL; and *A. ceylanicum* (72) as it was published.

The read counts from the *A. ceylanicum* and *B. malayi* data were pre-processed into TPM counts. We obtained TPM counts for the *S. stercoralis* and *G. pallida* datasets using

kallisto to align the read data and to quantify transcript abundances (100). Kallisto was preferable to DESeq at this stage of our analysis, as it allowed us to quickly and accurately quantify these large datasets. To increase comparability between all of the datasets, kallisto was used to re-quantify our own dauer RNA-seq data into TPM counts.

2.6 Figures

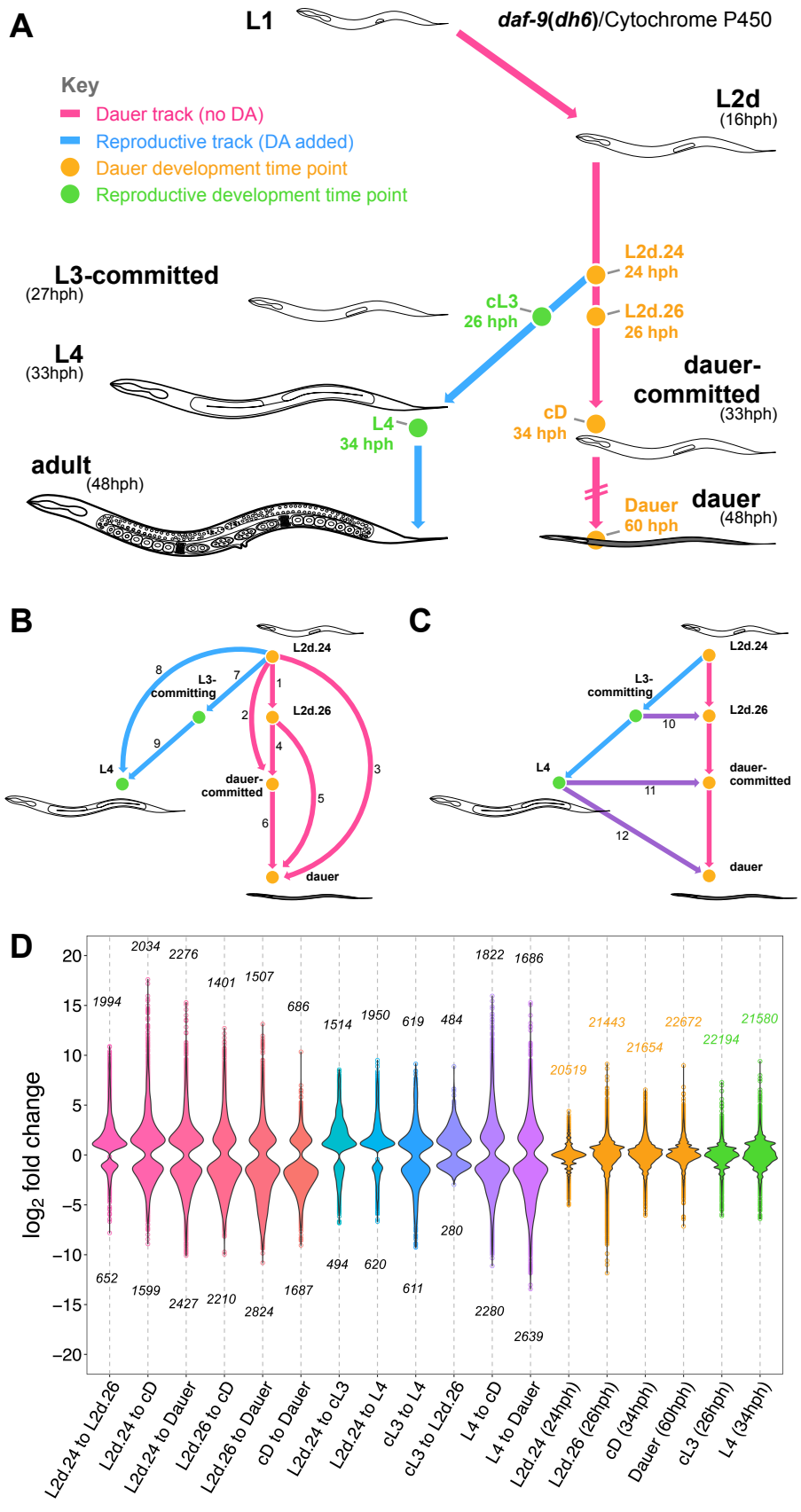
A
L1
daf-9(dh6)/Cytochrome P450
Key
Dauer track (no DA)
Reproductive track (DA added)
Dauer development time point
Reproductive development time point
L2d
(16hph)
L2d.24
24 hph
L3-committed
(27hph)
cL3
26 hph
L2d.26
26 hph
L4
(33hph)
dauer-
committed
(33hph)
cD
34 hph
L4
34 hph
adult
(48hph)
Dauer
60 hph
dauer
(48hph)
B
L2d.24
L3-
committing
L2d.26
L4
dauer-
committed
dauer
C
L2d.24
L3-
committing
L2d.26
L4
dauer-
committed
dauer
D
log2 fold change
20
15
10
5
0
−5
−10
−15
−20
1994
2034
2276
1401
1507
686
1514
1950
619
484
1822
1686
20519
21443
21654
22672
22194
21580
652
1599
2427
2210
2824
1687
494
620
611
280
2280
2639
L2d.24 to L2d.26
L2d.24 to cD
L2d.24 to Dauer
L2d.26 to cD
L2d.26 to Dauer
cD to Dauer
L2d.24 to cL3
L2d.24 to L4
cL3 to L4
cL3 to L2d.26
L4 to cD
L4 to Dauer
L2d.24 (24hph)
L2d.26 (26hph)
cD (34hph)
Dauer (60hph)
cL3 (26hph)
L4 (34hph)

Figure 2.1. 39% of the *C. elegans* genome is differentially expressed during dauer and reproductive development. (A) Experimental design for collecting dauer- and reproductively-developing *daf-9(dh6)* animals. The timing of molt events are indicated in parentheses (13). **(B-C)** Twelve comparisons between the six time points. Arrows are directed from the reference point to the end point of each comparison. **(D)** Violin plots of the significantly up- and down-regulated genes in each comparison. The number of up- and down-regulated genes in each comparison is indicated above and below its violin plot. The fold changes between the replicates of each sequenced time point are plotted for reference (orange and green plots). Abbreviations are hph: hours post hatch, DA: dafachronic acid, cL3: L3-committing, cD: dauer-committed.

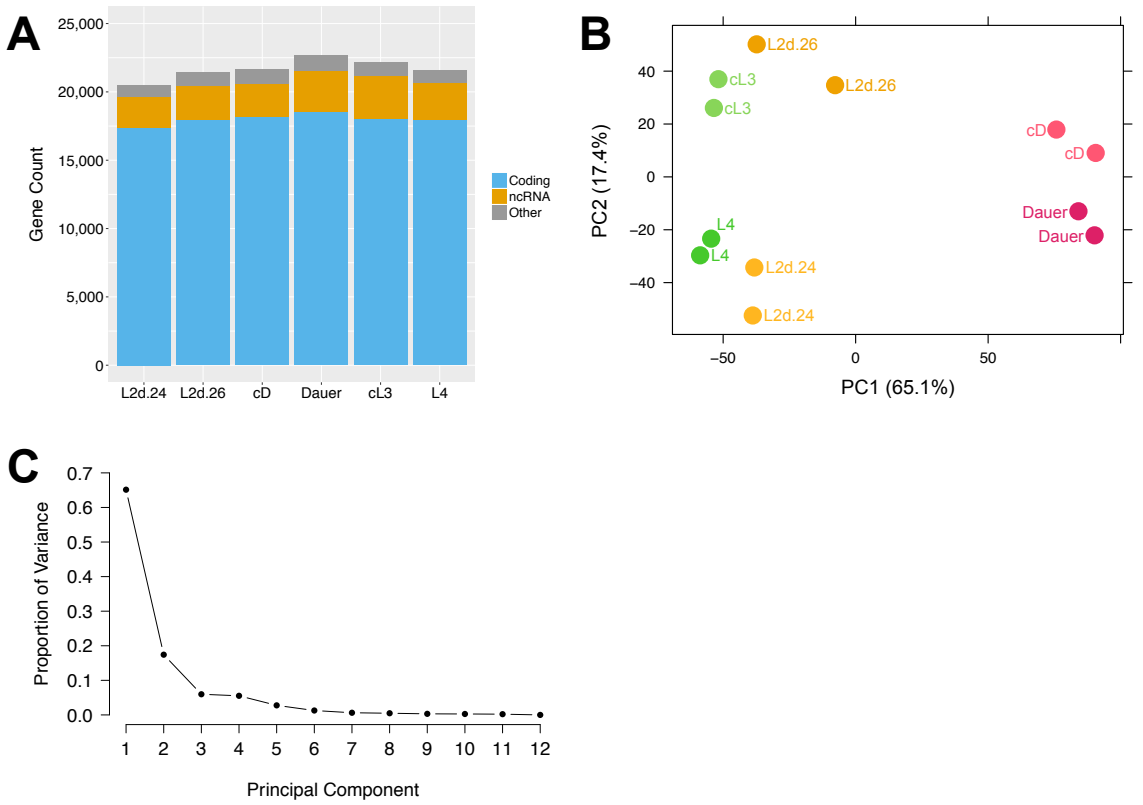

Figure 2.2. ***daf-9(dh6)*** **RNA-seq dataset summaries (A)** Detected gene counts from the six sequenced stages along dauer and reproductive development. **(B)** Principal component analysis plot of the variation in gene expression across the 12 sequenced samples. The proportion of total variation that is spanned by PC 1 and 2 are listed in parentheses. **(C)** Scree plot demonstrating the proportion of the total variation between the 12 sequenced samples that is explained by each principal component in the principal component analysis.

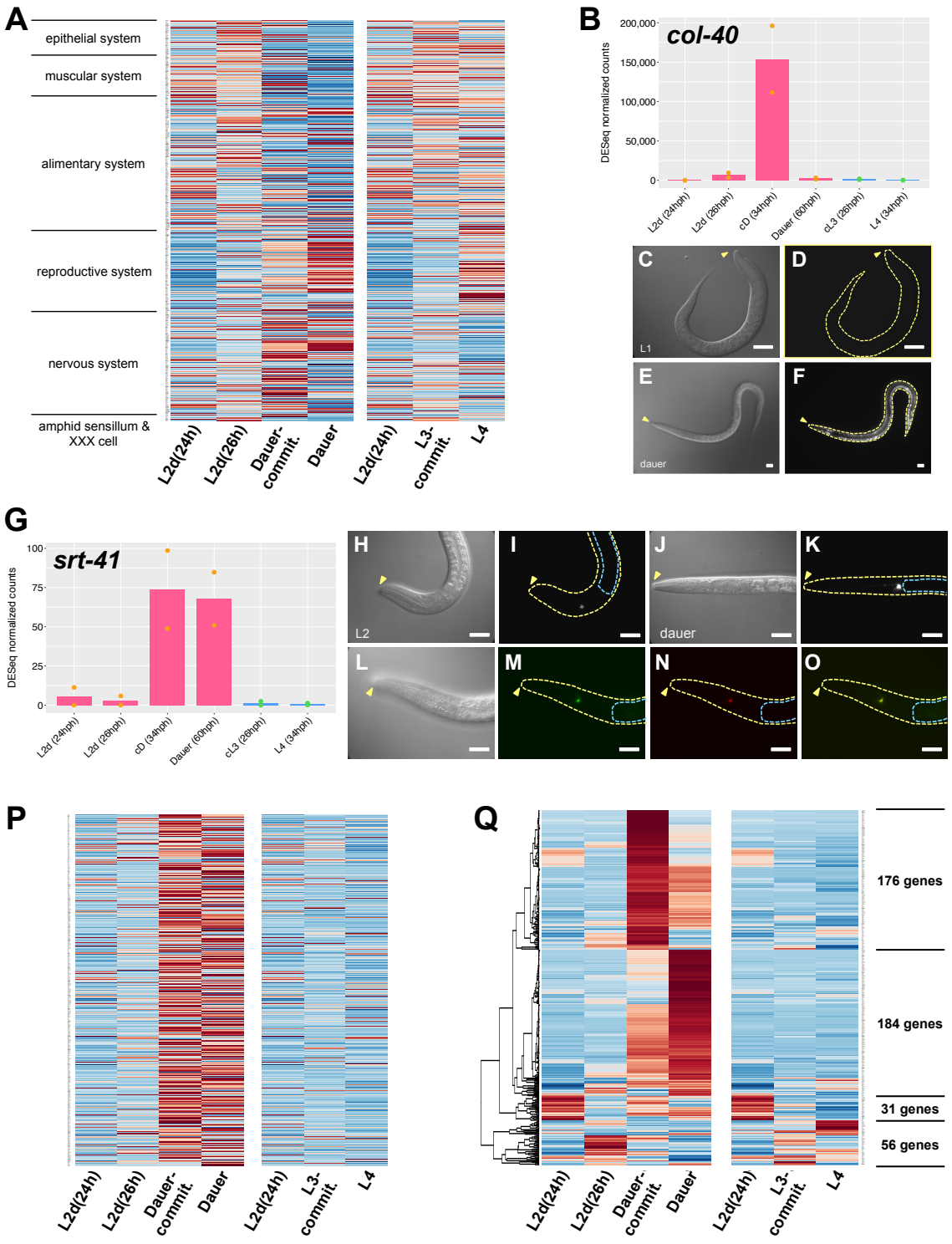
A
epithelial system
muscular system
alimentary system
reproductive system
nervous system
amphid sensillum & XXX cell
L2d(24h)
L2d(26h)
Dauer-commit.
Dauer
L2d(24h)
L3-commit.
L4
B
col-40
DESeq normalized counts
200,000
150,000
100,000
50,000
0
L2d (24hph)
L2d (26hph)
cD (34hph)
Dauer (60hph)
cL3 (26hph)
L4 (34hph)
C
L1
D
E
dauer
F
G
srt-41
DESeq normalized counts
100
75
50
25
0
L2d (24hph)
L2d (26hph)
cD (34hph)
Dauer (60hph)
cL3 (26hph)
L4 (34hph)
H
L2
I
J
dauer
K
L
M
N
O
P
L2d(24h)
L2d(26h)
Dauer-commit.
Dauer
L2d(24h)
L3-commit.
L4
Q
176 genes
184 genes
31 genes
56 genes
L2d(24h)
L2d(26h)
Dauer-commit.
Dauer
L2d(24h)
L3-commit.
L4

Figure 2.3. Differential expression was detected at high accuracy and single-cell resolution (A) The expression profiles of differentially expressed genes with putative tissue-specific expression in the epithelial system, muscular system, alimentary system, reproductive system, nervous system, amphid sensillum, and XXX cell. The expression data was scaled and heatmapped as in Figure 3. (B) Detected read counts for the col-40 gene. Points indicate count values from each sequenced replicate. The bar height represents the mean count value for each stage. Abbreviations are hph: hours post hatch, cL3: L3-committing, cD: dauer-committed. (C-D) Bright field and fluorescence images of the col-40 non-dauer expression pattern (shown is an L1). The body is traced in yellow dotted lines, and yellow arrows point to the mouth for reference. Scale bars represent a length of 20 μm. (E-F) Bright field and fluorescence images of the *col-40* dauer expression pattern. (H-I) Bright field and fluorescence images of the *srt-41* non-dauer expression pattern (shown is an L2). The intestine is traced in blue dotted lines for reference. (J-K) Bright field and fluorescence images of the *srt-41* dauer expression pattern. The two fluorescence images (I) and (K) were captured using the same imaging parameters. (L-O) *srt-41p::mCherry* expression in the AWC^{on} neuron. (M) GFP expressed from the AWC^{on} marker *str-2p::gfp* and (N) mCherry from *srt-41p::mCherry* co-localized in the same cell, as shown in (O) the merged image. Pictured is a non-dauer, since *str-2p::gfp* changes expression to the ASI neuron in dauers (4). (P) Venn diagram comparing our dataset to SAGE data published by Jones, et al. (2001), and microarray data published by Wang & Kim (2003), drawn using the eulerr package (5). Differential expression in our data was tested for using comparisons 2-6 and 11-12 to identify genes that were significantly up-regulated at dauer-commitment and dauer, relative to L2d and L4.

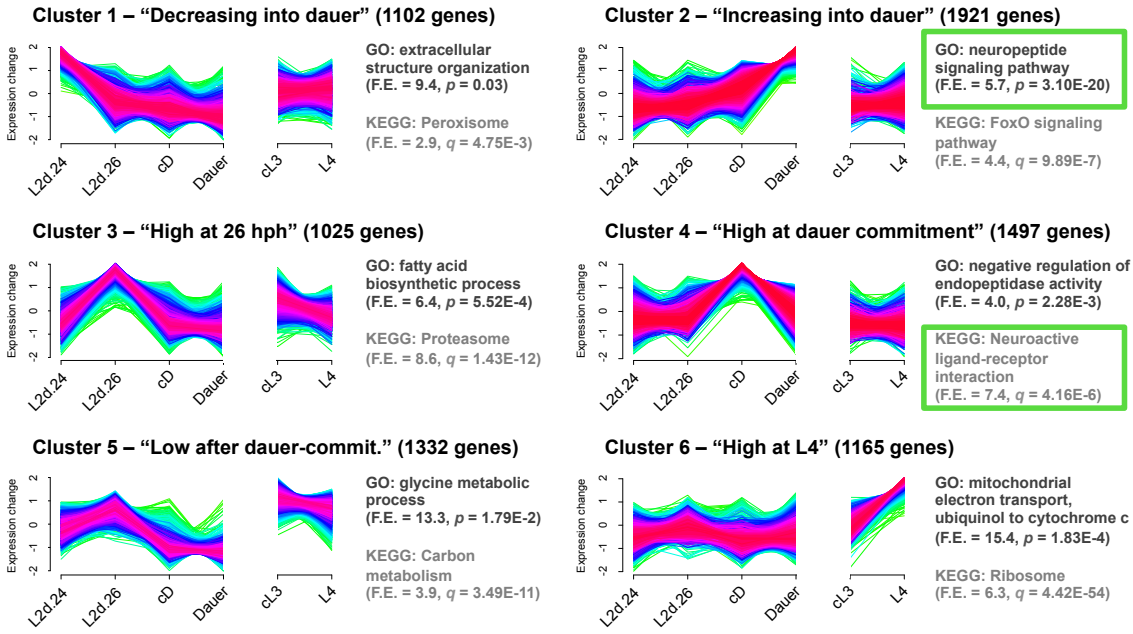

Figure 2.4. Clustering revealed six common expression profiles during dauer and reproductive development.

Soft clustering of the 8,042 differentially expressed genes into six common expression profiles. Yellow-green lines indicate genes with low cluster membership scores, and purple-red lines indicate genes with high membership scores. The top enriched GO and KEGG terms for each cluster are listed. Abbreviations: FE: fold enrichment.

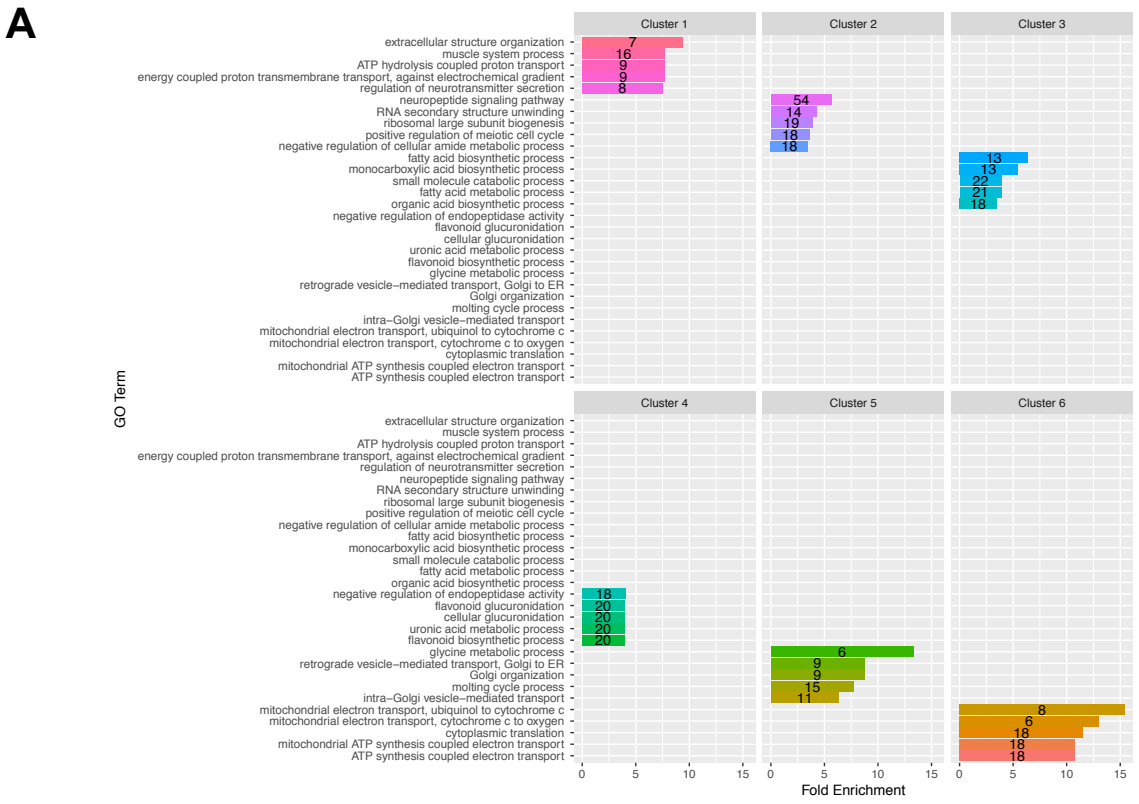
A
Cluster 1
Cluster 2
Cluster 3
Cluster 4
Cluster 5
Cluster 6
GO Term
extracellular structure organization
muscle system process
ATP hydrolysis coupled proton transport
energy coupled proton transmembrane transport, against electrochemical gradient
regulation of neurotransmitter secretion
neuropeptide signaling pathway
RNA secondary structure unwinding
ribosomal large subunit biogenesis
positive regulation of meiotic cell cycle
negative regulation of cellular amide metabolic process
fatty acid biosynthetic process
monocarboxylic acid biosynthetic process
small molecule catabolic process
fatty acid metabolic process
organic acid biosynthetic process
negative regulation of endopeptidase activity
flavonoid glucuronidation
cellular glucuronidation
uronic acid metabolic process
flavonoid biosynthetic process
glycine metabolic process
retrograde vesicle−mediated transport, Golgi to ER
Golgi organization
molting cycle process
intra−Golgi vesicle−mediated transport
mitochondrial electron transport, ubiquinol to cytochrome c
mitochondrial electron transport, cytochrome c to oxygen
cytoplasmic translation
mitochondrial ATP synthesis coupled electron transport
ATP synthesis coupled electron transport
0
5
10
15
Fold Enrichment

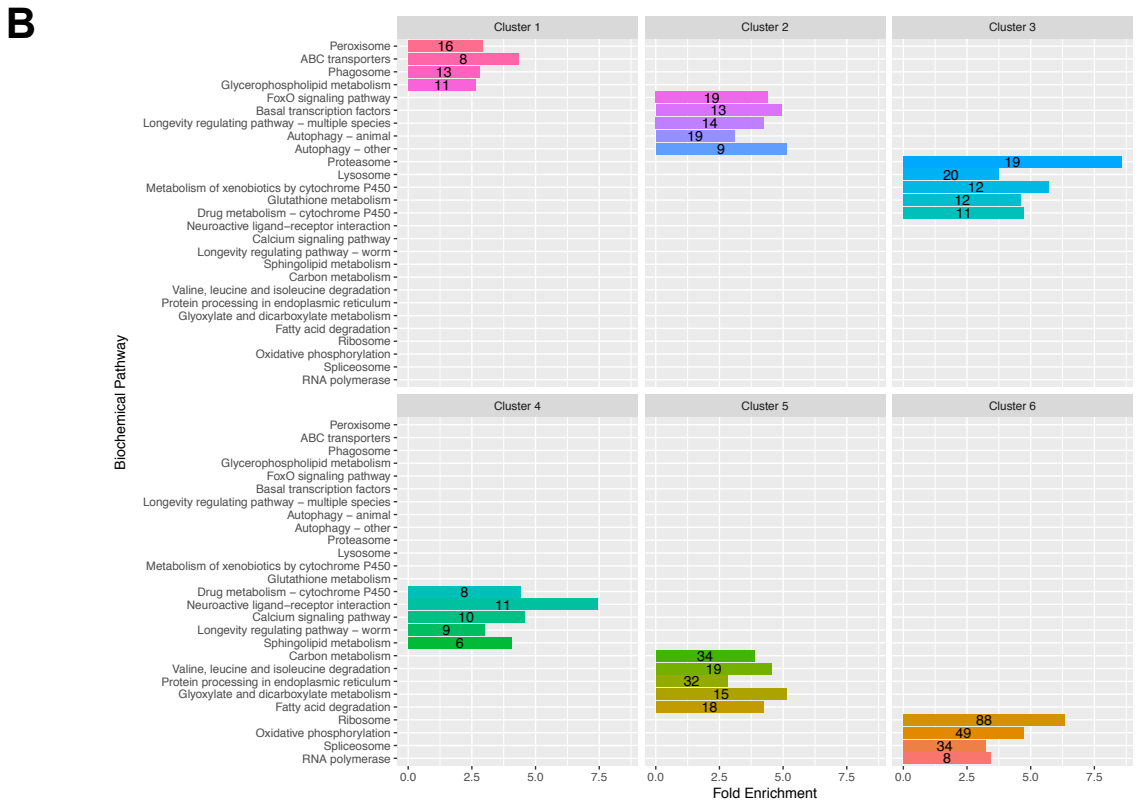
B
Cluster 1
Cluster 2
Cluster 3
Cluster 4
Cluster 5
Cluster 6
Biochemical Pathway
Peroxisome
ABC transporters
Phagosome
Glycerophospholipid metabolism
FoxO signaling pathway
Basal transcription factors
Longevity regulating pathway − multiple species
Autophagy − animal
Autophagy − other
Proteasome
Lysosome
Metabolism of xenobiotics by cytochrome P450
Glutathione metabolism
Drug metabolism − cytochrome P450
Neuroactive ligand−receptor interaction
Calcium signaling pathway
Longevity regulating pathway − worm
Sphingolipid metabolism
Carbon metabolism
Valine, leucine and isoleucine degradation
Protein processing in endoplasmic reticulum
Glyoxylate and dicarboxylate metabolism
Fatty acid degradation
Ribosome
Oxidative phosphorylation
Spliceosome
RNA polymerase
0.0
2.5
5.0
7.5
Fold Enrichment

Figure 2.5. Enriched GO terms and KEGG pathways in clusters 1 to 6. The number in each bar indicates the number of genes with that term in the cluster. (A) The five most enriched GO terms (based on descending fold enrichment) in clusters 1 to 6, using a cutoff of Bonferroni-adjusted p-value < 0.05. (B) The five most enriched biochemical pathways (based on ascending q-value) in clusters 1 to 6, using a cutoff of BH-corrected q-value < 0.05.

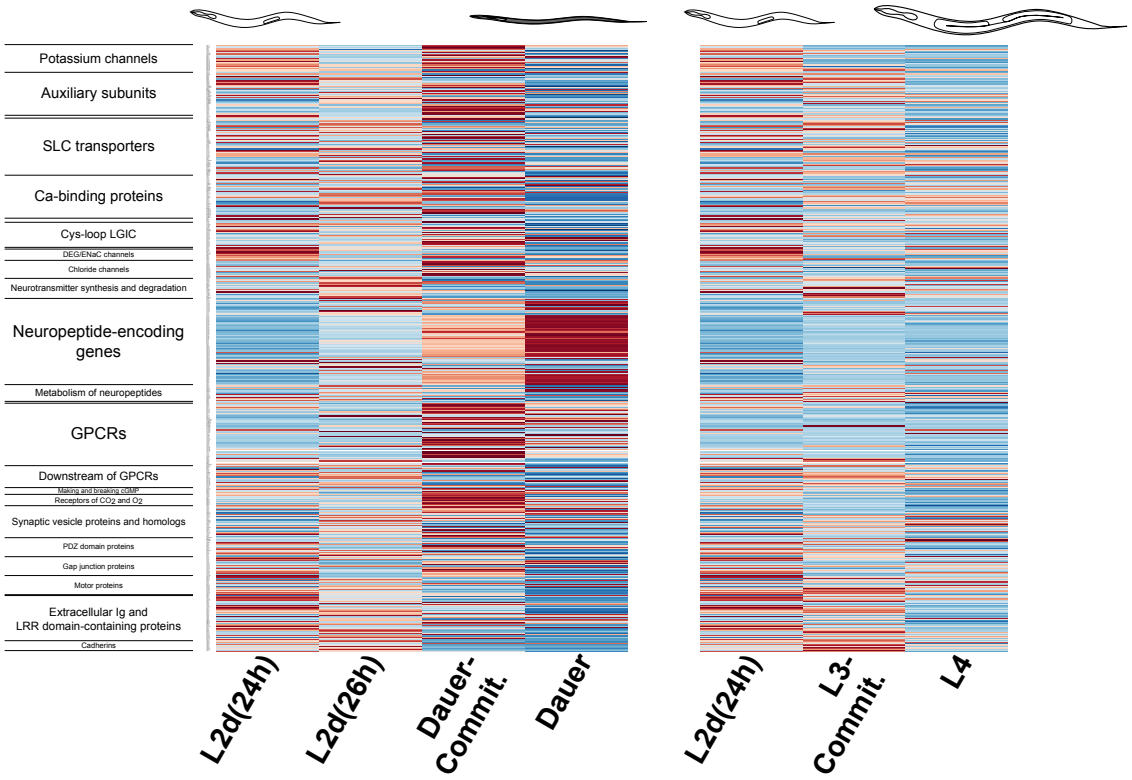

Figure 2.6. Differential expression of the neuronal effector genome of *C. elegans* during dauer and reproductive development. Heatmap of the expression of 606 differentially expressed neuronal effector genes. Each row represents a single gene, with the class that the gene belongs to indicated on the left. Red and blue indicate high and low expression scores, respectively.

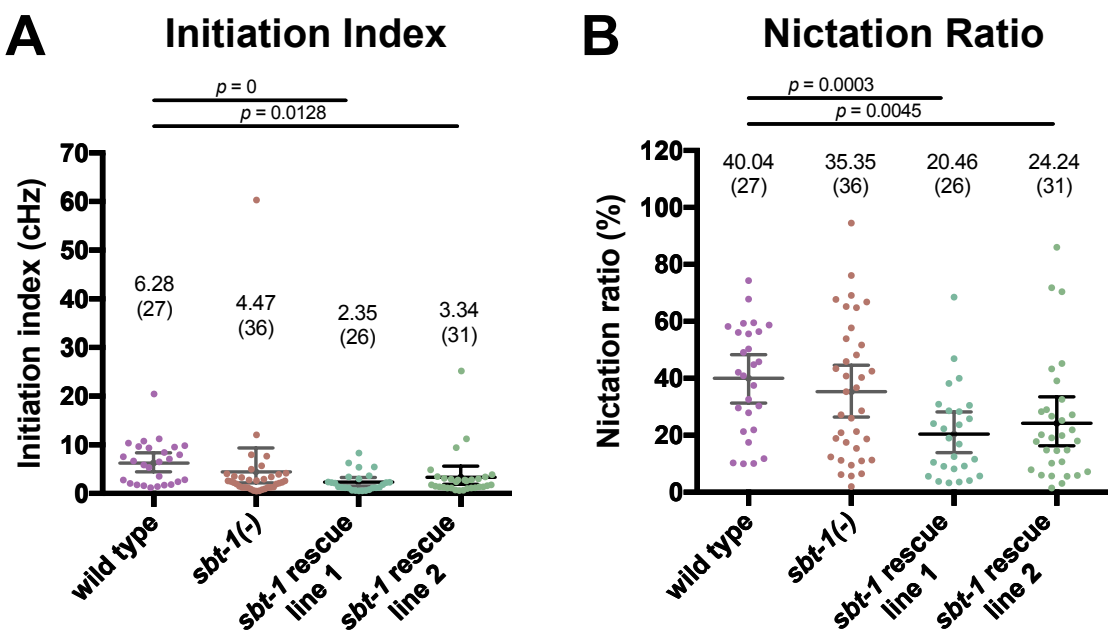

Figure 2.7. Nictation initiation and the proportion of time spent nictating are not significantly affected in *sbt-1* null mutants. (A-B) Nictation initiation (A) and ratio (B) measurements that were collected simultaneously with the nictation duration data in Figure 4D. Bootstrapped means and 99% confidence intervals are indicated. Statistic: permutation test.

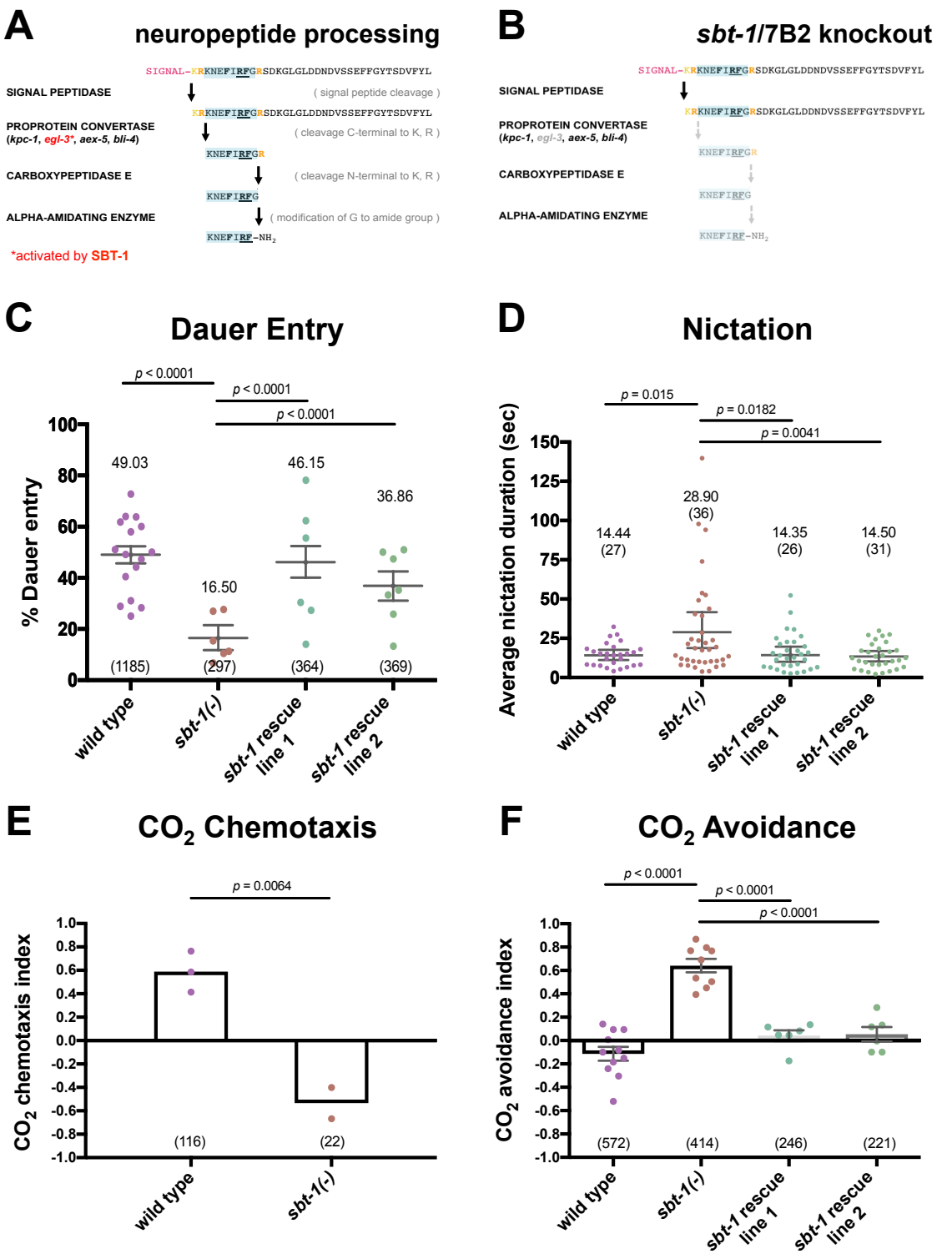

Figure 2.8. Neuropeptide signaling promotes dauer entry and dispersal behaviors. (A-B) Neuropeptide processing in wild type (A) and *sbt-1* null (B), using the FLP-8 peptide

sequence as an example. (C-D) Dauer entry (C) and nictation duration (D) assays. Bootstrapped means and 99% confidence intervals are indicated. (E-F) CO_2 chemotaxis (E) and avoidance (F) assays. Means and SEM are indicated. For (C-F), each dot is one trial, and the N tested is in parentheses. Statistic: permutation test (C-D), two-tailed t (E), one-way ANOVA (F).

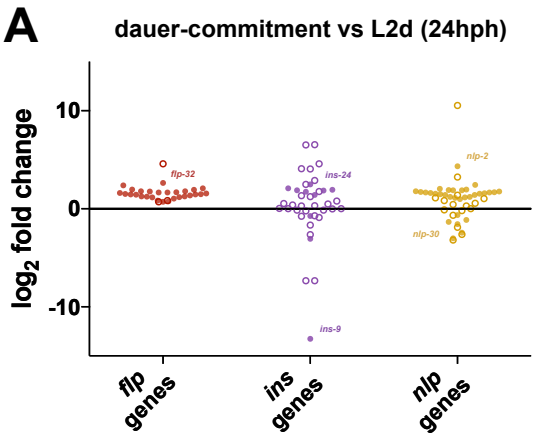

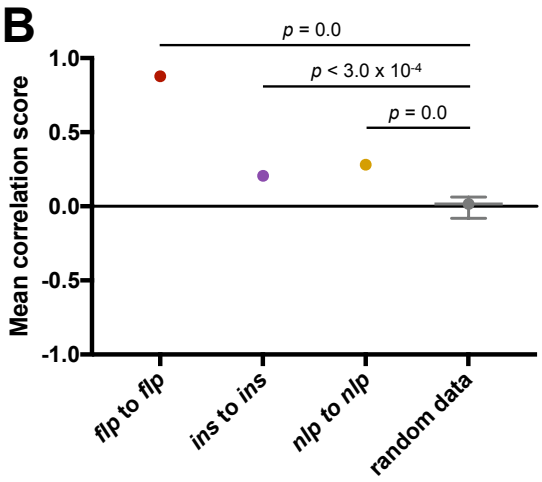

C Dauer Entry

Genotype	Mutant dauer entry %[a]	Wild type dauer entry %[a]	Δ Dauer entry prob.[b]	*p* value[c]	Significance[d]	N mutants tested	N wild type tested	Strain tested
flp-1(yn4)	12.12	72.27	-0.59	0.000	****	99	743	NY16
flp-2(ok3351)	81.15	46.51	0.34	0.000	****	260	744	PS7370[g]
W07E11.1 & flp-2(gk1039)	52.34	46.51	0.06	0.082	ns	321	744	PS7378[g]
flp-3(ok3265)	36.27	46.51	-0.10	0.013	ns	193	744	PS7379[g]
flp-6(ok3056)	88.36	72.27	0.16	0.000	****	292	743	VC2324
flp-7(ok2625)	50.84	56.50	-0.06	0.032	ns	419	1954	RB1990
flp-8(pk360)	24.19	85.51	-0.61	0.000	****	124	283	PT501[i]
flp-10(ok2624)	30.08	46.51	-0.16	0.001	*	123	744	RB1989
flp-11(tm2706)	43.02	72.27	-0.29	0.000	****	172	743	FX02706
flp-12(ok2409)	35.29	40.73	-0.05	0.294	ns	102	960	RB1863
flp-13 (tm2427)	44.21	47.96	-0.04	0.475	ns	190	196	PS6813[g]
flp-17(n4894)	20.47	40.73	-0.20	0.000	****	215	960	MT15933[i]
flp-18(db99)	90.11	54.39	0.35	0.000	****	91	706	AX1410[i]
flp-20(ok2964)	30.43	40.73	-0.10	0.058	ns	92	960	RB2188
flp-21(ok889)	52.38	56.50	-0.04	0.114	ns	462	1954	RB982
flp-21(pk1601)	20.57	56.50	-0.36	0.000	****	982	1954	AX1129[f]
flp-21(sy880)	29.79	47.96	-0.18	0.004	ns	94	196	PS7371[e]
flp-25(gk1016)	56.40	72.27	-0.16	0.000	****	344	743	VC1982
flp-26(gk3015)	45.06	72.27	-0.27	0.000	****	162	743	VC3017
flp-32(sy853)	38.18	49.03	-0.10	0.128	ns	55	1185	PS7219[h]
flp-34 (ok3071)	47.92	49.03	-0.01	0.882	ns	48	1185	PS7221[g]
flp-34 (sy810)	67.33	49.03	0.18	0.001	*	101	1185	PS7220[g]
flp-34 (sy811)	67.86	49.03	0.18	0.006	ns	56	1185	PS7279[f]

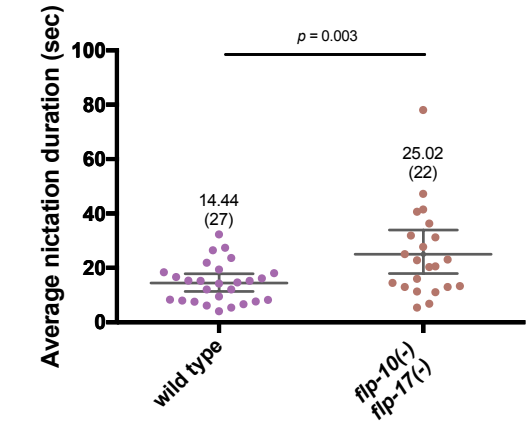

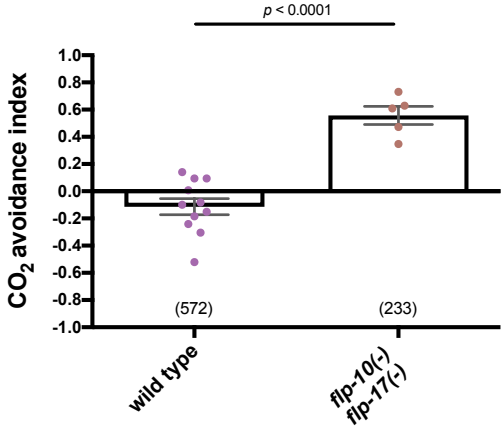

Figure 2.9. FMRFamide-like peptides are coordinately up-regulated during dauer development. (A) Fold changes in gene expression for all 118 *C. elegans* neuropeptide genes. Closed and open circles indicate significant and non-significant differential expression, respectively. The most up- and down-regulated genes of each family are labeled for reference. (B) Average Spearman correlation scores of genes to other genes of the same neuropeptide family, calculated across our RNA-seq dataset. Indicated is the bootstrapped mean and 99% confidence interval. (C) Survey for *flp* genes involved in the dauer entry decision. Footnotes: a−mean percentage calculated by nonparametric bootstrapping. b−the mean difference in dauer entry probability between wild type and mutant animals, calculated using Bayesian probability. c−calculated via permutation test. d−determined using a cutoff of Bonferroni-corrected p-value < 0.05: ****$p < 0.0001$, *$p < 0.05$, ns, not significant. e to j−strains outcrossed 1, 2, 3, 4, >4 and 6 times, respectively. (D-E) Nictation duration (D) and CO_2 avoidance (E) assays.

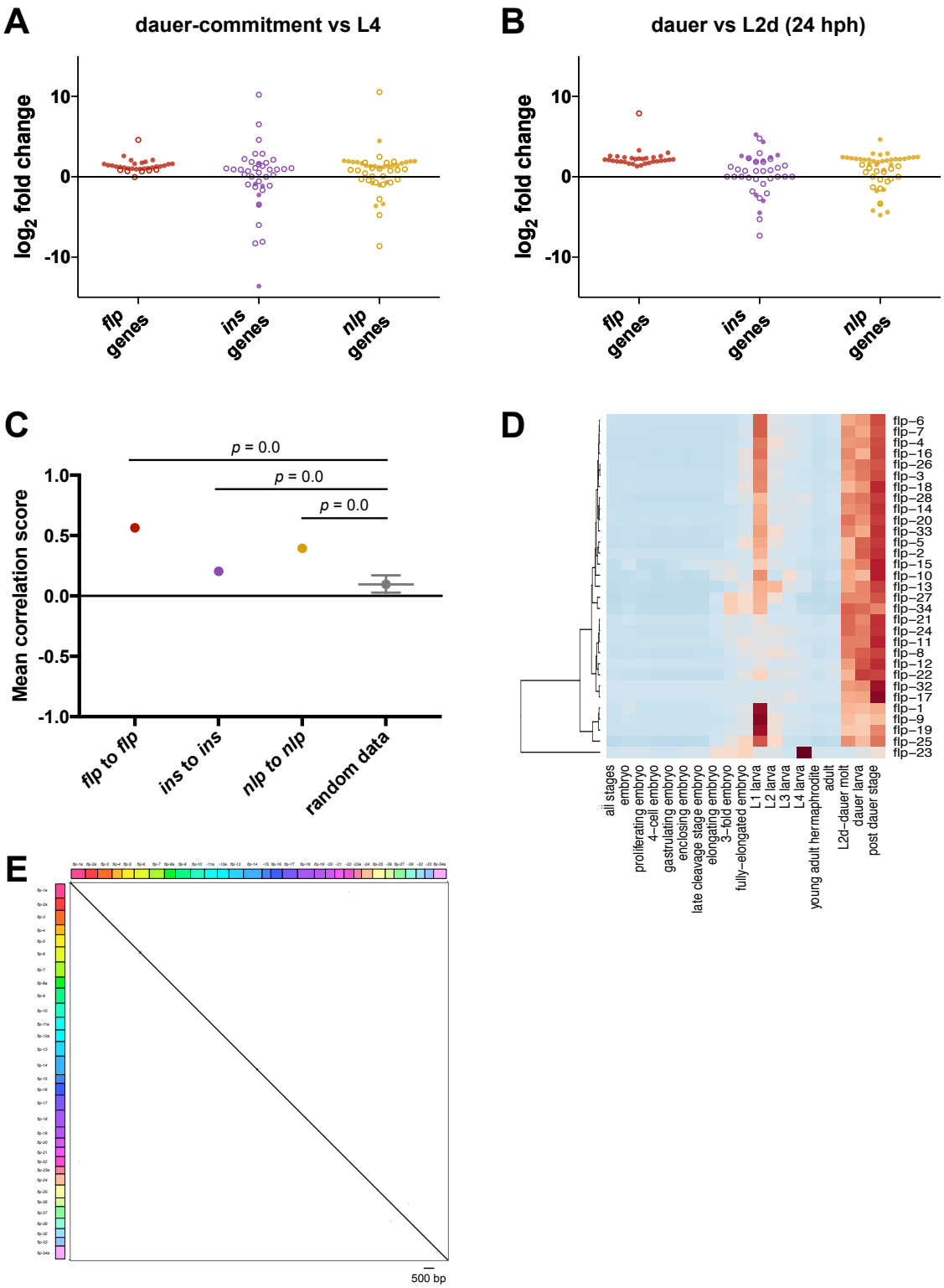
A
dauer-commitment vs L4
log2 fold change
10
0
-10
flp genes
ins genes
nlp genes
B
dauer vs L2d (24 hph)
log2 fold change
10
0
-10
flp genes
ins genes
nlp genes
C
p = 0.0
p = 0.0
p = 0.0
Mean correlation score
1.0
0.5
0.0
-0.5
-1.0
flp to flp
ins to ins
nlp to nlp
random data
D
flp–6
flp–7
flp–4
flp–16
flp–26
flp–3
flp–18
flp–28
flp–14
flp–20
flp–33
flp–5
flp–2
flp–15
flp–10
flp–13
flp–27
flp–34
flp–21
flp–24
flp–11
flp–8
flp–12
flp–22
flp–32
flp–17
flp–1
flp–9
flp–19
flp–25
flp–23
all stages
embryo
proliferating embryo
4–cell embryo
gastrulating embryo
enclosing embryo
late cleavage stage embryo
elongating embryo
3–fold embryo
fully–elongated embryo
L1 larva
L2 larva
L3 larva
L4 larva
young adult hermaphrodite
adult
L2d–dauer molt
dauer larva
post dauer stage
E
500 bp

Figure 2.10. FMRFamide-like peptides are coordinately up-regulated during dauer development. (A) Fold changes in gene expression for all 118 *C. elegans* neuropeptide genes during dauer-commitment versus L4 and (B) dauer versus L2d. Each circle represents an individual neuropeptide gene. Closed and open circles indicate significant and non-significant differential expression, respectively. (C) Average Spearman correlation scores of genes to other genes of the same neuropeptide family, calculated across 246 publically available RNA-seq datasets describing various *C. elegans* life stages and experimental conditions, including embryos, larvae, adults, and males (6). (D) Heatmap of *flp* median gene expression (analyzed in TPM) across the 246 RNA-seq datasets (6). The expression data was scaled and heatmapped as in Figure 3. (E) Dotplot of the coding sequences of all 31 *flp* genes, compared against each other. The x- and y-axes represent the concatenated coding sequences of the 31 *flp* genes (using only the a isoform, if multiple isoforms exist for that gene). Regions of sequence similarity are represented as a diagonal line of hits along the alignment space, and a minimum of 20 identical, consecutive nucleotides were required to generate a hit.

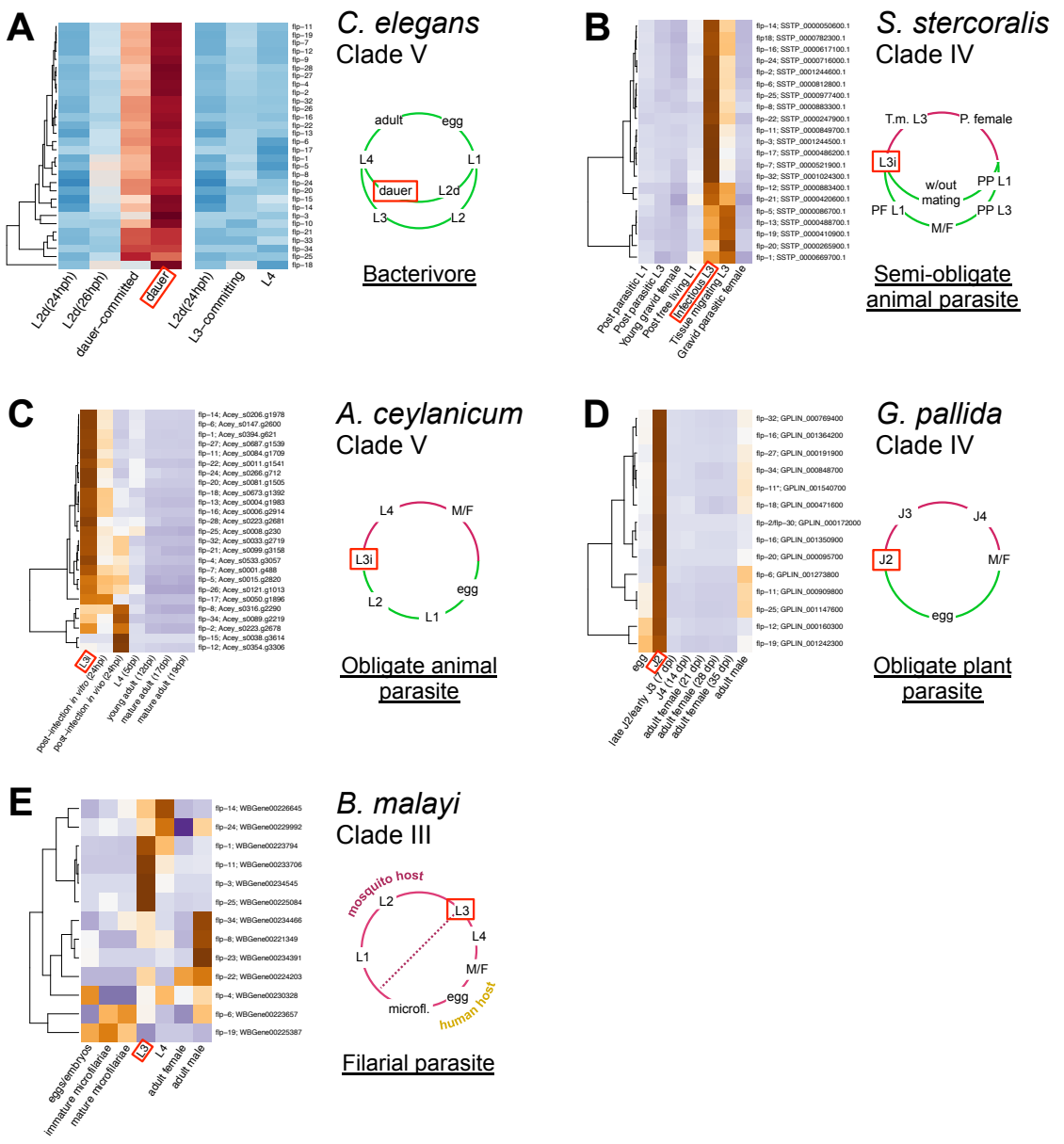

Figure 2.11. FMRFamide-like peptides are coordinately up-regulated in host-seeking infective juveniles of parasitic nematodes. The life cycle and clade membership (out of five major clades of Nematoda (108)) of each species are indicated to the right of each heatmap. Green life cycle regions indicate stages that are free-living or external to a host. Red life cycle regions indicate stages internal to a host. The dauer and infective juvenile stages are highlighted in red boxes. (A) Expression of *flp* genes in the free-living

C. elegans (from our data). Red and blue indicate high and low expression scores, respectively. (B-E) Expression of *flp* orthologs/analogs in the transcriptomes of (B) the semi-obligate animal parasite *Strongyloides stercoralis*, (C) the obligate animal parasite *Ancylostoma ceylanicum*, (D) the obligate plant parasite *Globodera pallida*, and (E) the filarial parasite *Brugia malayi*. Orange and purple indicate high and low expression scores, respectively. Transcriptomic data from (70-73). Abbreviations are PP: post-parasitic, M/F: adult male and female, PF: post-free-living, T.m.: tissue migrating, P. female: parasitic female.

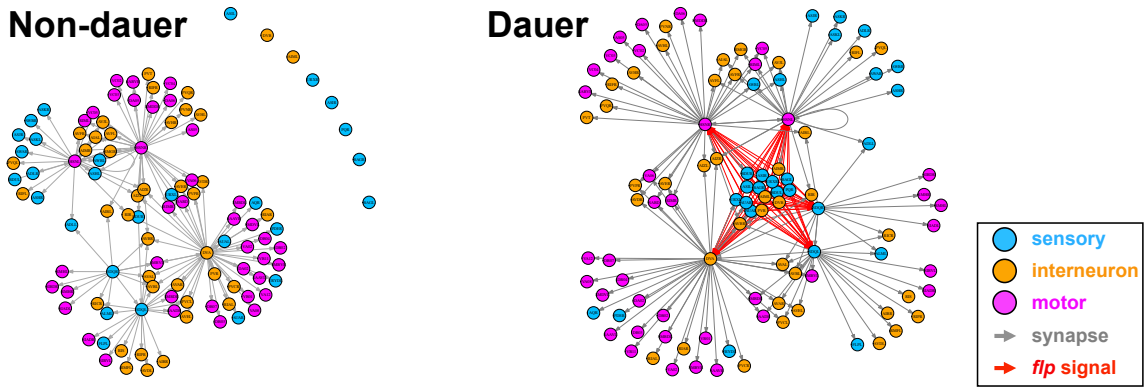

Figure 2.12. Model of circuit changes during dauer development via non-synaptic FLP signaling. The FLP-10 ligand EGL-6 receptor circuit is shown as an example. The synaptic connections that are indicated are (in pre-synaptic to post-synaptic order) from *flp-10* expressing neurons to *egl-6* expressing neurons to directly downstream synaptic targets. Expression pattern, connectomic, and biochemical data was used from (7-9), WormWiring, and WormBase.

2.7 References

1. McLaughlin KA*, et al.* (2015) Causal effects of the early caregiving environment on development of stress response systems in children. *Proceedings of the National Academy of Sciences of the United States of America* 112(18):5637-5642.

2. McQuaid RJ, McInnis OA, Stead JD, Matheson K, & Anisman H (2013) A paradoxical association of an oxytocin receptor gene polymorphism: early-life adversity and vulnerability to depression. *Frontiers in neuroscience* 7:128.

3. Reichmann F & Holzer P (2016) Neuropeptide Y: A stressful review. *Neuropeptides* 55:99-109.

4. Teicher MH, Samson JA, Anderson CM, & Ohashi K (2016) The effects of childhood maltreatment on brain structure, function and connectivity. *Nat Rev Neurosci* 17(10):652-666.

5. Gilbert SF (2000) Developmental Biology. (Sinauer Associates, Sunderland (MA)).

6. Fusco G & Minelli A (2010) Phenotypic plasticity in development and evolution: facts and concepts. Introduction. *Philosophical transactions of the Royal Society of London. Series B, Biological sciences* 365(1540):547-556.

7. Janzen FJ & Phillips PC (2006) Exploring the evolution of environmental sex determination, especially in reptiles. *J Evol Biol* 19(6):1775-1784.

8. Woodward DE & Murray JD (1993) On the effect of temperature-dependent sex determination on sex ratio and survivorship in crocodilians. *Proceedings of the Royal Society of London. Series B: Biological Sciences* 252(1334):149.

9. Newman RA (1992) Adaptive plasticity in amphibian metamorphosis. *BioScience* 42(9):671-678.

10. Cassada RC & Russell RL (1975) The dauerlarva, a post-embryonic developmental variant of the nematode *Caenorhabditis elegans*. *Developmental biology* 46(2):326-342.

11. Fielenbach N & Antebi A (2008) *Caenorhabditis elegans* dauer formation and the molecular basis of plasticity. *Genes & development* 22(16):2149-2165.

12. Golden JW & Riddle DL (1984) The *Caenorhabditis elegans* dauer larva: developmental effects of pheromone, food, and temperature. *Developmental biology* 102(2):368-378.

13. Schaedel ON, Gerisch B, Antebi A, & Sternberg PW (2012) Hormonal signal amplification mediates environmental conditions during development and controls an irreversible commitment to adulthood. *PLoS biology* 10(4):e1001306.

14. Wadsworth WG & Riddle DL (1989) Developmental regulation of energy metabolism in *Caenorhabditis elegans*. *Developmental biology* 132(1):167-173.

15. Oriordan VB & Burnell AM (1990) Intermediary metabolism in the dauer larva of the nematode *Caenorhabditis-Elegans*. 2. The Glyoxylate Cycle and Fatty-Acid Oxidation. *Comp Biochem Phys B* 95(1):125-130.

16. Albert PS & Riddle DL (1983) Developmental alterations in sensory neuroanatomy of the *Caenorhabditis elegans* dauer larva. *The Journal of comparative neurology* 219(4):461-481.

17. Schroeder NE*, et al.* (2013) Dauer-specific dendrite arborization in *Caenorhabditis elegans* is regulated by KPC-1/Furin. *Current Biology* 23(16):1527-1535.

18. Hallem EA*, et al.* (2011) A sensory code for host seeking in parasitic nematodes. *Current biology : CB* 21(5):377-383.

19. Lee H*, et al.* (2012) Nictation, a dispersal behavior of the nematode *Caenorhabditis elegans*, is regulated by IL2 neurons. *Nature neuroscience* 15(1):107-112.

20. Vanfleteren JR & Braeckman BP (1999) Mechanisms of life span determination in *Caenorhabditis elegans*. *Neurobiol Aging* 20(5):487-502.

21. Klass M & Hirsh D (1976) Non-ageing developmental variant of *Caenorhabditis elegans*. *Nature* 260(5551):523-525.

22. Erkut C*, et al.* (2013) Molecular strategies of the *Caenorhabditis elegans* dauer larva to survive extreme desiccation. *PloS one* 8(12):e82473.

23. Gerstein MB*, et al.* (2010) Integrative analysis of the *Caenorhabditis elegans* genome by the modENCODE project. *Science* 330(6012):1775-1787.

24. Wang J & Kim SK (2003) Global analysis of dauer gene expression in *Caenorhabditis elegans*. *Development* 130(8):1621-1634.

25. Karp X (2016) Working with dauer larvae. *WormBook : the online review of Caenorhabditis elegans biology*:1-19.

26. Husson SJ & Schoofs L (2007) Altered neuropeptide profile of *Caenorhabditis elegans* lacking the chaperone protein 7B2 as analyzed by mass spectrometry. *FEBS letters* 581(22):4288-4292.

27. Li C & Kim K (2014) Family of FLP peptides in *Caenorhabditis elegans* and related nematodes. *Frontiers in endocrinology* 5:150.

28. Pierce SB*, et al.* (2001) Regulation of DAF-2 receptor signaling by human insulin and *ins-1*, a member of the unusually large and diverse *Caenorhabditis elegans* insulin gene family. *Genes & development* 15(6):672-686.

29. Jia K, Albert PS, & Riddle DL (2002) DAF-9, a cytochrome P450 regulating *Caenorhabditis elegans* larval development and adult longevity. *Development* 129(1):221-231.

30. Motola DL*, et al.* (2006) Identification of ligands for DAF-12 that govern dauer formation and reproduction in *Caenorhabditis elegans*. *Cell* 124(6):1209-1223.

31. Gerisch B, Weitzel C, Kober-Eisermann C, Rottiers V, & Antebi A (2001) A hormonal signaling pathway influencing *Caenorhabditis elegans* metabolism, reproductive development, and life span. *Developmental cell* 1(6):841-851.

32. Sulston JE & Horvitz HR (1977) Post-embryonic cell lineages of the nematode, *Caenorhabditis elegans*. *Developmental biology* 56(1):110-156.

33. Marinov GK*, et al.* (2014) From single-cell to cell-pool transcriptomes: stochasticity in gene expression and RNA splicing. *Genome research* 24(3):496-510.

34. Miura F*, et al.* (2008) Absolute quantification of the budding yeast transcriptome by means of competitive PCR between genomic and complementary DNAs. *BMC genomics* 9:574.

35. Aken BL*, et al.* (2016) The Ensembl gene annotation system. *Database (Oxford)* 2016.

36. Howe KL*, et al.* (2016) WormBase 2016: expanding to enable helminth genomic research. *Nucleic Acids Res* 44(D1):D774-780.

37. Anders S & Huber W (2010) Differential expression analysis for sequence count data. *Genome biology* 11(10):R106.

38. Anders S*, et al.* (2013) Count-based differential expression analysis of RNA sequencing data using R and Bioconductor. *Nat Protoc* 8(9):1765-1786.

39. Jones SJ*, et al.* (2001) Changes in gene expression associated with developmental arrest and longevity in *Caenorhabditis elegans*. *Genome research* 11(8):1346-1352.

40. Futschik ME & Carlisle B (2005) Noise-robust soft clustering of gene expression time-course data. *J Bioinform Comput Biol* 3(4):965-988.

41. Kumar L & M EF (2007) Mfuzz: a software package for soft clustering of microarray data. *Bioinformation* 2(1):5-7.

42. Kanehisa M, Furumichi M, Tanabe M, Sato Y, & Morishima K (2017) KEGG: new perspectives on genomes, pathways, diseases and drugs. *Nucleic Acids Res* 45(D1):D353-D361.

43. Kanehisa M & Goto S (2000) KEGG: kyoto encyclopedia of genes and genomes. *Nucleic Acids Res* 28(1):27-30.

44. Kanehisa M, Sato Y, Kawashima M, Furumichi M, & Tanabe M (2016) KEGG as a reference resource for gene and protein annotation. *Nucleic Acids Res* 44(D1):D457-462.

45. Mi H*, et al.* (2017) PANTHER version 11: expanded annotation data from Gene Ontology and Reactome pathways, and data analysis tool enhancements. *Nucleic Acids Res* 45(D1):D183-D189.

46. Kaplan F*, et al.* (2011) Ascaroside expression in *Caenorhabditis elegans* is strongly dependent on diet and developmental stage. *PloS one* 6(3):e17804.

47. von Reuss SH*, et al.* (2012) Comparative metabolomics reveals biogenesis of ascarosides, a modular library of small-molecule signals in C. elegans. *J Am Chem Soc* 134(3):1817-1824.

48. Li C & Kim K (2008) Neuropeptides. *WormBook : the online review of C. elegans biology*:1-36.

49. Cohen M*, et al.* (2009) Coordinated regulation of foraging and metabolism in *Caenorhabditis elegans* by RFamide neuropeptide signaling. *Cell metabolism* 9(4):375-385.

50. Lee D, Lee H, Kim N, Lim DS, & Lee J (2017) Regulation of a hitchhiking behavior by neuronal insulin and TGF-beta signaling in the nematode *Caenorhabditis elegans*. *Biochem Biophys Res Commun* 484(2):323-330.

51. Braeckman BP, Houthoofd K, & Vanfleteren JR (2009) Intermediary metabolism. *WormBook : the online review of Caenorhabditis elegans biology*:1-24.

52. Ghosh S & Sternberg PW (2014) Spatial and molecular cues for cell outgrowth during *Caenorhabditis elegans* uterine development. *Developmental biology* 396(1):121-135.

53. Gupta BP, Hanna-Rose W, & Sternberg PW (2012) Morphogenesis of the vulva and the vulval-uterine connection. *WormBook : the online review of Caenorhabditis elegans biology*:1-20.

54. L'Hernault SW (2006) Spermatogenesis. *WormBook : the online review of Caenorhabditis elegans biology*:1-14.

55. Hobert O (2013) The neuronal genome of *Caenorhabditis elegans*. *WormBook : the online review of Caenorhabditis elegans biology*:1-106.

56. Kim Y, Bark S, Hook V, & Bandeira N (2011) NeuroPedia: neuropeptide database and spectral library. *Bioinformatics* 27(19):2772-2773.

57. Lindberg I, Tu B, Muller L, & Dickerson IM (1998) Cloning and functional analysis of *Caenorhabditis elegans* 7B2. *DNA and cell biology* 17(8):727-734.

58. Sieburth D*, et al.* (2005) Systematic analysis of genes required for synapse structure and function. *Nature* 436(7050):510-517.

59. Shen LL, Wang Y, & Wang DY (2007) Involvement of genes required for synaptic function in aging control in *Caenorhabditis elegans*. *Neuroscience bulletin* 23(1):21-29.

60. Kiontke K & Sudhaus W (2006) Ecology of *Caenorhabditis* species. *WormBook : the online review of Caenorhabditis elegans biology*:1-14.

61. Felix MA & Braendle C (2010) The natural history of *Caenorhabditis elegans*. *Current biology : CB* 20(22):R965-969.

62. Hallem EA & Sternberg PW (2008) Acute carbon dioxide avoidance in *Caenorhabditis elegans*. *Proceedings of the National Academy of Sciences of the United States of America* 105(23):8038-8043.

63. Krumsiek J, Arnold R, & Rattei T (2007) Gepard: a rapid and sensitive tool for creating dotplots on genome scale. *Bioinformatics* 23(8):1026-1028.

64. Smith ES, Martinez-Velazquez L, & Ringstad N (2013) A chemoreceptor that detects molecular carbon dioxide. *Journal of Biological Chemistry* 288(52):37071-37081.

65. Kim K & Li C (2004) Expression and regulation of an FMRFamide-related neuropeptide gene family in *Caenorhabditis elegans*. *J Comp Neurol* 475(4):540-550.

66. Ringstad N & Horvitz HR (2008) FMRFamide neuropeptides and acetylcholine synergistically inhibit egg-laying by *Caenorhabditis elegans*. *Nature neuroscience* 11(10):1168-1176.

67. Viney ME (2009) How did parasitic worms evolve? *BioEssays : news and reviews in molecular, cellular and developmental biology* 31(5):496-499.

68. Okumura E & Yoshiga T (2014) Host orientation using volatiles in the phoretic nematode *Caenorhabditis japonica*. *J Exp Biol* 217(18):3197-3199.

69. McCoy CJ*, et al.* (2014) New insights into the FLPergic complements of parasitic nematodes: informing deorphanisation approaches. *EuPA open proteomics* 3:262-272.

70. Choi YJ*, et al.* (2011) A deep sequencing approach to comparatively analyze the transcriptome of lifecycle stages of the filarial worm, *Brugia malayi*. *PLoS neglected tropical diseases* 5(12):e1409.

71. Cotton JA*, et al.* (2014) The genome and life-stage specific transcriptomes of *Globodera pallida* elucidate key aspects of plant parasitism by a cyst nematode. *Genome biology* 15(3):R43.

72. Schwarz EM*, et al.* (2015) The genome and transcriptome of the zoonotic hookworm *Ancylostoma ceylanicum* identify infection-specific gene families. *Nature genetics* 47(4):416-422.

73. Stoltzfus JD, Minot S, Berriman M, Nolan TJ, & Lok JB (2012) RNAseq analysis of the parasitic nematode *Strongyloides stercoralis* reveals divergent regulation of canonical dauer pathways. *PLoS neglected tropical diseases* 6(10):e1854.

74. Bain O & Babayan S (2003) Behaviour of filariae: morphological and anatomical signatures of their life style within the arthropod and vertebrate hosts. *Filaria journal* 2(1):16.

75. Felix MA & Duveau F (2012) Population dynamics and habitat sharing of natural populations of *Caenorhabditis elegans* and *C. briggsae*. *BMC biology* 10:59.

76. Nusbaum MP, Blitz DM, Swensen AM, Wood D, & Marder E (2001) The roles of co-transmission in neural network modulation. *Trends in neurosciences* 24(3):146-154.

77. Salio C, Lossi L, Ferrini F, & Merighi A (2006) Neuropeptides as synaptic transmitters. *Cell Tissue Res* 326(2):583-598.

78. Landgraf R & Neumann ID (2004) Vasopressin and oxytocin release within the brain: a dynamic concept of multiple and variable modes of neuropeptide communication. *Frontiers in neuroendocrinology* 25(3-4):150-176.

79. Bargmann CI (2012) Beyond the connectome: how neuromodulators shape neural circuits. *BioEssays : news and reviews in molecular, cellular and developmental biology* 34(6):458-465.

80. Jekely G (2013) Global view of the evolution and diversity of metazoan neuropeptide signaling. *Proceedings of the National Academy of Sciences of the United States of America* 110(21):8702-8707.

81. Dockray GJ (2004) The expanding family of -RFamide peptides and their effects on feeding behaviour. *Experimental physiology* 89(3):229-235.

82. Elphick MR & Mirabeau O (2014) The evolution and variety of RFamide-type neuropeptides: insights from deuterostomian invertebrates. *Frontiers in endocrinology* 5:93.

83. Cardoso JC, Felix RC, Fonseca VG, & Power DM (2012) Feeding and the rhodopsin family g-protein coupled receptors in nematodes and arthropods. *Frontiers in endocrinology* 3:157.

84. Guillermin ML, Castelletto ML, & Hallem EA (2011) Differentiation of carbon dioxide-sensing neurons in *Caenorhabditis elegans* requires the ETS-5 transcription factor. *Genetics* 189(4):1327-1339.

85. White JG, Southgate E, Thomson JN, & Brenner S (1986) The structure of the nervous system of the nematode *Caenorhabditis elegans*. *Philosophical transactions of the Royal Society of London. Series B, Biological sciences* 314(1165):1-340.

86. Dalzell JJ, McMaster S, Fleming CC, & Maule AG (2010) Short interfering RNA-mediated gene silencing in *Globodera pallida* and *Meloidogyne incognita* infective stage juveniles. *International journal for parasitology* 40(1):91-100.

87. Morris R*, et al.* (2017) A neuropeptide modulates sensory perception in the entomopathogenic nematode *Steinernema carpocapsae*. *PLoS Pathog* 13(3):e1006185.

88. Sudhaus W (2010) Preadaptive plateau in Rhabditida (Nematoda) allowed the repeated evolution of zooparasites, with an outlook on evolution of life cycles within Spiroascarida. *Palaeodiversity* 3, Supplement:117-130.

89. De Ley P (2006) A quick tour of nematode diversity and the backbone of nematode phylogeny. *WormBook : the online review of Caenorhabditis elegans biology*:1-8.

90. Han Z, Boas S, & Schroeder NE (2015) Unexpected variation in neuroanatomy among diverse nematode species. *Front Neuroanat* 9:162.

91. Brenner S (1974) The genetics of *Caenorhabditis elegans*. *Genetics* 77(1):71-94.

92. Mello C & Fire A (1995) DNA transformation. *Methods in cell biology* 48:451-482.

93. Maduro M & Pilgrim D (1995) Identification and cloning of *unc-119,* a gene expressed in the *Caenorhabditis elegans* nervous system. *Genetics* 141(3):977-988.

94. Arribere JA*, et al.* (2014) Efficient marker-free recovery of custom genetic modifications with CRISPR/Cas9 in *Caenorhabditis elegans*. *Genetics* 198(3):837-846.

95. Wickham H (2009) *ggplot2: Elegant Graphics for Data Analysis* (Springer-Verlag New York).

96. Yu G, Wang LG, Han Y, & He QY (2012) clusterProfiler: an R package for comparing biological themes among gene clusters. *OMICS* 16(5):284-287.

97. Warnes GR*, et al.* (2016) gplots: Various R programming tools for plotting data.

98. Neuwirth E (2014) RColorBrewer: ColorBrewer Palettes. R package version 1.1-2.

99. Jones E, Oliphant T, & Peterson P (2001) SciPy: open source scientific tools for Python.

100. Bray NL, Pimentel H, Melsted P, & Pachter L (2016) Near-optimal probabilistic RNA-seq quantification. *Nature biotechnology* 34(5):525-527.

101. Pachter L (2011) Models for transcript quantification from RNA-Seq. *arXiv*. eprint arXiv:1104.3889(eprint arXiv:1104.3889):eprint arXiv:1104.3889.

102. Golden JW & Riddle DL (1984) A pheromone-induced developmental switch in *Caenorhabditis elegans*: Temperature-sensitive mutants reveal a wild-type temperature-dependent process. *Proceedings of the National Academy of Sciences of the United States of America* 81(3):819-823.

103. Efron B & Tibshirani RJ (1994) *An introduction to the bootstrap* (CRC press).

104. Sivia DS & Skilling J (2006) *Data analysis: a Bayesian tutorial* (Oxford University Press).

105. Jones E, Oliphant T, & Peterson P (2001) SciPy: open source scientific tools for Python.

106. Bargmann CI, Hartwieg E, & Horvitz HR (1993) Odorant-selective genes and neurons mediate olfaction in *Caenorhabditis elegans*. *Cell* 74(3):515-527.

107. McVeigh P*, et al.* (2005) Analysis of FMRFamide-like peptide (FLP) diversity in phylum Nematoda. *International journal for parasitology* 35(10):1043-1060.

108. Blaxter M & Koutsovoulos G (2015) The evolution of parasitism in Nematoda. *Parasitology* 142 Suppl 1:S26-39.

Chapter 3

GENETIC MARKERS ENABLE THE VERIFICATION AND MANIPULATION OF THE DAUER ENTRY DECISION

(This work was done in collaboration with James Lee)

3.1 Abstract

Phenotypic plasticity allows animals to survive in changing environments through the alteration of phenotypes or development. One of the best-studied examples of phenotypic plasticity is dauer larval development in the free-living roundworm *Caenorhabditis elegans*. When faced with hostile environments, *C. elegans* larvae can exit reproductive development and enter the stress-resistant and spore-like dauer larval stage. However, knowledge about how the dauer entry decision is made, and how the different tissues of the animal coordinate to execute transformation into dauer is limited. This is because identifying animals that make the entry decision, or that fail to coordinately remodel its tissues during dauer development is time-consuming and labor-intensive. Utilizing our previously reported RNA-seq of animals going through dauer or reproductive development (Lee et al., 2017), we have identified genetic markers for conveniently tracking and manipulating the dauer entry decision. These include *col-183* (which tracks dauer fate in the hypodermis), *ets-10* (neurons and intestine), *nhr-246* (intestine and muscle), and *F53F1.4* (reproductive fate in hypodermis). Using condition shift experiments, we demonstrate that the dauer-specific fluorescence expressions of the markers correspond to the commitment event of the dauer entry decision, and therefore label when the decision is made. We show that these markers can be used to manipulate the entry decision by driving the reproduction-promoting gene *daf-9*/Cytochrome P450 under the control of the dauer-specific marker *col-183*, through which we could shift animals into non-dauer development. We further demonstrate that the markers can be used to track tissue coordination and its breakdown in partial dauer mutants, as *daf-9*, *daf-15*, and *daf-18* partial dauers exhibit partial expression of the *ets-10* reporter. We therefore propose strategies for

using the markers to identify the intercellular signals that coordinate the dauer entry decision. Our findings thus provide strong molecular tools for studying phenotypic plasticity during a whole animal decision.

3.2 Introduction

Phenotypic plasticity enables organisms to respond to changing environments through activation of different phenotypes or alternative developmental courses (1). For example, nutritional factors contribute to the development of morphological distinct ants castes in some species (2), and also influence neuronal plasticity in human (3).

Caenorhabditis elegans can go through two different developmental trajectories depending on the conditions of the environment. In favorable environments, they proceed from L1, L2, L3, and L4 larvae stages to reproductive adults. When the animal senses harsh stimuli, including high temperature, low food, and high amount of pheromone, L1 larva can enter an alternative pre-dauer stage, L2d, and commit to become a dauer if the unfavorable conditions persist. The dauer entry decision is a whole animal decision that involves remodeling of individual tissues to transform the entire animal to have dauer-specific physiology and behaviors. The specialized physiology, the thickened cuticle for example, makes dauer more resistant to environmental insult (4, 5), and the special behaviors enable dauers to disperse to better environments and resume reproductive development (6, 7).

Genes involved in dauer development, including genes in insulin and TGF-beta signaling pathways, have been identified through intense genetic screening (8–11). However, our knowledge regarding how the dauer entry decision is made and how the decision is coordinately executed across different tissues is still limited (12). First, it is difficult to identify L2d, the stage when environmental signals are integrated and the dauer-commitment decision is made, because of its lack of distinct features (13). Additionally, it can be labor-intensive to look for non-dauer features in dauers that fail to coordinately

remodel all the tissues. SDS sensitivity and fluorescent beads are two available tools for dauer hypodermis and pharynx selection (14, 15), but not for other tissues.

We previously reported the time-resolved gene expression profiles from animals going through dauer or reproductive development (16). From the rich dataset, we were able to find genes that are specifically regulated in either of the developmental tracks as potential readouts of the decision. Here we describe four molecular markers that can track the decision at the level of different tissues, and are predictive of the decision. We verified that the markers could also be used to drive gene expression during the dauer entry decision, and to parse incomplete dauer development phenotypes. Our findings provide strong molecular tools for studying phenotypic plasticity during a whole animal decision.

3.3 Results

Dauer and reproductive markers demonstrated specific expression patterns

Unfavorable conditions promote L1 larvae to develop into pre-dauer L2d. Depending on whether the environment improves and enough dafachronic acid (DA) growth hormone gets amplified, L2d larvae can progress to either reproductive or dauer development. In our previous study, we controlled the animals' binary developmental choice by withholding or adding synthetic DA at 24 hours post hatch (hph) to *daf-9(dh6)* mutant, which lack intrinsic DA, and we profiled the transcriptional changes from animals going through dauer (L2d, dauer-committed, and dauer) or reproductive (L3-committing and L4) development (16). To find good markers for dauer, we selected candidate genes based on the following criteria: (i) genes that have high expression specifically during dauer or reproductive development; (ii) genes that are expressed in large tissues, including collagen genes, for convenient observation under low magnification; (iii) genes that might shed light on dauer biology, including transcription factors and unknown genes.

First, 156 of 164 genes in the collagen (*col*) family were detected and differentially expressed in the RNA-seq dataset. Within those, five collagen genes (*col-2*, *col-37*, *col-85*, *col-40* and *col-183*) have the highest transcripts per million (tpm) counts at the dauer-commitment, while having low counts in other stages (Figure 3.1.). Indeed, *col-2* and *col-40* have previously been reported to have specific expression in dauer (16, 22). We made a *col-183p::mcherry* transcriptional reproter strain, and we observed strong mCherry expression exclusively in dauer but not other stages (Figure 3.2.A-3.2.C). *col-*

85 also has similarly high dauer expression, but dauers expressing *col-85p::mcherry* were abnormally sensitive to SDS treatment (data not shown), possibly caused by promoter quenching or toxicity. Because SDS-resistant is a standard way for selecting and verifying dauers, we excluded *col-85* in further experiments.

Second, we detected 274 transcription factor genes that are differentially expressed during dauer and reproductive development. We clustered those genes by their expression profiles, looked for dauer marker candidates, and found 119 that fit our criteria (Figure 3.3). We chose to focus on *ets-10*, a member of the ETS-domain family of transcription factors. The *ets-10* gene had the highest tpm counts during dauer-committed and dauer relative to other stages (Figure 3.2.D). We observed that *ets-10* is expressed in different tissues during dauer and non-dauer (Figure 3.2E-F and Figure 3.4). During dauer, *ets-10p::gfp* was expressed in two sets of neurons and the intestine (Figure 3.2.E-F). In non-dauers, its expression was only observed in uterine cells in L4 animals and spermatheca in adults (Figure 3.4.).

We also investigated the transcription factor *nhr-246*. The tpm counts of *nhr-246* only increased during dauer development and was at its highest level at the dauer-commitment time point (Figure 3.2.G). Other than intestinal expression in embryo and L1 stages, *nhr-246p::gfp* was only detected in dauer in intestine and muscle (Figure 3.2.H-I and Figure 3.5.).

In addition to dauer-specific genes, we also looked for genes that are downregulated specifically in dauer. Out of the five genes we tested — *asp-1*, *F53F1.4*, *sqt-3*, *dpy-13* and *col-156* — *F53F1.4* marker animals were the healthiest, and had the highest tpm reads in reproductive development (Figure 3.6. and Figure 3.2.J). We found that

F53F1.4p::gfp is expressed in the hypodermis at all stages (Figure 3.2.K-L), and the fluorescence intensity was reduced in dauer (data not shown). Because of its expression profile, we propose the gene name *led-1*, which stands for "Low Expression in Dauer".

To sum up, we have developed three dauer markers (*col-183p::mcherry*, *ets-10p::gfp*, and *nhr-246p::gfp*) that have increased expression level and distinct expression patterns in dauers. We have also detected intensity changes in *led-1p::gfp* that mark non-dauers from dauers.

col-183, *ets-10* and *nhr-246* label the dauer commitment decision

Because the dauer marker genes have high expression levels at dauer-commitment, we expected that the fluorescence of these genes might be useful for indicating the dauer-commitment event. If the markers do label the animals that are committed to dauer, then: (i) all dauers will have fluorescence expression (Figure 3.7.A) and (ii) fluorescent animals will still become dauer even if the environment improves (Figure 3.7.B). We found that the fluorescence markers were turned on in all the dauers examined (100% for all three markers strains, with 174-311 animals examined per marker) (Figure 3.7.C). Moreover, after we transferred animals from unfavorable to favorable condition as soon as the fluorescence was detected, we observed that 96% to 100% of the animals still entered dauer despite the shift to reproduction-promoting environment (*col-183p::mcherry* 100%, n=22; *ets-10p::gfp* 100%, n=18; *nhr-246p::gfp* 96%, n=26) (Figure 3.7.D). These data suggest that *col-183* and *ets-10* label the dauer commitment decision, and *nhr-246* labels the decision or slightly before commitment.

The promoters of the dauer markers can be used to manipulate the dauer decision

Reproductive development in *C. elegans* requires the synthesis of DA, the product of DAF-9/cytochrome P450. The timing of *daf-9* expression and the amplification of DA in the hypodermis has been shown to coincide with the critical period of time when L2d animals decide to go through reproductive instead of dauer development (23) (Figure 3.8.A-3.8.B). However, it is not known whether ectopically expressing *daf-9* during dauer-commitment can alter developmental trajectory. We therefore used the *col-183* promoter to overexpress *daf-9* in hypodermis during dauer-commitment when *daf-9* would otherwise be expressed at its lowest (Figure 3.8.C). We then examined the animals' decision between dauer and reproductive development under dauer-inducing conditions. We observed that animals with *daf-9* overexpression were 0.5 times as likely to become dauers compared to those with control *gfp* (*col-183p::daf-9* bootstrap mean = 30%, n = 336; *col-183p::gfp* bootstrap mean = 59%, n = 262) (Figure 3.8.D). This data suggests that the promoters of the dauer markers can be used to drive ectopic gene expression during dauer-commitment, and that *daf-9* hypodermal expression can shift animal development from dauer to adulthood.

The dauer markers can be used to study the coordination between tissues

The dauer entry decision is a whole-animal decision, with all the tissues coordinating dauer development programs. Previous studies have identified partial dauers, where one or more of the tissues fail to coordinate and therefore exhibit non-dauer features. Known partial dauer phenotypes include continued pharyngeal pumping, indistinct dauer alae on the cuticle, and L2/L3-like pharynx, neuron, intestine, or excretory gland morphologies.

For example, *daf-9(e1406)*/cytochrome P450 dauers have a non-dauer intestine, cuticle, pharynx, and neurons(24); *daf-15(m81)*/RAPTOR dauers fail to remodel the cuticle, pharynx, neurons intestine and excretory gland (24); *daf-18(e1375)*/PTEN dauers have an unremodeled, still pumping pharynx, and an intestine that is neither fully dauer nor L3(25).

Because identifying partial dauers relies on close examination of the animal's morphology, it can be time-consuming and requires experience. We therefore utilized the dauer-specific *ets-10p::gfp* expression in neurons and intestine to pinpoint partial dauer phenotypes.

In *daf-9(e1406)* dauers, we confirmed their partial dauer phenotype in the intestine: we observed a 3-fold decrease in *ets-10p::gfp* expression in the intestine compared to wild type dauers (average intensity in wild type = 9017 arbitrary units (a.i.), n = 26; average intensity in *daf-9(e1406)* = 2998 a.i., n = 25) (Figure 3.9.A-B and 3.9.K), providing a clear indication of the non-dauer feature of *daf-9(e1406)* intestines.

We were also able to confirm the intestinal partial dauer phenotype of *daf-15(m81)* animals as well: we observed a 4-fold reduction in *ets-10p::gfp* intestinal expression compared to wild type (average intensity in wild type = 7166 a.i., n = 12; average intensity in *daf-15(m81)* = 1512 a.i., n = 16) (Figure 3.9.C-D and 3.9K). Additionally, we confirmed the neuronal partial dauer phenotype of *daf-15(m81)*, as neuronal *ets-10p::gfp* fluorescence was present in all wild type animals (n=20), but was undetectable (16 out of 20 animals) or dimly expressed (4 out of 20) in *daf-15(m81)* (Figure 3.9.G-H and 3.9.L).

In *daf-18(e1375)*, we observed a slight increase in *ets-10p::gfp* intestinal expression (average intensity in wild type = 3299 a.i., n = 11; average intensity in *daf-18(e1375)* = 5169 a.i., n = 9) (Figure 3.9.E-F and 3.9.K), and the disappearance of neuronal expression in most of the animals (9 out of 10) (Figure 3.9.I-J and 3.9.L). These results not only confirmed the partial dauer characteristic of *daf-18(e1375)* intestine, but also revealed the previously unknown non-dauer characteristic of *daf-18(e1375)* neurons.

From our results, we have identified *ets-10p::gfp* as a tool for studying the execution of the dauer decision in different tissues. We propose a model for how *ets-10* expression is differentially regulated in the dauer intestine and neurons by DAF-9, DAF-15 and DAF-18 (Figure 3.9.M). In the dauer intestine, DAF-15 and DAF-9 promote *ets-10* expression and DAF-18 inhibit *ets-10*; both DAF-15 and DAF-18, but not DAF-9, positively regulate *ets-10* expression in the dauer nervous system. This model suggests that the same signal (*e.g.* DA produced by DAF-9/cytochrome P450) can have distinct effects on the differentiation of different tissues in dauer.

3.4 Discussion

We have described four genetic markers that label dauer or non-dauer animals, and which can be used for conveniently assaying the dauer entry decision. We demonstrated that the dauer markers in fact mark the dauer-commitment decision using condition-shift experiments. Beyond fluorescence labeling, we were able to use the promoter region to manipulate the commitment decision, and to tease apart the tissue-specific defects of partial dauer mutants.

We picked members of the hypodermis-expressed collagen gene family as one of our dauer marker candidates because they fit our criteria of being expressed at high levels and in a large tissue. In addition, they offered the opportunity to learn more about the role of hypodermal *daf-9* expression in the developmental decision. When animals commit to reproductive development, *daf-9* functions by promoting a positive feedback amplification loop in the hypodermis to lock in the decision (23). Even under dauer-inducing conditions, when we introduced *daf-9* expression under the control of *col-183* promoter, we were able to shift the animal's decision toward reproduction.

Notably, dauer-specific collagen expression has been reported before for *col-2* (22), but we are the first to connect the expression of a collagen gene with the dauer-committment decision. We speculate that the biological function of *col-183* is to shape the stress-resistance and impermeability of dauer cuticle starting from the commitment decision (4, 26).

We also looked at the transcription factor gene class for additional marker candidates. We found that both *ets-10* and *nhr-246* demonstrated dauer-specific expression patterns

during dauer-commitment, suggesting their function in execution and maintainance of the dauer program. For instance, the expression of *ets-10* and *nhr-246* in intestine might help establish the specialized intestine structure and metabolism of dauers. We speculate that they participate in remodeling the dauer intestine or switching metabolism from the TCA cycle to long-term lipid metabolism (27, 28).

The full coordination of tissue physiology and function is important for dauer survival. Using these markers, we can study how tissue-coordination is achieved during dauer development. Partial dauers represent breaks in tissue-coordination, and by using the markers we can read out their phenotypes on a molecular level. Using *ets-10* markers, we were able to not only recapitulate known partial dauer phenotypes in *daf-9*, *daf-15* and *daf-18*, but identify the previously unknown function of DAF-18 in remodeling dauer neurons. Moreover, we found that DA and insulin signals (controlled by *daf-9* and *daf-15*, *daf-18*, respectively) are combined in discrete ways to control *ets-10* expression in different tissues. It would be intriguing to figure out how different tissues might use different *cis*-regulatory elements and signaling receptors to interpret the same signal to meet their specialized needs.

We have described three dauer-specific markers and one reproductive-specific marker selected from our previously published dauer RNA-seq time course. We have demonstrated that these markers are useful for tracking the dauer-committment decision, driving gene expression during dauer-committment, and for teasing apart partial dauer phenotypes tissue by tissue. 117 transcription factor genes and 6 collagen genes also fit the selection criteria we used to pick our markers. This selection opens up the exciting

potential of using these genes for further tracking, manipulating, and parsing the dauer entry decision.

3.5 Material and Method

Animal strains.

C. elegans strains were grown using standard protocols with the *Escherichia coli* strain OP50 as a food source (17). The wild type strain is N2 (Bristol). Other animal strains are listed below.

Transgenic strains.

Transcriptional reporter strains. All of the transcriptional reporters were built suing fusion PCR (18). Primers used to amplify the promoter regions and the amplified promoter sizes were as follows: *col-183p* (*col-183* promoter, 1695bp)

forward- AATCGCAAACCTTCAACGAAGAG,

reverse- tcacccttgagaccattaagcGGTTGACTGGTTGCTGTTGCT;

ets-10p (1111bp)

forward- GGTTGACTGGTTGCTGTTGCT,

reverse-agtcgacctgcaggcatgcaagct GTTTGTCAGCTAGTTTGCGG;

nhr-246p (3069bp)

forward- GTTTGTCAGCTAGTTTGCGG,

reverse- agtcgacctgcaggcatgcaagctATTGTTGAAATTGAAAATTATTTTGAA;

F53F1.4p (1851bp)

forward- ATTATGTAGGCCCAATATAAAGTTTGA,

reverse- agtcgacctgcaggcatgcaagct GTTGAAAATGTTGAAAGTCAAAAGAG.

The promoter regions of *ets-10*, *nhr-246* and *F53F1.4* were fused to *gfp::unc-54* 3'UTR (amplified from pPD95_75 from Addgene), and the promoter region of *col-183* was fused to *mCherry::unc-54* 3'UTR (amplified from pGH8 from Addgene). Injection mixture was prepared at a concentration of 20 ng/μL reporter construct, 50 ng/μL *unc-119(+)* rescue construct, and 130 ng/μL 1-kb DNA ladder carrier DNA. Transgenic strain was obtained by microinjecting the mixtures into the adult gonads of *unc-119(ed4)* animals. The *ets-10p::gfp* and *F53F1.4p::gfp* were further integrated into the genome by X-ray (19, 20). The fluorescent transcriptional reporter strains generated were as follows: PS6725 *unc-119(ed4); syEx1337[col-183p::mcherry; unc-119(+)]*; PS7127: *unc-119(ed4); syIs360[ets-10p::gfp; unc-119(+)]* (outcrossed 3 times); PS7921 *unc-119(ed4); syEx1539[nhr-246p::gfp; unc-119(+)]*; PS7920 *unc-119(ed4);* PS6724: *unc-119(ed4); syIs263[F53F1.4p::gfp; unc-119(+)]* (outcrossed 10 times).

Transcriptional reporter in partial dauer mutant backgrounds. The strains with *ets-10p::gfp* expression in *daf-15(m81)* or *daf-9(e1406)* background were generated by crossing PS7127 with DR732 *daf-15(m81) unc-22(s7)/nT1* or AA823 *daf-9(e1406) dhEx354[sdf-9::daf-9cDNA::GFP; lin-15(+)]*. The strain with *ets-10p::gfp* expression in *daf-18(e1375)* background was obtained by microinjecting the injection mixture (20 ng/μL reporter construct, 50 ng/μL *ofm-1p::rfp* coelomocyte co-injection marker, and 130 ng/μL 1-kb DNA ladder carrier DNA) into the adult gonads of CB1375 *daf-18(e1375)*.

daf-9 overexpression strain. col-183 promoter region were cloned into the pSM vector that contains *gfp* or *daf-9* cDNA. *daf-9* cDNA sequence was obtained from Wormbase and

amplified with forward primer ATGCACTTGGAGAACCGTG and reverse primer TTAGTTGATGAGACGATTTCCG. Injection mixture was prepared at a concentration of 20 ng/μL *col-183p::gfp* or *col-183p::daf-9* cDNA, 50 ng/μL *ofm-1p::rfp* coelomocyte co-injection marker, and 130 ng/μL 1-kb DNA ladder carrier DNA. Transgenic strain was obtained by microinjecting the mixtures into the adult gonads of wild type animals. The transgenic strains generated were PS7949 *syEx1628[col-183p::gfp; ofm-1p::rfp]* and PS7931 *syEx1629[col-183p::daf-9 cDNA; ofm-1p::rfp]*.

Dauer induction.

The preparation of crude pheromone and the induction of dauers on pheromone plates were performed with previously described methods (16, 21). Briefly, crude pheromone plates (NGM-agar with added crude pheromone and no peptone) were used to induce synchronized dauers: For each pheromone plate, 20 μL of heat-killed OP50 (8 g/100 mL) were spotted and 12-15 young adult animals were picked onto the plate to lay eggs at 20°C for 3 (for *environmental condition shift*) or 12 hours (for examing fluorescence expression in dauer) before being removed. The plates were then moved to 25.5°C incubation for 48 hours.

Verification of dauer markers.

SDS assay on fluorescent animals

Dauers induced on pheromone plate were identified by morphology and examined for the presence of fluorescence expression. The fluorescence animals were further transferred to

unseeded plates and treated with 1% SDS. The numbers of total and survived animals were scored after 15 minutes.

Environmental condition shift of fluorescent animals.

The fluorescence expression in the transcriptional reporter strains was detectable under dissecting microscope staring around 30-32 hours after egg laid. At 33-34 hour, we transferred the fluorescent animals from dauer-inducing pheromone plates to reproduction-inducing plates, which contain high amount of bacteria and no pheromone. 24 hours after the transfer, the animals were treated with 1% SDS, and the numbers of total and survived animals were scored after 15 minutes.

Quantification of fluorescence intensity.

The fluorescence intensity of *ets-10p::gfp* was measured using ZEISS ZEN microscope software. The regions of interests were drawn on both the intestine and the background area, and the net fluorescence intensity was calculated as the subtraction of the two measurements.

Dauer formation assay.

The preparation of crude pheromone and the dauer entry assay were performed with previously described methods (16, 21). On the day of the experiment, seven to ten young adults were picked onto each pheromone plate (NGM-agar with added crude pheromone and no peptone), and allowed to lay approximately 50-60 eggs before being removed. 20 µl of heat-killed OP50 was added to the plates as a food source for the un-hatched larvae.

After 48 hours of incubation at 25.5°C, dauers and non-dauers were counted on each plate based on their distinct morphologies. The permutation test was used to calculate statistics as previously describe (16).

3.6 Figures

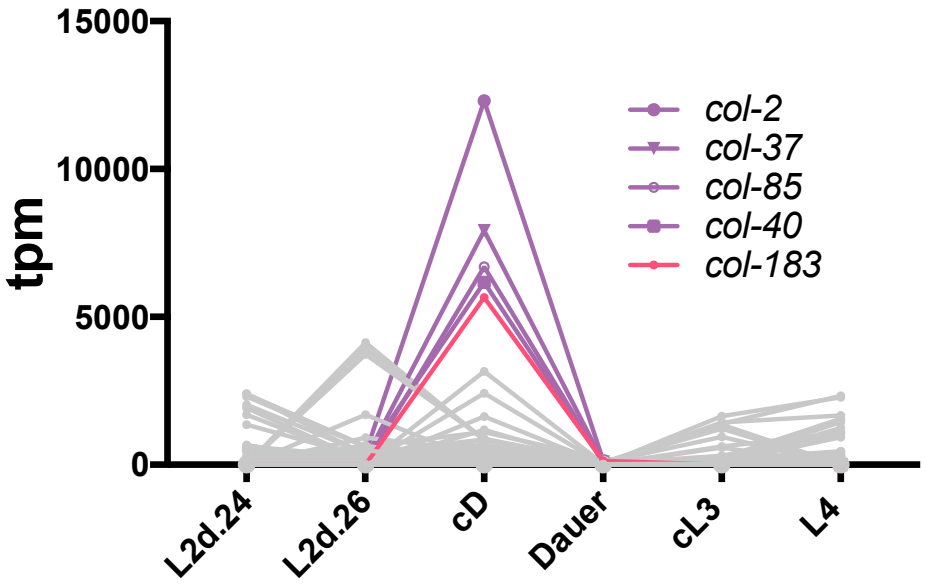

Figure 3.1. Expression profiles of collagen gene

Expression profiles of all the collagen genes detected. Each line represents one collagen gene. The top five genes with the highest expression level were highlighted in purple (*col-2*, *col-37*, *col-85*, and *col-40*) and pink (*col-183*). The rest of the genes were colored in grey for simplicity. All the expression data plotted were from our previous paper (16).

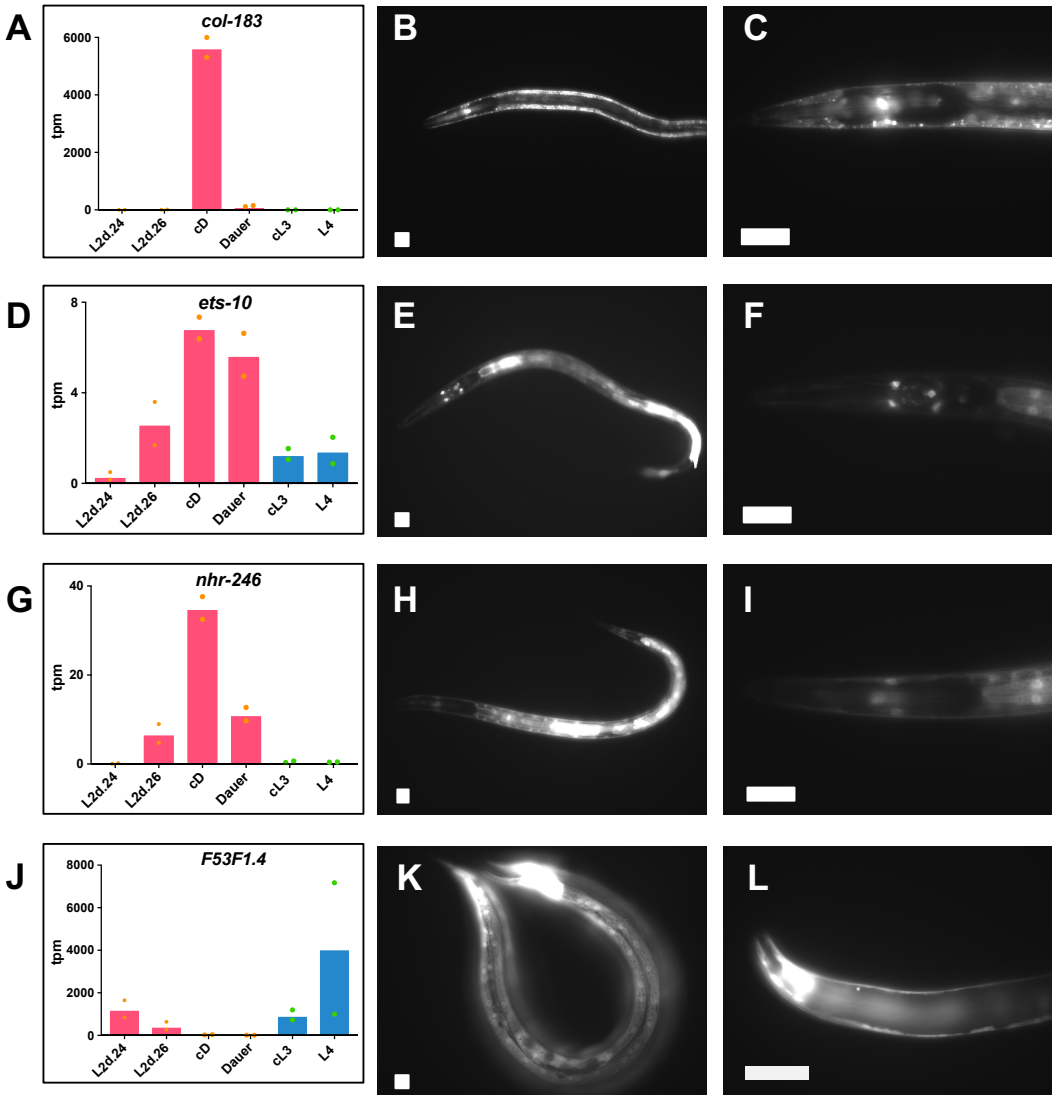

Figure 3.2. *col-183*, *ets-10*, *nrh-246* and *led-1*(*F53F1.4*) Genetic markers demonstrates dauer- or reproductive-specific expression pattern

(A-C) *col-183*: detected read counts of the *col-183* gene across developmental stages **(A)**, and fluorescence images of the *col-183* expression pattern in dauer **(B-C)**. **(D-F)** *ets-10*: detected read counts of the *ets-10* gene across developmental stages **(D)**, and fluorescence images of the *ets-10* expression pattern in dauer **(E-F)**. **(G-I)** *nhr-246*: detected read counts

of the *nhr-246* gene across developmental stages **(G)**, and fluorescence images of the *nhr-246* expression pattern in dauer **(H-I)**. **(J-L)** *led-1(F53F1.4)*: detected read counts of the *F53F1.4* gene across developmental stages **(J)**, and fluorescence images of the *led-1(F53F1.4)* expression pattern in dauer **(L)**. In read count figures **(A, D, G, and J)**, points indicate the values from each sequenced replicate, and the bar height represents the mean count value for each developmental stage. Red and blue bars represent dauer and reproductive development, respectively. tpm, transcripts per million; L2d.24, L2d at 24 hours post hatch (hph); L2d.26, L2d at 26 hph; cD, dauer-committed; cL3, L3-committing. All the plotted read counts data were from Lee and Shih *et al.* (16). Scale bar: 0.1mm.

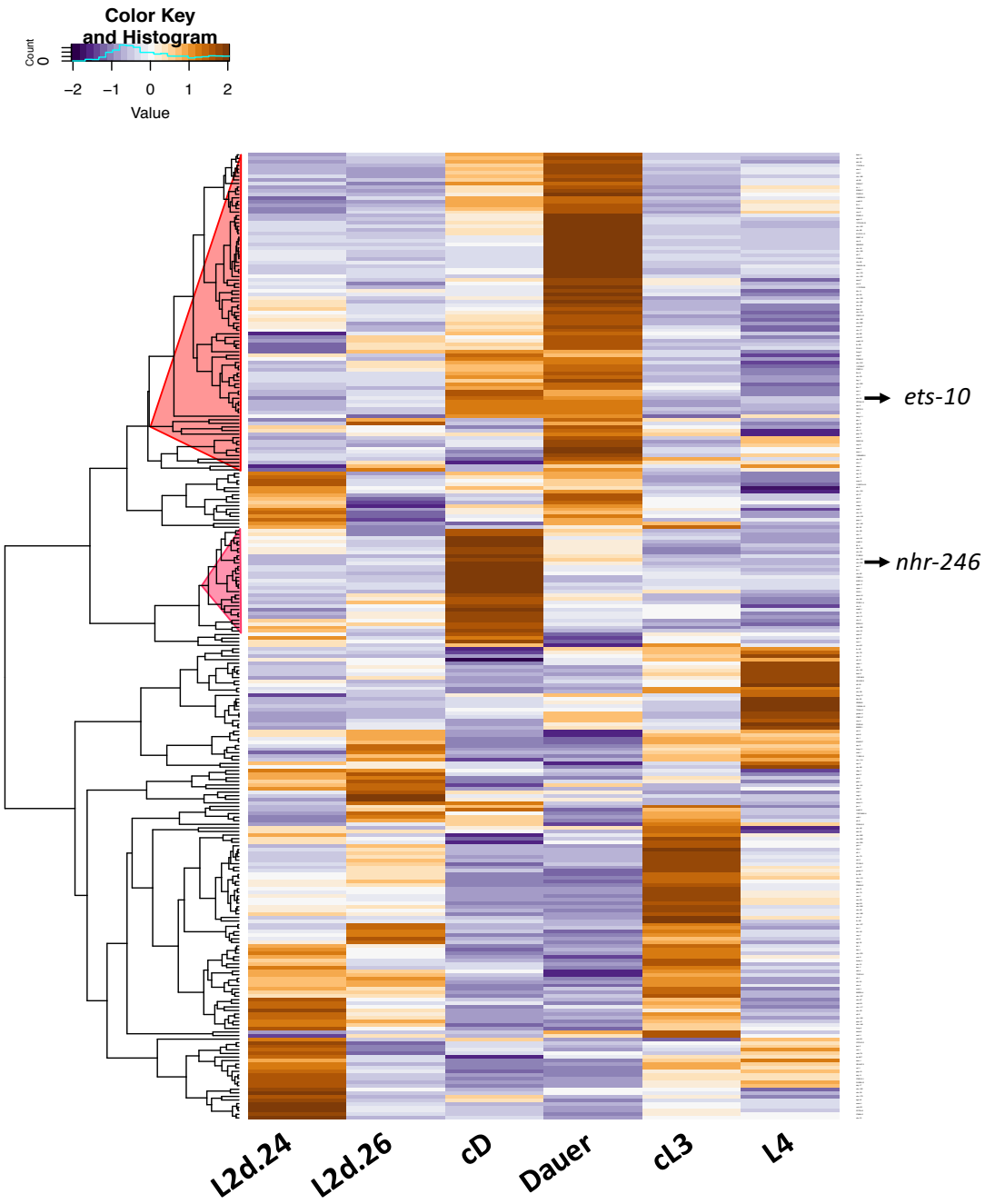
Color Key
and Histogram
Count
0
−2
−1
0
1
2
Value
ets-10
nhr-246
L2d.24
L2d.26
cD
Dauer
cL3
L4

Figure 3.3 Expression profiles of transcription factors

The expression profiles of genes encoding transcription factors were scaled and plotted on the heatmap. High and low expression level were shown in brown and purple color, respectively. Each row represents one single gene, and the genes were clustered based on their expression patterns. *ets-10* and *nhr-246* belong to the two gene clusters that have increased expression in dauer and dauer-committed (cD) stage, respectively. The heatmap was generated using packages in R, as described previously (16).

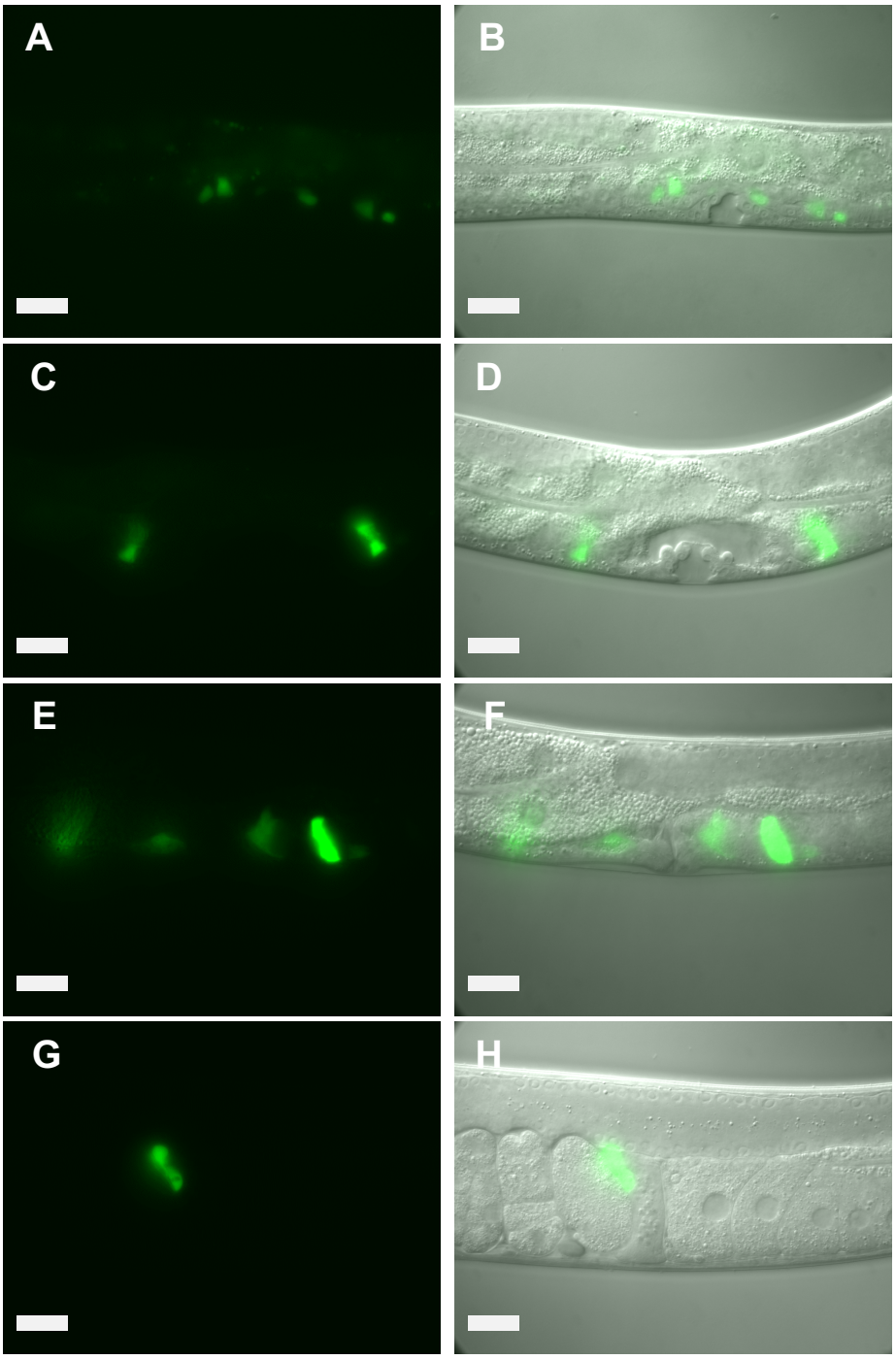
A
B
C
D
E
F
G
H

Figure 3.4. *ets-10* expression pattern in non-dauer stages (L4-adult)

Fluorescence **(A, C, E, and G)**, and the corresponding brightfiled and fluorescence merged images **(B, D, F, and H)** of *ets-10* across different life stages: early-mid L4 **(A-B)**, mid-L4 **(C-D)**, L4 lethargus **(E-F)** and adult **(G-H)**. Scale bar: 0.02mm.

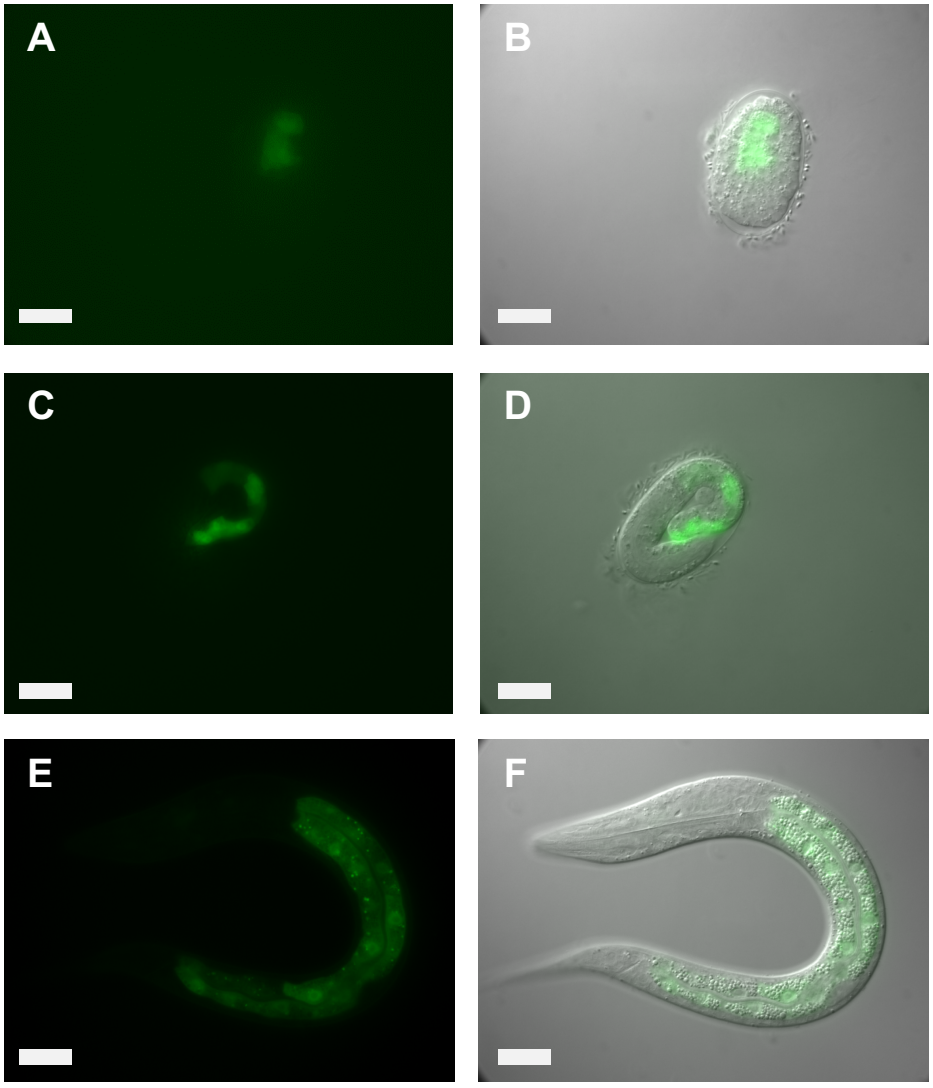

Figure 3.5. *nhr-246* expression pattern in non-dauer stage (embryo-L1)

Fluorescence **(A, C, and E)**, and the corresponding brightfiled and fluorescence merged images **(B, D, and F)** of *nhr-246* across different life stages: embryo **(A-D)** and L1 **(E-F)**. Scale bar: 0.02mm.

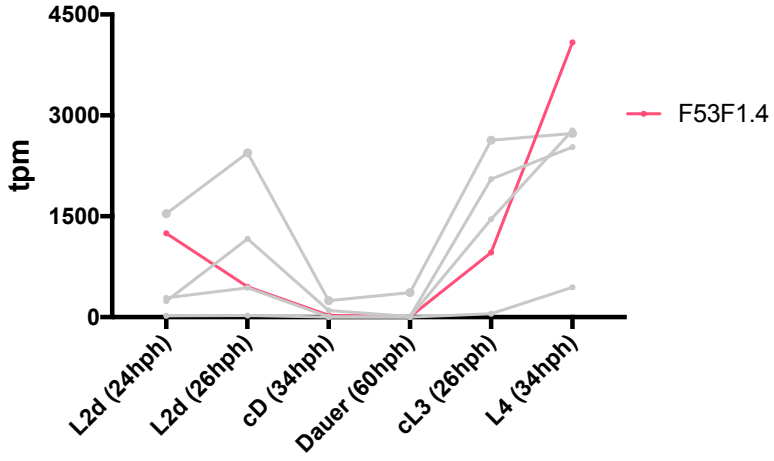

Figure 3.6. Expression profiles of genes that are down-regulated in dauer

Expression profiles of genes that are down-regulated specifically in dauer. Each line represents the average read counts of one single gene across different stages. *led-1(F53F1.4)*, the one we studied, was labeled in pink, and the rest of the genes were colored in grey for simplicity.

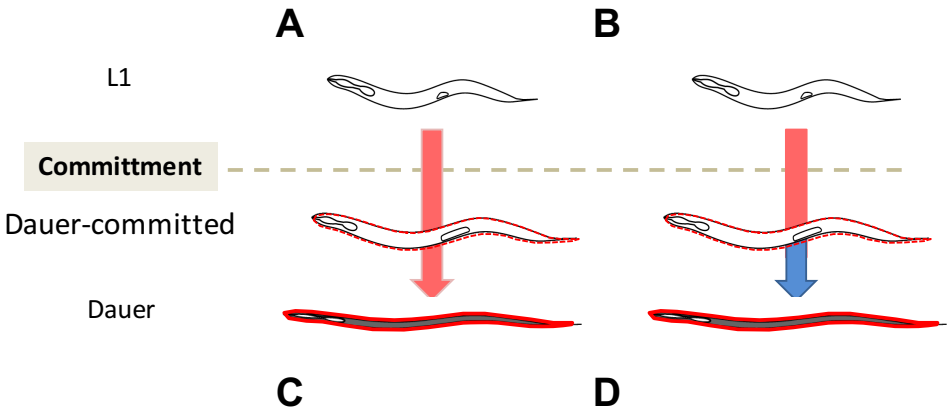

	dauers with fluorescence	dauers after shifted to favorable
col-183p::mecherry	100% (192/192)	100% (22/22)
ets-10p::gfp	100% (311/311)	100% (18/18)
nhr-246p::gfp	100% (174/174)	96% (25/26)

Figure 3.7. The appearance of fluorescence correlates with the dauer-commitment decision and stays on in dauer

(A-B) Cartoon diagram showing the experimental design with red hypodermal marker as an example. The red and blue arrows indicate the developmental progression in unfavorable and favorable conditions, respectivly. **(C-D)** The results from each of the marker strains. The numbers in parentheses represent the number of animals with positive results / total number of animals tested.

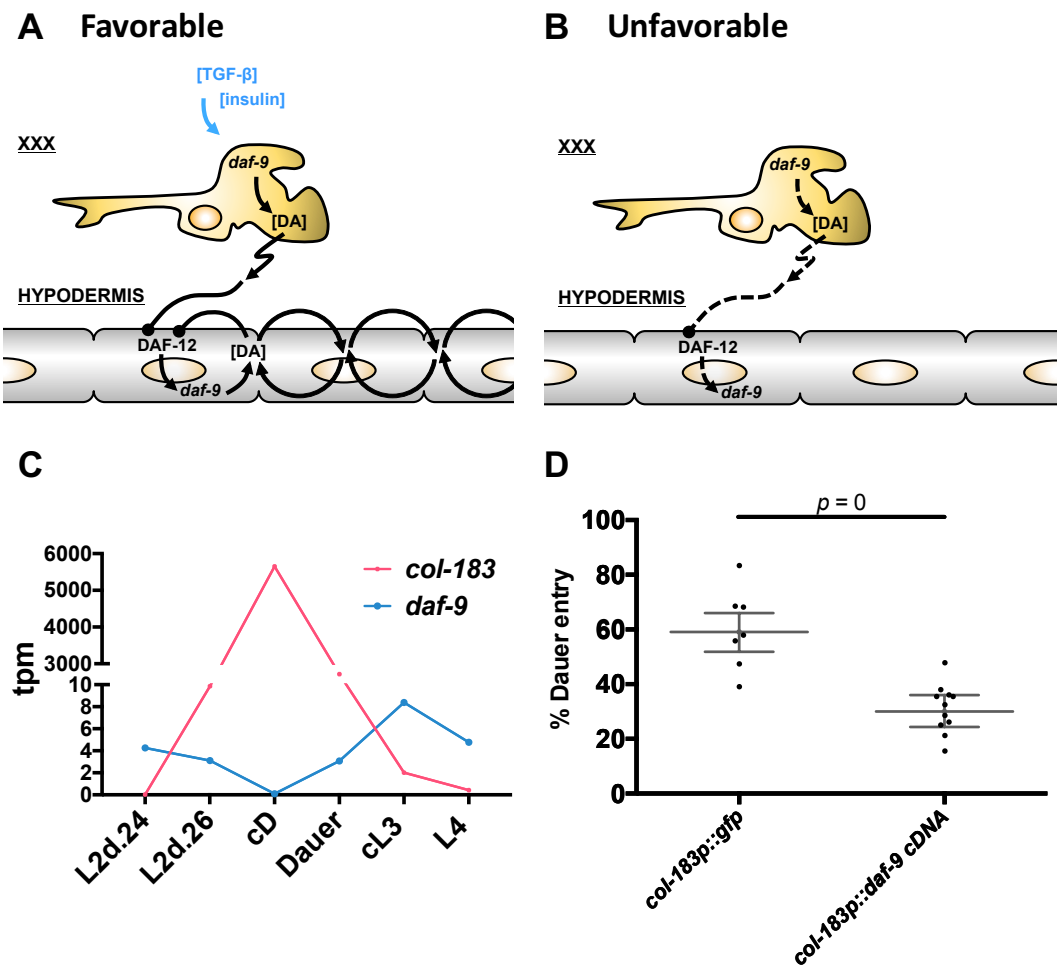

Figure 3.8. Overexpressing *daf-9* in the hypodermis during commitment increases the reproduction decision

(A-B) Cartoon diagram showing the amplification of dafachornic acid in hypodermis through TGF-beta and insulin signaling under favorable condition **(A)**, and the lack of dafachornic acid amplification in dauer-inducing environment **(B)**. **(C)** Average detected read counts of the *col-183* and *daf-9* gene across developmental stages. **(D)** Dauer entry assay on animals with *col-183* promoter driving expression of *gfp* or *daf-9* cDNA. The long horizontal line indicates the bootstrapped mean, and the error bar shows the 99%

confidence intervals. Each dot is one trial, and the data were collected from at least three different days. Statistics: permutation test. XXX: XXX cell; DA, dafachronic acid; tpm, transcripts per million.

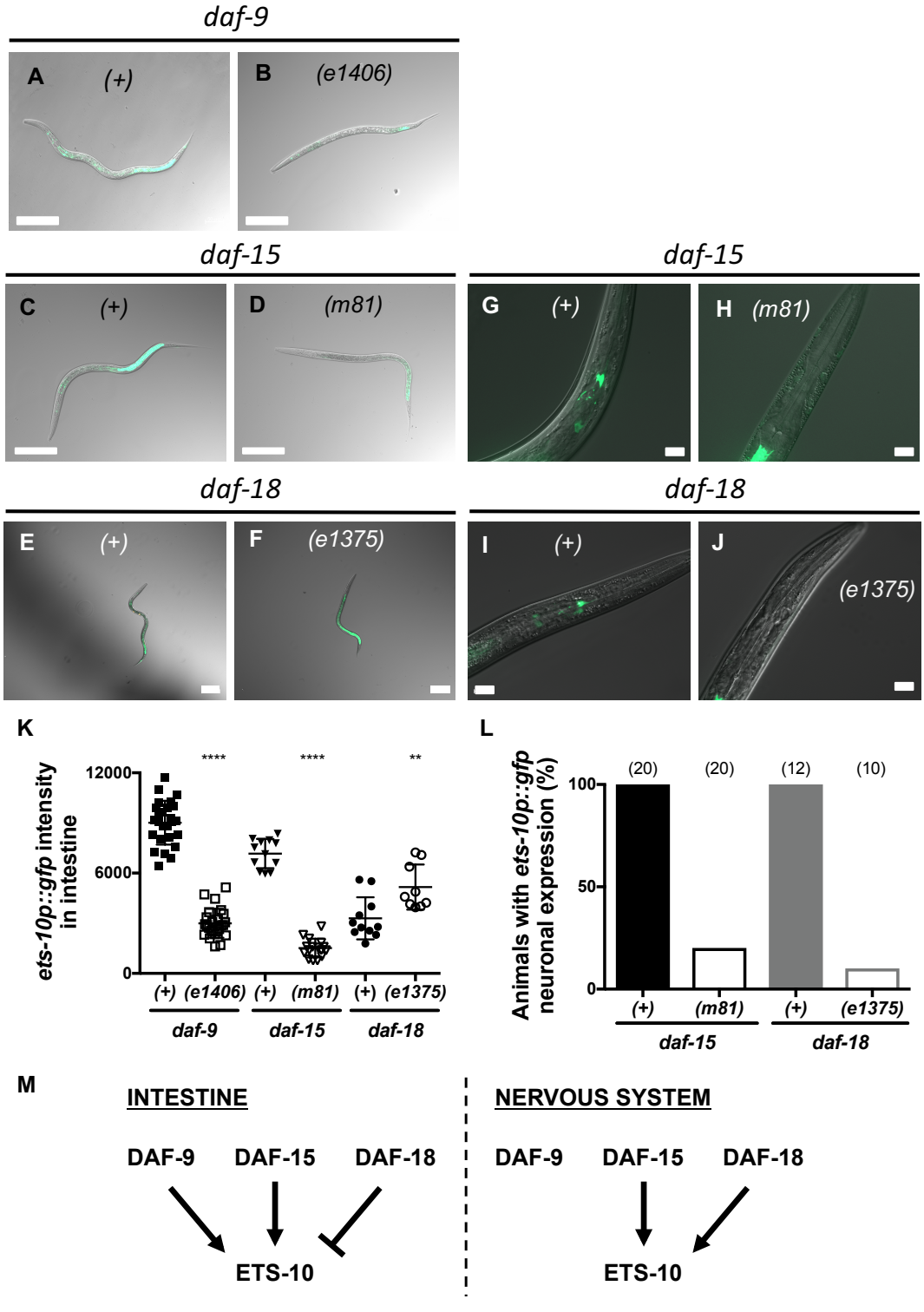
daf-9
A (+)
B (e1406)
daf-15
C (+)
D (m81)
daf-15
G (+)
H (m81)
daf-18
E (+)
F (e1375)
daf-18
I (+)
J (e1375)
K
ets-10p::gfp intensity in intestine
12000
6000
0
****
****
**
(+) (e1406) (+) (m81) (+) (e1375)
daf-9
daf-15
daf-18
L
Animals with ets-10p::gfp neuronal expression (%)
100
50
0
(20)
(20)
(12)
(10)
(+) (m81) (+) (e1375)
daf-15
daf-18
M
INTESTINE
DAF-9
DAF-15
DAF-18
ETS-10
NERVOUS SYSTEM
DAF-9
DAF-15
DAF-18
ETS-10

Figure 3.9. Partial dauers mis-express dauer markers

(A-J) Representative images of *ets-10p::gfp* expression pattern in wild type **(A, C, E, G and I)**, *daf-9(e1406)* **(B)**, *daf-15(m81)* **(D and H)**, *daf-18(e1375)* **(F and J)** animals. **(K)** Quantification of *ets-10p::gfp* intestinal fluorescence intensity in wild type, *daf-9(e1406)* and *daf-15(m81)* animals. Each dot represented one animal. The error bars showed standard deviation. Statistic: nonparametric two-tailed t test. **** $p < 0.0001$; ** $p < 0.01$ **(L)** The percentage of wild type, *daf-15(m81)* and *daf-18(e1375)* animals with *ets-10p::gfp* neuronal expression. The number in parenthesis indicates the number of animals examined. **(M)** A proposed model for how DAF-9, DAF-15, and DAF-18 influence ETS-10 expression in the intestine and nervous system. Scale bar: 100um **(A-F)** and 10um **(G-J)**.

3.7 References

1. Kelly SA, Panhuis TM, Stoehr AM (2012) Phenotypic plasticity: molecular mechanisms and adaptive significance. *Comprehensive Physiology* 2(2):1417–39.

2. Schwander T, Lo N, Beekman M, Oldroyd BP, Keller L (2010) Nature versus nurture in social insect caste differentiation. *Trends in ecology & evolution* 25(5):275–82.

3. Nithianantharajah J, Hannan AJ (2006) Enriched environments, experience-dependent plasticity and disorders of the nervous system. *Nature reviews Neuroscience* 7(9):697–709.

4. Cox GN, Staprans S, Edgar RS (1981) The cuticle of *Caenorhabditis elegans*. II. Stage-specific changes in ultrastructure and protein composition during postembryonic development. *Developmental biology* 86(2):456–70.

5. Page AP, Johnstone IL (2007) The cuticle. *WormBook*:1–15.

6. Hallem EA, et al. (2011) A sensory code for host seeking in parasitic nematodes. *Current biology : CB* 21(5):377–83.

7. Lee H, et al. (2011) Nictation, a dispersal behavior of the nematode *Caenorhabditis elegans*, is regulated by IL2 neurons. *Nature neuroscience* 15(1):107–12.

8. Fielenbach N, Antebi A (2008) *Caenorhabditis elegans* formation and the molecular basis of plasticity. *Genes & development* 22(16):2149–65.

9. Ren P, et al. (1996) Control of *Caenorhabditis elegans* larval development by neuronal expression of a TGF-beta homolog. *Science* 274(5291):1389–1391.

10. Li W, Kennedy SG, Ruvkun G (2003) *daf-28* encodes a *Caenorhabditis elegans* insulin superfamily member that is regulated by environmental cues and acts in the DAF-2 signaling pathway. *Genes Dev* 17(7):844–858.

11. Schackwitz WS, Inoue T, Thomas JH (1996) Chemosensory neurons function in parallel to mediate a pheromone response in *Caenorhabditis elegans*. *Neuron* 17(4):719–728.

12. Androwski RJ, Flatt KM, Schroeder NE (2017) Phenotypic plasticity and remodeling in the stress-induced *Caenorhabditis elegans* dauer. *Wiley interdisciplinary reviews Developmental biology*. doi:10.1002/wdev.278.

13. Karp X (2018) Working with dauer larvae. *WormBook*:1–19.

14. Cassada RC, Russell RL (1975) The dauerlarva, a post-embryonic developmental variant of the nematode *Caenorhabditis elegans*. *Developmental biology* 46(2):326–42.

15. Nika L, Gibson T, Konkus R, Karp X (2016) Fluorescent beads are a versatile tool for staging *Caenorhabditis elegans* in different life histories. *G3* 6(7):1923–33.

16. Lee JS, et al. (2017) FMRFamide-like peptides expand the behavioral repertoire of a densely connected nervous system. *Proceedings of the National Academy of Sciences of the United States of America* 114(50):E10726–E10735.

17. Brenner S (1974) The genetics of *Caenorhabditis elegans*. *Genetics* 77(1):71–94.

18. Hobert O (2002) PCR fusion-based approach to create reporter gene constructs for expression analysis in transgenic *Caenorhabditis elegans*. *BioTechniques* 32(4):728–30.

19. Maduro M, Pilgrim D (1995) Identification and cloning of *unc-119*, a gene expressed in the *Caenorhabditis elegans* nervous system. *Genetics* 141(3):977–88.

20. Mello C, Fire A (1995) DNA transformation. *Methods in cell biology* 48:451–82.

21. Schroeder NE, Flatt KM (2014) In vivo imaging of dauer-specific neuronal remodeling in *Caenorhabditis elegans*. *Journal of visualized experiments : JoVE* (91):e51834.

22. Kramer JM, Cox GN, Hirsh D (1985) Expression of the *Caenorhabditis elegans* collagen genes *col-1* and *col-2* is developmentally regulated. *The Journal of biological chemistry* 260(3):1945–51.

23. Schaedel ON, Gerisch B, Antebi A, Sternberg PW (2012) Hormonal signal amplification mediates environmental conditions during development and controls

an irreversible commitment to adulthood. *Plos Biology* 10(4). doi:10.1371/journal.pbio.1001306.

24. Albert PS, Riddle DL (1988) Mutants of *Caenorhabditis elegans* that form dauer-like larvae. *Developmental biology* 126(2):270–93.

25. Vowels JJ, Thomas JH (1992) Genetic analysis of chemosensory control of dauer formation in *Caenorhabditis elegans*. *Genetics* 130(1):105–23.

26. Blaxter ML (1993) Cuticle surface proteins of wild type and mutant *Caenorhabditis elegans*. *J Biol Chem* 268(9):6600–6609.

27. Popham JD. W JM (1979) Aspects of the fine structure of the dauer larva of the nematode *Caenorhabditis elegans*. *Canadian Journal of Zoology* 57(4):794–800.

28. Braeckman BP (2009) Intermediary metabolism. *WormBook*:1–24.

Chapter 4

EXTREMOPHILE NEMATODES IN AND AROUND MONO LAKE DEMONSTRATE ADAPTATION TO AN ARSENIC-RICH ENVIRONMENT

(This work was done in collaboration with James Lee, Ryoji Shinya, Jean Marie Badroos, Elizabeth Goetz, and Amir Sapir)

4.1 Abstract

Studying extremophile organisms have expanded our understanding of the limits and adaptability of life. Nevertheless, the dynamics of animal habitation of harsh environments and the mechanisms of resilience and plasticity underlying this habitation remain largely unknown. Here we describe the discovery of extremophile nematodes in and around Mono Lake, CA, a unique basic, arsenic-rich, and hypersaline environment. In contrast to the limited number of animal species previously reported to live in the lake, we have isolated at least eight species of nematodes, including five previously unidentified species. Finding live nematodes in the same niches of Mono Lake in two consecutive years show that the lake hosts a stable population of worms. Phylogenetic analyses show that the nematodes belong to diverse clades across the phylum Nematoda, supporting a model of multiple colonization events. Consistent with this model, different mouth morphologies of these nematodes suggest diverse feeding strategies including bacterial grazers and predatory nematodes. We were able to culture one species of Mono Lake worms, *Auanema tufa* n. sp., and found that it is resistant to arsenite (As(III)) and arsenate (As(V)) — the two primary arsenic species in the lake. Integration of niche environmental conditions with the prevalence of worms at each of these niches suggests that arsenic resistance preceded the adaptation to other environmental conditions in the lake. Our finding highlights the previously unappreciated complexity of the animal life in the unique ecosystem of Mono Lake and provides insights into the dynamics and type of adaptations of animals to extreme environments.

4.2 Introduction

Among the largest habitats on Earth are "extreme" environments where the physical and chemical conditions differ from the habitable zone of humans. These environments include, for example, the Deep Sea, sub-terrestrial niches, the high atmosphere, and specific terrestrial lakes. However, we know very little about the organisms that live in these habitats (extremophiles) and their strategies for adapting and thriving in such hostile environments, partly due to sampling challenges and limited access to these habitats. Moreover, the difficulties of growing and maintaining organisms from extreme habitats in the laboratory limit our understanding of the dynamics and the mechanisms underlying the adaptation of these organisms to their niches.

One phylum of organisms that seem to be particularly adapted to thrive in extreme environments are nematodes. These roundworms have been found in a variety of hostile environments, including deep subterranean niches (1, 2), extreme arid soil (3), frozen Antarctic water (4) and the Deep Sea (5, 6). Moreover, nematodes were found to dominate many of the habitats with environmental conditions so harsh as to almost not support animal life including the subterrane surface (7) and anoxic underwater sediments (8).

Nematodes have developed several protective strategies of modified life cycle to ensure the survival of the current or subsequent generations. For example, in response to unfavorable environmental conditions *Caenorhabditis elegans* enters an alternative developmental stage, the dauer, that allows its survival in harsh conditions (9, 10). Specific adaptive genetic programs facilitate the unique physiology of the dauer state including the development of specialized morphology such as thickening of the cuticle, and an anaerobic metabolism. These adaptations result in an animal that is highly resistant to environmental

insults and long-lived. The diverse lifestyle and feeding strategies of nematodes that range from free-living bacterial and fungal feeders, predator nematodes, to parasitic worms of plant and animal hosts often result in the cohabitation of worms in the same ecological niche. It is not clear, however, what specific adaptations enable nematodes to survive and thrive in extreme environments. Moreover, the sequences of events that underlie the habitation of nematodes in hostile environments remain largely unknown.

Mono Lake, a natural basin located in the Inyo National Forest of California, is an extreme environment that is high in pH, salt, and arsenic (11). It was formed as a closed basin since at least 50,000 years ago (12), but in 1941 some freshwater streams feeding the lake were diverted, making the drop of the lake level even more severe (13). The result of this level drop not only concentrated the salts (14, 15), but also facilitated arsenic to dissolve from sediments to its aqueous forms (16). Arsenic is a chemical element that is toxic to most organisms. At a biochemical level, inorganic arsenic in concentrations found in Mono Lake replace phosphate in several reactions and may react with critical thiols in proteins and inhibit their activity. Thus, arsenic has a negative pleiotropic effect on living organisms causing genotoxicity, altered DNA methylation and cell proliferation, oxidative stress, apoptosis, and mutagenesis (17). The level of arsenic in Mono Lake is approximately 0.2 mM, which is 1,500 times higher than the maximum limit for drinking water (18). Consistent with the harshness of the environment, the number of living animals reported in the lake has been limited to two animal species, the alkali fly (*Ephydra hians*) and brine shrimp (*Artemia monica*) (19). The adaptation of these two species is polyphyletic, suggesting that an independent habitation of the lake took place in a process of strong purifying selection. Nevertheless, the sequence of events of this colonization process and the type of the specific

adaptations that enable these animals to live in Mono Lake remain largely unknown.

Here we report eight species isolated in and around Mono Lake. These species were isolated from polyphyletic nematode clades, suggesting that Mono Lake has been inhabited by nematodes independently and multiple times. One of these species, *Auanema tufa* is culturable in laboratory conditions and exhibits resistance to arsenic, highlighting a probable hallmark of adaptation of animals to arsenic-rich environments.

4.3 Results

Nematodes were isolated from three sampling sites around Mono Lake

Mono Lake covers 13 miles east to west and 8 miles north to south, and the lake shores are characterized by variable levels of human intervention and environment conditions. To survey for animal life in the sediments of Mono Lake, we collected soil from three different sites around Mono Lake to sample across various levels of human activities, and chemical and physical conditions. The three sites located in the north-east (site A), south (site B), and west (site C) (**Figure 4.1A** and **Figure 4.2**). Not approachable by vehicles, site A (Pristine Beach) on the north-east side of the lake is a large, sandy open field with the least visitors and observable biological activity of the three sites. Site B (Navy Beach) on the south attracts the most tourists. It contains emerged tufa structures, which are the precipitation products of calcium-bearing springs and the lake's carbonated waters (19). Site C (Old Marina) on the west has a rocky shore with small tufa structures. In all the sites we found the brine shrimps *Artemia monica* in the lake water and upper surface of the sediment, larvae of the *Ephydra hians* alkali fly in the sediments, and adult alkali flies on the lake's shores.

At each sampling site, we collected soil samples from three zones with various distances relative to the shore: dry zone, tide zone and in-lake (**Figure 4.1B**). Within each niche, we sampled different sub-niches, for example, "in-lake" sampling involved the sampling of sediments in an increasing distance from the shoreline. We isolated live nematodes from all three sampling sites. From site A, most samples were collected from the tide zone and in-lake, and nematodes were isolated in samples across -1 to 100 m away from the shore in sediments under water columns of 0 to 110 cm deep (**Figure 4.1B-C**). Nematodes were also found from site B dry and tide zones, and from dry, tide and in-like zones in site C. In contrast

to the sediments, we did not find nematodes along the water columns. During the survey of the soil samples, we found that nematodes that were isolated in the wet tide zone and in-lake niches coexist with brine shrimp and the larvae of the alkali fly. These three taxa were the only animals isolated from the samples demonstrating the harshness of the environment that apparently can host a limited number of animal species that developed specific adaptations.

Mono Lake is not an isolated ecological system; it collects the waters of several streams from the nearby mountains, and it is amenable for different human interventions. To rule out the possibility that the isolated nematodes are the result of an environmental contamination, for example due to human activity, we sampled the isolated Pristine Beach site (**Figure 4.1A**). Sampling this site in two consecutive years, 2016 and 2017, we found nematodes at Pristine Beach at both years indicating that the lake hosts an ecologically-stable community of nematodes (**Figure 4.1C**). From the many morphologically different nematodes we found, we choose to characterize eight morphologically distinct species by DNA analysis (species a-h. **Figure 4.1D** (species b), **Figure 4.1E** (species e) and **Figure 4.3**). One species was isolated from in-lake in site A (species g), six species were isolated in site B (species a-f), and one was from both site B and C (species h). Importantly, in 2017, we found two of the species (species e and f) again, from different locations (site B tide zone in 2016 and site C dry zone in 2017) (**Figure 4.4E**). This observation suggests that particular species of nematodes are ecologically stable and widespread in the lake.

Some of the nematodes in Mono Lake live in pH 10.

To understand the environmental conditions at the niches inhabitant by Mono Lake nematodes, we measured the pH and soil salinity of our samples (**Table 4.1**). Consistent with

previous reports, the average pH of the samples fell within the range of 9-10 across different zones and sites (minimum: 9.0 ± 0.7 from site B tide zone, maximum: 10.01 ± 0.1 from site C dry zone), except for one sample from site B dry zone (pH=7.815). In contrast, the salinity of the samples varied by site and zone (**Figure 4.4A**). Overall, samples from site A were more saline (tide zone 15.0 ± 3.0 ppt and in-lake 11.5 ± 3.5 ppt), and samples from site B were less saline (dry zone 1.0 ppt, tide zone 0.9 ± 0.7 ppt and in-lake 2.7 ± 1.9 ppt). This chemical analysis is consistent with the geography of Mono Lake in which site A, the most secluded from human interventions and the entry points of freshwater streams, is the most chemically extreme among the three sites we sampled. Nevertheless, site A hosts a large population of nematodes in the tide zone and in the lake, suggesting that nematodes were adapted to thrive even at extreme niches of the lake.

Mono Lake's nematodes belong to different nematode clades and represent diverse lifestyles

We integrated morphological and phylogenetic tools to study the biodiversity of the isolated nematodes and their lifestyle in the Mono Lake ecosystem. Within the eight species, we identified a variety of mouth structures (**Figure 4.5**), including grinders (**Figure 4.4B**, species a), teeth (**Figure 4.4C**, species d) and long esophagus (**Figure 4.4D**, species f). The mouth structure of nematodes is an indicator of its feeding style (28). Base on the mouth structure analysis, we predict that species a and species d are a bacterial feeder and a predator, respectively. Species d may develop its tooth to prey on nematodes that are bacterial feeders in cases of harsh environmental conditions similar to what was shown for the interaction between the predatory nematode, *Pristionchus pacificus,* and its prey, *C. elegans* (29).

Species e belongs to the family Mermithidae (see below), whose members have been observed to parasitize arthropods, such as spiders and grasshopper (30). This structure raises the possibility that species e could be parasitic of the other animals living in the lake. Taken together, our data show that the ecosystem of Mono Lake is much more complex than previously thought encompassing bacterial grazers, predators of other animals, and probably parasitic nematodes.

Five nematodes isolated are likely new species

We used molecular signatures, including ribosome large subunit (LSU) 28rDNA and small subunit (SSU) 18rDNA, to identify the species in order to understand the course and dynamics of lake colonization by these nematodes. The sequence analysis suggested that three of the isolated nematodes are known species, and five of the isolated nematodes are likely new species (**Figure 4.4E**, **Figure 4.6**). Moreover, the isolates are from across the phylogeny of Nematoda (Blaxter and Helder classification (31)(32)) (**Figure 4.4E-F**). The known species include Clade V/9 nematodes *Mononchoides americanus* (species c, **Figure 4.11-12**) and *Diplogaster rivalis* (species d, **Figure 4.13-14**), and Clade II/1 nematode *Prismatolaimus dolichurus* (species f, **Figure 4.17**). Two of the new species belong to Clade V/9, including *Auanema sp.* (species a, **Figure 4.7-8**) and *Pellioditis sp.* (species b, **Figure 4.9-10**). We assigned the other three new species in family instead of genus because of the lack of phylogenetically close species: species e is in *Mermithidae* family, which belongs to Clade I/2 (**Figure 4.4F** and **Figure 4.15**); species g and h are in *Diplolaimelloides* family, which is classified between Clade II and III/5 (**Figure 4.4F** and **Figure 4.18-19**). We concluded that species g and h are different because the sequence similarity between them is

96.77%, which is less than our criteria of 98% (**Figure 4.20**). Taken together, the diverse distribution across the phylum Nematoda suggests that the colonization of Mono Lake by nematodes happened independently and multiple times.

Auanema tufa is culturable in lab

The difficulty in replicating the exact conditions of extreme environments in order to culture the organisms that live in these habitats is a major obstacle in the study of life in the extremes. Thus, employing different culturing methods and conditions, we sought to establish a stable culturing system of Mono Lake nematodes in the laboratory. Of the eight species identified, we were able to culture in our laboratory, using *C. elegans* culturing methods, one species which we identified as belonging to the *Auanema* genus (species a). Because this *Auanema sp.* shares only 89% (LSU) and 96%(SSU) sequence identity with its closest related *A. rhodensis* (**Figure 4.6-8**), we concluded that *Auanema sp.*is a new species. Based on the tufa-rich environment we isolated it from, we named the species *Auanema tufa.* Notably, while its close related nematode species have been found in diverse habitats, only *A. tufa* was isolated from extreme environment (**Figure 4.21**). The reproductive lifespan of *A. tufa* at 22.5°C is around 2.5-3 days, which is comparable to *C. elegans*. *A. tufa* shares some similarities with *A. rhodensis* and *A. freiburgensis* but also show some unique characteristics of their reproduction traits (33). The adult of all three species has a vulva located at mid-body and a two-armed gonad (**Figure 4.21B-C**). *A. rhodensis* and *A. freiburgensis* have three genders (hermaphrodite, male and female), wherease *A. tufa* might be hermaphroditic or parthenogenic. We have observed male in *A. tufa*, but it appears very rarely. Moreover, *A. tufa* live-birth hatched larvae from their vulva (ovoviviparity) (**Figure**

4.21B) instead of laying embryos like other nematodes of the *Auanema* genus such as *A. rhodensis* and *A. freiburgensis*. Ovoviviparity has been considered an adaptation to thrive in extreme environments (34, 35), thus yet representing another conceivable adaptation of *A. tufa* to the conditions of the lake.

A. tufa is an arsenic-resistant nematode

Mono Lake water and sediments are unique environments of high pH, salinity, and high concentrations of arsenic species, primarily As(III) and (V) (11). It is known that a high concentration of arsenic is toxic to most living organisms thereby limiting animal life in arsenic-rich environments. To understand how Mono Lake nematodes survive in this hostile environment, we exposed *A. tufa* and a control nematode, the culturable soil worm *C. elegans,* with increasing concentrations of As(III) and As(V) solutions and examined their ability to survive over time. After 2.5 hours of exposure, we observed increased survival of *A. tufa* in both 1.5 and 3 mM of As(III) solutions in comparison to *C. elegans* (**Figure 4.22A-B**). Even more striking is the ten fold more resistance of *A. tufa* to As(V). Specifically, *A. tufa* could withstand a concentration of 30mM As(V) compared to *C. elegans* (**Figure 4.22C-D**). As a control we incubated the two strains in water and we detected 100% survival of the two species within the time window of the assay (**Figure 4.22E**). *A. tufa* was isolated from near the surface of the tide zone, where As(V) is reported to be the dominant arsenic species (36). The results strongly suggest that evolving of mechanisms of arsenic resistance is a critical step in the adaptation of nematodes, including *A. tufa,* to the conditions of Mono Lake.

An increasing body of evidenc show that in *C.elegans*, SKN-1 is a transcription factor dedicated to promote many protective stress responses. Specifically, an activated form of *skn-1* mediates arsenic resistance in *C. elegans* (37). Thus, it is possible that activation of SKN-1 is one of the mechanisms that collectively underlie the adaptation of Mono Lake nematodes to Arsenic. To test if *skn-1* gene activity could explain the observed arsenic resistance of *A. tufa*, we compared the survival rate of *A. tufa* with different strains of *C. elegans*. These strains include the wild-type background as a control and an *skn-1* allele, *lax188,* in which the SKN-1 protein is activated constitutively. We choose to expose the worms to 10mM As(V) solution in which the survival rate of *A. tufa* is significantly higher than wild-type *C. elegans* worms (**Figure 4.22C**). Consistent with previous reports, we found that the activation of SKN-1 leads to arsenic resistance. Importantly, *A. tufa* survive better than wild-type and *skn-1* gain of function *C. elegans* worms (**Figure 4.22F**). Thus, activation of the *skn-1* pathway might play a critical role in the adaptation of *A. tufa* and other Mono Lake nematodes to the extreme environmental conditions in the lake.

4.4 Discussion

Because Mono Lake is an extreme natural environment it was thought to host limited animal biodiversity. Here we report that, in addition to what was previously known, nematodes live in Mono Lake. We found spatial and temporal stable populations of nematodes all across the lake (A, B, and C sites) and at various zones (dry zone, tide zone, and in-lake), indicating there are multiple niches within the ecosystem of Mono Lake where nematodes can thrive. Mono Lake nematodes have multiple lifestyles for survival, as suggested by their diverse morphologies. In total we identified, using molecular phylogeny, eight species that belong to diverse clades across the phylum Nematoda. This polyphyletic diversity suggests that multiple colonization events took place in Mono Lake. Moreover, we found that one of the nematodes, *Auanema tufa* is culturable in lab and is more resistant to arsenic than *C. elegans*.

Due to the high level of protection of Mono Lake, we believe that our sampling was far from being saturated. Indeed, when we isolated the same species (species in *Mermithidae* and *Tripylidae*) in subsequent years, we did not find them in the same site. Our unsaturated sampling may also explain why the nematodes we observed at low abundance in the first year (*A. tufa*) were not observed in the subsequent year.

We suspect that there are several ways for the nematodes to adapt to Mono Lake. First, it is possible that nematodes around Mono Lake develop pre-adaptations to arsenic, which may allow them to evolve and further adapt to the high pH and salinity conditions in-lake. That could explain the adaptation strategy of the arsenic-resistant *A. tufa* found in site B, where the salinity is the lowest and the pH varies the most among the three sampling sites. Secondly, upregulation of arsenic resistance genes, such as *skn-1,* may be a critical aspect of

this adaptation. Further investigation is required to test directly if *skn-1* or other stress-related genes are involved. Finally, entering the dauer stage, a stress-resistant and developmentally arrested period (38)(39), might help nematodes survive in Mono Lake and find relatively favorable places within the harsh environment via dauer-specific dispersal behaviors (40). Our sampling technique did not favor the isolation of dauers, but it is possible that dauer formation is one strategy of resistance that facilitated the habitation of the lake by dauer-forming nematodes.

The fact that nematodes have been found in several harsh environments, including Mono Lake, raises the question: what makes nematodes good extremophiles? Because nematode genomes can very quickly and dramatically through high rates of gene acquisition and loss (41), it is likely that nematodes can adapt to challenging conditions. Moreover, the small size of nematodes is probably beneficial, allowing the utilization of neuroendocrine signaling to engage and enact whole animal survival programs in response to stress. Lastly, as mentioned before, dauer animals have well-equipped physiology and behaviors to cope with stress.

We have investigated extremophile biology in nematodes and have identified yet another harsh environment where nematodes can survive. We identified eight species from across the diversity of Nematoda, suggesting that Mono Lake was invaded independently and multiple times. The arsenic resistance of *A. tufa* that lives in the relatively safe harbor of the B site suggests that preadaptation to arsenic could lead to the genomic evolution necessary to survive the pH and salinity of inner Mono Lake.

4.5 Material and Method

Sites and sampling

Soil and water samples were collected from three sites around Mono Lake (**Figure 4.1**) in August 2016, June 2017 and July 2017. Site A, which we named Pristine Beach, (38° 3′ 27.91″ N, 119° 1′ 50.66″ W), site B is at Navy Beach (37° 56′ 21.90″ N, 119° 1′ 25.93″ W), and site C is at Old Marina (37° 59′ 12.80″ N, 119° 8′ 18.70″ W).

At each site, soil samples were collected from inside the lake, tide zone, and dry zone, with each sample weight ranging from 15 to 375 g. Total numbers of samples collected from each site were: 25 from site A (9 in 2016 and 16 in 2017), 34 from site B (19 in 2016 and 15 in 2017), and 22 from site C (7 in 2016 and 15 in 2017). The sampling permits were issued to Amir Sapir by the California Fish and Wildlife Department (SCP-13436) and from the Californian State Parks Department. All of the sample information, including location, pH, salinity, and the presence of nematodes, is listed in Table S1.

Soil salinity and pH measurement

Each soil sample was mixed with Milli-Q water in a 1:2 ratio (weight:volume) for salinity and pH measurements (20). Soil salinity was estimated by measuring the conductivity with two meters: Orion conductivity meter model 126 (for 2016 samples) and TPS WP-81 conductivity meter (for 2017 samples). Soil pH was measured using VWR pH meter model 8015.

Nematode isolation and species identification

Nematodes were isolated directly from the soil samples either using a dissecting microscope

on-site or in the laboratory by the Baermann funnel method for overnight extraction (21). The isolated nematodes were further identified by morphology and molecular signatures. For molecular analysis, individual worm lysate was prepared in worm lysis solution (100µl DirectPCR lysis reagent (Viagen Biotech), 10.5µl proteinase K (10 mg/ml) and 5µl 1M DTT). The gene fragments of ribosome large subunit (LSU) 28rDNA and small subunit (SSU) 18rDNA were amplified (22)(23) and sequenced. MEGA7 was used to build phylogenetic tree from the resulting sequences (24). The tree was estimated by using Maximum Likelihood (ML) analysis and 1,000 bootstrap replicates, and the species identification was done with General Time Reversible model (25). The isolated nematode is considered as a new species when it exhibits <98% sequence similarity compared with its nearest neighbor (26, 27).

Nematode culture

Maintenance

Both *C. elegans* wild-type strain N2 (Bristol) and *Auanema tufa* n. sp. were grown using standard *C. elegans* culturing protocol with *Escherichia coli* strain OP50 as a food source (19). *Auanema tufa* was maintained at 22.5°C.

Freezing

Auanema tufa was frozen using Trehalose-DMSO method (personal communication with Dr. Kevin F. O'Connell). Briefly, *Auanema tufa* n. sp. from freshly starved plates was washed off with M9 buffer (3 g KH_2PO_4, 6 g Na_2HPO_4, 5 g NaCl and 1 ml 1 M $MgSO_4$ in 1L ddH_2O) and collected in a 15ml centrifuge tube. The worm pellet was washed once, re-

suspended with Trehalose-DMSO freezing buffer (15.1 g Trehalose (Fisher BioReagents, PA, Cat# BP2687-25) and 17.7 ml DMSO in 500 ml M9 buffer), and transferred to cryogenic vials. The vials were stored in -80°C freezer after 30 minutes incubation at room temperature.

Survival assay

As(III) and As(V) solutions were prepared by dissolving sodium (meta)arsenite (Sigma-Aldrich, MO, Cat S7400) and sodium arsenate dibasic heptahydrate (Sigma-Aldrich, MO, Cat# S9663) in Milli-Q water, respectively. Adults of *C. elegans* wild-type N2, *skn-1(lax188)*, and *Auanema tufa* were washed with Milli-Q water for 4 times and transferred to 12-well tissue culture plates (Corning, NY) containing 0.9 ml of Milli-Q water and various concentration of As(III) or As(V) per well. Each well has on average 34 animals, ranging from 10 to 66. Final concentrations of 1.5 and 4.5 mM of As(III), and 10 and 30 mM of As(V) was used to treat animals. Animals were incubated at 22°C and the numbers of surviving animals, determined by their physiology and touch-provoked movement (in response to eyelash touch), were counted at different time points (1, 2.5, 5 and 7 hours).

4.6 Figures

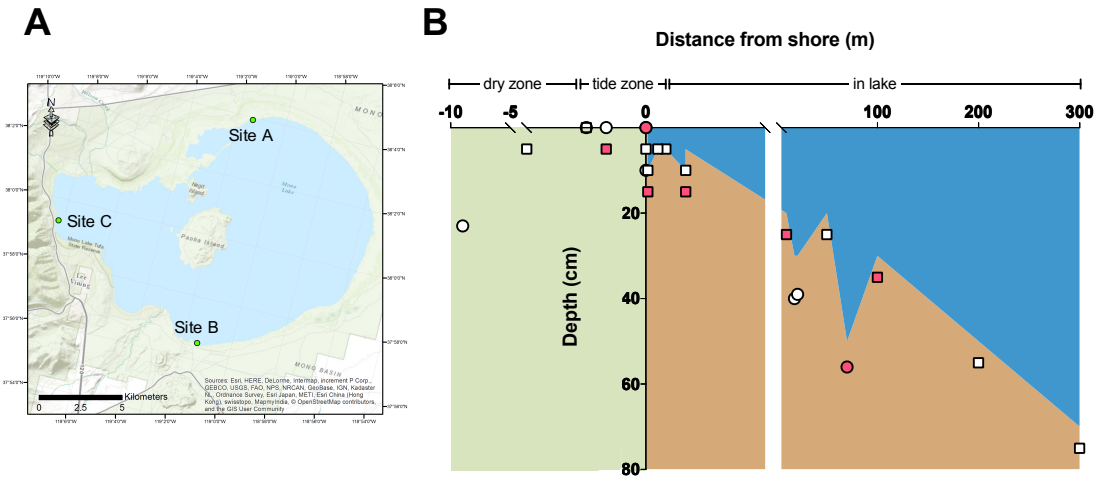

C

Year	Site A			Site B			Site C		
	dry zone	tide zone	lake	dry zone	tide zone	lake	dry zone	tide zone	lake
2016	0/1	1/5	1/3	2/3	9/14	0/1	1/1	0/6	NA
2017	0/1	2/6	3/8	NA	1/3	0/9	6/14	3/4	4/11
Total	0% (0/2)	27% (3/11)	36% (4/11)	67% (2/3)	59% (10/17)	0% (0/10)	47% (7/15)	30% (3/10)	36% (4/11)

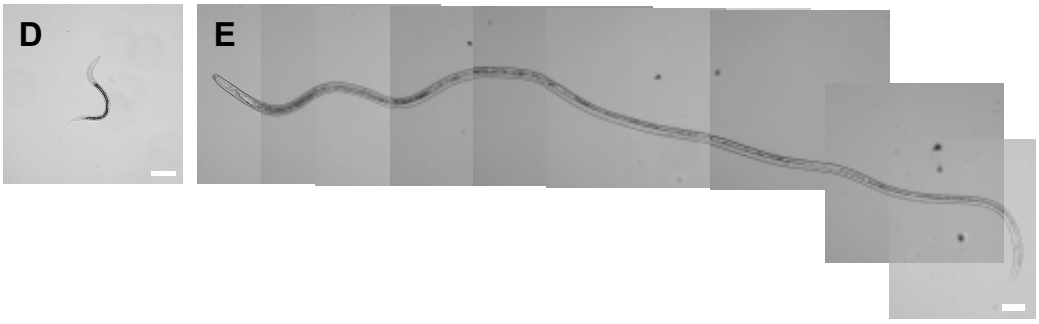

Figure 4.1. Nematodes were isolated from in and around Mono Lake. (A) The locations of the three sampling sites A, B and C around Mono Lake. Samples were collected in August 2016 and June 2017. **(B)** Plot showing the locations at site A where samples were collected, relative to the shore (x-axis) and surface (y-axis). The boundaries of three different kinds of locations, dry zone, tide zone, and in-lake, were shown by the brackets. Blue indicates lake water and brown indicates the soil. Circles and squares represent samples collected in 2016

and 2017, respectively. The samples in which nematodes were found were colored in pink. **(C)** Summary table of the origins of the samples. Samples were collected from dry zone, tide zone or lake from each site. The numbers in the cells indicate the number of samples with nematodes isolated versus the total number of samples collected. The locations that have nematodes found were highlighted in beige for 2016 samples and grey for 2017 ones. NA, non-applicable. **(D-E)** Representative images of two nematodes isolated. One was isolated from site B dry and tide zones in 2016 **(D)**, and the other one was isolated from site B tide zone in 2016 and site C dry zone in 2017 **(E)**.

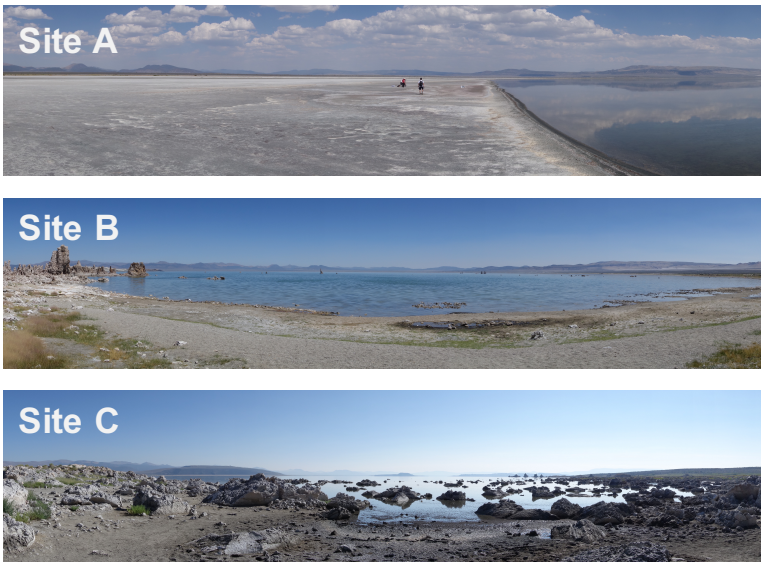

Figure 4.2. Pictures of three sampling sites around Mono Lake. Pictures of site A (10 Mile Road), site B (Navy Beach), and site C (Old Marina).

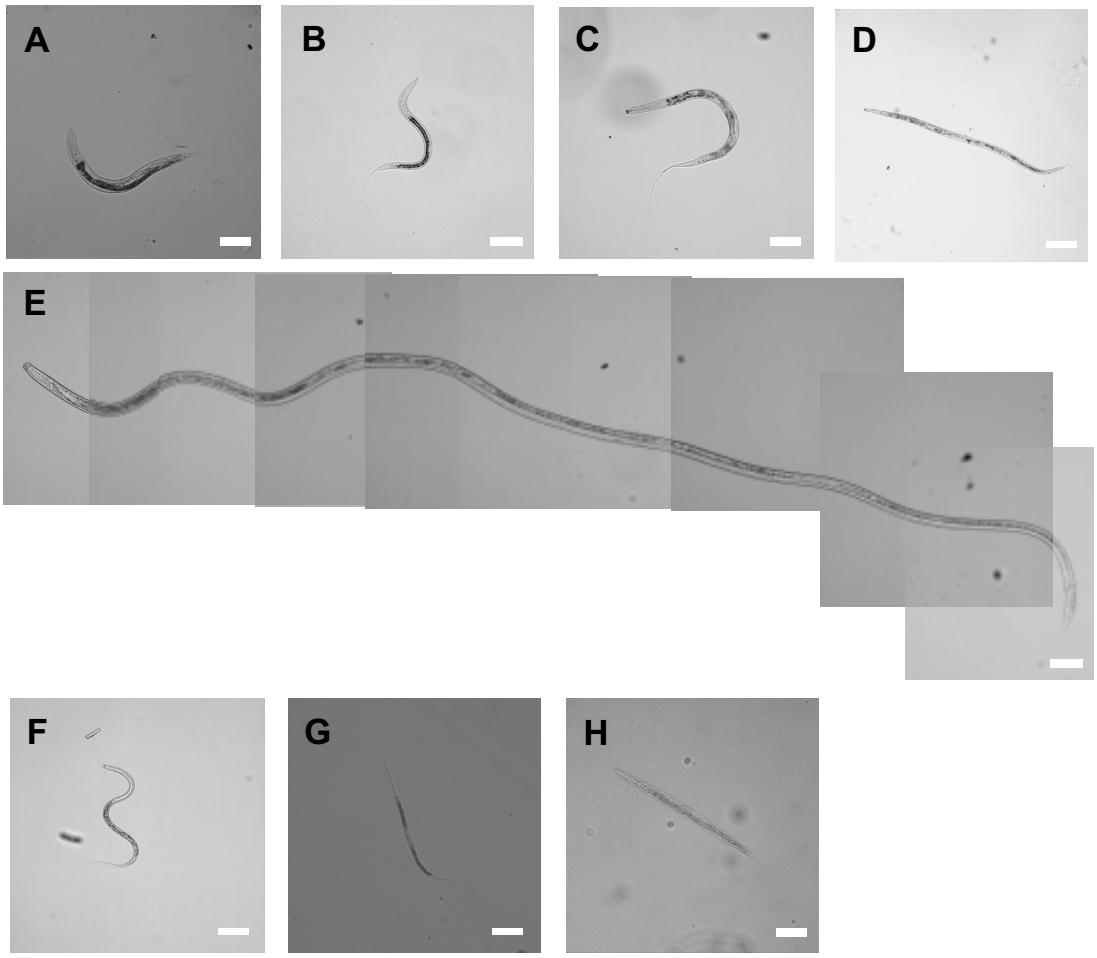

I

Species	Clade		Site A		Site B		Site C		
	Blaxter[3]	Helder[4]	tide zone	lake	dry zone	tide zone	dry zone	tide zone	lake
a. *Auanema sp.*[1,2]	V	9				B8 (2016) B14 (2016)			
b. *Pellioditis sp.*[1,2]	V	9			B20 (2016)	B9 (2016)			
c. *Mononchoides americanus*[1,2]	V	9			B20 (2016)	B7 (2016) B9 (2016)			
d. *Diplogaster rivalis*[1,2]	V	9				B8 (2016)			
e. species in Mermithidae[1,2]	I	2				B9 (2016)	C131 (2017) C133 (2017)		
f. *Prismatolaimus dolichurus*[1]	II	1				B7 (2016)	C130 (2017)		
g. species in Monhysteridae[2]	(II, III)	5		A9 (2016)					
h. species in Monhystreidae[2]	(II, III)	5				B8 (2016)	C7 (2016)		

Figure 4.3. Nematodes isolated from the three sites are diverse in morphology. (A-H) Morphology of species a-h under low magnification. **(I)** Identification and classification of the eight nematodes isolated. The species were identified by either 28S LSU rRNA (Footnote 1) or 18S SSU rRNA (Footnote 2). The classification system was based on the ones introduced by Blaxter (Clade I-V) or Heider (Clade 1-13). Some species fall between Clade II and III, which were indicated with parenthesis in the table. The sample number, location, and the year collected were indicated in the corresponding cell. Highlighted squares denote sites where the species was observed. Samples from 2016 are in beige, and those from 2017 are in grey. Scale bar: 100μm

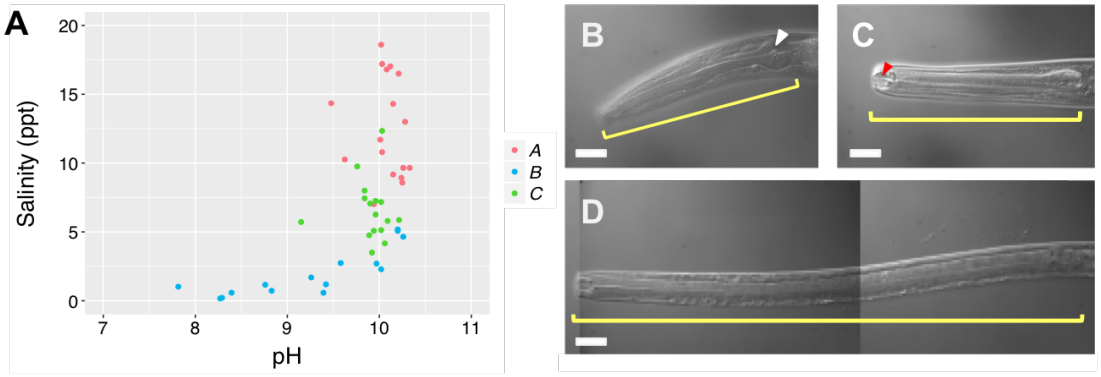

E

Species	Clade		Site A		Site B		Site C		
	Blaxter[3]	Helder[4]	tide zone	lake	dry zone	tide zone	dry zone	tide zone	lake
a. *Auanema sp.*[1,2]	V	9				B8 (2016) B14 (2016)			
b. *Pellioditis sp.*[1,2]	V	9			B20 (2016)	B9 (2016)			
c. *Mononchoides americanus*[1,2]	V	9			B20 (2016)	B7 (2016) B9 (2016)			
d. *Diplogaster rivalis*[1,2]	V	9				B8 (2016)			
e. species in Mermithidae[1,2]	I	2				B9 (2016)	C131 (2017) C133 (2017)		
f. *Prismatolaimus dolichurus*[1]	II	1				B7 (2016)	C130 (2017)		
g. species in Monhysteridae[2]	(II, III)	5		A9 (2016)					
h. species in Monhystreidae[2]	(II, III)	5				B8 (2016)	C7 (2016)		

F

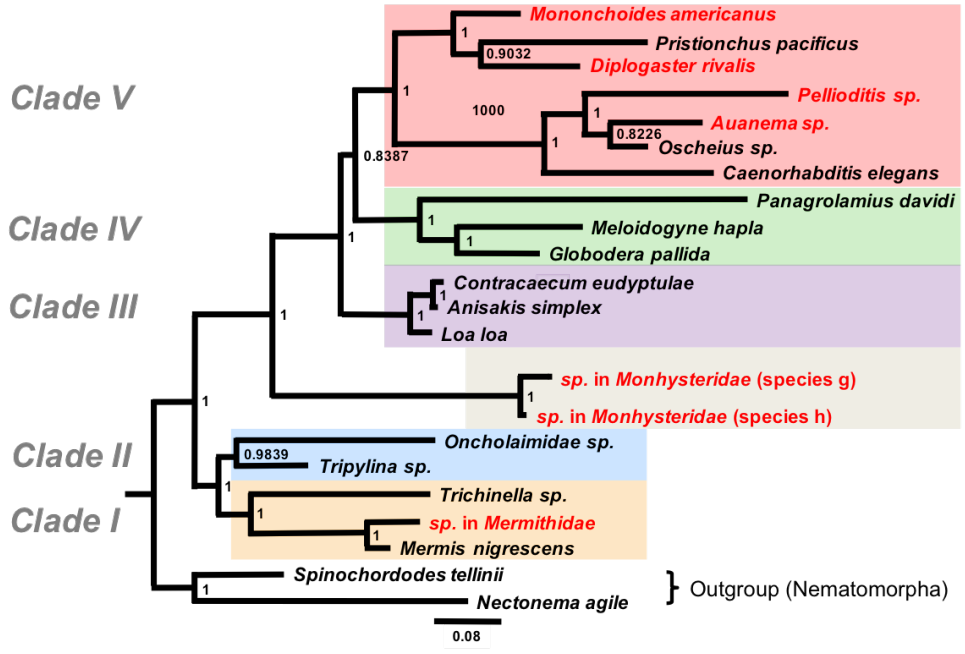

Figure 4.4. The nematodes isolated are phylogenetically and morphologically diverse. **(A)** Plot showing the salinity and pH of all the samples collected. Each dot represents the measurements from one single sample, and the color corresponds to the site where the sample were collected from. **(B-D)** Mouth/head structures of three representative nematodes (Species a, d and f, respectively). The white and red arrowheads indicate the grinder and tooth, respectively. The yellow bracket shows the length of the esophagus. Scale bar: 20μm. **(E)** Identification and classification of the eight nematodes isolated. The species were identified by either 28S LSU rRNA or 18S SSU rRNA. The classification system was based on the ones introduced by Blaxter (Clade I-V) or Heider (Clade 1-13). Some species fall between Clade II and III, which were indicated with parenthesis in the table. The sample number, location, and the year collected were indicated in the corresponding cell. Highlighted squares denote sites where the species was observed. Samples from 2016 are in beige, and those from 2017 are in grey. **(F)** Phylogenetic tree of the eight of the nematodes based on SSU sequences. The nematodes we isolated were highlighted in red. The numbers show the bootstrap score out of 1000 runs. Footnotes: 1, confirmed by LSU rRNA sequence; 2, confirmed by SSU rRNA sequence; 3, reference (31) ; 4, reference (32)

Sample number	Location	From shore (cm)	Under ground (cm)	Water depth (cm)	pH	Salinity (ppt)	Presence of neamtdoes	Number of nematodes/species
A1	tide zone	0	0	0	ND	ND	NO	
A2	tide zone	-150	0	0	ND	ND	NO	
A3	tide zone	0	10	0	ND	ND	NO	
A4	tide zone	0	0	0	9.477	14.342	YES	1 / 1
A5	tide zone	-100	0	0	ND	ND	NO	
A6	dry zone	-900	23	0	ND	ND	NO	
A7	in lake	1800	10	30	ND	ND	NO	
A8	in lake	7000	6	50	9.624	10.26	YES	~5 / 1
A9	in lake	2100	9	30	ND	ND	NO	
A100	tide zone	5	10	0	10.21	16.5	NO	
A101	tide zone	5	5	0	10.08	16.8	YES	1 / 1
A102	dry zone	-300	5	0	10.12	17.02	NO	
A103	tide zone	50	0	5	10.15	14.3	NO	
A104	tide zone	0	5	0	10.02	18.6	NO	
A105	in lake	30	0	5	10.01	11.7	NO	
A106	tide zone	-150	0	0	10.03	17.2	NO	
A107	tide zone	-100	0	5	10.03	10.8	YES	4 / ND
A108	in lake	100	5	10	10.28	13	YES	33 / ND
A109	in lake	1000	5	20	10.33	9.65	YES	1 / 1
A110	in lake	5000	5	20	10.24	8.93	NO	
A111	in lake	10000	5	30	10.25	8.58	YES	4 / ND
A112	in lake	20000	5	50	9.94	7.02	NO	
A113	in lake	30000	5	70	10.15	9.17	NO	
A114	in lake	100	5	5	10.26	9.65	NO	
B1	tide zone	0	0	0	ND	ND	NO	
B2	tide zone	0	0	0	ND	ND	NO	
B3	in lake	300	0	10	ND	ND	NO	
B4	tide zone	0	8	0	ND	ND	NO	
B5	tide zone	20	10	0	ND	ND	YES	2 / 1
B6	tide zone	10	10	0	ND	ND	YES	1 / 1
B7	tide zone	0	5	0	9.3925	0.581	YES	~15 / 2
B8	tide zone	-100	5	0	ND	ND	YES	20 / ≥2
B9	tide zone	-100	5	0	5.967[a]	0.779	YES	~50 / 3
B10	tide zone	0	0	0	ND	ND	YES	1 / 1
B12	tide zone	0	0	0	ND	ND	YES	1 / 1
B13	tide zone	-75	8	0	ND	ND	NO	
B14	tide zone	-75	0	0	8.394	0.586	YES	~200 / ≥3
B15	tide zone	0	0	0	ND	ND	NO	
B16	dry zone	-300	6.5	0	ND	ND	YES	2 / ND
B19	dry zone	-300	5	0	ND	ND	NO	
B20	dry zone	0	0	0	7.815	1.022	YES	~20 / 2
B21	tide zone	-120	4	0	ND	ND	YES	1 / 1
B100	in lake	30	10	0	9.42	1.19	NO	
B101	tide zone	0	10	0	8.83	0.725	NO	
B102	in lake	300	10	0	8.27	0.166	NO	
B103	in lake	50	10	30	9.58	2.74	NO	
B104	in lake	10	10	10	9.97	2.7	NO	
B106	in lake	10	10	10	8.76	1.16	NO	
B107	in lake	30	10	10	9.26	1.692	NO	
B108	tide zone	-100	10	0	8.29	0.214	YES	40 / 1
B111	tide zone	0	10	0	10.02	2.29	NO	
B112	in lake	100	10	40	10.2	5.08	NO	
B113	in lake	300	10	50	10.26	4.65	NO	
B114	in lake	1000	10	100	10.2	5.18	NO	
C1	tide zone	0	5	0	ND	ND	NO	
C2	tide zone	0	0	0	ND	ND	NO	
C3	tide zone	-30	0	0	ND	ND	NO	
C4	tide zone	0	4	0	ND	ND	NO	
C6	tide zone	0	5	0	ND	ND	NO	
C7	dry zone	-200	5	0	10.2145	5.87	YES	3 / 2
C8	tide zone	0	3	0	9.175	22.361[a]	NO	
C100	in lake	300	0	0	10.06	4.17	YES	1 / 1
C101	tide zone	5	0	0	9.89	4.76	YES	2 / ND
C102	dry zone	-20	0	0	10.02	7.17	YES	8 / 1
C103	in lake	10	20	0	10.02	5.13	NO	
C104	dry zone	-1000	0	0	10.03	12.34	YES	52 / ND
C105	in lake	20	20	20	9.92	3.5	NO	
C106	tide zone	0	0	0	9.15	5.72	YES	1 / 1
C108	in lake	100	0	20	9.94	5.08	NO	
C109	in lake	100	10	0	9.96	7.26	NO	
C110	in lake	300	10	40	9.9	7.06	YES	2 / ND
C111	in lake	1000	0	50	10.09	5.8	YES	2 / ND
C112	in lake	3000	10	50	9.84	7.44	YES	1 / 1
C113	in lake	5000	0	50	9.96	6.26	NO	
C114	in lake	7000	10	70	9.84	8	NO	
C115	in lake	10000	10	100	9.76	9.76	NO	
C130	dry zone	-300	5	0	ND	ND	YES	~400 / 1
C131	dry zone	-500	5	0	ND	ND	YES	131 / 2
C132	tide zone	-30	5	0	ND	ND	NO	
C133	dry zone	-1000	5	0	ND	ND	YES	10 / 1
C134	dry zone	-1000	15	0	ND	ND	NO	
C135	dry zone	-1000	28	0	ND	ND	NO	
C136	dry zone	-500	15	0	ND	ND	YES	1 / 1
C137	dry zone	-500	48	0	ND	ND	NO	
C138	dry zone	-50	5	0	ND	ND	NO	
C139	dry zone	-50	48	0	ND	ND	NO	
C140	dry zone	-50	28	0	ND	ND	NO	
C141	dry zone	-50	15	0	ND	ND	NO	
C142	dry zone	-10000	2	0	ND	ND	NO	
C143	tide zone	-30	5	10	ND	ND	YES	1 / 1

Table 4.1. Detailed information of the soil samples collected. Sample numbers include the information of both sampling site (A, B, or C) and sampling year (2016 samples start from 1, 2017 samples start from 100). The sign of the distance from the shore indicates the direction of the sampling site in respect to the lake: positive is into the lake, and negative is away from the lake. Footnote: a, outliers, excluded from further analysis. ND: not determined.

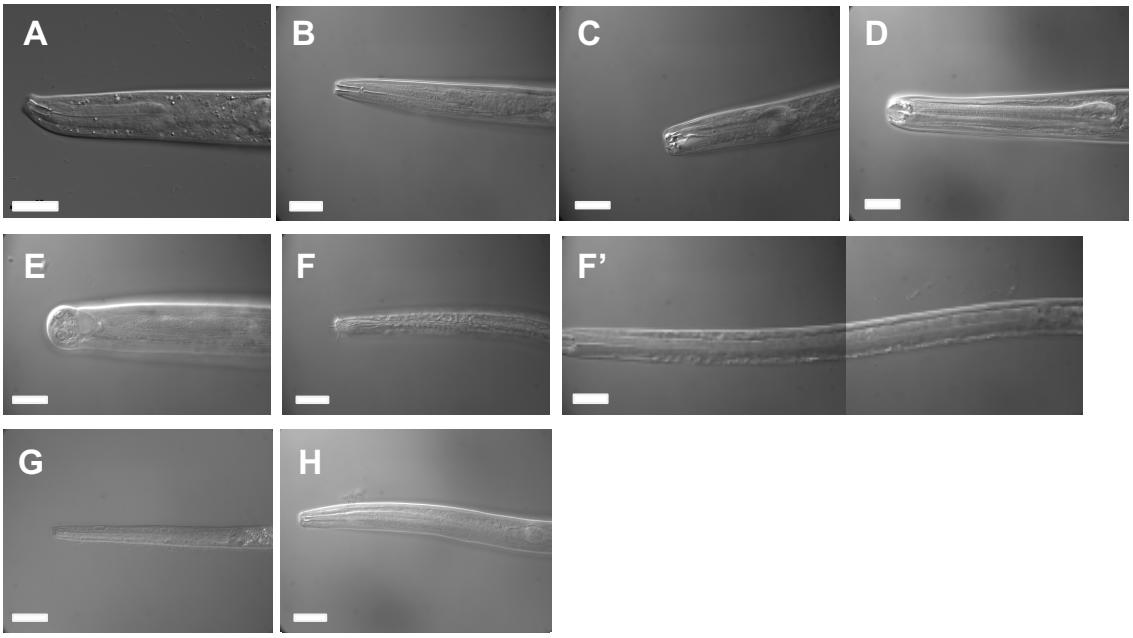

I

Species	Clade		Site A		Site B		Site C		
	Blaxter[3]	Helder[4]	tide zone	lake	dry zone	tide zone	dry zone	tide zone	lake
a. *Auanema sp.*[1,2]	V	9				B8 (2016) B14 (2016)			
b. *Pellioditis sp.*[1,2]	V	9			B20 (2016)	B9 (2016)			
c. *Mononchoides americanus*[1,2]	V	9			B20 (2016)	B7 (2016) B9 (2016)			
d. *Diplogaster rivalis*[1,2]	V	9				B8 (2016)			
e. species in Mermithidae[1,2]	I	2				B9 (2016)	C131 (2017) C133 (2017)		
f. *Prismatolaimus dolichurus*[1]	II	1				B7 (2016)	C130 (2017)		
g. species in Monhysteridae[2]	(II, III)	5		A9 (2016)					
h. species in Monhystreidae[2]	(II, III)	5				B8 (2016)	C7 (2016)		

Figure 4.5. Nematodes isolated from the three sites are diverse in morphology. (A-H) Morphology of species a-i under high magnification. (F) and (F') were taken from the same animal but on different focal planes. **(I)** Identification and classification of the eight nematodes isolated. The sample number, location, and the year collected were indicated in the corresponding cell. Scale bar: 20μm

Species	Sequence identity （%）	
	LSU	SSU
a	89	96
b	88	95
c	90	98 (to Mononchoides americanus)
d	92	99 (to Diplogaster rivalis)
e	85	93
f	99 (to Prismatolaimus dolichurus)	NA
g	NA	92
h	NA	96

Figure 4.6. Percent of sequence identity of each isolate compared to its closest related species. Based on LSU and SSU sequences. NA: not applicable

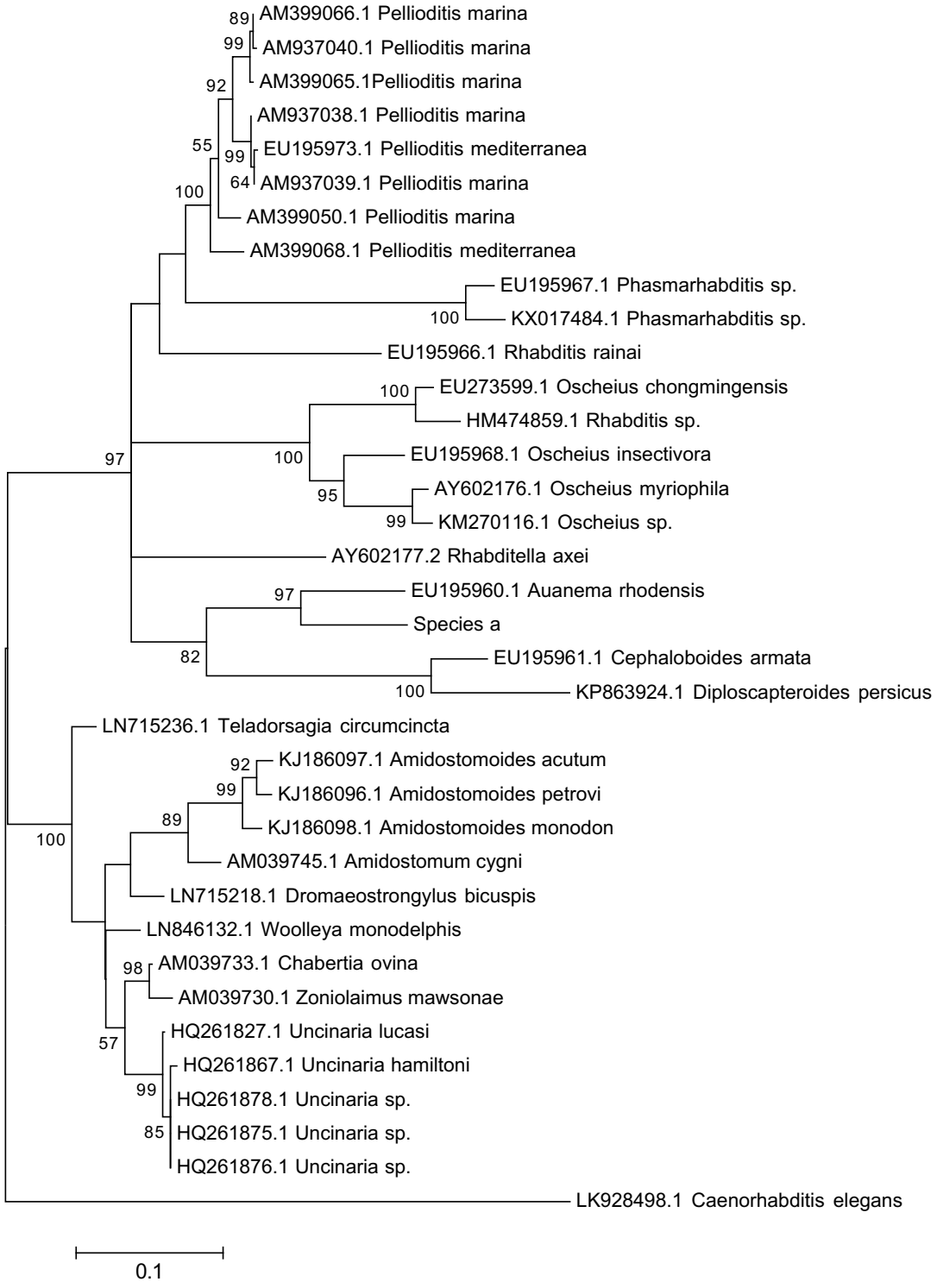

Figure 4.7. Phylogenetic tree of species a (based on LSU sequence)

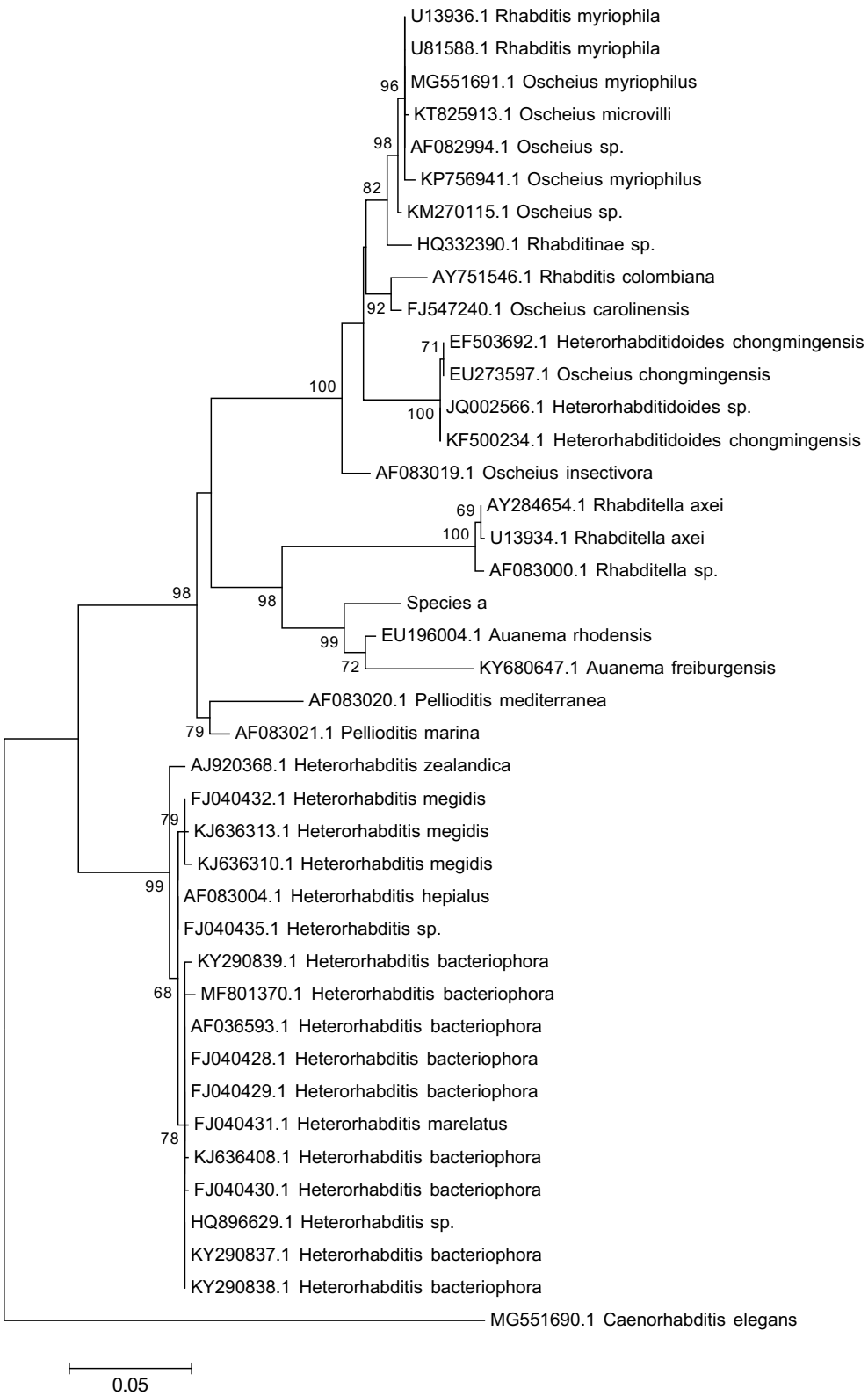

Figure 4.8. Phylogenetic tree of species a (based on SSU sequence)

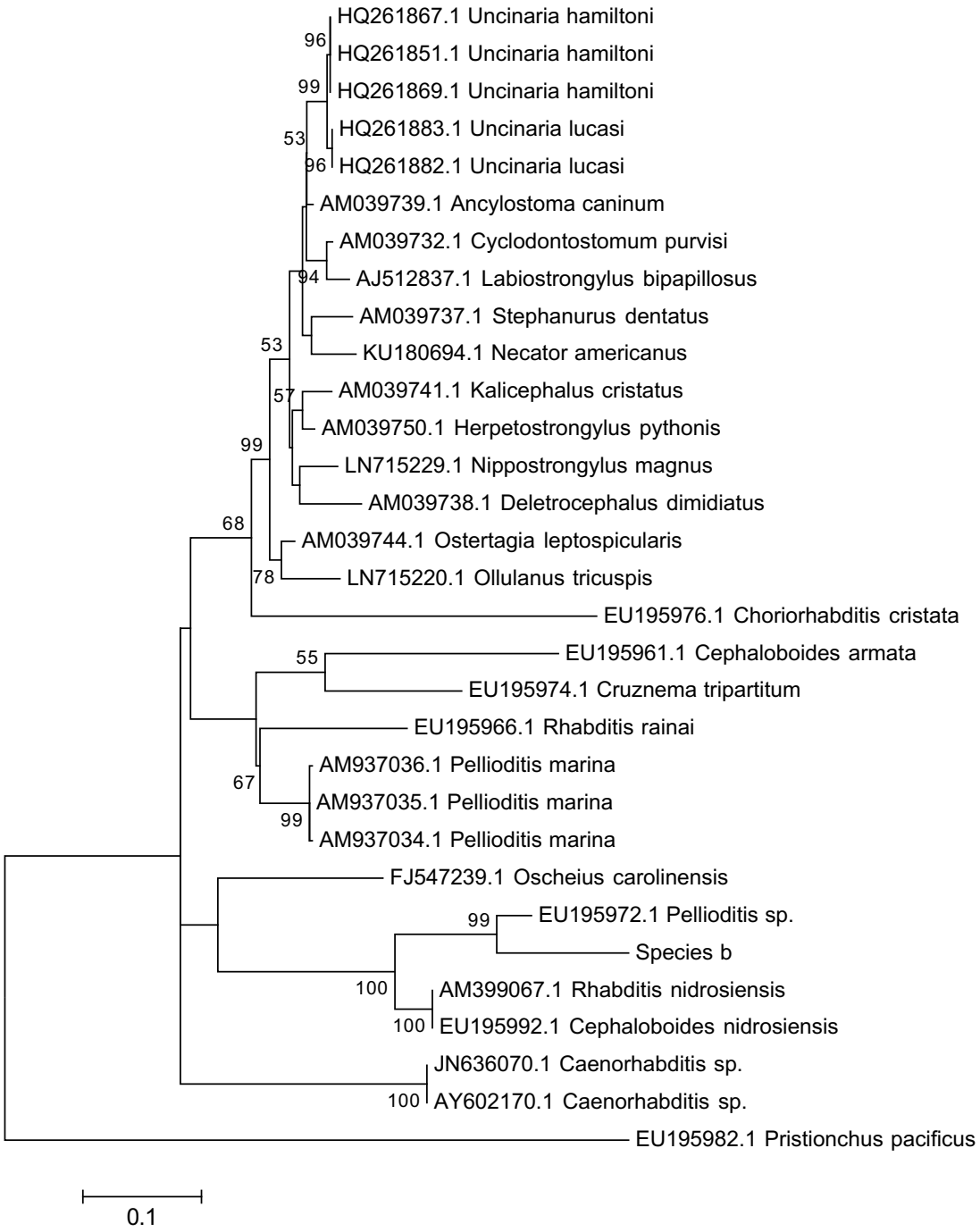

Figure 4.9. Phylogenetic tree of species b (based on LSU sequence)

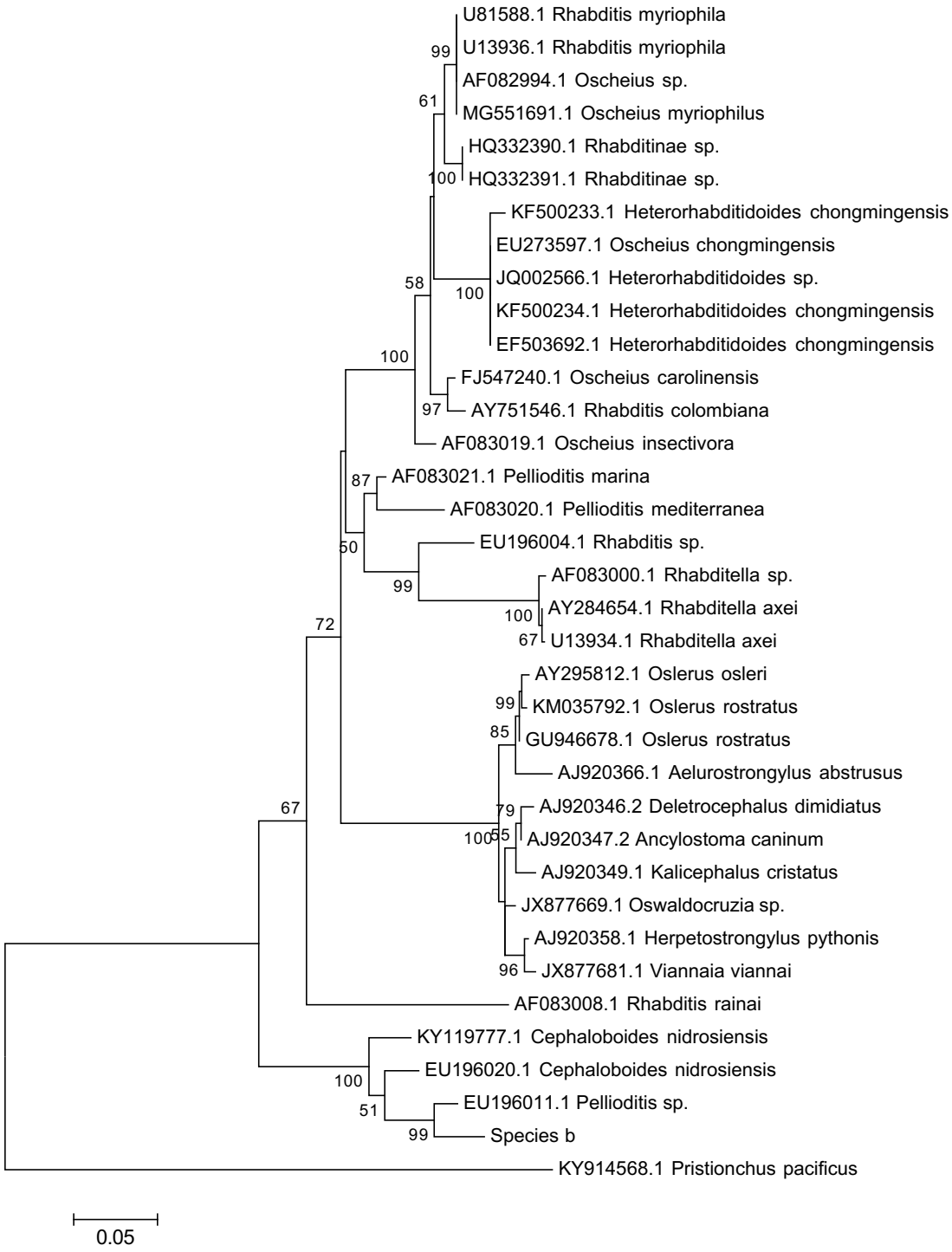

Figure 4.10. Phylogenetic tree of species b (based on SSU sequence)

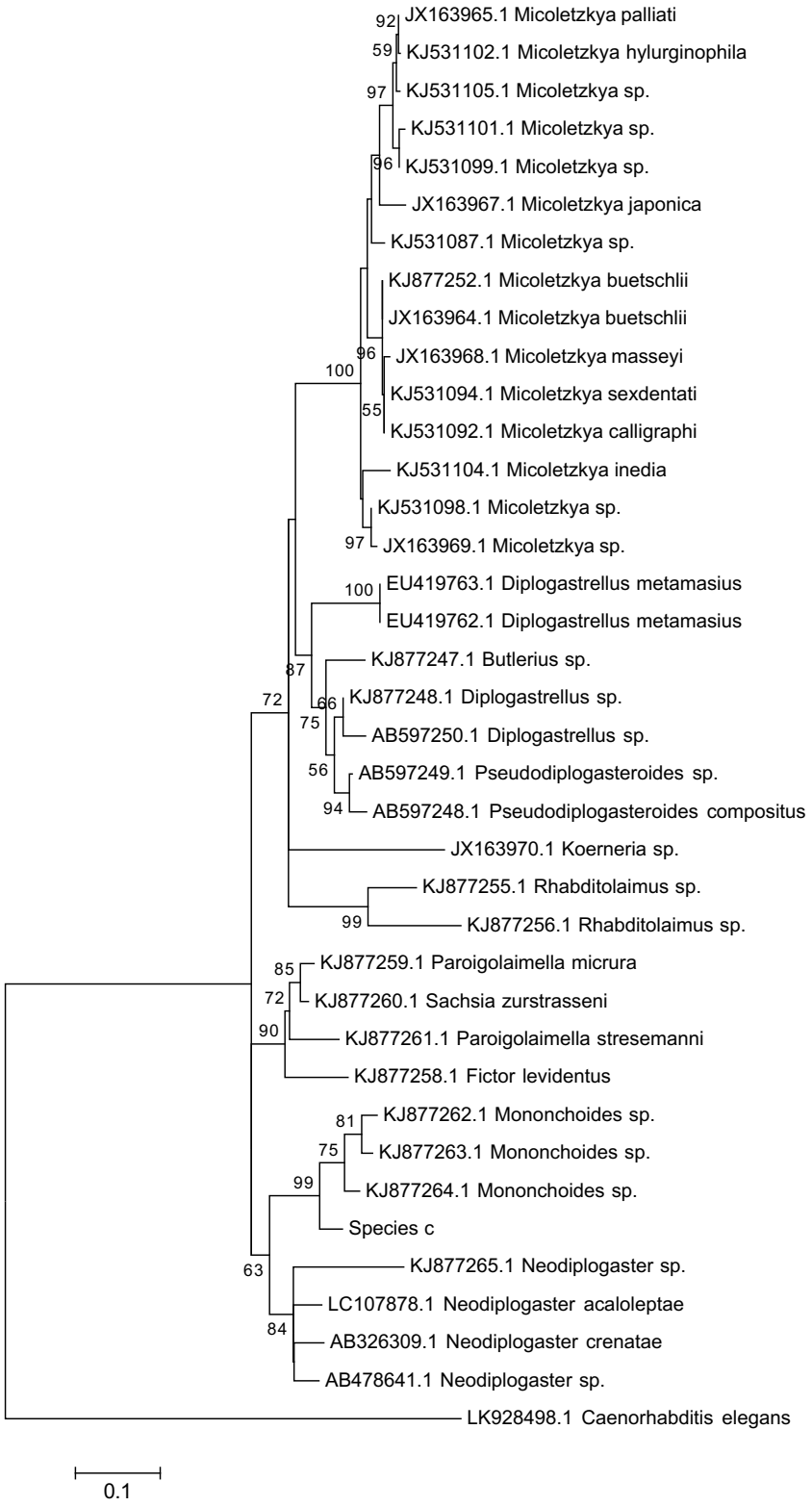

Figure 4.11. Phylogenetic tree of species c (based on LSU sequence)

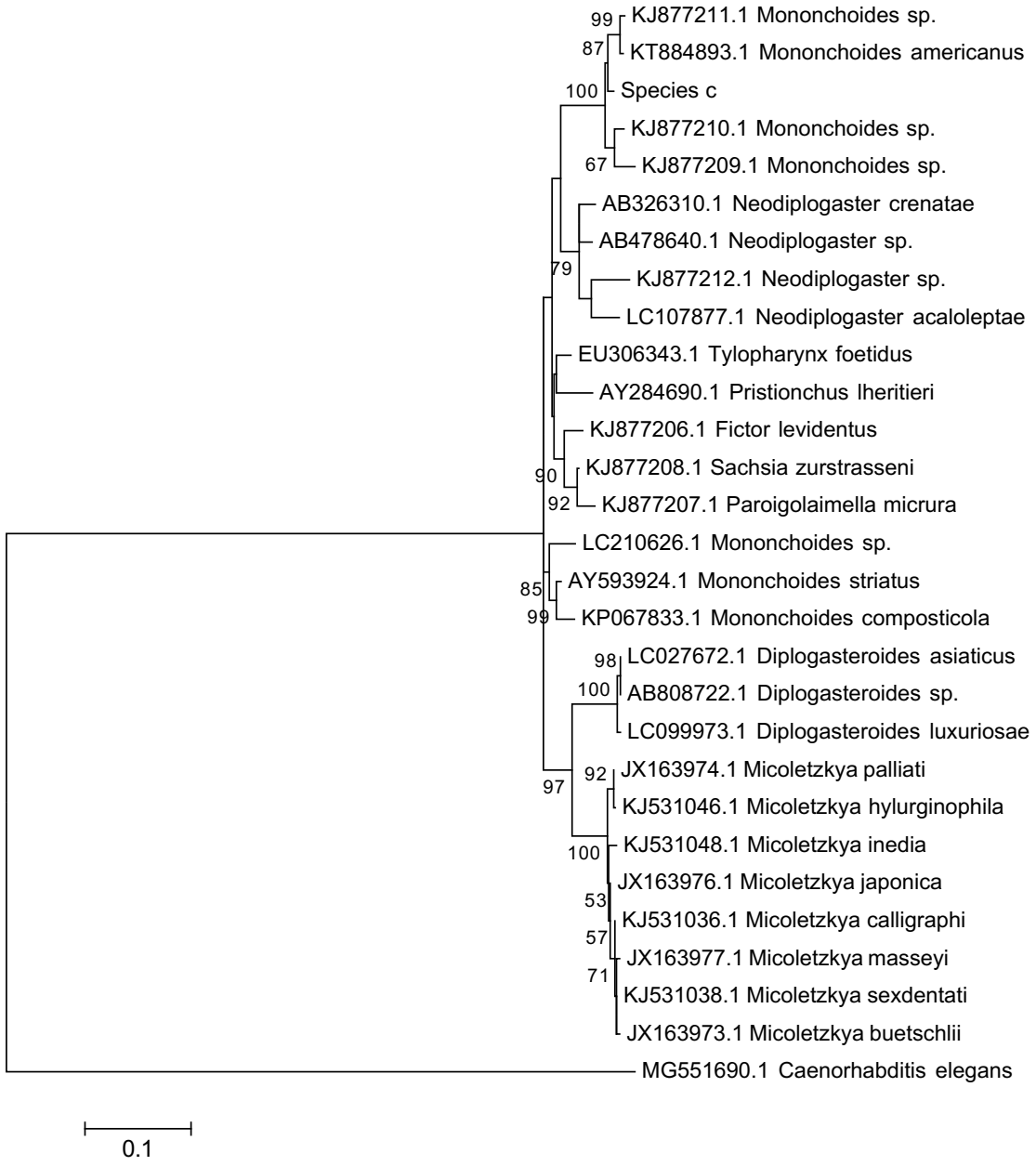

Figure 4.12. Phylogenetic tree of species c (based on SSU sequence)

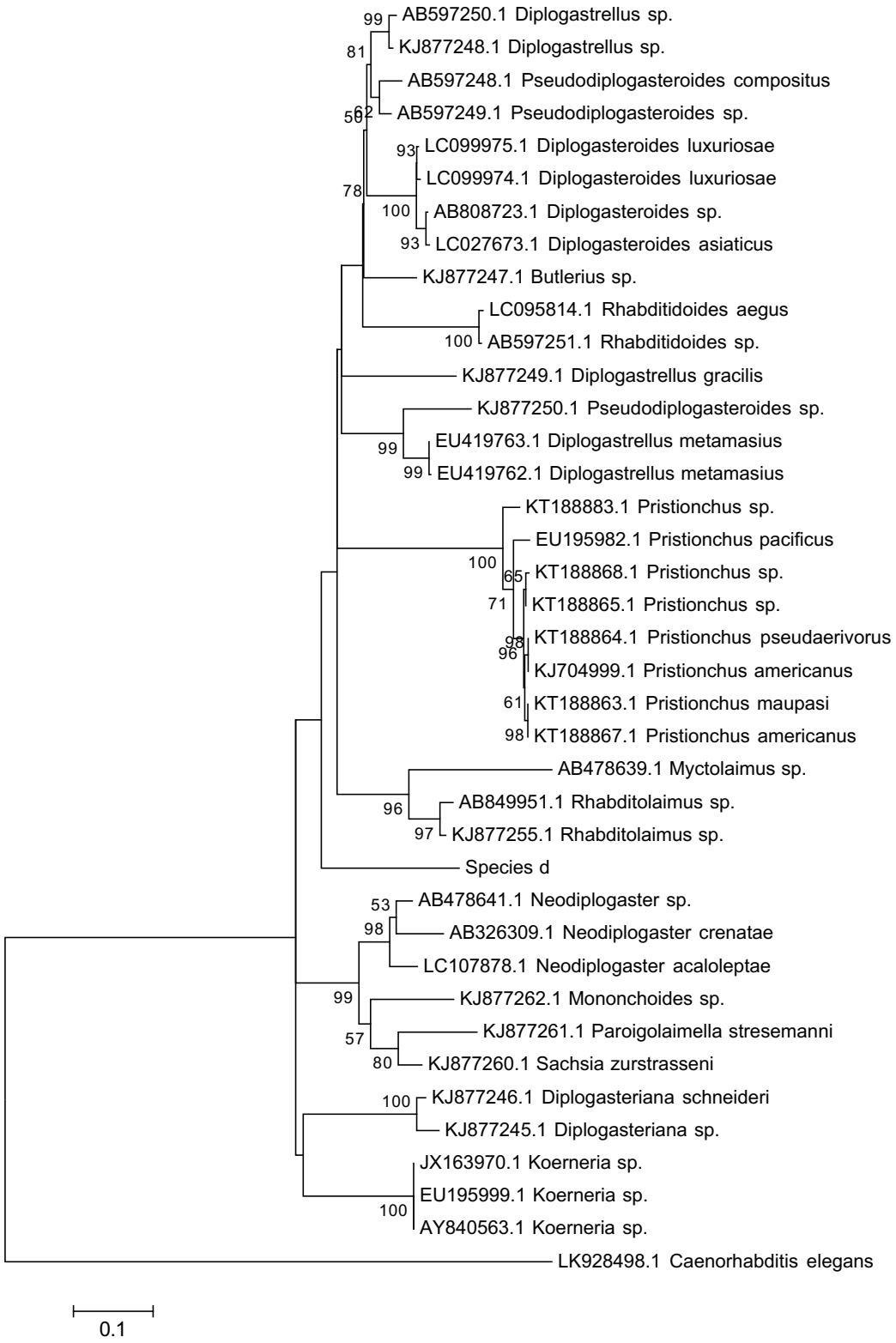

Figure 4.13. Phylogenetic tree of species d (based on LSU sequence)

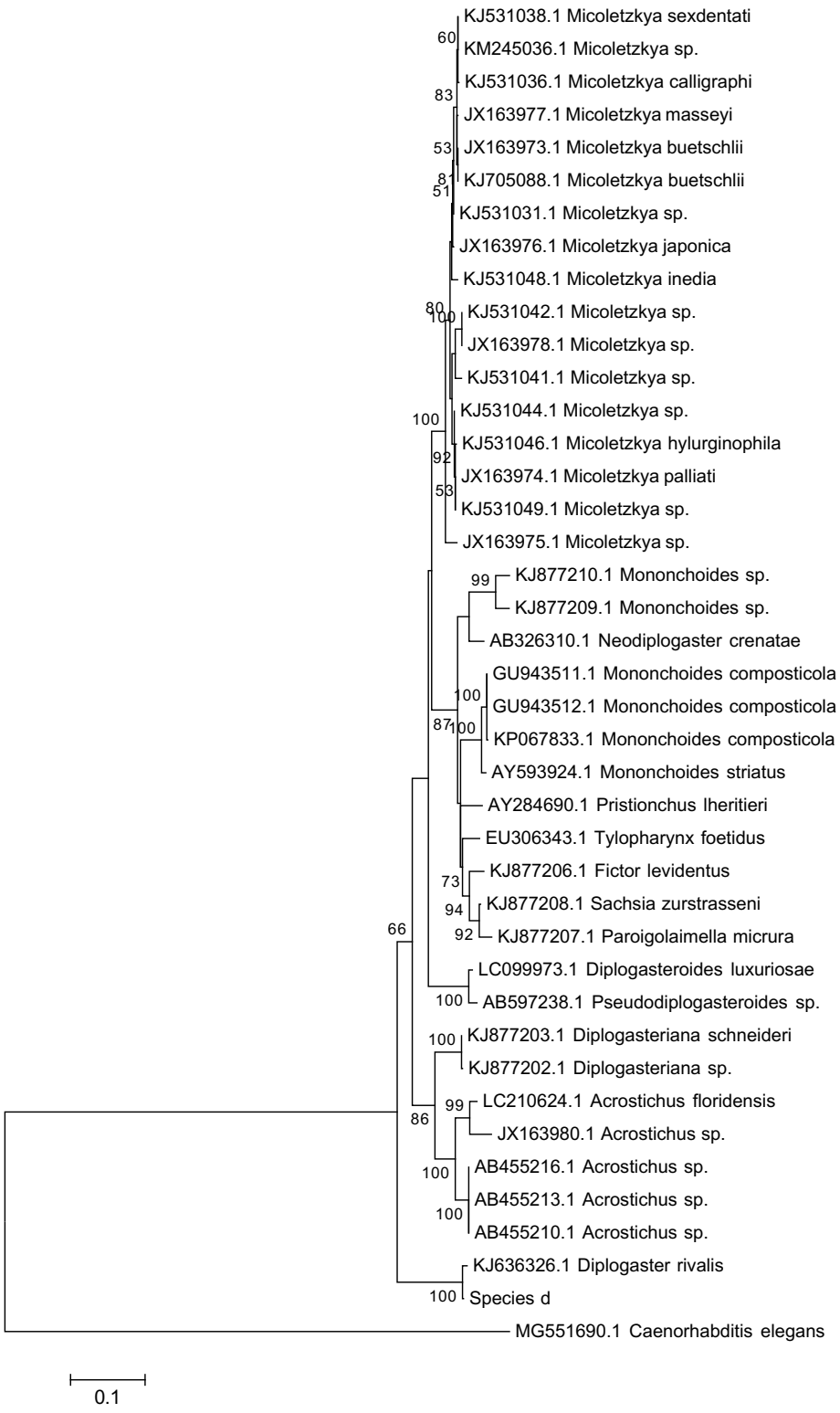

Figure 4.14. Phylogenetic tree of species d (based on SSU sequence)

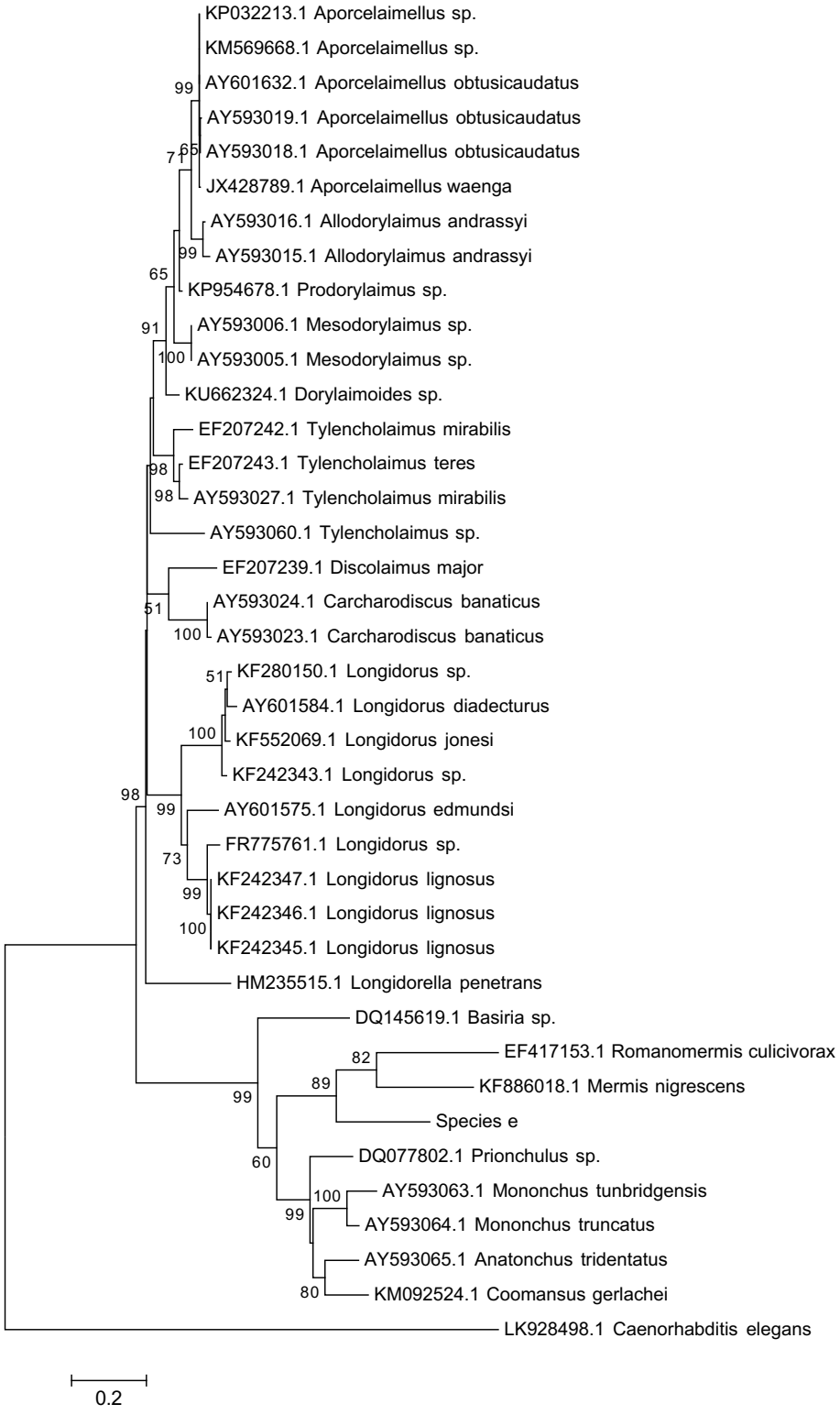

Figure 4.15. Phylogenetic tree of species e (based on LSU sequence)

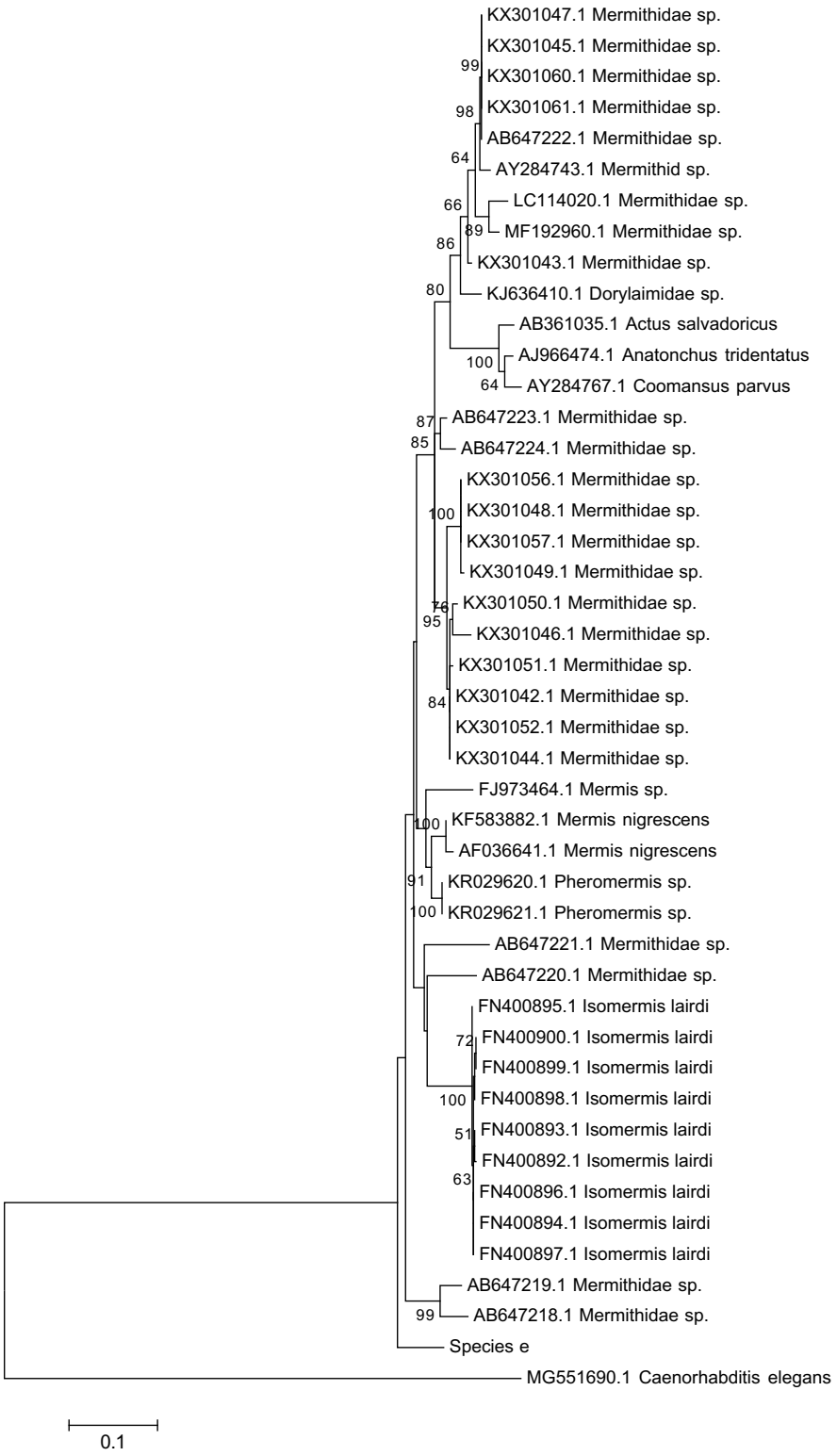

Figure 4.16. Phylogenetic tree of species e (based on SSU sequence)

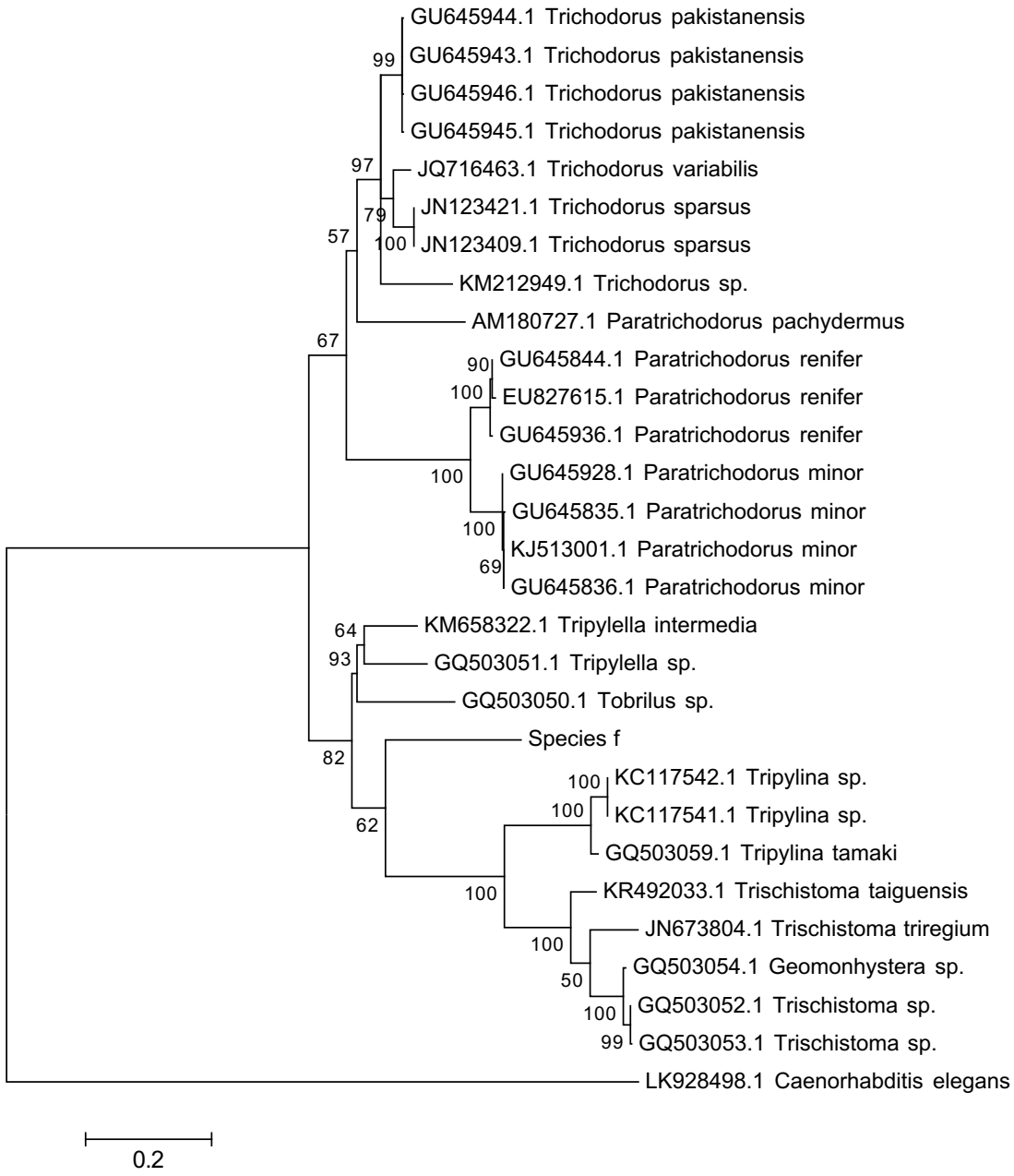

Figure 4.17. Phylogenetic tree of species f (based on LSU sequence)

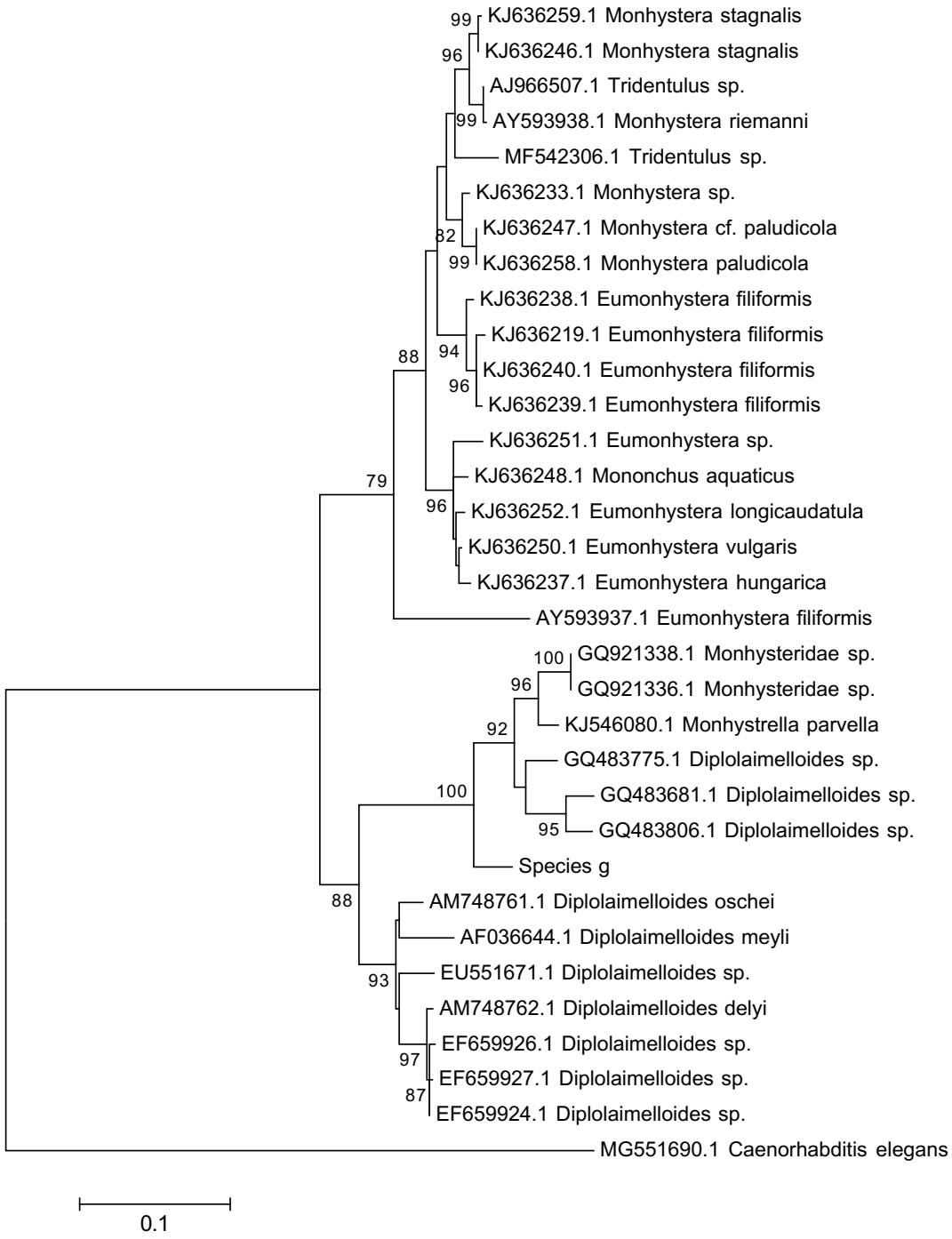

Figure 4.18. Phylogenetic tree of species g (based on SSU sequence)

Figure 4.19. Phylogenetic tree of species h (based on SSU sequence)

```
g       -------------------ATTACAACAGCCGTTGTTTCTTGGATCTCTTCTCTACTTGGA     42
h       ----AGCCGCGATAGCTCATTACAACAGCCGTTGTTTCTTGGATCTCTTCTCTACTTGGA     56
i       AGTGAGCCGCGATAGCTCATTACAACAGCCGTTGTTTCTTGGATCTCTTCTCTACTTGGA     60
                     ****************************************

g       TAACTGTGGTAATTCTAGAGCTAATACATGCAATCAAGCCCTGAACTTACGTGACGGGCG     102
h       TAACTGTGGTAATTCTAGAGCTAATACATGCAACCAAGCCCTGAACTTACGTGACGGGCG     116
i       TAACTGTGGTAATTCTAGAGCTAATACATGCAACCAAGCCCTGAACTTACGTGACGGGCG     120
        ******************************** ************************

g       CATTTATTAGAACAAAACCATCCGGCTTTGC--CGTGCTTTGGTGACTCTGAATAACTGA     160
h       CATTTATTAGAACAAAACCATCTGGCCTCGCGCCATCTAATGGTGACTCTGAATAACTGA     176
i       CATTTATTAGAACAAAACCATCTGGCCTCGCGCCATCTAATGGTGACTCTGAATAACTGA     180
        ********************** *** * **  * *    ********************

g       GCCGATCGCACGGGCTTGTCCCGGCGACATATCTTTCAAGTGTCTGCCTTATCAGGTTTC     220
h       GCCGATCGCACGGGCTCGTCCCGGCGACGTATCTTTCAAGTGTCTGCCTTATCAGGTTTC     236
i       GCCGATCGCACGGGCTTGTCCCGGCGACATATCTTTCAAGTGTCTGCCTTATCAGGTTTC     240
        **************** *********** ********************************

g       GTTGGCGGTTTATGTGACCGCCAAGCCTGTAACGGGTAACGGAGGATCAGGGTCTGACTC     280
h       GTTGGCGGTTTATGTGACCGCCAAGCCTGTAACGGGTAACGGAGGATCAGGGTCTGACTC     296
i       GTTGGCGGTTTATGTGACCGCCAAGCCTGTAACGGGTAACGGAGGATCAGGGTCTGACTC     300
        ************************************************************

g       CGGAGAGGGAGCCTGAGAAACGGCTACCACTTCTAAGGAAGGCAGCAGGCGCGCAAATTA     340
h       CGGAGAGGGAGCCTGAGAAACGGCTACCACTTCTAAGGAAGGCAGCAGGCGCGCAAATTA     356
i       CGGAGAGGGAGCCTGAGAAACGGCTACCACTTCTAAGGAAGGCAGCAGGCGCGCAAATTA     360
        ************************************************************

g       CCCACTCTTGGAGCAAGGAGGTAGTGACGAAAAATACCAAGGTCAGGCTCATTGAGCTTG     400
h       CCCACTCTTGGAGCAAGGAGGTAGTGACGAAAAATACCAAGGTCAGGCTCATCGAGCTTG     416
i       CCCACTCTTGGAGCAAGGAGGTAGTGACGAAAAATACCAAGGTCAGGCTCATCGAGCTTG     420
        ************************************************** *******

g       ACCATTGGAATGAGAACAATCTAAATCCTTTAACGAGGATCTAGTGGAGGGCAAGTCTGG     460
h       ACCATTGGAATGAGAACAATCTAAATCCTTTAACGAGGATCTAGTGGAGGGCAAGTCTGG     476
i       ACCATTGGAATGAGAACAATCTAAATCCTTTAACGAGGATCTAGTGGAGGGCAAGTCTGG     480
        ************************************************************

g       TGCCAGCAGCCGCGGTAATTCCAGCTCCGCAAGTGTATTCCTATACTGTTGCGTTTAAAT     520
h       TGCCAGCAGCCGCGGTAATTCCAGCTCCGCAAGTGTATTCCTATACTGTTGCGTTTAAAT     536
i       TGCCAGCAGCCGCGGTAATTCCAGCTCCGCAAGTGTATTCCTATACTGTTGCGTTTAAAT     540
        ************************************************************

g       AGCTCGTAGTTGGATCTGCGTGTTTAGCGCGTGGTGCTGCTTTTTGTGGTTACTGCGACG     580
h       AGCTCGTAGTTGGATCTGCGTGTTTAGCGCGCGGTGCTGCTTTTTGCAGTTACTGCGACG     596
i       AGCTCGTAGTTGGATCTGCGTGTTTAGCGCGCGGTGCTGCTTTTTGCAGTTACTGCGACG     600
        ******************************** **************  ************

g       CGACACAGTGTTGCTTTCTGCCACGATGCTCTCGCGAGTGTCGTGTCGATAAGCAGAGTT     640

h       CGACACAGTGTTGCTTGCTGCCACGATGCTCCCACAAGG----------------------     635
i       CGACACAGTGTTGCTTGCTGCCACGATGCTC------------------------------     631
        **************** **************

g       TACTTTGAACAAATCAGAGTGCTCAAAACGGGCGTTTCGCTCGAATGTTCTTGCATGGAA     700
h       ------------------------------------------------------------     635
i       ------------------------------------------------------------     631


g       TAATGGAATA       710
h       ----------       635
i       ----------       631
```

Figure 4.20. Species g and h SSU sequence alignment

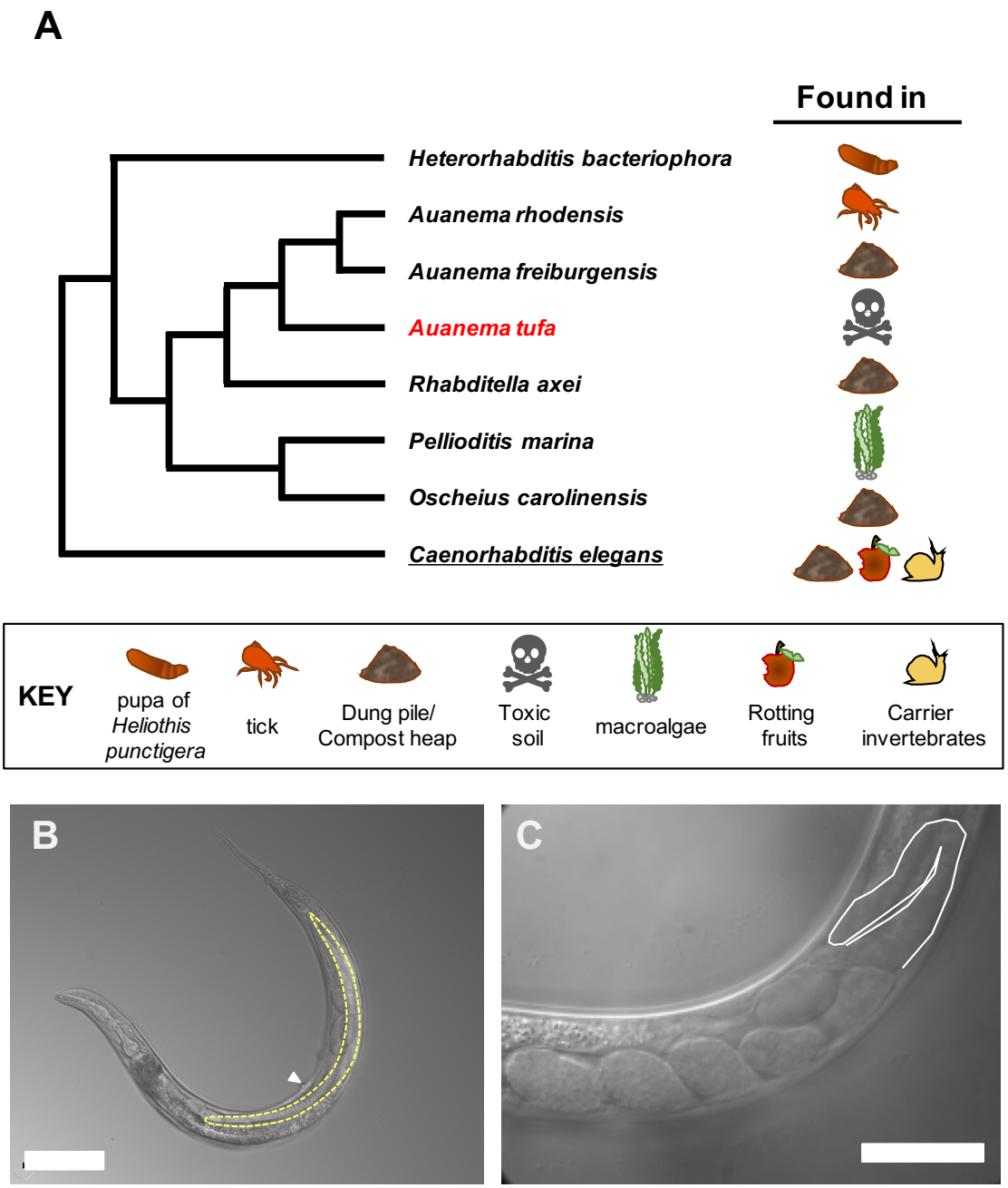

Figure 4.21. Characteristics of *Auanema tufa*. (A) Simplified phylogenetic tree showing the phylogenetic relationships of *Auanema tufa* (highlighted in red) and selected Rhabditina based on SSU sequences. **(B)** One of the two arms of the *A. tufa* adult gonad. The gonad arm is outlined with white line. Scale bar: 20μm. **(C)** The representative image of an adult *A. tufa*. The position of the vulva was indicated by the white arrow. Scale bar: 100μm

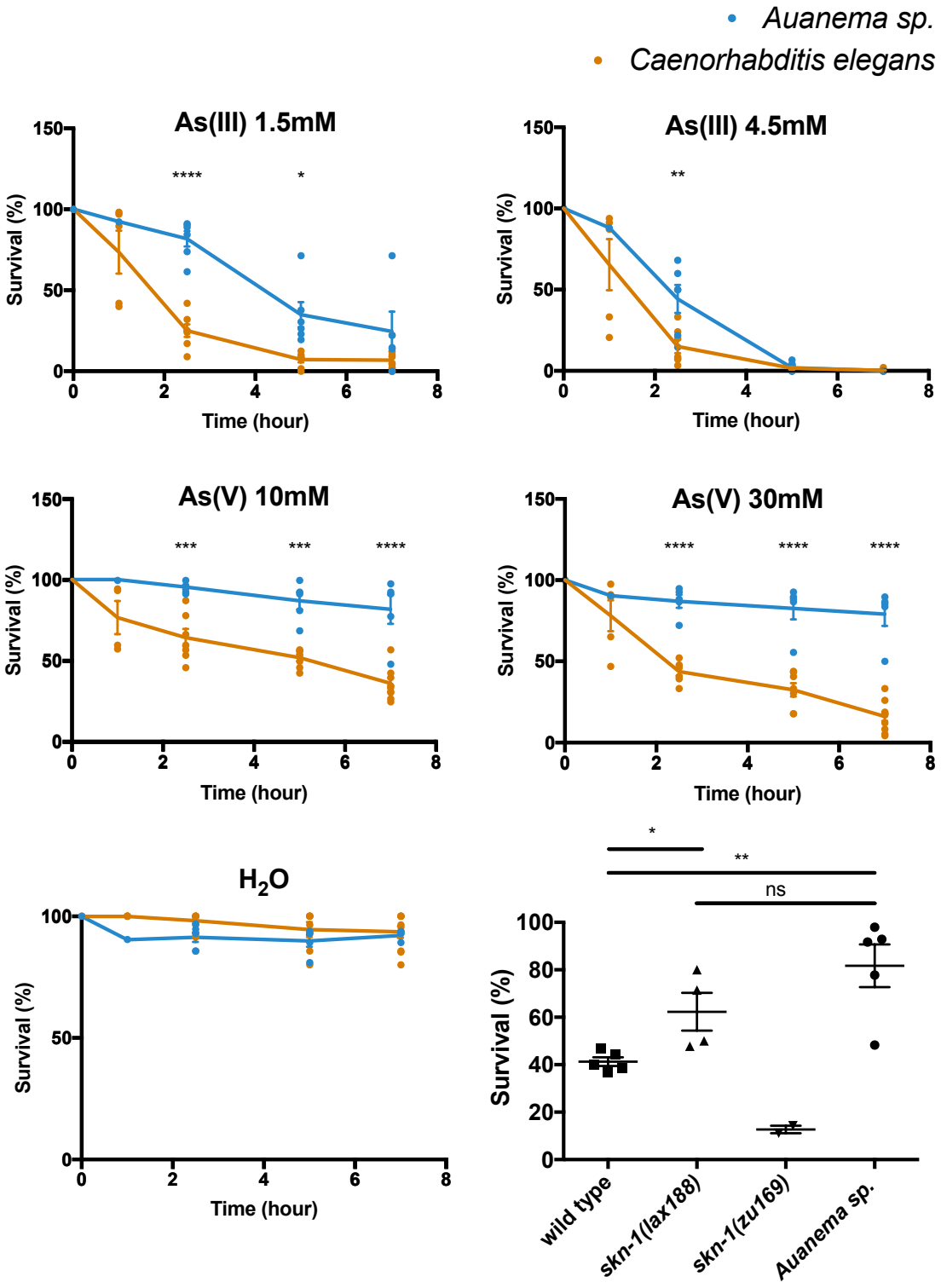
Auanema sp.
Caenorhabditis elegans
As(III) 1.5mM
As(III) 4.5mM
As(V) 10mM
As(V) 30mM
H2O
Survival (%)
Time (hour)
****
*
**
***
ns
wild type
skn-1(lax188)
skn-1(zu169)
Auanema sp.

Figure 4.22. *A. tufa* is resistant to arsenic. (A-D) The survival curve of *A. tufa* (blue) and *C. elegans* (orange) in 1.5mM As(III) (A), 4.5mM As(III) (B),10mM As(V) (C), or 30 mM As(V) (D). **(E)** The survival of *Auanema sp.* (blue) and *C. elegans* (orange) in water over time. Statistics: two-way ANOVA with Bonferroni correction. "*"<0.05, "**"<0.01, "***"< 0.001, "****" <0.0001. **(F)** The survival percentage of *C. elegans,* wild-type animals, *skn-1* mutants (with gain-of-function *(lax188)* and *A. tufa* with 10mM As(V) treatment for seven hours. WT, wild-type; gf, gain-of-function. Statistics: One-way ANOVA with Tukey's post hoc test after the validation of normal distribution using the SPSS software "*" $p<0.05$. Error bars indicate the standard error of the mean.

4.7 References

1. Borgonie G, et al. (2011) Nematoda from the terrestrial deep subsurface of South Africa. Nature 474(7349):79–82.

2. Borgonie G, et al. (2015) Eukaryotic opportunists dominate the deep-subsurface biosphere in South Africa. Nature communications 6:8952.

3. Treonis AM, Wall DH (2005) Soil nematodes and desiccation survival in the extreme arid environment of the antarctic dry valleys. Integrative and comparative biology 45(5):741–50.

4. Wharton D, Ferns D (1995) Survival of intracellular freezing by the Antarctic nematode Panagrolaimus davidi. The Journal of experimental biology 198(Pt 6):1381–7.

5. Sapir A, et al. (2014) Microsporidia-nematode associations in methane seeps reveal basal fungal parasitism in the deep sea. Front Microbiol 5:43.

6. Vanreusel A, De Groote A, Gollner S, Bright M (2010) Ecology and biogeography of free-living nematodes associated with chemosynthetic environments in the deep sea: a review. PLoS ONE 5(8):e12449.

7. Borgonie G, et al. (2015) Deep subsurface mine stalactites trap endemic fissure fluid Archaea, Bacteria, and Nematoda possibly originating from ancient seas. Frontiers in microbiology 6:833.

8. Danovaro R, et al. (2010) The first metazoa living in permanently anoxic conditions. BMC Biol 8:30.

9. Riddle DL, Albert PS (1997) Genetic and environmental regulation of dauer larva development. C. Elegans II, eds Riddle DL, Blumenthal T, Meyer BJ, Priess JR (Cold Spring Harbor (NY)). 2nd Ed. Available at: http://www.ncbi.nlm.nih.gov/pubmed/21413222.

10. Vanfleteren JR, Braeckman BP (1999) Mechanisms of life span determination in Caenorhabditis elegans. Neurobiol Aging 20(5):487–502.

11. Oremland RS, Stolz JF, Hollibaugh JT (2004) The microbial arsenic cycle in Mono Lake, California. FEMS microbiology ecology 48(1):15–27.

12. Reheis MC, Stine S, Sarna-Wojcicki AM (2002) Drainage reversals in Mono Basin during the late Pliocene and Pleistocene. GSA Bulletin 114(8):991–1006.

13. Cloud P, Lajoie KR (1980) Calcite-impregnated defluidization structures in littoral sands of mono lake, California. Science 210(4473):1009–1012.

14. Nielsen LC, DePaolo DJ (2013) Ca isotope fractionation in a high-alkalinity lake system: Mono Lake, California. Geochimica et Cosmochimica Acta 118:276–294.

15. Jellison R, Melack JM (1993) Meromixis in hypersaline Mono Lake, California. 1. Stratification and vertical mixing during the onset, persistence, and breakdown of meromixis. Limnology and Oceanography 38(5):1008–1019.

16. Smedley PL, Kinniburgh D (2002) A review of the source, behaviour and distribution of arsenic in natural waters. Applied Geochemistry 17(5):517–568.

17. Hughes MF (2002) Arsenic toxicity and potential mechanisms of action. Toxicol Lett 133(1):1–16.

18. Council NR (2001) Arsenic in Drinking Water: 2001 Update (The National Academies Press, Washington, DC) doi:10.17226/10194.

19. Wiens JA, Patten DT, Botkin DB (1993) Assessing ecological impact assessment: Lessons from Mono Lake, California. Ecological applications : a publication of the Ecological Society of America 3(4):595–609.

20. Raymond MW DA and Marshall, CJ (2013) Factors determining nematode distributions at Cape Hallett and Gondwana station, Antarctica. Antarctic Science 25(3):347–357.

21. Hooper DJ (1986) Extraction of free-living stages from soil. In Laboratory Methods for Work with Plant and Soil Nematodes, ed Southey JF (HMSO, London), pp 5–30.

22. Nunn GB (1992) Nematode molecular evolution: an investigation of evolutionary patterns among nematodes based upon DNA sequences. Ph.D. (University of Nottingham, United Kingdom).

23. Floyd R, Abebe E, Papert A, Blaxter M (2002) Molecular barcodes for soil nematode identification. Molecular ecology 11(4):839–50.

24. Hall BG (2013) Building phylogenetic trees from molecular data with MEGA. Molecular biology and evolution 30(5):1229–35.

25. Guindon S, Gascuel O, Rannala B (2003) A simple, fast, and accurate algorithm to estimate large phylogenies by maximum likelihood. Syst Biol 52(5):696–704.

26. Schlaberg R, Simmon KE, Fisher MA (2012) A systematic approach for discovering novel, clinically relevant bacteria. Emerg Infect Dis 18(3):422–430.

27. Marande W, López-García P, Moreira D (2009) Eukaryotic diversity and phylogeny using small- and large-subunit ribosomal RNA genes from environmental samples. Environ Microbiol 11(12):3179–3188.

28. Yeates GW Coleman, DC (1982) Role of nematodes in decomposition. Nematodes in Soil Ecosystems, ed Freckman DW (University of Texas Press Austin), pp 55–80.

29. Bento G, Ogawa A, Sommer RJ (2010) Co-option of the hormone-signalling module dafachronic acid-DAF-12 in nematode evolution. Nature 466(7305):494–497.

30. Nickle WR (1972) A contribution to our knowledge of the Mermithidae (Nematoda). J Nematol 4(2):113–146.

31. Blaxter ML, et al. (1998) A molecular evolutionary framework for the phylum Nematoda. Nature 392(6671):71–5.

32. Holterman M, et al. (2006) Phylum-wide analysis of SSU rDNA reveals deep phylogenetic relationships among nematodes and accelerated evolution toward crown Clades. Molecular biology and evolution 23(9):1792–800.

33. Kanzaki N, et al. (2017) Description of two three-gendered nematode species in the new genus Auanema (Rhabditina) that are models for reproductive mode evolution. Sci Rep 7(1):11135.

34. Gaever SV, Moodley L, Beer D de, Vanreusel A (2006) Meiobenthos at the Arctic Håkon Mosby Mud Volcano, with a parental-caring nematode thriving in sulphide-rich sediments. Marine Ecology Progress Series 321:143–155.

35. Zeppilli D, et al. (2015) Rapid colonisation by nematodes on organic and inorganic substrata deployed at the deep-sea Lucky Strike hydrothermal vent field (Mid-Atlantic Ridge). Mar Biodiv 45(3):489–504.

36. Oremland RS, et al. (2000) Bacterial dissimilatory reduction of arsenate and sulfate in meromictic Mono Lake, California. Geochimica et Cosmochimica Acta 64(18):3073–3084.

37. Inoue H, et al. (2005) The C. elegans p38 MAPK pathway regulates nuclear localization of the transcription factor SKN-1 in oxidative stress response. Genes Dev 19(19):2278–2283.

38. Golden JW, Riddle DL (1984) The Caenorhabditis elegans dauer larva: developmental effects of pheromone, food, and temperature. Dev Biol 102(2):368–378.

39. Fielenbach N, Antebi A (2008) C. elegans dauer formation and the molecular basis of plasticity. Genes & development 22(16):2149–65.

40. Campbell JF, Gaugler R (1993) Nictation behaviour and its ecological implications in the host search strategies of entomopathogenic nematodes (Heterorhabditidae and Steinernematidae). Behaviour 126(3/4):155–169.

41. Rödelsperger C, Streit A, Sommer RJ (2013) Structure, function and evolution of the nematode genome. ELS, ed John Wiley & Sons, Ltd (John Wiley & Sons, Ltd, Chichester, UK). doi:10.1002/9780470015902.a0024603.

Chapter 5

CONCLUSIONS

5.1 Concluding remarks

In working on my thesis, I have thought about how stress affects development and behavior. For example, chronic stress in mammals can affect the structure and function of the brain region associated with memory and emotion (1). Under stressful conditions, tardigrades can hibernate and even survive in the vacuum of space (2).

In the case of nematodes, I discovered that *Caenorhabditis elegans* use neuropeptides to respond to stress and to change their neural states (3). I also discovered around 8,000 other molecular correlates to stress, and used a selection as molecular markers to track and manipulate the dauer entry decision. Going outside of the lab, I discovered nematodes surviving in Mono Lake, and proposed an idea for how pre-adaptation to arsenic in the tide zone could lead to the genomic evolution needed to invade inner Mono Lake.

Here, I speculate that the *C. elegans* strategy of using FMRFamide neuropeptides to change their neural state during dauer is especially important for overcoming the constraints of their physically limited nervous system. That is, because *C. elegans* neurons are over-connected, the nervous system lacks compartmentalization, and does not contain an obvious region that could be specialized for dauer functions (4, 5). Instead, specialized connections between neurons could be created through the different combinations of neuropeptides and their particular receptors. Therefore, species with limited compartmentalization might rely on neuropeptides to allow them to switch neural states, potentially for responding to environmental stresses.

In the case of the human brain, which is compartmentalized into regions tasked with functions such as vision, learning, and memory, one might suspect neuropeptides to be less

important. In fact, even with compartmentalization, neuropeptides might help set up neural states within a region as well. For example, the dynamic visual information processing in mammalian retina requires the modulation of neuropeptdie NPY(6, 7).

On working on my thesis, I have also thought about the importance of field trip and look at biology in the nature. In-lab experiments are useful for precise quantitative measurements of complex and noisy animal development and behaviors. However, because lab condition is so controlled, we might lose our insight in studying biological relevant questions. That's why I think sufficient balance of in- and out-of-lab experiments is ideal.

From my perspective and experience, I believe there are several exciting directions the dauer field can go. Studying how tissues are coordinated in a way to execute the dauer decision appropriately, especially the mechanism for neuronal tissues to remodel and function properly for dauer-specific behaviors, would be fascinating. Moreover, studying dauer recovery decision, which requires the animal to constantly gauge the environmental changes and their internal energy storage, could provide a better understanding of how the interplay between external and internal states affects decision.

5.2 References

1. McEwen BS, Nasca C, Gray JD (2016) Stress effects on neuronal structure: Hippocampus, amygdala, and prefrontal cortex. *Neuropsychopharmacology* 41(1):3–23.

2. Persson D, et al. (2011) Extreme stress tolerance in tardigrades: surviving space conditions in low earth orbit. *Journal of Zoological Systematics and Evolutionary Research* 49(s1):90–97.

3. Lee JS, et al. (2017) FMRFamide-like peptides expand the behavioral repertoire of a densely connected nervous system. *Proceedings of the National Academy of Sciences of the United States of America* 114(50):E10726–E10735.

4. Bargmann CI (2012) Beyond the connectome: how neuromodulators shape neural circuits. *Bioessays* 34(6):458–465.

5. White JG, Southgate E, Thomson JN, Brenner S (1986) The structure of the nervous system of the nematode *Caenorhabditis elegans*. *Philos Trans R Soc Lond, B, Biol Sci* 314(1165):1–340.

6. Geffen MN, Vries SEJ de, Meister M (2007) Retinal ganglion cells can rapidly change polarity from off to on. *PLOS Biology* 5(3):e65.

7. Santos-Carvalho A, Ambrósio AF, Cavadas C (2015) Neuropeptide Y system in the retina: From localization to function. *Prog Retin Eye Res* 47:19–37.

A p p e n d i x

CAENORHABDITIS ELEGANS CAN USE MECHANOSENSATION TO PREDICT ENVIRONMENTAL COLLAPSE

(This work was done in collaboration with Lee J, Chin-Sang I, and Brugman K)

A.1 Abstract

Animals make decisions to alter aspects of their development based on signals from the environment. The roundworm *Caenorhabditis elegans* can escape environmental collapse by entering a spore-like dauer larval stage. Food, pheromone, and temperature have long been known to input into the dauer entry decision, but some inputs are clearly missing in models of the decision. Here we report a role for mechanosensation as an overlooked input into the decision. We show that gentle, harsh, and piezo touch promote dauer entry, using quantitative entry assays on CRISPR knock-ins and existing mutants in mechanosensation. We demonstrate that touch and pheromone likely work in parallel to promote dauer entry, by examining pheromone sensation and signal transmission in mechanosensation-defective mutants. We confirm that direct mechanical stimulation of *C. elegans* promotes dauer entry, and we provide a plausible role for mechanosensation in sensing dauer-promoting weather and crowding conditions. Our findings reveal that the dauer entry decision is more complex than previously recognized, and illuminates how animals can make robust decisions, even with a numerically simple nervous system.

A.2 Introduction

Most if not all organisms undergo developmental decisions to survive in changing environments (1, 2). By altering aspects of their development, organisms including bacteria (3, 4), insects (5), plants (6, 7), and mammals (8, 9) can adapt their metabolism, physiology, and reproductive strategy to meet resource availability. In this way, *Caenorhabditis elegans* roundworms can escape environmental collapse by becoming dauer larvae (10). Dauers are spore-like, stress-resistant, and capable of long-range dispersal (11-13). In addition, dauers have a remodeled nervous system and cease feeding, reproduction, and aging, making dauer entry one of the most dramatic postembryonic switches to be reported (14-16).

Dauer entry is a complex decision, requiring multiple inputs from food, pheromone, and temperature to assess the quality of the environment (17). Seven amphid sensory neurons (**Figure A.1A**) transduce these signals over an integration period of several hours, presumably to extract trend information on the environment's decline (18-20). Dauer entry is therefore an anticipatory decision that aims to predict whether environmental conditions will continue to support growth.

Despite being one of the best studied life cycle decisions, no satisfying model of dauer entry exists (but see (12, 18)), likely because a complete accounting of all of the inputs into the decision has not been made (21). We therefore investigated the possibility that mechanosensory inputs affect the dauer entry decision. Indeed, mechanosensation is useful for assessing population density in plants and bacteria (7, 22), and can be used to self-assess growth rate in insects (23). In the wild, *C. elegans* is found in rotting vegetation, where it can come into contact with bacteria, fungi, insects, predators, and other nematodes (24). *C. elegans* can use several types of touch, including discriminative gentle touch (25, 26) and

nociceptive harsh touch (27, 28), to help navigate through such complex physical environments (29, 30). Conceivably, information captured by mechanosensation could complement food, pheromone, and temperature signals to assess crowding, nutrition status, or other cues.

Using quantitative dauer entry assays, we demonstrate that CRISPR mutants and existing strains of mechanosensation-defective animals make inaccurate dauer entry decisions. By examining pheromone sensation and signal transmission, we find that pheromone and touch work in parallel pathways to promote dauer entry. Using direct mechanical stimulation, we further demonstrate that mechanosensation promotes dauer entry. Finally, we provide a plausible role for mechanosensation in assessing weather and crowding conditions that promote dauer entry. Our findings reveal that *C. elegans* use mechanosensation to enhance the accuracy of their dauer entry decision, demonstrating that the decision is more complex than previously recognized.

A.3 Results

The dauer entry life cycle decision is modulated by mechanosensation.

Gentle touch in *C. elegans* is sensed by the ALM, AVM, PLM, and PVM touch receptor neurons (TRNs) (25). The MEC-3/LIM homeodomain transcription factor is necessary for the differentiation of the TRNs during development (31). Using pheromone to induce dauer entry (19, 32), we tested the ability of *mec-3(e1338)* null mutants to enter dauer, relative to wild type. We observed that *mec-3(e1338)* entered dauer at a 3.4-fold lower rate than wild type (*mec-3(e1338)* dauer entry rate = 16%, N = 147; wild type dauer entry rate = 55%, N = 245) (**Figure A.1B-C**). This data suggests that MEC-3, and likely the TRNs, promotes dauer entry.

Mechanotransduction in the TRNs relies on the MEC-4/ MEC-10/MEC-2/MEC-6 channel complex (33). The MEC-4 channel subunit is essential for the activity of this complex, and is expressed exclusively in the TRNs (25, 34). Additionally, MEC-4 is believed to be required specifically for mechanotransduction, since other ionic currents are unaffected in *mec-4* nulls (33). Using CRISPR, we knocked in a 43-nucleotide stop cassette (35) into the *mec-4* gene to generate 3 putative null alleles: *sy1124*, *sy1125*, and *sy1126* (**Figure A.2**). We observed that the pheromone-induced dauer entry of these mutants occurred at an average 2.0-fold lower rate than wild type (*e.g. mec-4(sy1124)* dauer entry = 21%, N = 315; wild type dauer entry = 58%, N = 520) (**Figure A.1B-C**, **Figure A.3**).

We also tested the canonical *mec-4(u253)* null allele (36), which demonstrated a 126-fold decrease in dauer entry (*mec-4(u253)* dauer entry = 0%, N = 267; wild type dauer entry = 47%, N = 446). The stronger phenotype of the *u253* allele may indicate that *sy1124*, *sy1125*, and *sy1126* are loss-of-function alleles instead of nulls, or could be due to genetic background

effects in the *mec-4(u253)* strain.

Furthermore, we observed that *mec-4(e1611)* gain-of-function mutants have a 2.0-fold increased dauer entry rate as compared to wild type (*mec-4(e1611)* dauer entry = 79%, N = 228; wild type dauer entry = 37%, N = 167). Although the *e1611* gain-of-function allele causes neurodegeneration in the TRNs through hyperactivity of the mechanotransduction channel (37), the AVM touch neuron is not fully degenerated until adulthood (38). It is therefore likely that mechanotransduction is hyperactive in the AVM during the dauer entry decision in *mec-4(e1611)* animals. These data suggest that MEC-4 promotes dauer entry through the activity of the mechanotransduction channel.

We further confirmed this by testing the MEC-10 subunit of the channel complex, which regulates the ionic activity of the complex (39). We used CRISPR to generate 2 putative null alleles of *mec-10*: *sy1127*, and *sy1129* (**Figure A.2**), and observed that they entered dauer at an average 1.9-fold lower rate than wild type (*e.g. mec-10(sy1127)* dauer entry = 35%, N = 341; wild type dauer entry = 58%, N = 520) (**Figure A.1B-C**).

We also tested the *mec-10(e1515)* point mutant, which dramatically reduces the mechanoreceptor current (MRC) of the transduction complex (39). *mec-10(e1515)* mutants entered dauer at a 37.9-fold lower rate than wild type (*mec-10(e1515)* dauer entry = 1%, N = 181; wild type dauer entry = 42%, N = 241). Furthermore, the loss-of-function allele *mec-10(ok1104)*, which only mildly decreases the peak MRC of the channel complex (39), did not significantly affect dauer entry (*mec-10(ok1104)* dauer entry = 38%, N = 236; wild type dauer entry = 46%, N = 299). These data suggest that MEC-10 promotes dauer entry through the MRC of the transduction complex.

MEC-18/Firefly luciferase-like protein and MEC-19/novel membrane protein modulate

gentle touch (40, 41). We observed that *mec-18(u228)* decreased dauer entry by 5.1-fold (*mec-18(u228)* dauer entry = 9%, N = 167; wild type dauer entry = 46%, N = 418) and *mec-19(ok2504)* modestly decreased dauer entry by 1.4-fold (*mec-19(ok2504)* dauer entry = 44%, N = 233; wild type dauer entry = 60%, N = 430) (**Figure A.1B-C**). These data further indicate that gentle touch promotes dauer entry.

We also tested the role of harsh touch on dauer entry by assaying the *trp-4(sy695)* and *trp-4(sy696)* putative null alleles (42). The TRP-4/TRPN channel subunit is expressed in the ADE, DVA, and PDE harsh touch neurons and regulates posterior harsh touch (27). We observed that *trp-4(sy695)* and *trp-4(sy696)* decreased dauer entry by an average 3.9-fold (*e.g. trp-4(sy695)* dauer entry = 10%, N = 143; wild type dauer entry = 50%, N = 294) (**Figure A.1B-C**). These data suggest that harsh touch mediated by TRP-4 promotes dauer entry.

Since *mec* and *trp-4* mutants disrupt the function of several neurons, we used *ceh-17(np1)* nulls to test the effects of an incomplete nervous system on the dauer entry decision. The CEH-17 transcription factor is necessary for the proper axonal outgrowth of the ALA and 4 SIA neurons (43, 44), neither of which have known functions in dauer entry or mechanosensation. We observed that *ceh-17(np1)* did not significantly affect dauer entry, relative to wild type (*ceh(np1)* dauer entry = 39%, N = 185; wild type dauer entry = 49%, N = 239) (**Figure A.1B**). Therefore, the effects of the *mec* and *trp-4* mutants on dauer entry are likely beyond those of an incomplete nervous system. These data indicate that the dauer entry decision is modulated by gentle and harsh touch.

Touch and pheromone are parallel inputs into the dauer entry decision

To understand how the dauer entry decision is affected in touch mutants, we tested the dauer entry dose-response of *mec-4*, *trp-4*, and *mec-4;trp-4* mutants to pheromone. Using concentrations of 0.25%, 0.75%, and 2.25% pheromone to drive dauer entry, we observed a logarithmic dose-response to pheromone in wild type, as expected (45), with an EC50 of 0.64% ($R^2 = 0.99$) (**Figure A.4A**). *mec-4(sy1124)* mutants demonstrated an EC50 of 2.22% ($R^2 = 0.99$), corresponding to a decreased dose-response to pheromone across 0.75%-2.25%. *trp-4(sy695)* mutants demonstrated an EC50 of 0.98% ($R^2 = 0.99$), corresponding to a modest decrease in dose-response across all concentrations. The *mec-4(sy1124);trp-4(sy695)* double mutant demonstrated a similar dose-response to that of the *mec-4(sy1124)* single, with an EC50 of 2.07% ($R^2 = 0.99$). The decreased dose-response of the mutants suggests that *mec-4* and *trp-4* affect dauer entry by modulating pheromone sensation, or by affecting the decision as a parallel input to pheromone.

Aside from dauer entry, another method for assaying pheromone sensation is to measure *str-3* gene expression in the ASI neuron (46). STR-3 is a chemosensory receptor, and its expression in the ASI is repressed by sensation of pheromone in ASI and ASK. As a result, *str-3::gfp* is useful for identifying mutants that disrupt pheromone sensation and signal transmission (47, 48). We observed that STR-3::GFP fluorescence in the ASI did not vary between L2d animals with wild type *mec-4*, null *mec-4(sy1124)*, and gain-of-function *mec-4(e1611)* (**Figure A.4B-C**). In addition, STR-3::GFP fluorescence was the same between wild type, *mec-4(sy1124)*, and *mec-4(e1611)* young adults (**Figure A.4D**). Furthermore, STR-3::GFP levels did not vary in wild type adults that were mechanically stimulated via drop test (49) (**Figure A.4E**). These data suggest that touch does not affect pheromone sensation or signal transmission. A simple interpretation is that touch affects the dauer entry

decision as a parallel input to pheromone.

mec-4 and *trp-4* act additively with *pezo-1* to promote dauer entry

Despite being the major mechanotransducer in mammals (50, 51), the role of PEZO-1/Piezo in *C. elegans* remains unclear. In addition, *pezo-1* is expressed in neurons but not the TRNs (**Table A.1**). We used CRISPR to generate 3 loss-of-function alleles of *pezo-1*: *sy1184*, *sy1199*, and *sy1200*, and we observed that *pezo-1(sy1199)* decreased dauer entry by 2.0-fold (*pezo-1(sy1199)* dauer entry = 28%, N = 172; wild type dauer entry = 57%, N = 1039) (**Figure A.5**). This data suggest that *pezo-1* acts similarly to the *mec-4* and *trp-4* mechanotransducers and promotes dauer entry.

mec-4(sy1124);pezo-1(sy1200) double mutants decreased dauer entry by 2.5-fold (dauer entry = 23%, N = 137; wild type dauer entry = 57%, N = 1039), though this effect was not significantly different from the effect of the *mec-4* and *pezo-1* single mutants (**Figure A.5**). On the other hand, *mec-4(sy1124);trp-4(sy695);pezo-1(sy1184)* triple mutants decreased dauer entry by 4.2-fold (dauer entry = 14%, N = 190; wild type dauer entry = 57%, N = 1039) (**Figure A.5**). The effect of the *mec-4;trp-4;pezo-1* triple mutant was significantly greater than the effect of the single mutants, as well as the *mec-4;trp-4* double. These data suggest that *mec-4* and *trp-4* act additively with *pezo-1* to modulate dauer entry.

Direct mechanical stimulation promotes dauer entry

We investigated whether direct mechanical stimulation of animals could drive them into dauer entry. We used two methods for inducing mechanosensation: (1) we added 150-212 um glass beads to dauer entry plates to increase the roughness of the culture surface, and (2)

we used a servo shaker to gently agitate culture plates every 10 to 20 seconds.

We observed that the addition of 0.2 to 0.6 mg/cm^2 glass beads did not affect wild type dauer entry (dauer entry without beads = 64%, N = 215; dauer entry with beads = 64%, N = 325) (**Figure A.6A**). However, we observed that gently agitating sensitized *daf-2(e1370)* mutants—which enter dauer mildly at room temperature (52)—increased dauer entry by 1.7-fold (*daf-2(e1370)* dauer entry = 59%, N = 76; *daf-2(e1370)* with vibration = 100%, N = 44%) (**Figure A.6B**). These results suggest that direct mechanical stimulation, at least from vibration, can promote the dauer entry decision.

A.4 Discussion

Developmental decisions allow organisms to survive in changing environments (2). One of the best studied developmental decisions is *C. elegans* dauer entry. The principal regulators of this decision have been identified through genetic analysis of dauer-constitutive and -defective mutants, which highlighted the major inputs of food and pheromone (53-58). However, no satisfying model of the entry decision exists, likely because all of the inputs have not been identified (21).

Indeed, the known inputs into the dauer entry decision—food, pheromone, and temperature—are not the only cues that nematodes are exposed to in the wild, and in some cases these cues may be unreliable for assessing the environment. For instance, pheromones may be quenched by organic matter in soils (59), and may be used as dishonest signals to manipulate other nematodes into disadvantageous dauer decisions (60, 61).

Here we have demonstrated a role for mechanosensation as an overlooked modulator of the dauer entry decision. *C. elegans* can sense several types of touch, presumably to help navigate its natural environments where it can come into contact with bacteria, fungus, insects, carriers, predators, and other nematodes (62). These types of touch include gentle touch, harsh touch, nose touch, and food texture sensation (30). Gentle touch is likely analogous to low-threshold, discriminative touch in humans, which helps to detect light touch, hair movements, vibrations, quivering, and social touch (26, 63, 64). On the other hand, harsh touch is likely analogous to high-threshold nociception, which detects physically damaging forces (26-28). Curiously, the major mechanotransducers in nematodes are MEC-4/10 and TRP-4, while the major mechanotransducer in mammals in Piezo.

Using quantitative dauer entry assays on CRISPR knock-ins and existing mutants of

gentle touch (*mec-3*, *mec-4*, *mec-10*, *mec-18*, and *mec-19*), harsh touch (*mec-3* and *trp-4*), and piezo touch (*pezo-1*), we showed that mechanosensation promotes the dauer entry decision. We further confirmed this using direct mechanical stimulation, and demonstrated that vibration can promote dauer entry. We mostly did not observe large effect sizes for the mechanosensation-defective single mutants, and this is to be expected since the principal regulators of the decision have already been identified. Therefore, mechanosensation is a modulator of the decision, much like temperature which enhances pheromone-induced dauer entry (17).

Because of the moderate effect size of *trp-4(sy695)* on dauer entry, the *mec-4(sy1124)*;*trp-4(sy695)* phenotype could not be used to determine if *mec-4* and *trp-4* act additively or in the same pathway (65). However, close connections between the harsh touch and gentle touch neurons suggest it is likely that *mec-4* and *trp-4* act in the same circuit pathway to modulate dauer entry: The harsh touch PDE neuron is directly gap junctioned to the gentle touch PVM, and is gap junctioned to the gentle touch PLM via PVC (66, 67). In addition, the harsh touch DVA is gap junctioned to the gentle touch ALM and PLM via PVR and PVC/PVR, respectively. On the other hand, we demonstrated that *mec-4* and *trp-4* act additively with *pezo-1* to promote dauer entry, indicating that there are parallel pathways for mechanosensation to input into the decision.

We propose that mechanosensation could be used to assess at least two conditions that correlate with dauer entry: humidity and crowding. First, humidity is sensed, in part, by MEC-10 (68), and has been suggested by some groups to promote dauer entry (21). Moreover, moisture has been shown to affect the dispersal of parasitic nematodes (69), suggesting it may affect dauer dispersal as well. Indeed, we and others have shown that

dauers and parasitic nematodes share common strategies for dispersal (32, 70). Thus, while dauers can survive dessication for a few days (13), it may be advantageous for *C. elegans* to enter dauer when humidity levels are favorable for dispersal.

Second, *C. elegans* can sense crowding via pheromone signals (71), which can be inaccurate (59-61). We speculate that *C. elegans* could also measure crowding via contact-dependent signaling, such as in bacteria (22), plants (7), and insects (5). We have shown that touch and pheromone likely act in parallel to affect the dauer entry decision, and it is conceivable that they might jointly assess crowding in order to increase the accuracy of the decision.

The input of mechanosensation into dauer entry has revealed the decision to be more complex than previously recognized. This growing complexity raises the intriguing possibility that other cues such as light, O_2/CO_2, pH, and osmotic stress may input into the decision as well (**Figure A.7**). This hypothesis is supported by recent findings that the dauer entry decision is modulated by noxious stimuli, which may facilitate pheromone signaling (48). It is plausible that multiple inputs assessing various aspects of the environment may be crucial for making robust developmental decisions in *C. elegans*. Finally, since mechanosensation is important for growth and development in invertebrates to vertebrates (72), and is used to make developmental decisions in fungi (73), plants (7), and insects (5), we speculate that mechanosensation may be a common input into developmental decisions across biology.

A.5 Materials and Methods

Animal strains

C. elegans strains were grown using standard protocols with *Escherichia coli* OP50 as a food source (74). The wild type strain was N2 (Bristol). Strains obtained from the *Caenorhabditis* Genetics Center (CGC) include CB1515 *mec-10(e1515)*, RB1115 *mec-10(ok1104)*, TU228 *mec-18(u228)*, RB1925 *mec-19(ok2504)*, and IB16 *ceh-17(np1)* 3x outcrossed. TQ526 *mec-3(e1338)* 4x outcrossed, TQ253 *mec-4(u253)*, and TQ1243 *mec-4(e1611)* 6x outcrossed were gifts from the Xu laboratory. PS4492 *trp-4(sy695)* 7x outcrossed and PS4493 *trp-4(sy696)* 6x outcrossed were generated in the Sternberg laboratory.

CRISPR-generated strains

CRISPR alleles of *mec-4*, *mec-10*, and *pezo-1* were generated by knocking in the 43-nucleotide stop cassette:
GGGAAGTTTGTCCAGAGCAGAGGTGACTAAGTGATAAgctagc (35).

PS7913 *mec-4(sy1124)*, PS7914 *mec-4(sy1125)*, and PS7915 *mec-4(sy1126)* were generated using the guide RNA ACGACGTGCCGGTTTTGTGG. Flanking sequences

(Left) CCGAACCACCCACCACCCCTGCACCCACCA

(Right) CAAAACCGGCACGTCGTCGAGGAAAACGTG.

PS8039 *trp-4(sy695)*;*mec-4(sy1124)* was generated by crossing PS7913 males to PS4492.

PS7916 *mec-10(sy1127)* and PS7918 *mec-10(sy1129)* were generated using the guide RNA TATACAATTTATCAATCAGG. Flanking sequences

(Left) TTCTAATCTGTGCTATACAATTTATCAATC

(Right) AGGCGGTCGCTGTGATTCAGAAGTATCAGA.

PS8111 *pezo-1(sy1199)*, PS8112 *pezo-1(sy1200);mec-4(sy1124)*, and PS8084 *trp-4(sy695);pezo-1(sy1184);mec-4(sy1124)* were generated using the guide RNA CCAGAAGCTCGTAAGCCAGG. Putative flanking sequences

(Left) CGCTGTTTCTGAACCAGAAGCTCGTAAGCC

(Right) AGGAGGCACTGAAGAAACGGATGGTGATGA.

Dauer entry assay

Pheromone-induced dauer entry assays were performed as previously described (32). The conditions used to induce dauer entry were: 20 uL of 8% w/v heat-killed OP50 and incubation at 25.5^{o}C for 48 hours, with approximately 50 animals per plate. For phenotypic screening (**Figure A.1B**), we used 1.5% pheromone to induce approximately 50% dauer entry in wild type in order to detect increased or decreased dauer entry in mutants.

Mechanical perturbation of animals

Glass beads: 2 to 6 mg of autoclaved glass beads (Millipore Sigma G1145, 150-212 um) were added to the surface of 0.75% pheromone dauer entry plates, to an approximate density of 0.2 to 0.6 mg/cm^2. Dauer entry was assayed as above.

Vibration assay: We used the *daf-2(e1370)* sensitized mutant, which enters dauer modestly at room temperature (52). We attached culture plates containing *daf-2(e1370)* animals to a servo shaker and gently agitated every 10 to 20 seconds at room temperature for 48 hours.

Drop test assay

Culture plates were parafilmed, put in a cardboard box, and dropped as in (49): from a height of 5 cm, 30 times, with a 10 second interstimulus interval.

Pheromone sensitivity assay

For measurements in L2d, larvae were grown on 2.25% pheromone dauer entry plates for 23 to 27 hours at 25.5^{o}C. For measurements in young adults, 20 L4 animals were picked onto seeded NGM plates the day before the assay. For the drop test assay, 15 L4 animals were picked the day before the assay. Fluorescence measurements of STR-3::GFP in the ASI neuron were made using ZEISS ZEN software. Average fluorescence intensities were obtained from regions drawn around the ASI and image backgrounds, and fluorescence was corrected by subtracting the background. All fluorescence intensities were normalized to measurements from the same-day CX3596 *str-3::gfp* control.

A.6 Figures and tables

A

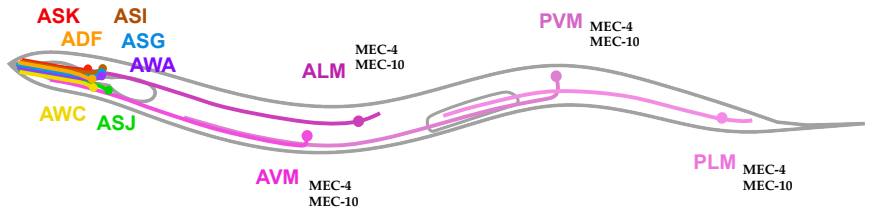

B

Genotype	Function Effect	Mutant Entry %	WT Entry %	Relative Entry (WT % / Mutant %)	Adjusted *P*	Trials Tested	Mutant N_{tested}	WT N_{tested}
mec-3(e1338) x4 out.	null	16	55	3.4	***	3	147	245
mec-4(sy1124)	putative null	21	58	2.7	***	6	315	520
mec-4(sy1125)	putative null	29	54	1.9	***	4	279	419
mec-4(sy1126)	putative null	41	58	1.4	***	4	261	520
mec-4(u253)	null	0	47	126.3	***	4	267	446
mec-4(e1611) x6 out.	gf	79	37	0.5	***	4	228	167
mec-10(sy1127)	putative null	35	58	1.6	***	6	341	520
mec-10(sy1129)	putative null	28	58	2.1	***	4	165	520
mec-10(e1515)	gf	1	42	37.9	***	3	181	241
mec-10(ok1104)	lf	38	46	1.2	n.s.	4	236	299
mec-18(u228)	unknown	9	46	5.1	***	3	167	418
mec-19(ok2504)	putative null	44	60	1.4	***	4	233	430
trp-4(sy696) x6 out.	putative null	19	50	2.7	***	3	176	294
trp-4(sy695) x7 out.	putative null	10	50	5.1	***	3	143	294
ceh-17(np1) x3 out.	null	39	49	1.3	n.s.	3	185	239

C

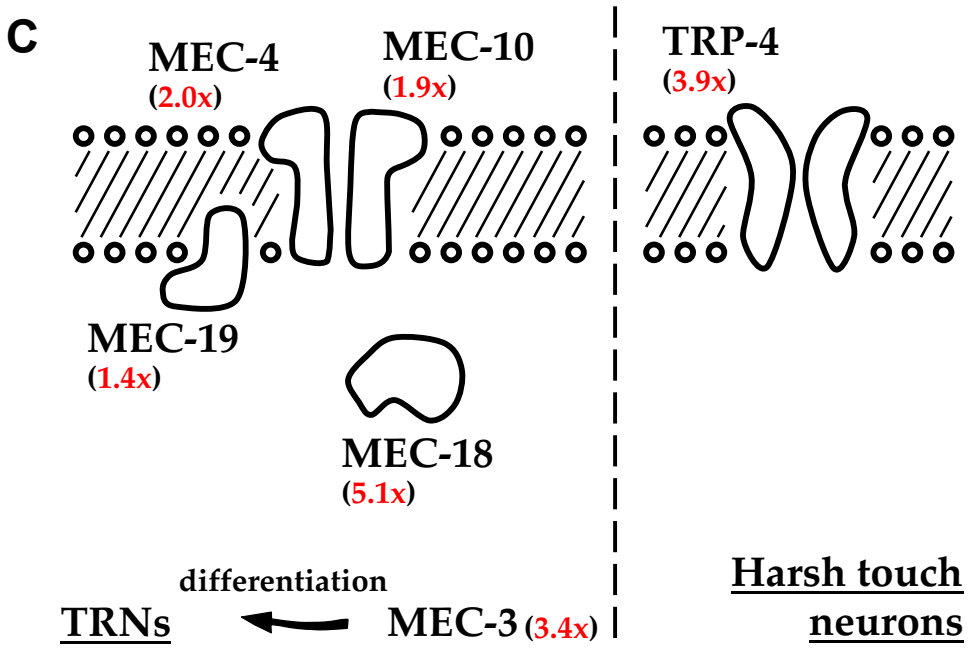

Figure A.1. The dauer entry life cycle decision is modulated by mechanosensation. (A) Schematic of the gentle touch mechanosensory neurons (magenta) and amphid neurons (rainbow) of *C. elegans*. The expression of MEC-4 and MEC-10 mechanoreceptors in the gentle touch neurons is indicated. **(B)** Dauer entry rates of *mec* mutants. *P* calculated via nonparametric permutation test and adjusted using Bonferroni correction. out., outcrossed. **(C)** Schematic of gentle (left) and harsh (right) touch neurons. Top, ECM; bottom, cytoplasm. Numbers in parentheses represent the relative dauer entry rate of wild type to mutant. Red, dauer entry promoting.

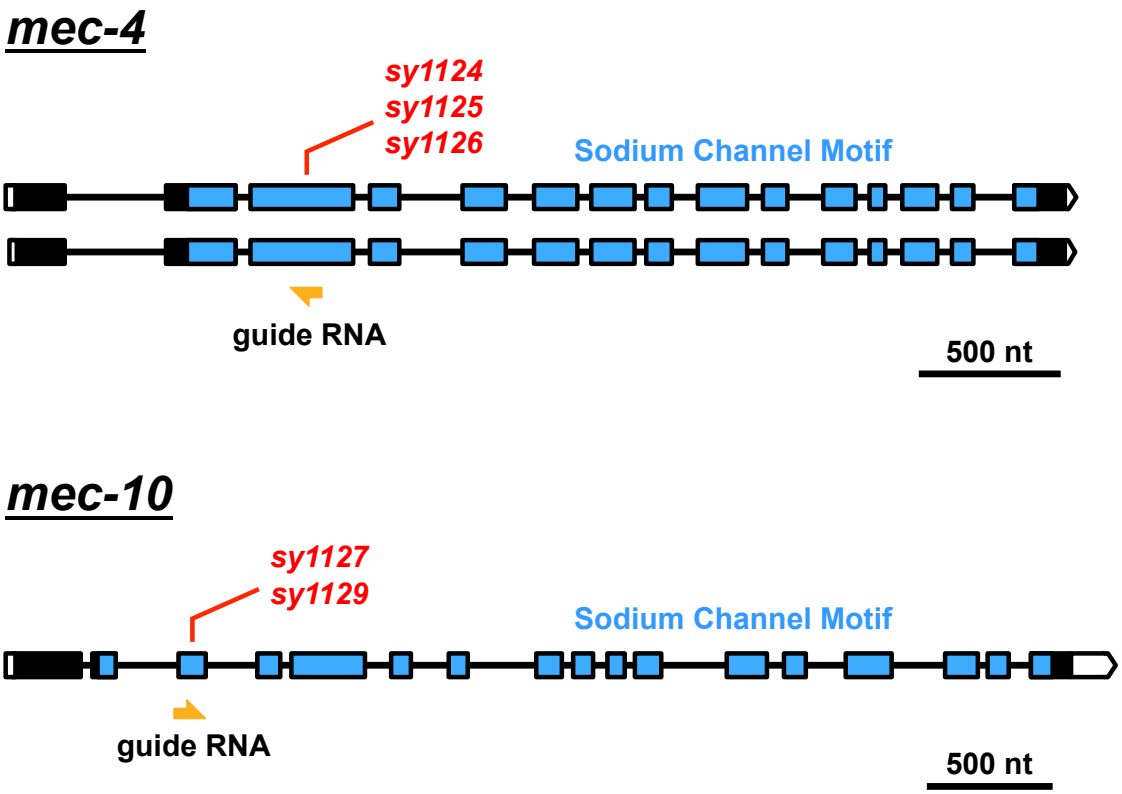

sy1124 – 1126, 1127, 1129
STOP-IN allele: GGGAAGTTTGTCCAGAGCAGAGGTGACTAAGTGATAAgctagc

Figure A.2. *mec-4* and *mec-10* CRISPR alleles are putative nulls. Gene models of *mec-4* and *mec-10*. The location of the *sy* CRISPR alleles are indicated in red. White, untranslated regions; black, exons; blue, sodium channel-encoding exon regions; lines, introns. Arrow indicates the direction of the guide RNA.

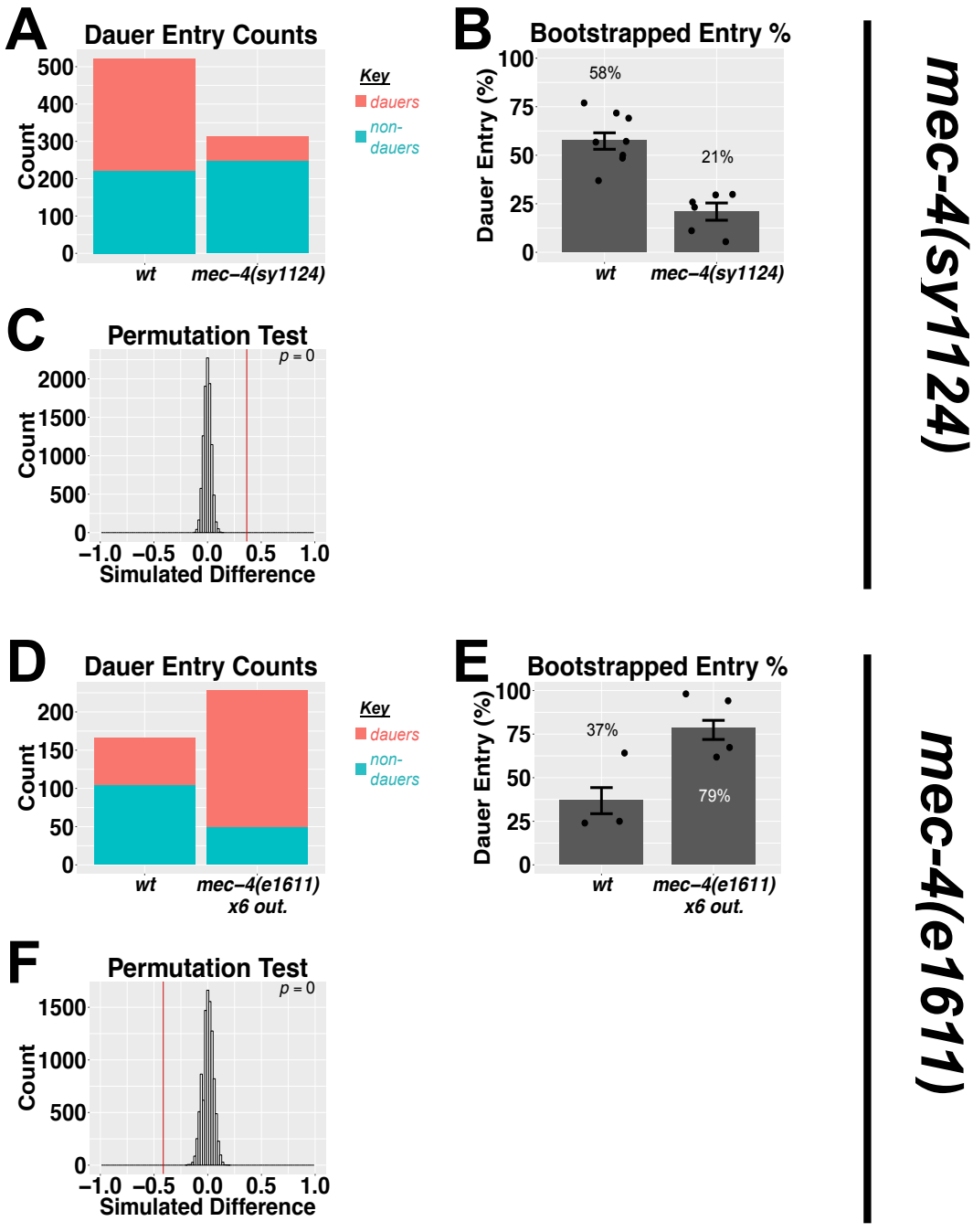
A
Dauer Entry Counts
Count
500
400
300
200
100
0
wt
mec–4(sy1124)
Key
dauers
non-dauers
B
Bootstrapped Entry %
Dauer Entry (%)
100
75
50
25
0
58%
21%
wt
mec–4(sy1124)
C
Permutation Test
p = 0
Count
2000
1500
1000
500
0
–1.0 –0.5 0.0 0.5 1.0
Simulated Difference
mec-4(sy1124)
D
Dauer Entry Counts
Count
200
150
100
50
0
wt
mec–4(e1611) x6 out.
Key
dauers
non-dauers
E
Bootstrapped Entry %
Dauer Entry (%)
100
75
50
25
0
37%
79%
wt
mec–4(e1611) x6 out.
F
Permutation Test
p = 0
Count
1500
1000
500
0
–1.0 –0.5 0.0 0.5 1.0
Simulated Difference
mec-4(e1611)

Figure A.3. *mec-4* promotes dauer entry. (A, D) The number of animals that decided to enter dauer (red) or reproductive development (blue) for the wild type control, (A) *mec-4(sy1124)* nulls, and (D) *mec-4(e1611)* gain-of-function mutants. **(B, E)** Representation of dauer entry counts as percentages. Points, independent trials; bar, bootstrapped dauer entry percentage; whiskers, 95% confidence interval. **(C, F)** Histogram of the 9,999 simulated differences between wild type and (C) *mec-4(sy1124)* nulls or (F) *mec-4(e1611)* gain-of-function mutants in non-parametric permutation tests. Red line, observed difference.

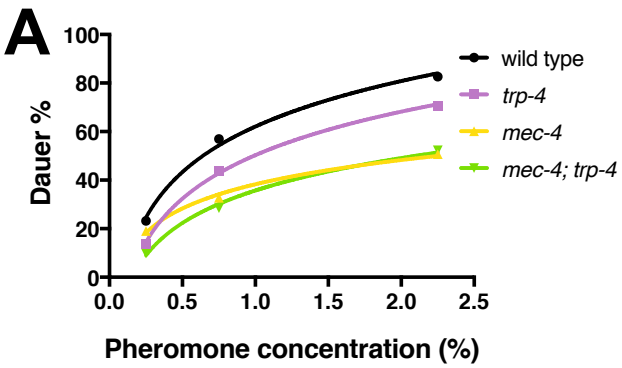

0.25%	wild type	*mec-4*	*trp-4*	*mec-4; trp-4*
wild type				
mec-4	n.s.			
trp-4	*	n.s.		
mec-4; trp-4	*	n.s.	n.s.	

0.75%	wild type	*mec-4*	*trp-4*	*mec-4; trp-4*
wild type				
mec-4	***			
trp-4	**	*		
mec-4; trp-4	***	n.s.	**	

2.25%	wild type	*mec-4*	*trp-4*	*mec-4; trp-4*
wild type				
mec-4	***			
trp-4	***	***		
mec-4; trp-4	***	n.s.	***	

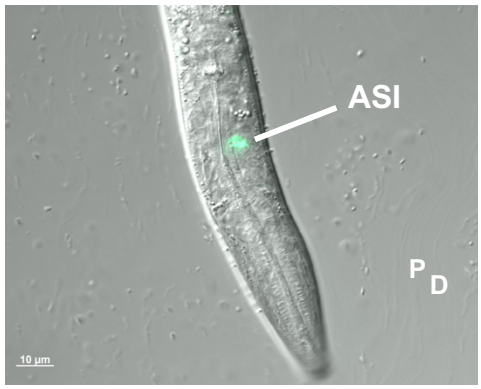

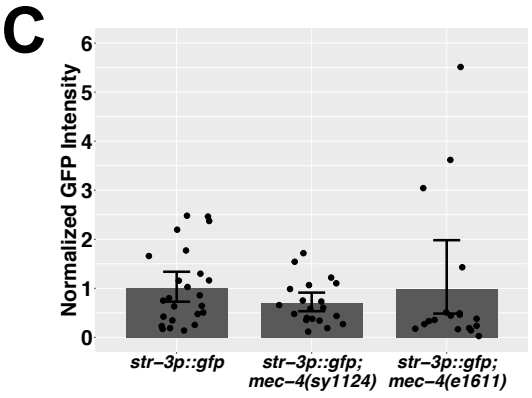

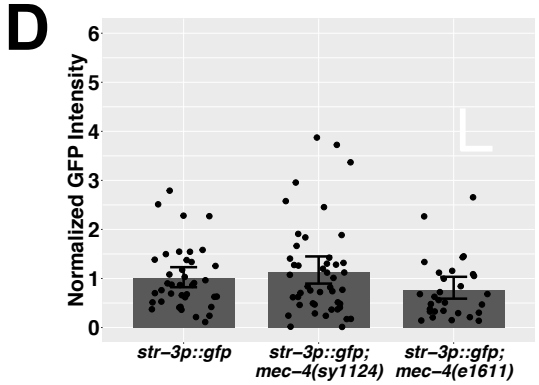

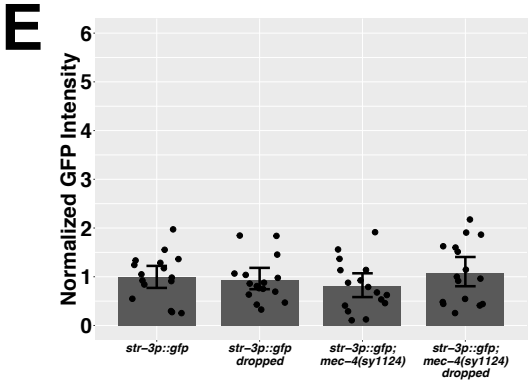

Figure A.4. Touch and pheromone are parallel inputs into the dauer entry decision. (A) Pheromone dose-response curve of dauer entry for wild type, *mec-4(sy1124)* nulls, *trp-4(sy695)* nulls, and *mec-4(sy1124)*;*trp-4(sy695)* double mutants. Points represent averages from 3-17 independent trials. Pairwise adjusted *P* values are indicated in the matrices corresponding to each pheromone concentration point. Shades of green, increasing statistical confidence. **(B)** Representative image of *str-3::gfp* fluorescence in the ASI neuron of *mec-4(wt)* L2d larvae. **(C-D)** STR-3::GFP intensity in (C) L2d and (D) adult animals. **(E)** STR-3::GFP intensity in adults mechanically stimulated via dropping. Points, individual animals; bar, bootstrapped mean intensity; whiskers, 95% confidence interval.

Gene	Protein Type	Expression	Strain	Allele	Protein Effect	Function Effect	Phenotype	Citation
mec-3	LIM homeodomain protein	AIZ, ALM, AVM, FLP, PLM, PVD, PVM, VNC	TQ526	*mec-3(e1338)*	Insertion and frameshift	Putative loss-of-function or null	TRNs fail to differentiate	Way & Chalfie 1989; Xue, Tu, & Chalfie 1993; Bounoutas *et al*. Chalfie 2009; Kubanek *et al*. Goodman 2018
mec-4	DEG / ENaC channel	ALM, AVM, PLM, PVM	TU253	*mec-4(u253)*	Deletion	Null	Abolished mechanoreceptor currents	Hong, Mano, & Driscoll 2000; O'Hagan, Chalfie, & Goodman 2005
			TQ1243	*mec-4(e1611)*	T442A	Gain-of-function	Touch insensitivity, touch cell degeneration	Driscoll & Chalfie 1991
			CB1339	*mec-4(e1339)*	G230E	Loss-of-function	Partially touch insensitive	O'Hagan, Chalfie, & Goodman 2005; Chalfie & Sulston 1981
mec-10	DEG / ENaC channel	ALM, AVM, FLP, PLM, PVD, PVM, tail neuron	CB1515	*mec-10(e1515)*	S105F	Gain-of-function	Touch insensitive (but weaker than *u20*, *u390*, *u332*, *e1715*)	Huang & Chalfie 1994; Arnadottir *et al*. Chalfie 2011
			RB1115	*mec-10(ok1104)*	Deletion	Loss-of-function	Partially touch insensitive (weaker than *e1515*)	Arnadottir et al. Chalfie 2011
mec-18	Firefly luciferase-like	ALM, AVM, PLM, PVM	TU228	*mec-18(u228)*	Uncurated	Unknown	Partial abnormality in mechanosensation	WormBase; CGC
mec-19	Novel membrane protein	ALM, AVM, FLP, PLM, PVD, PVM	RB1925	*mec-19(ok2504)*	Deletion	Putative null	Enhanced *mec-4(d)* degeneration	Barstead *et al*. Zapf 2012; Chen *et al*. Chalfie 2016
pezo-1	Piezo-type mechanosensitive ion channel	head neurons, HOA, HOB, male tail interneurons, PCS, CAN, ray neurons, spermatheca, vulval muscle	PS8111	*pezo-1(sy1199)*	Insertion, stop, and frameshift	Putative loss-of-function or null	Male mating defective (falling off), reduced fecundity	Brugman & Sternberg *unpublished*
trp-4	TRPN channel pore-forming subunit	ADE, CEP, DVA, DVC, PDE	PS4492	*trp-4(sy695)*	Deletion	Putative null	Abnormal body bends	Li *et al*. Xu 2011
			PS4493	*trp-4(sy696)*	Deletion	Putative null	Abnormal body bends	Li et al. Xu 2011
ceh-17	Q_{50} paired-like homeodomain protein	ALA, DA8, DB5, DNC, head muscle, RMED, SIA, SIBV, VNC	IB16	*ceh-17(np1)*	Deletion	Null	ALA and SIA axonal outgrowth impaired	Pujol et al. Brunet 2000; Buskirk & Sternberg 2007

Table A.1. Expression pattern and allele effects of mechanosensation genes. Magenta, gentle touch receptor neurons; Orange, harsh touch receptor neurons.

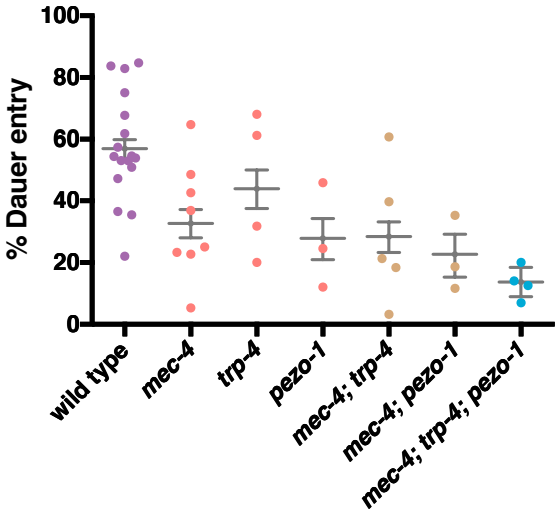

0.75%	wild type	*mec-4*	*trp-4*	*pezo-1*	*mec-4; trp-4*	*mec-4; pezo-1*	*mec-4; trp-4; pezo-1*
wild type							
mec-4	***						
trp-4	**	*					
pezo-1	***	n.s.	**				
mec-4; trp-4	***	n.s.	**	n.s.			
mec-4; pezo-1	***	n.s.	***	n.s.	n.s.		
mec-4; trp-4; pezo-1	***	***	***	*	**	n.s.	

Figure A.5. *mec-4* and *trp-4* act additively with *pezo-1* to promote dauer entry. Dauer entry *mec-4*, *trp-4*, and *pezo-1* at 0.75% pheromone. Points, independent trials; center line, bootstrapped dauer entry percentage; whiskers, 95% confidence interval.

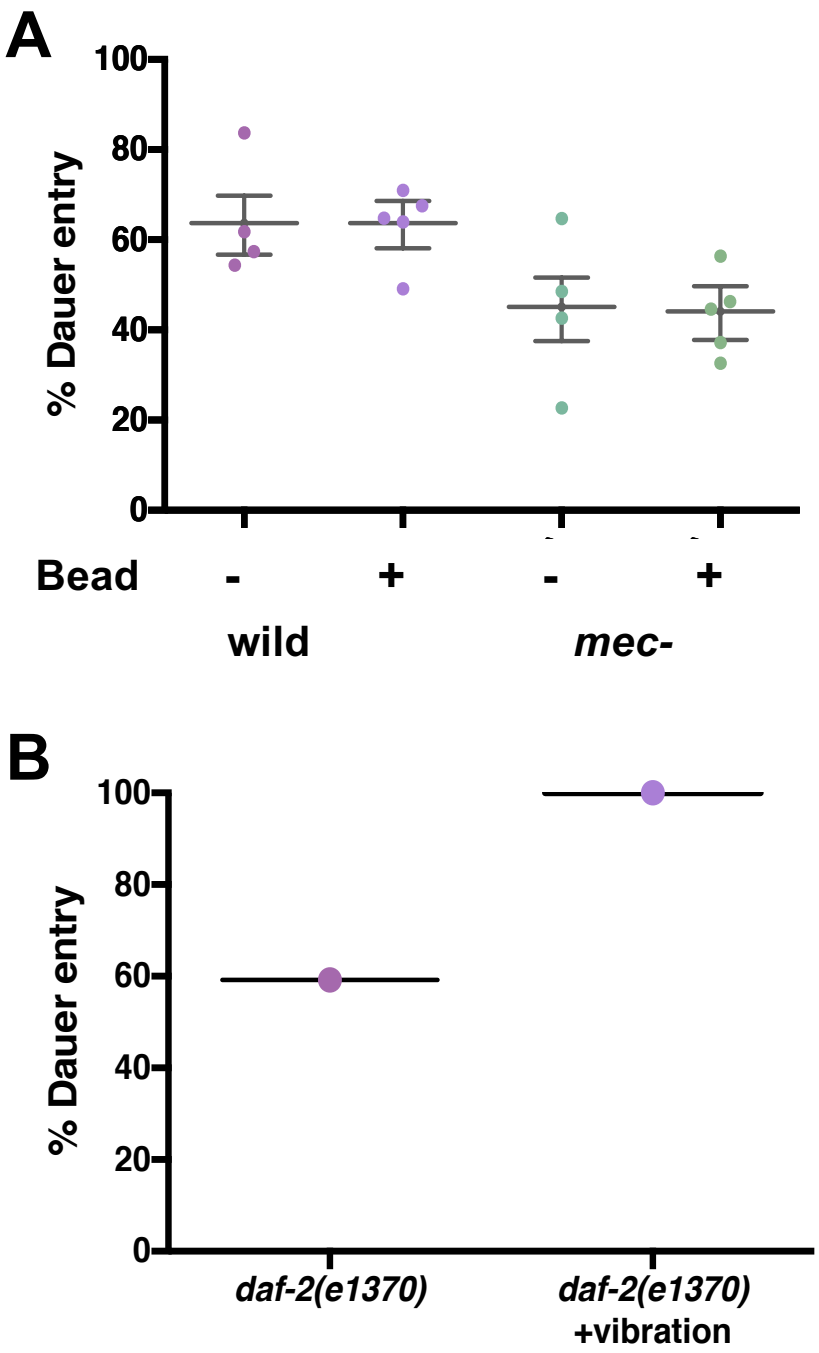

Figure A.6. Direct mechanical stimulation promotes dauer entry. (A) Dauer entry percentages for wild type animals grown with glass bead perturbation. **(B)** Dauer entry for *daf-2(e1370)* with vibration perturbation. Points, independent trials; bar, bootstrapped dauer entry percentage.

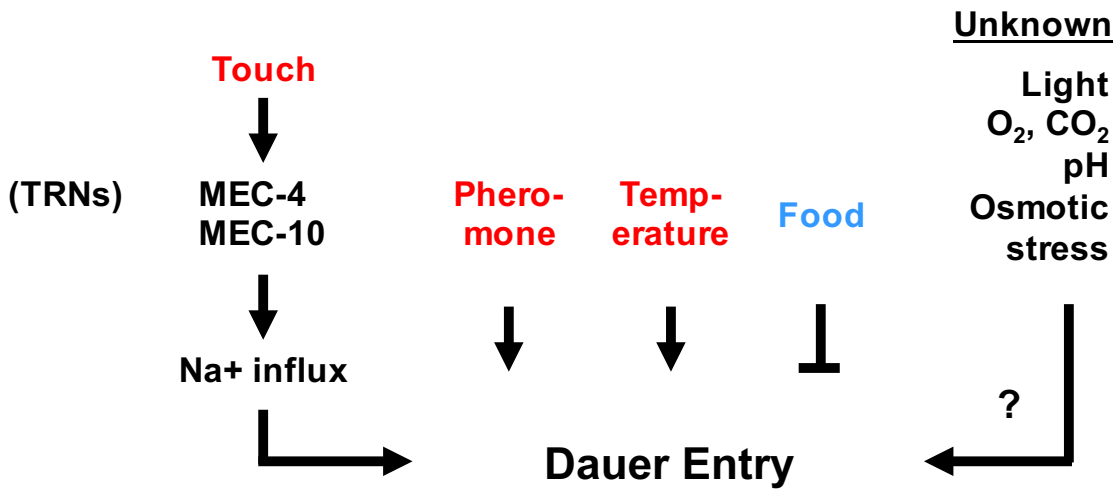

Figure A.7. Model of the complex dauer entry decision. Red, dauer-promoting inputs; blue, dauer-inhibiting.

A.7 References

1. Ackermann M (2015) A functional perspective on phenotypic heterogeneity in microorganisms. *Nat Rev Microbiol* 13(8):497-508.
2. Fusco G & Minelli A (2010) Phenotypic plasticity in development and evolution: facts and concepts. Introduction. *Philosophical transactions of the Royal Society of London. Series B, Biological sciences* 365(1540):547-556.
3. Perkins TJ & Swain PS (2009) Strategies for cellular decision-making. *Mol Syst Biol* 5:326.
4. Tagkopoulos I, Liu YC, & Tavazoie S (2008) Predictive behavior within microbial genetic networks. *Science* 320(5881):1313-1317.
5. Simpson SJ, Sword GA, & Lo N (2011) Polyphenism in insects. *Current biology : CB* 21(18):R738-749.
6. Gruntman M, Gross D, Majekova M, & Tielborger K (2017) Decision-making in plants under competition. *Nat Commun* 8(1):2235.
7. de Wit M*, et al.* (2012) Plant neighbor detection through touching leaf tips precedes phytochrome signals. *Proceedings of the National Academy of Sciences of the United States of America* 109(36):14705-14710.
8. Ptak GE*, et al.* (2012) Embryonic diapause is conserved across mammals. *PloS one* 7(3):e33027.
9. Renfree MB & Fenelon JC (2017) The enigma of embryonic diapause. *Development* 144(18):3199-3210.

10. Cassada RC & Russell RL (1975) The dauerlarva, a post-embryonic developmental variant of the nematode Caenorhabditis elegans. *Developmental biology* 46(2):326-342.

11. Felix MA & Duveau F (2012) Population dynamics and habitat sharing of natural populations of Caenorhabditis elegans and C. briggsae. *BMC biology* 10:59.

12. Fielenbach N & Antebi A (2008) C. elegans dauer formation and the molecular basis of plasticity. *Genes & development* 22(16):2149-2165.

13. Kiontke K & Sudhaus W (2006) Ecology of Caenorhabditis species. *WormBook : the online review of C. elegans biology*:1-14.

14. Albert PS & Riddle DL (1983) Developmental alterations in sensory neuroanatomy of the Caenorhabditis elegans dauer larva. *The Journal of comparative neurology* 219(4):461-481.

15. Klass M & Hirsh D (1976) Non-ageing developmental variant of Caenorhabditis elegans. *Nature* 260(5551):523-525.

16. Vanfleteren JR & Braeckman BP (1999) Mechanisms of life span determination in Caenorhabditis elegans. *Neurobiol Aging* 20(5):487-502.

17. Golden JW & Riddle DL (1984) The Caenorhabditis elegans dauer larva: developmental effects of pheromone, food, and temperature. *Developmental biology* 102(2):368-378.

18. Avery L (2014) A model of the effect of uncertainty on the C elegans L2/L2d decision. *PloS one* 9(7):e100580.

19. Golden JW & Riddle DL (1984) A pheromone-induced developmental switch in Caenorhabditis elegans: Temperature-sensitive mutants reveal a wild-type

temperature-dependent process. *Proceedings of the National Academy of Sciences of the United States of America* 81(3):819-823.

20. Schaedel ON, Gerisch B, Antebi A, & Sternberg PW (2012) Hormonal signal amplification mediates environmental conditions during development and controls an irreversible commitment to adulthood. *PLoS biology* 10(4):e1001306.
21. Karp X (2016) Working with dauer larvae. *WormBook : the online review of C. elegans biology*:1-19.
22. Blango MG & Mulvey MA (2009) Bacterial landlines: contact-dependent signaling in bacterial populations. *Curr Opin Microbiol* 12(2):177-181.
23. Nijhout HF & Callier V (2015) Developmental mechanisms of body size and wing-body scaling in insects. *Annu Rev Entomol* 60:141-156.
24. Frezal L & Felix MA (2015) C. elegans outside the Petri dish. *eLife* 4.
25. Chalfie M & Sulston J (1981) Developmental genetics of the mechanosensory neurons of Caenorhabditis elegans. *Developmental biology* 82(2):358-370.
26. Lumpkin EA, Marshall KL, & Nelson AM (2010) The cell biology of touch. *J Cell Biol* 191(2):237-248.
27. Li W, Kang L, Piggott BJ, Feng Z, & Xu XZ (2011) The neural circuits and sensory channels mediating harsh touch sensation in Caenorhabditis elegans. *Nat Commun* 2:315.
28. McClanahan PD, Xu JH, & Fang-Yen C (2017) Comparing Caenorhabditis elegans gentle and harsh touch response behavior using a multiplexed hydraulic microfluidic device. *Integr Biol (Camb)* 9(10):800-809.

29. Maguire SM, Clark CM, Nunnari J, Pirri JK, & Alkema MJ (2011) The C. elegans touch response facilitates escape from predacious fungi. *Current biology : CB* 21(15):1326-1330.

30. Schafer WR (2015) Mechanosensory molecules and circuits in C. elegans. *Pflugers Arch* 467(1):39-48.

31. Way JC & Chalfie M (1989) The mec-3 gene of Caenorhabditis elegans requires its own product for maintained expression and is expressed in three neuronal cell types. *Genes & development* 3(12A):1823-1833.

32. Lee JS*, et al.* (2017) FMRFamide-like peptides expand the behavioral repertoire of a densely connected nervous system. *Proceedings of the National Academy of Sciences of the United States of America* 114(50):E10726-E10735.

33. O'Hagan R, Chalfie M, & Goodman MB (2005) The MEC-4 DEG/ENaC channel of Caenorhabditis elegans touch receptor neurons transduces mechanical signals. *Nature neuroscience* 8(1):43-50.

34. Lai CC, Hong K, Kinnell M, Chalfie M, & Driscoll M (1996) Sequence and transmembrane topology of MEC-4, an ion channel subunit required for mechanotransduction in Caenorhabditis elegans. *J Cell Biol* 133(5):1071-1081.

35. Sternberg PW, Wang H, Park H, & Liu J (2018) An efficient genome editing strategy to generate putative null mutants in Caenorhabditis elegans using CRISPR/Cas9. *bioRxiv*.

36. Hong K, Mano I, & Driscoll M (2000) In vivo structure-function analyses of Caenorhabditis elegans MEC-4, a candidate mechanosensory ion channel subunit. *J Neurosci* 20(7):2575-2588.

37. Brown AL, Fernandez-Illescas SM, Liao Z, & Goodman MB (2007) Gain-of-function mutations in the MEC-4 DEG/ENaC sensory mechanotransduction channel alter gating and drug blockade. *J Gen Physiol* 129(2):161-173.

38. Calixto A, Jara JS, & Court FA (2012) Diapause formation and downregulation of insulin-like signaling via DAF-16/FOXO delays axonal degeneration and neuronal loss. *PLoS Genet* 8(12):e1003141.

39. Arnadottir J, O'Hagan R, Chen Y, Goodman MB, & Chalfie M (2011) The DEG/ENaC protein MEC-10 regulates the transduction channel complex in Caenorhabditis elegans touch receptor neurons. *J Neurosci* 31(35):12695-12704.

40. Chen Y, Bharill S, O'Hagan R, Isacoff EY, & Chalfie M (2016) MEC-10 and MEC-19 Reduce the Neurotoxicity of the MEC-4(d) DEG/ENaC Channel in Caenorhabditis elegans. *G3 (Bethesda)* 6(4):1121-1130.

41. Topalidou I, van Oudenaarden A, & Chalfie M (2011) Caenorhabditis elegans aristaless/Arx gene alr-1 restricts variable gene expression. *Proceedings of the National Academy of Sciences of the United States of America* 108(10):4063-4068.

42. Li W, Feng Z, Sternberg PW, & Xu XZ (2006) A C. elegans stretch receptor neuron revealed by a mechanosensitive TRP channel homologue. *Nature* 440(7084):684-687.

43. Pujol N, Torregrossa P, Ewbank JJ, & Brunet JF (2000) The homeodomain protein CePHOX2/CEH-17 controls antero-posterior axonal growth in C. elegans. *Development* 127(15):3361-3371.

44. Van Buskirk C & Sternberg PW (2010) Paired and LIM class homeodomain proteins coordinate differentiation of the C. elegans ALA neuron. *Development* 137(12):2065-2074.

45. Schroeder NE & Flatt KM (2014) In vivo imaging of Dauer-specific neuronal remodeling in C. elegans. *J Vis Exp* (91):e51834.

46. Peckol EL, Troemel ER, & Bargmann CI (2001) Sensory experience and sensory activity regulate chemosensory receptor gene expression in Caenorhabditis elegans. *Proceedings of the National Academy of Sciences of the United States of America* 98(20):11032-11038.

47. Kim K*, et al.* (2009) Two chemoreceptors mediate developmental effects of dauer pheromone in C. elegans. *Science* 326(5955):994-998.

48. Neal SJ*, et al.* (2016) A Forward Genetic Screen for Molecules Involved in Pheromone-Induced Dauer Formation in Caenorhabditis elegans. *G3 (Bethesda)* 6(5):1475-1487.

49. Rose JK, Sangha S, Rai S, Norman KR, & Rankin CH (2005) Decreased sensory stimulation reduces behavioral responding, retards development, and alters neuronal connectivity in Caenorhabditis elegans. *J Neurosci* 25(31):7159-7168.

50. Geng J, Zhao Q, Zhang T, & Xiao B (2017) In Touch With the Mechanosensitive Piezo Channels: Structure, Ion Permeation, and Mechanotransduction. *Curr Top Membr* 79:159-195.

51. Ranade SS*, et al.* (2014) Piezo2 is the major transducer of mechanical forces for touch sensation in mice. *Nature* 516(7529):121-125.

52. Gems D*, et al.* (1998) Two pleiotropic classes of daf-2 mutation affect larval arrest, adult behavior, reproduction and longevity in Caenorhabditis elegans. *Genetics* 150(1):129-155.

53. Gerisch B, Weitzel C, Kober-Eisermann C, Rottiers V, & Antebi A (2001) A hormonal signaling pathway influencing C. elegans metabolism, reproductive development, and life span. *Developmental cell* 1(6):841-851.

54. Gottlieb S & Ruvkun G (1994) daf-2, daf-16 and daf-23: genetically interacting genes controlling Dauer formation in Caenorhabditis elegans. *Genetics* 137(1):107-120.

55. Jia K, Albert PS, & Riddle DL (2002) DAF-9, a cytochrome P450 regulating C. elegans larval development and adult longevity. *Development* 129(1):221-231.

56. Riddle DL, Swanson MM, & Albert PS (1981) Interacting genes in nematode dauer larva formation. *Nature* 290(5808):668-671.

57. Thomas JH, Birnby DA, & Vowels JJ (1993) Evidence for parallel processing of sensory information controlling dauer formation in Caenorhabditis elegans. *Genetics* 134(4):1105-1117.

58. Vowels JJ & Thomas JH (1992) Genetic analysis of chemosensory control of dauer formation in Caenorhabditis elegans. *Genetics* 130(1):105-123.

59. Torr P, Heritage S, & Wilson MJ (2004) Vibrations as a novel signal for host location by parasitic nematodes. *International journal for parasitology* 34(9):997-999.

60. Bose N*, et al.* (2014) Natural variation in dauer pheromone production and sensing supports intraspecific competition in nematodes. *Current biology : CB* 24(13):1536-1541.

61. Diaz SA*, et al.* (2014) Diverse and potentially manipulative signalling with ascarosides in the model nematode C. elegans. *BMC Evol Biol* 14(1):46.

62. Schulenburg H & Felix MA (2017) The Natural Biotic Environment of Caenorhabditis elegans. *Genetics* 206(1):55-86.

63. McGlone F, Wessberg J, & Olausson H (2014) Discriminative and affective touch: sensing and feeling. *Neuron* 82(4):737-755.

64. Tan PL & Katsanis N (2009) Thermosensory and mechanosensory perception in human genetic disease. *Hum Mol Genet* 18(R2):R146-155.

65. Huang LS & Sternberg PW (2006) Genetic dissection of developmental pathways. *WormBook : the online review of C. elegans biology*:1-19.

66. Chen BL, Hall DH, & Chklovskii DB (2006) Wiring optimization can relate neuronal structure and function. *Proceedings of the National Academy of Sciences of the United States of America* 103(12):4723-4728.

67. White JG, Southgate E, Thomson JN, & Brenner S (1986) The structure of the nervous system of the nematode Caenorhabditis elegans. *Philosophical transactions of the Royal Society of London. Series B, Biological sciences* 314(1165):1-340.

68. Russell J, Vidal-Gadea AG, Makay A, Lanam C, & Pierce-Shimomura JT (2014) Humidity sensation requires both mechanosensory and thermosensory pathways

in Caenorhabditis elegans. *Proceedings of the National Academy of Sciences of the United States of America* 111(22):8269-8274.

69. dos Santos CN*, et al.* (2011) Seasonal dynamics of cyathostomin (Nematoda - Cyathostominae) infective larvae in Brachiaria humidicola grass in tropical southeast Brazil. *Veterinary parasitology* 180(3-4):274-278.

70. Viney ME (2009) How did parasitic worms evolve? *BioEssays : news and reviews in molecular, cellular and developmental biology* 31(5):496-499.

71. Ludewig AH & Schroeder FC (2013) Ascaroside signaling in C. elegans. *WormBook : the online review of C. elegans biology*:1-22.

72. Ardiel EL & Rankin CH (2010) The importance of touch in development. *Paediatr Child Health* 15(3):153-156.

73. Vidal-Diez de Ulzurrun G & Hsueh YP (2018) Predator-prey interactions of nematode-trapping fungi and nematodes: both sides of the coin. *Appl Microbiol Biotechnol* 102(9):3939-3949.

74. Brenner S (1974) The genetics of Caenorhabditis elegans. *Genetics* 77(1):71-94.